เพื่อแม่และพ่อ

Acknowledgement

I would like express my sincere gratitude to Prof. Amparo Acker-Palmer who has given me the great opportunity to pursue my PhD work in the newly started up group. Without her stimulating enthusiasm, constructive comments, inspiring suggestions, and endless positive energy, the project would never have been in the same shape as it is right now. And more importantly, I would never be the same researcher I am now without the support she constantly gave me to develop my own ideas and to try things that others would not even waste their time to think twice.

I am very grateful for all the supports I have constantly received from Prof. Ruediger Klein. His constructive suggestions and generous support of devices and reagents, even when our group had moved out of his department, all have been an indispensable contribution to the success of my work.

My special thank goes to Alessandro Filosa, my best friend, my tutor, my endless source of knowledge, the one whom I always turn to with every possible kinds of problem. Not only the great contribution on ideas for the project that he provided, but also his patience, learning eagerness, and stimulating motivation that brought me to where I am now and still enthusiastic to step forward.

The work could not be completed without the great collaborators, Till Acker and Sacha Siedel who took care of tumor experiments, George Wilkinson and Ralf Adams who provided transgenic animals, and Clara Essmann who helped with biochemistry experiments.

Last but not least, I would also like to thank all the members of the Acker-Palmer group for all the great times we shared and such a great working environment they created. An ex-member of the group Inmaculada Segura, who was always there for me when I just started in the vascular biology field knowing very little about endothelial cells, also rightly deserve my appreciation.

EphrinB2 regulates VEGFR2 function in developmental and tumor angiogenesis

Dissertation

Der Facultät für Biologie

Lugwig-Maximilians-Universität

München

Vorgelegt von

Suphansa Sawamiphak

München, Juni 2010

Erstgutachter: Prof. Dr. Rüdiger Klein

Zweitgutachter: Prof. Dr. Angelika Böttger

Tag der mündlichen Prüfung: 27. Juli 2009

The work presented in this thesis was performed in the laboratory of Dr. Amparo Acker-Palmer, Junior Group – Signal transduction, at the Max-Planck-Institute of Neurobiology, Martinsried, Germany.

Erklärung

Ich versichere, daβ ich die Dissertation “EphrinB2 regulates VEGFR2 function in developmental and tumor angiogenesis” selbstständig, ohne unerlaubte Hilfe angefertigt, und mich dabei keiner anderen als der von mir ausdrücklich bezeichneten Hilfen und Quellen bedient habe.

Die Dissertation wurde in der jetzigen oder ähnlichen Form bei keiner anderen Hochschule eingereicht und hat noch keinen sonstigen Prüfungszwecken gedient.

_____ _____

(Ort, Datum) (Suphansa Sawamiphak)

Zusammenfassung

Die Blutgefäßbildung ist nicht nur wäherend der frühen Entwicklungsstadien von großer Bedeutung, sondern ist auch ausschlaggebend bei der Entstehung von Krebs beteiligt.

Spezialisierte Zellen, die sogenannten „Tip-Zellen“, können durch die Ausbildung von fadenförmigen Ausstülpungen (Filopodien), entweder die Umgebung nach Signalmolekülen aus dem umliegenden Gewebe absuchen oder auch als physikalische Anker fungieren, dabei stabilisieren sie den Zellkontakt mit der extrazellulaeren Matrix, bei der Vorwärtsbewegung beim vaskulären Wachstum.

Intensive Untersuchungen in den letzten Jahren lieferten einen beständigen Beweis dafür, dass „Tip-Zellen“ eine Schlüßelrolle beim Wachstum von Blutgefäßen während der Angiogenese spielen. Dies hat das Verständniss der molekularen Mechanismen für die Spezialisierung der „Tip-Zellen“ stark beeinflußt.Jedoch ist zum derzeitigen Stand das Wissen über die molekulare Mechanerie, welcher die „Tip-Zell“-Lenkung unterliegt nur sehr wenig bekannt.

Vaskuläre endothel „Tip-Zellen“ gehören zu den gut charakterisierten axonalen Wachstumskegeln. Diese spielen eine wichtige Rolle bei der Migration von wachsenden Axone während der Vernetzungen des bestehenden Nervensystems. Neben den morphologischen Gemeinsamkeiten lassen noch mehr Anhaltspunkte dafür finden, dass der axonale Wachstumskegel und die Kapillargefäß „Tip-Zellen“ einige gemeinsame Signalmoleküle teilen. Als weiterer Beleg dafür ist das vorhanden sein von verwandten Rezeptoren auf der Zelloberfläche von sowohl Nerven- als auch Blutgefäßzellen, desweiteren ist anzuführen die in beiden Arten gemeinsame Umwandlung von Signalen aus der Umgebung in eine Zellantwort und letztendlich die Anordnung des Nerven- und des Blutgefäßsystems im gesamten Körper.

Die bidirektionale Signalverarbeitung von Eph-Rezeptoren und ihren Ephrin transmembran Liganden machen das wichtigste Leitsingal bei der axonalen Migration aus. EphrinB2 is bekannt dafür intrinsische Singale auzulösen, welche für den Umbau von sowohl Blut- als auch lymphatischen Gefäßen während der Entwicklung beteiligt sind. Allerdings sind die molekularen

Mechanismen, die der EphrinB2 Funktion während der Vaskularisierung unterliegen noch weitgehendst unverstanden.

Die sehr genau definierte Rolle von EphrinB Liganden während des axonalen Wachstums führt zur Annahme, dass EphrinB2 vielleicht genauso bei der Migration von endothelalen „Tip-Zellen“ beteiligt sein könnte. Die Analyse der Vaskularisierung von mäuse Retinas, isoliert nach der Geburt, bei EphrinB2 Signal Mutanten zeigt, dass die Defekte im EphrinB2 PDZ-Signal (ephrinB2ΔV), jedoch nicht das fehlen der EphrinB2 Tyrosinphosphorylierung (ephrinB25Y), zu einem Defekt in der vaskulären Entwicklung bei EphrinB2ΔV Mäusen führt. Dieser Defekt führt zu einer ernsthaften Reduktion der fadenförmigen Ausstülpungen an der Wachstumsfront des sich entwickelnden vaskulären Netzwerkes. Umgekehrt führt die Aktivierung des EprinB2 „reverse signaling“ in Explantaten gewonnen aus Retina genauso wie die Überexpression von EprinB2 in Kulturen von primären Endothelzellen zu einer Ausdehnung der fadenförmigen Ausstülpungen.

Mechanistisch konnte in dieser Arbeit zum ersten Mal gezeigt werden, dass EprihnB2 als Schlüsselregulator beim vaskulären endothel Wachstums Faktor Rezeptor2 (VEGFR2) fungiert. Dies konnte bei den verschiedensten Versuchssystemen, wie zum Beispiel ex vivo, in vitro und biochemischen Versuchen, gezeigt werden. Daher bietet diese Arbeit einige starke Hinweise auf die äußerst wichtige Rolle der EphrinB2 PDZ- abhängigen Signale während der Internalisierung von VEGFR2 von der Zelloberfläche. Doch weitaus wichtiger, gegen das frühere Dogma, ist die Internalisierung von VEGFR2 notwendig für die anhaltende Signal Aktivierung des Rezeptors. Ausserdem, können die fadenförmigen Ausstülpungen als Antwort auf die Stimulation mit VEGFR2, auch endozytotische Prozesse erfüllen, dies konnte in Explantaten aus der Retinas gezeigt werden. Ferner wurde die funktionelle relevanz der Rezeptorinternalisierung für die einwandtfreie Signalweiterleitung bewiesen. In pathologischen Ansaetzen, wurde das EphrinB2 PDZ-Signal blockiert und somit eine Reduktion des Tumorwachstums erreicht, diese Verringerung ging einher mit der Abnahme der Tumorvaskularisierung. Die angiogene Bildung der Tumorblutgefäße ist vergleichbar mit der Tumorvaskularisierung in EphrinB2ΔV Mutanten Mäusen. Diese Funktion von EphrinB2 bei der

Regulation von Angiogenese bei der Tumorblutgefäßbildung ist auf die spezifität der Endothelzellen zurückzuführen und kann in Mäusen, welchen das EphrinB2 (ephrinB1iΔEC) fehlt ebenfalls beobachtet werden.

Abschließend lässt sich sagen, dass diese Arbeit einen neuen molekularen Mechanismus bei der Kontrolle des vaskulären Wachstum aufzeigt. Wobei EphrinB2, durch die PDZ-Wechselwirkung, sowohl bei der Endozytose als auch die Aktivierung des VEGFR2 Signalweg benötigt, um die Funktion der gerichteten Migration von endothel „Tip-Zellen“ sowohl während der Entwicklung als auch in pathologischen Ansätzen zu aktivieren. Die direkte Regulation der VEGFR2 Funktion durch EphrinB2 PDZ Wechselwirkung verkörpert eine reizvolle kombinatorisch oder alternative anti-angiogene Therapie mit einer sehr viel höheren spezifität für die Behandlung gegen Tumore.

Table of contents

1. List of figures and tables 1

2. Publication from the work presented in the dissertation 4

3. Abbreviations 5

4. Summary 9

5. Introduction 11

5.1 Blood vessel formation 11

5.1.1 Vasculogenesis 12

5.1.2 Sprouting angiogenesis 14

5.1.2.1 Selection of sprouting endothelial cells 15

5.1.2.2 Directional migration of endothelial sprouts 19

5.1.2.2.1 Neurovascular cues in angiogenesis 19

5.1.2.3 Converting sprouts into vessels 22

5.1.3 Intussusceptive angiogenesis 24

5.1.4 Arteriovenous differentiation 24

5.1.5 Mouse retinal angiogenesis model 26

5.2 Tumor angiogenesis 27

5.3 VEGF and their receptors 30

5.3.1 General characteristics of VEGFs and VEGFRs 30

5.3.2 VEGFR2 signaling 32

5.4 Eph receptors and ephrin ligands 35

5.4.1 General characteristics of Eph receptors and ephrin ligands 35

5.4.2 Eph forward signaling 38

5.4.3 Ephrin reverse signaling 40

5.4.3.1 EphrinA reverse signaling 40

5.4.3.2 EphrinB reverse signaling 40

5.4.4 Regulation of adhesion and repulsion 42

5.4.5 Eph-ephrin in vascular morphogenesis 43

5.5 Receptor endocytosis 46

5.5.1 Endocytosis in control of signaling 49

5.6 The thesis project 50

6 Results..... 52
6.1 EphrinB2 PDZ-signaling controls endothelial tio cell filopodial extension during sprouting angiogenesis 52
6.1.1 EphrinB2 reverse signaling through PDZ-interaction is indispensable for developmental angiogenesis 52
6.1.2 Angiogenic growth of blood vessels is unaffected in the absence of ephrinB2 tyrosine phosphorylation 56
6.1.3 The requirement of ephrinB2 PDZ-signaling in angiogenic growth of blood vessels is widespread throughout the central nervous system..... 57
6.1.4 Lack of ephrinB2 PDZ-signaling specifically affects filopodial extension in endothelial tip cells, without alteration of cell proliferation 58
6.1.5 Complementary expression of ephrinB2 in spouting retinal vessels and EphB receptors in the scaffolding astrocytic network 61
6.1.6 EphrinB2 gain-of-function promotes filopodial protrusion in cultures endothelial cells 63
6.1.7 EphrinB2 PDZ-interactions confers contact-mediated Repulsive activity to endothelial cells..... 64
6.1.8 Supplementary information on CD-Rom 57
6.2 EphrinB2 PDZ-interaction is crucial for VEGFR2 internalization and signal transduction 68
6.2.1 VEGF-induced endocytosis of VEGFR2 requires PDZ interactions downstream of ephrinB2..... 69
6.2.2 Expression levels of ephrinB2, VEGFRs, and NICD are unaltered in *ephrinB2*$^{\Delta V/\Delta V}$ mutant mice and endothelial cells..... 71
6.2.3 Activation of ephrinB2 induces VEGFR2 internalization..... 72
6.2.4 Kinetics of ephrinB2-induced VEGFR2 internalization 76
6.2.5 VEGFR2 and ephrinB2 are potential interaction partners 77
6.2.6 VEGFR2 activation is compromised in absence of ephrinB2 PDZ-interactions.. 78
6.2.7 Endocytosis is essential for VEGFR2 downstream signaling 81
6.2.8 VEGFR2 signaling intensity and duration depend on endocytosis of the receptor..... 82
6.3 EphrinB2 regulates endothelial tip cell filopodial extension by triggering VEGFR2 internalization..... 83
6.3.1 VEGF-induced extension of endothelial tip cell filopodia requires endocytosis .. 84

6.3.2 Activation of ephrinB2 signaling is sufficient to rescue Compromised filopodial extension caused by VEGF deprivation 85
6.4 EphrinB2 PDZ-signaling in endothelial cells influences tumor growth by regulating tumor angiogenesis 87
6.4.1 Blockade of ephrinB2 PDZ-signaling decreases brain tumor growth and reduces angiogenic sprouting of tumor vasculature 88
6.4.2 Endothelial-specific loss of ephrinB2 is sufficient to inhibit tumor angiogenesis 91
6.4.3 Pathological angiogenesis in different vascular beds are commonly controlled by ephrinB2 93

7 Discussion 96
7.1 VEGFR2 internalization is required for the full activation of downstream signaling 97
7.2 Endocytosis and spatial distribution of VEGFR2 during guided migration 99
7.3 EphrinB2 and VEGFR2 in control of tip cell filopodial extension 101
7.4 Triggering VEGFR2 signaling: A team effort of VEGF and ephrinB2 104
7.5 Interaction between VEGFR2 and ephrinB2 104
7.6 Molecular mechanism underlying ephrinb2 function in the endocytosis of VEGFR2 105
7.7 Control ephrinB2 expression by Notch signaling and tip cell function of ephrinB2 107
7.8 Different roles of ephrinB2 during angiogenic growth of blood vessels 109
7.9 Eph/ephrin signaling in tumor progression: angiogenesis and beyond 111

8 Materials and methods 113
8.1 Materials 113
8.1.1 Chemicals, enzymes and commercial kits 113
8.1.2 Bacteria 113
8.1.3 Cell lines 113
8.1.4 Primary cells 113
8.1.5 Media and dissection buffers 113
8.1.6 Plasmids 116
8.1.7 Oligoneucleotides 117
8.1.8 Solutions and buffers 117
8.1.9 Antibodies 124
8.1.10 Mouse lines 126

8.2 Methods 127
8.2.1 Molecular biology 127
8.2.2 Cell culture 130
8.2.3 Angiogenesis assay with primary endothelial cells 135
8.2.4 Immunocytochemistry 136
8.2.5 Biochemistry 138
8.2.6 Analysis of postnatal retinal angiogenesis 139
8.2.7 Retinal explantation 141
8.2.8 Surface biotinylation assay in cortial slices 142
8.2.9 Histology 142

9 Bibliography 146

10 *Curriculum vitae* 162

1. List of figures and tables

Introduction

Figure 5-1 Development of blood vasculature 12
Figure 5-2 Cellular events during angiogenic sprouting of a blood vessel 15
Figure 5-3 Stimulation Regulatory mechanism in control of tip-stalk cell specification 17
Figure 5-4 Morphological similarities between axonal growth cone and endothelial tip cell 19
Figure 5-5 Common cues for neural and vascular guidances 21
Figure 5-6 Molecular regulators of arterial and venous differentiation 24
Figure 5-7 Development of blood vessels of postnatal mouse retina 26
Figure 5-8 Tumor-induced angiogenic growth of blood vessels 28
Figure 5-9 VEGFR2 signaling 33
Figure 5-10 Eph receptors and ephrin ligands 36
Figure 5-11 Eph receptor forward signaling 38
Figure 5-12 EphrinB reverse signaling 41
Figure 5-13 Endocytosis pathways 47

Results

Figure 6-1 EphrinB2 PDZ interactions are required for expansion of superficial retinal vasculature in new born mice 53
Figure 6-2 Vascular branching and formation of vascular sprouts are impaired in absence of ephrinB2 PDZ-dependent signaling 54
Figure 6-3 The vascular phenotype caused by loss of ephrinB2 PDZ-interactions are persisted in adult mice 55
Figure 6-4 EphrinB2 phosphotyrosine dependent signaling is dispensable for *in vivo* retinal angiogenesis 56-57
Figure 6-5 *EphrinB2*$^{\Delta V/\Delta V}$ mice show vascular defects throughout the central nervous system 58
Figure 6-6 Disruption of ephrinB2 PDZ-dependent signaling causes severe defect in endothelial tip cell filopodial extension 59-60
Figure 6-7 Endothelial cell proliferation is not affected in *ephrinB2*$^{\Delta V/\Delta V}$ mutant retinas 60

Figure 6-8 EphrinB2 is expressed throughout the developing retinal vascular network and its receptos EphB are abundant in the astrocytic scaffold 61-62
Figure 6-9 Overexpression of ephrinB2 induces filopodial dynamics in endothelial cells.....63
Figure 6-10 Characterization of ephrinB2 knockout endothelial cells.....64
Figure 6-11 EphrinB2 reverse signaling mediates repulsive activity in endothelial cells.....65-66
Figure 6-12 Contact-mediated repulsion of endothelial cells requires ephrinB2 PDZ-interaction, but not tyrosine phosphorylation.....67
Figure 6-13 EphrinB2 PDZ-signaling is necessary for VEGFR2 internalization.....70-71
Figure 6-14 Characterization of *ephrinB2*$^{\Delta V/\Delta V}$ mutant mice and endothelial cells 72
Figure 6-15 Stimulation of ephrinB2 reverse signaling by EphB4-Fc is sufficient to induce VEGFR2 internalization 73-74
Figure 6-16 The effect of ephrinB2 activation on VEGFR2 trafficking was confirmed in live tissue 75
Figure 6-17 Kinetics of VEGFR2 internalization following ephrinB2 activation in endothelial cells 76
Figure 6-18 EphrinB2 and VEGFR2 co-localized at the cell membrane and co-immunoprecipitated.....77-78
Figure 6-19 VEGF-stimulated phosphorylation of VEGFR2 is compromised in *ephrinB2*$^{\Delta V/\Delta V}$ endothelial cells 79
Figure 6-20 *EphrinB2*$^{\Delta V/\Delta V}$ mutant mice show general impairment of VEGFR2 phosphorylation at different tyrosine residues 80
Figure 6-21 Endocytic trafficking is necessary for VEGF-stimulated VEGFR2 phosphorylation 81
Figure 6-22 Activation and prolongation of signaling downstream of VEGFR2 require receptor endocytosis.....83
Figure 6-23 Acute stimulation of explanted retina with VEGF induces tip cell filopodial extension in an endocytic-dependent manner 84-85
Figure 6-24 Activation of ephrinB2 induces tip cell filoipodial extension in explanted retinas 85-86
Figure 6-25 EphrinB2 activation rescues tip cell filopodial dynamics following VEGF sequestering 87
Figure 6-26 Characterization of high grade astrocytomas.....89

Figure 6-27 Intracranial astrocytoma growth is reduced in *ephrinB2*$^{\Delta V/\Delta V}$ mice compared with wild type littermates 89
Figure 6-28 Angiogenic sprouting of intracranial grown in *ephrinB2*$^{\Delta V/\Delta V}$ mice is impaired 90-91
Figure 6-29 Endothelial-specific ephrinB2 knockout mice show Arrested intracranial tumor growth 92
Figure 6-30 EphrinB2 function during pathological sprouting angiogenesis is endothelial cell specific 93
Figure 6-31 Subcutaneous tumor growth is reduced in *ephrinB2*$^{\Delta V/\Delta V}$ mice compared with wild type littermates 94
Figure 6-32 Angiogenesis is impaired in tumors developed subcutaneously in *ephrinB2*$^{\Delta V/\Delta}$ mutant mice 95

Discussion

Figure 7-1 Role of ephrinB2 in endothelial tip cell 96
Figure 7-2 Possible role of endocytosis in control of localization and intensity of VEGFR2 signaling 100

Materials and methods

Table 8-1 Primary antibodies 124
Table 8-2 Secondary antibodies 125

2. Publication from the work presented in this dissertation

Suphansa Sawamiphak, Sascha Seidel, Clara L. Essmann, George A. Wilkinson, Mara Pitulescu, Till Acker and Amparo Acker-Palmer

EphrinB2 regulates VEGFR2 function in developmental and tumour angiogenesis.

Nature 2010 May; 465(7297): 487/91

3. Abbreviation

°C	degree celsius
µ	micro
ACSF	artificial cerebrospinal fluid
ADAM	A-Disintegrin-And-Metalloprotease
AP2	adaptor protein-2
BAD	Bcl-2-associated death promoter
Bcl-2	B-cell lymphoma 2
bFGF	basic fibroblast growth factor
BME	Basal Medium Eagle
CAS	Crk-associated substrate
CCM	cerebral cavernous malformation
Cdc42	cell division cycle 42
CXCR4	CXC-motif chemokine receptor-4
DAG	diacylglycerol
DCC	deleted colorectal carcinoma receptor
DEP-1	density-enhanced phosphatase-1
DLAV	dorsal longitudinal anastomotic vessel
Dll4	Delta-like 4
DMEM	Dulbecco's modified Eagle's medium
D-PBS	Dulbecco's phosphate buffer saline
Dvl	Dishevelled
EC	endothelial cell
EGFR	Epidermal growth factor receptor
EPS15	(EGFR)-pathway substrate-15
Eph	Erythropoietin-producing hepatocellular
Ephrin	Eph family receptor interacting protein
eNOS	endothelial nitric oxide synthase
ERK1/2	extracellular-signal-regulated kinase-1/2
ESCRT	endosomal sorting complex required for transport
FAK	focal adhesion kinase
FBS	fetal bovine serum
Fc	fragment crystallizable, constant part of the antibody
Flt-1	fms-related tyrosine kinase 1
Gα	G protein α subunit

GAP	GTPase-activating proteins
GEF	Guanine nucleotide exchange factor
Girdin	Girders of actin filament
GIT1	G protein-coupled receptor kinase-interacting protein 1
GPCR	G protein-coupled receptors
GPI	glycosylphosphatidylinositol
GRIP	glutamate-receptor-interacting-protein
grl	gridlock
HBSS	hank's buffered salt solution
HEK	human embryonic kidney
HeLa	Henrietta Lacks
Hes	Hairy/Enhancer of Split
Hey	Hairy/E(spl)-related with YRPW motif
HIF1α	hypoxia-inducible factor 1, alpha subunit
Ig	immunoglobulin
INL	inner nuclear layer
Jag1	Jagged1
KUZ	Kuzbanian
LB	Luria-Bertani
M	molar
m	milli
MAPK	mitogen-activated protein kinase
MCAM	melanoma cell adhesion molecule
Min	minute
N	nano
Nck	non-catalytic region of tyrosine kinase adaptor protein
NO	nitric oxide
NICD	Notch intracellular domain
Nrarp	Notch-regulated ankyrin repeat protein
Nrp	Neuropilin
P	postnatal day
PAK	p21-activated kinase
PAR6	partitioning-defective protein 6
PDGFβ	platelet-derived growth factor beta
PDZ	postsynaptic density-95/discs large/zonula occludens-1

PFA	paraformaldehyde
pH	potential hygenii
Pick1	protein kinase C-interacting protein
PIP_2	phosphatidylinositol-4,5-bisphosphate
PI3K	phosphoinositol 3-kinase
PKB	protein kinase B
PKC	protein kinase C
PLC-γ	phospholipase C-γ
PlGF	placenta growth factor
Plxn	Plexin
PtdIn	phosphatidylinositol
PTFE	polytetrafluoroethylene
PTP-BL	protein tyrosine phosphatase BAS-like
PVR	PDGF/VEGF receptor
Rac1	RAS-related C3 botulinum substrate 1
RBPJ	recombination signal binding protein for immunoglobulin kappa J region
RGC	retinal ganglion cell
RhoA	Ras homolog gene family: member A
RTK	receptor tyrosine kinase
SDF1	stromal-derived factor-1
Sema	Semaphorin
Shb	SH2 domain-containing adaptor protein B
Shc	SH2 domain-containing transforming protein
SH2	Src (sarcoma virus transforming gene product) homology 2
TCPTP	T-cell protein tyrosine phosphatase
TGFβ	transforming growth factor β receptors
Tiam1	T-cell lymphoma invasion and metastasis 1
TIE2	tunica internal endothelial cell kinase 2
TNFR	tumor necrosis factor receptor
TrkB	Tropomycin-related kinase B
TSP1	thrombospondin 1
Tyr	Tyrosine
UIM	Ubiquitin interaction motif
Unc5b	Uncoordinated-5 homolog B
VE-cadherin	vascular endothelial cadherin

VEGF	Vascular endothelial growth factor
VEGFR	vascular endothelial growth factor receptor
VRAP	VEGF receptor-associated protein

4. Summary

Vessel sprouting is not only essential for normal development in the early stage of life, but also a decisive process for the progression of cancer. Specialized cells so called ‘tip cells’, by dynamically extending and retracting filopodial processes, function as a sensor for guidance cues in the surrounding tissues and might also serve as physical clutches that stabilize cell-extracellular matrix contacts to facilitate forward movement of vascular sprouts. Extensive studies in these recent years have provided a solid proof of the pivotal role of these tip cells in angiogenic growth of blood vessel and pushed forward our understanding of the molecular players in control of tip cell specification. On the contrary, our current knowledge of the molecular machineries that regulate guidance of tip cells is very limited. Vascular endothelial tip cells bear striking resemblance to the well-characterized axonal growth cones that lead the migration of growing axons during nerve wiring. In support of their morphological similarities, emerging evidences suggest that axonal growth cones and capillary tip cells share several guidance molecules that, upon engagement with their cognate receptors on the cell surfaces, transduce environmental signals into internal molecular responses and ultimately dictate the direction of growing nerves and vessels through the body. Bidirectional signaling from the Eph receptors and their transmembrane ligands ephrins represents one of the most important guidance cues involved in axon path finding. EphrinB2 is well-known to possess intrinsic signaling capabilities that are critical for angiogenic remodeling of both blood and lymphatic vessels during development. However, the cellular and molecular mechanisms underlying ephrinB2 function in the vasculatures are poorly understood.

The well-defined role of ephrinB ligands in axon guidance leads to an attractive speculation that ephrinB2 might be involved in guided migration of endothelial tip cells. Analysis of postnatal retinal vasculatures of ephrinB2 signaling mutant mice reveals that the deficiency in ephrinB2 PDZ-signaling (ephrinB2ΔV), but not the lack of ephrinB2 tyrosine-phosphorylation (ephrinB25Y), causes defective vascular development. EphrinB2ΔV mice exhibit a severe reduction of filopodia extensions at the sprouting front of growing vascular network. Conversely, activation of ephrinB2 reverse signaling in explanted retinas as well as overexpression of ephrinB2 in cultured primary endothelial cells can promote the extension

of filopodia processes. Mechanistically, it has been shown for the first time here that ephrinB2 serves as a key regulator of the vascular endothelial growth factor receptor 2 (VEGFR2) signaling. Employing a broad range of *ex vivo*, *in vitro*, and biochemical assays the work presented here has provided several evidences of the crucial requirement of ephrinB2 PDZ-dependent signaling in the internalization of VEGFR2 from cell surface. More importantly, against earlier dogma, internalization of VEGFR2 is necessary for the activation of prolonged signaling activities downstream of the receptor. Moreover, extension of filopodia structures in response to stimulation of VEGFR2, as demonstrated in explanted retinas, also requires functional endocytic process, further proven the functional relevance of receptor internalization for the proper signal transduction. In pathological settings, blockade of ephrinB2 PDZ-signaling reduces tumor growth associated with decreased tumor vascularization. Angiogenic sprouting of tumor blood vessels is compromised in tumors grown in ephrinB2ΔV mutant mice. The function of ephrinB2 in the regulation of angiogenic growth of tumor blood vessel is endothelial-specific given that the defect in tumor vascularization is reproduced in mice lacking ephrinB2 specifically in endothelial cells (ephrinB1iΔEC).

Taken together, the work presented in this thesis reveals the novel molecular machinery in control of vascular sprouting whereby ephrinB2, through PDZ-interactions, regulates endocytosis and activation of VEGFR2 signaling required for endothelial tip cell function during guided migration of growing vessels in both developmental and pathological settings. The direct regulation of VEGFR2 function by ephrinB2 PDZ-interactions represents an attractive combinatorial or alternative anti-angiogenic therapy with a more specific target for tumor treatment.

5. Introduction

The development of the vascular system is among the earliest events in vertebrate organogenesis. The complex closed circuit that consists of numerous interconnected conduits of the vascular tree is essential for supplying individual organs with oxygen, nutrients, signaling molecules, and immune cells, as well as efficient removal of CO_2 and waste products, all of which is required from early embryogenesis and sustained throughout life. In adults, growth and remodeling of the vascular network is essential for tissue metabolism and wound repair processes. Excessive growth of the vasculature, on the other hand, could lead to chronic inflammatory diseases. Moreover many tumors recruit host blood vessels to support their own growths and to facilitate their metastasis to distant tissues. Understanding the mechanisms that govern the complex process of vessel formation might therefore yield therapeutic benefits for example in cancer therapy. Largely driven by the need for therapeutic improvements, a number of key players and signaling events involved in the process of vascular formation have been identified (Coultas et al., 2005). However, given the complex nature of the vascular formation process that requires the tight coordination of many cellular and molecular events controlled by different signaling pathways, our knowledge of the process is still far from completed.

Our recent understanding about the cellular and molecular mechanisms underlying the formation of blood vessels during development and tumor progression, and the brief overview about the well-known key regulator of vascular development, the vascular endothelial growth factor (VEGF) receptors will be introduced first. Secondly, I will introduce the Eph/ephrin system and signaling, whose role in axon guidance had been well established, and has previously been shown to be essential in blood vessel remodeling. Deciphering the role of ephrin in the process of blood vessel formation in both physiological and pathological conditions at the molecular level was the main focus of this thesis project.

5.1 Blood vessel formation

During development, as soon as the early mesoderm has developed via gastrulation, the first step in the formation of the blood vasculature, process termed “vasculogenesis” begins. Vasculogenesis involves in the differentiation of mesodermal precursors to

endothelial progenitors (so called 'angioblasts') and the *de novo* formation of a primary capillary structure from those progenitors (Risau and Flamme, 1995); Fig. 5-1).

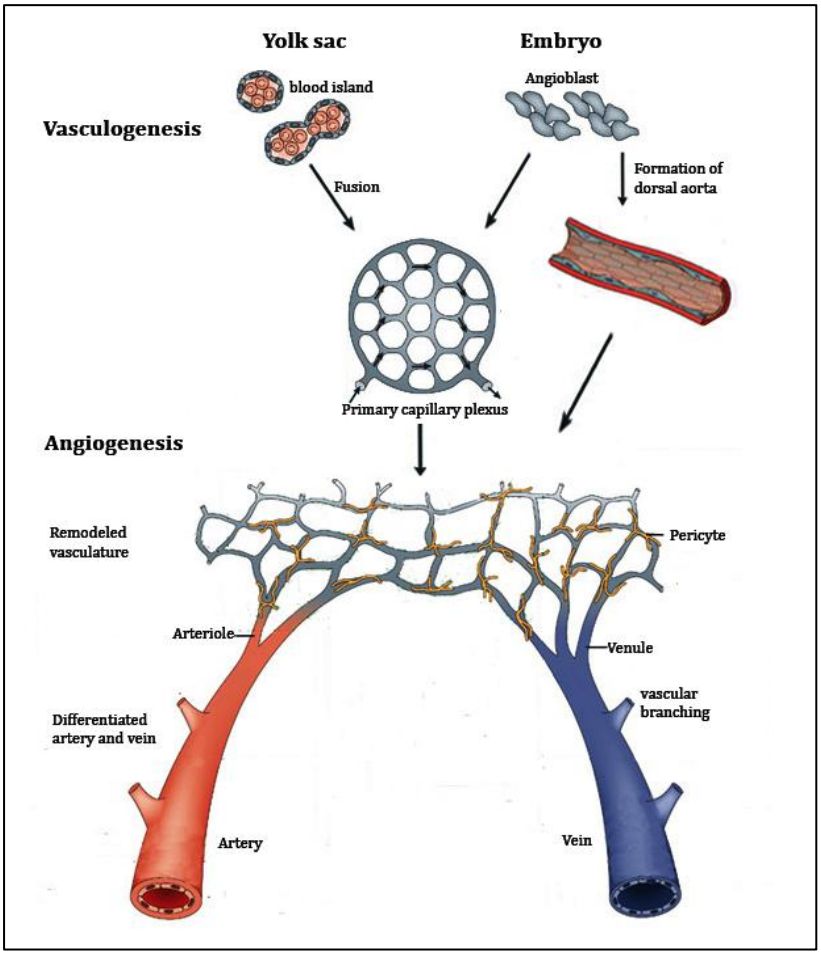

Figure 5-1 Development of blood vasculature. Schematic representation of vasculogenic assembly of endothelial precursors into primitive capillary structure which further remodel into highly ordered vascular networks via angiogenic sprouting. Scheme is adapted from Adams and Alitalo, 2007.

Further expansion and remodeling of the primitive capillary plexi occurs through a process called "angiogenesis", the formation of new blood vessels from the pre-existing ones (Carmeliet and Jain, 2000). Two distinct mechanisms during angiogenic growth of blood vessels, sprouting and non-sprouting or intussusception, have been described (Djonov et al., 2002). Through angiogenesis remodeling and recruitment of pericytes and smooth muscle cells, the primitive uniformed capillary plexi are developed in to hierarchically organized structure consisting of arteries, veins, and capillaries.

5.1.1 Vasculogenesis

Cellular mechanisms The earliest sign of vascular system development and therefore the first signature of vasculogenesis is the emergence of the yolk sac blood islands, clusters of

mesodermal cells that differentiate into solid clumps of hematopoietic cells enclosed with angioblasts. Subsequent fusion of blood islands gives rise to the primitive vascular plexus (Risau and Flamme, 1995). Inside the embryo, the dorsal aorta (which will later on fuse into one single vessel) and the vitelline arteries and veins are formed by direct aggregation of angioblasts without plexus intermediates (Ambler et al., 2001; Coultas et al., 2005; Patan, 2000).

The cardinal vein was thought to form by the same mechanism until very recently. Employing the zebrafish (*Danio rerio*) model, a third mode of blood vessel formation, where dorsal aorta and cardinal vein arise from a common precursor vessel, has been proposed. This process involves selective sprouting and migration of venous-fated endothelial progenitors from the precursor vessel, which results in the segregation of the cardinal vein from the dorsal aorta (Herbert et al., 2009).

The precise mechanism of the generation of endothelial cells and hematopoietic cells from mesodermal precursors remains debatable. A model involving bipotential common precursor known as ‘hemangioblast’ which could differentiate independently to produce hematopoietic and endothelial progenitor cells has long been postulated. The strongest evidence in favor of this model came from an *in vitro* clonal analysis of mouse embryonic stem (ES) cells which could directly differentiate into both hematopoietic and endothelial cells (Choi et al., 1998). A more recent model involves the generation of hematopoietic progenitor cells from hemangioblasts through a subset of early endothelial cells called ‘hemogenic endothelial cells’. Several recent studies provide compelling evidences in support of this model (Chen et al., 2009; Eilken et al., 2009; Lancrin et al., 2009).

Cells with endothelial characteristics circulating in the blood stream, so called ‘circulating endothelial cells’ (CECs), were observed and more importantly were found to be increased in many pathological conditions (Blann et al., 2005). Among these CECs which exhibit mature endothelial cell characteristics, a subpopulation with progenitor-like phenotype known as ‘circulating endothelial progenitor cells’ was also observed (Bertolini et al., 2006). Growing evidences suggest the contributions of these progenitor cells in neovascularization during regenerative and pathological conditions in the adult (Bertolini et al., 2006; Rafii et al., 2002).

Molecular regulators Bone marrow-derived circulating progenitor cells have been suggested to contribute to the formation of new vessels by differentiation into endothelial cell (EC) and incorporation into the developing vessels as well as retaintion in the perivascular area to promote vascular sprouting. Recruitment of these circulating cells to the growing vasculature requires chemotactic signals and adhesive molecules (Adams and Alitalo, 2007). VEGF secreted into the tissue microenvironment can recruit VEGFR1-positive bone-marrow-derived circulating cells, predominantly expressing hematopoietic markers, to specific sites of the body to facilitate adult neovascularization (Grunewald et al., 2006). Interestingly, the CXC-motif chemokine receptor-4 (CXCR4) which is also expressed in these circulating cells retains the cells in the perivascular space where its ligand stromal-derived factor-1 (SDF1) is locally secreted by fibroblast and smooth muscle cells in response to VEGF (Grunewald et al., 2006). Similarly, a subpopulation of circulating monocytes expressing TIE2 (tunica internal endothelial cell kinase 2) known as TIE2-expressing monocytes (TEM) homes to perivascular regions and acts in a paracrine manner to induce outgrowth of blood vessels without being incorporated into the endothelium (De Palma et al., 2005).

5.1.2 Sprouting angiogenesis

Upon stimulation with growth factors and chemokines, a subpopulation of endothelial cells lining inside the vessel wall acquires a motile and invasive activity which drive the modulation of cell-cell contact and local basement membrane matrix degradation. This leads to the sprouting of these activated endothelial cells from the pre-existing vessels. Endothelial sprouts migrate directionally toward areas with insufficient blood supply via the concentration gradient of growth factors and several guidance cues. Longitudinal and circumferential growth of the sprouts is acquired by proliferation of endothelial cells. Subsequent fusion of adjacent sprouts and lumen formation leads to the establishment of vascular tubules and the initiation of blood flow. To maintain vascular integrity of the newly formed tubules endothelial cell junctions need to be established. Blood flow and deposition of basement membrane together with the recruitment of mural cells contribute to maturation of the new vessels (all the cellular processes are depicted in figure 5-2).

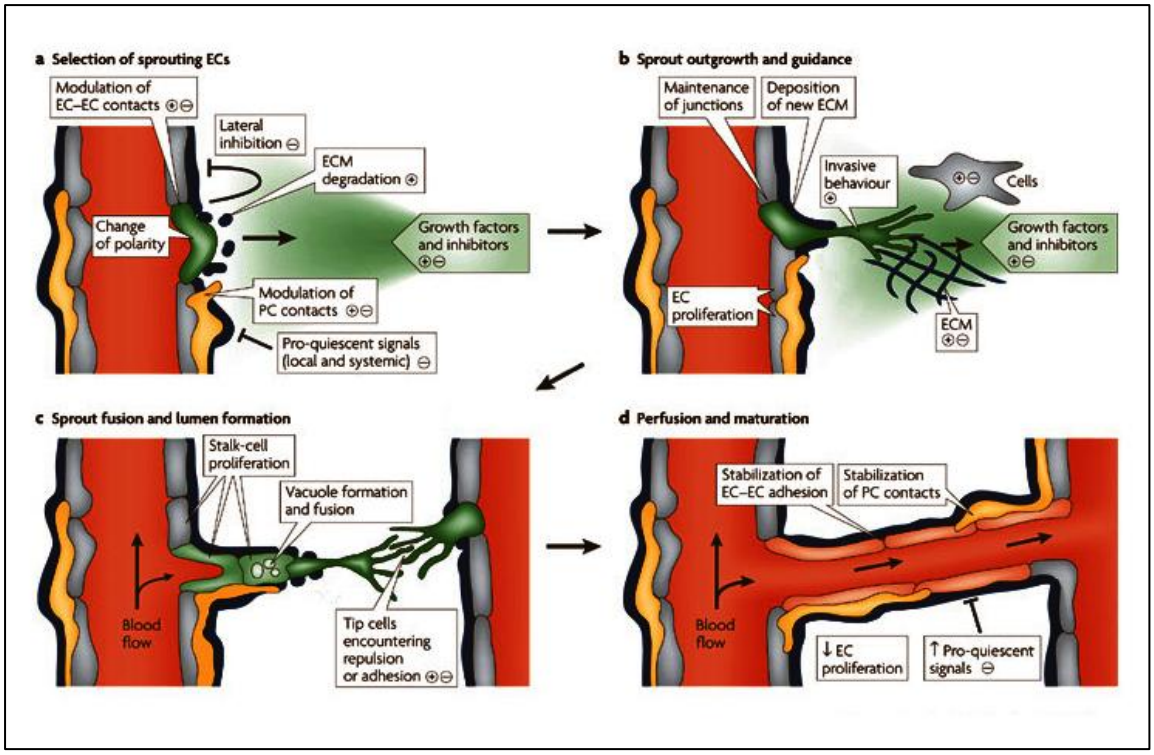

Figure 5-2 Cellular events during angiogenic sprouting of a blood vessel. A balance between pro- (+) and anti-angiogenic (-) stimuli derived from endothelial cells themselves, pericytes which have direct contact to the endothelium, guidepost cells and extracellular matrix along the migration path of the endothelial sprout determine the progression of each event. Model is adapted from Adams and Alitalo, 2007.

5.1.2.1 Selection of sprouting endothelial cells

VEGF (see topic 5.3 for detail) has been long known as the most prominent chemoattractant for endothelial cells. VEGF produced in response to local hypoxia promotes polarized EC sprouting and migration along VEGF gradients as shown in the well-established angiogenesis model in mammals, the retina (Gerhardt et al., 2003; Stone et al., 1995). Interestingly, ECs within the vessel wall respond differentially upon receiving VEGF stimulant. Only some ECs are selected to initiate sprouting. These cells, so called ‘tip cells’, extend long dynamic filopodia to probe their environment for guidance cues and lead the migration of the new sprouts. Not only their morphology, but also their gene expression profiles distinguish these tip cells from the adjacent ‘stalk cells’ that follow them in the growing sprouts. Expression levels of VEGFR2, VEGFR3, Dll4 (Delta-like 4), PDGFβ (Platelet-derived growth factor beta), and Unc5b (Uncoordinated-5 homolog B) are higher in

tip cells as compared to stalk cells (Phng and Gerhardt, 2009). Specification of tip and stalk cells is of great importance in the initiation of sprouting angiogenesis. ECs, in close contact to each other, are exposed to similar concentrations of VEGF. Without a signaling regulator to specify which cells become tip or stalk cells, all ECs will response indifferently. This would lead to an imbalance in the number of tip/stalk cells which may cause vascular disintegration. The best known regulator of endothelial tip and stalk cell specification to date are the Notch receptors and their ligands Dll4 and Jag1 (Jagged1).

Notch signaling in control of ECs specification First discovered in *Drosophila melanogaster* in which mutant allele causes notched wing, four Notch receptors (Notch1-Notch4), and five ligands (Dll1, Dll3, Dll4, Jag1, and Jag2, collectively called DSL from Delta, Serrate, LAG-2) have been identified in mammals. Notch receptors are expressed on the cell surface as heterodimers consist of an extracellular domain (NECD) and a transmembrane intracellular domain (NICD) linked together by a non-covalent bond (Roca and Adams, 2007). Upon *trans*-interaction of Notch and its ligand between adjacent cells the extracellular region of Notch is cleaved by a member of disintegrin and metalloprotease (ADAM) leaving the transmembrane region susceptible to γ-secretase, by which cleavage release the NICD from the cell surface. NICD translocates to the nucleus where it binds to the transcription factor RBPJ (recombination signal binding protein for immunoglobulin kappa J region, also known as CSL from mammalian CBF1, *Drosophila* Su(H), and *Caenorhabditis elegans* LAG1) and results in the replacement of the corepressor complex bound to CSL with the transcriptional activation complex. This process turns on the transcription of Notch target genes such as *Hes* (*Hairy/Enhancer of Split*), *Hey* (*Hes-related proteins*), *Nrarp* (*Notch-regulated ankyrin repeat protein*), and *efnb2* (*EphrinB2*) (Grego-Bessa et al., 2007; Phng and Gerhardt, 2009). Hes and Hey proteins, in turn, act as transcription repressors of genes further downstream (Phng and Gerhardt, 2009).

The crucial role of Notch and Dll4 in the regulation of endothelial tip/stalk cells specification has been demonstrated by several recent studies employing different model systems. Endothelial-specific inducible knockout of Notch1 or global deletion of one allele of Dll4 causes excessive tip cell formation in mouse retinas. In addition, in this model, where

there is a mosaic expression pattern of Notch1 due to the different degrees of Cre recombination, the majority of Notch1-deficient cells displayed tip cell characteristics (Hellstrom et al., 2007). In zebrafish, Rbpj or Dll4-deficient embryos exhibit enhanced sprouting and dramatic increased number of cells within the intersegmental vessel sprouts. Furthermore, in the chimeric setting, Rbpja knockdown cells transplanted into wild type embryo failed to integrate to the dorsal aorta and preferentially localized to tip cell position in the intersegmental sprouts (Siekmann and Lawson, 2007). Acquisition of tip cell characteristics in the Notch signaling-deficient cells therefore indicates that Notch is required to suppress these highly motile behaviors to allow only a subpopulation of cells to become tip cells.

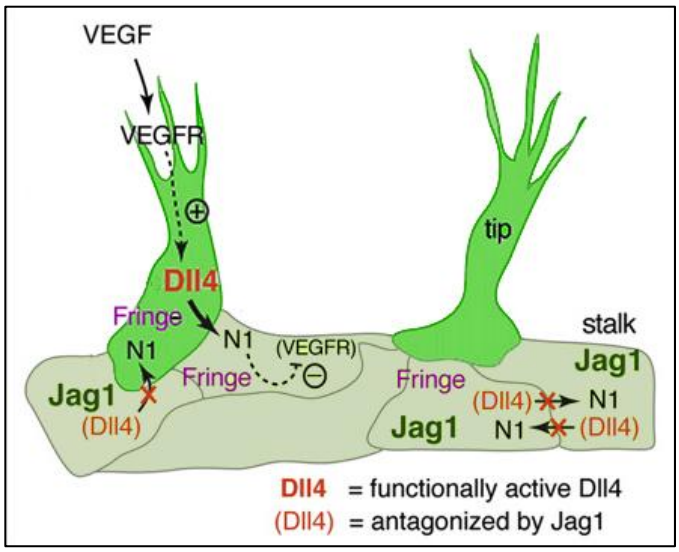

Figure 5-3 Regulatory mechnisms in control of tip/stalk cell specification. VEGF-stimulated activation of VEGFR2 induces expression of Dll4 which, in turn, activates Notch signaling to suppress tip cell phenotype in adjacent cells by downregulation of VEGFR. Concurrently, Jagged1 (Jag1) in these stalk cells antagonizes Dll4 to prohibit activation of Notch in tip cells. Dotted lines represent regulation of protein expression; filled lines represent signaling activation. Scheme is adapted from Benedito et al., 2009

Although the role of Notch in coordinating the balance of tip and stalk cells is widely appreciated, the downstream molecular mechanism mediating this function of Notch is not fully resolved. The most prominent angiogenesis regulator VEGFR2 (detail in topic 5.3) enters the scheme from several evidences demonstrated that Notch signaling negatively regulates its expression (Henderson et al., 2001; Holderfield et al., 2006; Suchting et al., 2007; Williams et al., 2006), possibly through the transcriptional repressor Hey1 (Holderfield et al., 2006). Retinal endothelium of Dll4 heterozygous mice shows an up-regulation and wider distribution of *VEGFR2* mRNA, normally abundant in the sprouting front, also in the vascular bed. Furthermore, VEGF has been shown to induce Dll4 expression in angiogenic active vessels (Hainaud et al., 2006; Lobov et al., 2007; Patel et

al., 2005), which is in agreement with the ligand prominent (albeit not exclusive) expression in the tip cells localized at the sprouting front of growing vessels (Hellstrom et al., 2007; Hofmann and Iruela-Arispe, 2007). There, they are exposed to higher concentrated gradient of VEGF as compared to vascularized regions within the vascular bed.

These findings together prompt a model in which VEGF triggers expression of Dll4 which, in turn, activate Notch signaling in the adjacent cells. As a consequence, VEGFR2 in the Notch-activated cells is down-regulated and the cells are thereby non-responsive to VEGF stimulus. Cells that produce more Dll4 are then selected as tips, whereas their neighbors with active Notch remain stalks (Fig. 5-3). The specification of tip/stalk fates is most likely a very dynamic process. Live microscopy of Dll4-deficient zebrafish embryo shows that the tip cells abnormally sprout from the dorsal longitudinal anastomotic vessel (DLAV) at the dorsal-most aspect of the somites with invasive migratory behavior can be readily integrated into the DLAV (Leslie et al., 2007). It has also been shown that Dll4 can be up-regulated not only by VEGF but also by Notch (Benedito et al., 2009; Carlson et al., 2005), adding complexity to the Dll4-Notch-VEGF reciprocal regulation model. Another Notch ligand, Jag1, has recently been shown to play a part in the scheme. Jag1 is enriched in stalk cells and very weakly expressed in tip cells. Jag1-deficient ECs preferentially occupy tip cell positions, whereas overexpression of Jag1 results in the stalk sorting of ECs in the growing mouse retinal vasculatures (Benedito et al., 2009). Glycosylation of Notch by the glycosyltransferase Fringe has been reported to enhance the receptor activation by Delta-like ligand, but inhibit its response to Serrate/Jagged ligands (Yang et al., 2005). Combining Dll4 and Jag1 stimulation in EC overexpressed Manic Fringe reduces Dll4-stimulated Notch response, suggesting that Jag1 antagonizes Dll4 when Notch is glucosaminylated (Benedito et al., 2009). It has therefore been proposed that Jag1 highly expressed in stalk cells might antagonize the more potent ligand Dll4 to prohibit activation of Notch in adjacent tip cells (Fig. 5-3). Jag1 counteraction of Dll4-induced Notch activation between stalk cells might also be required to sustain VEGFR2 expression which is important for proliferation of these cells during active angiogenesis (Benedito et al., 2009).

5.1.2.2 Directional migration of endothelial sprouts

Wiring of the vascular system into a complex hierarchical network that is capable of effective delivery of oxygen and nutrients to different organs throughout the body is of utmost importance and requires the precisely coordinated series of guidance decisions. Clues to the complex nature of vessel guidance come from the anatomical similarities of the vascular and nervous network and moreover, the paralleled patterns of blood vessels and peripheral nerve fiber (Mukouyama et al., 2002). The task of axon navigation through a complex environment over considerable distances to reach the appropriate targets is carried out by a specialized structure at the leading tip of growing axons, the growth cones. The filopodia-riched structure and the dynamic nature of the growth cone that continuously extend and retract their filopodia to reassess the environment and to select the correct routes hold striking similarities to the endothelial tip cell (fig. 5-4). A complement of these structural and behavioral similarities comes from increasing evidences demonstrated that nerves and vessels share several guidance molecules (fig. 5-5), which transduce environmental cues to cytoskeletal changes required for cell migration (Carmeliet and Tessier-Lavigne, 2005).

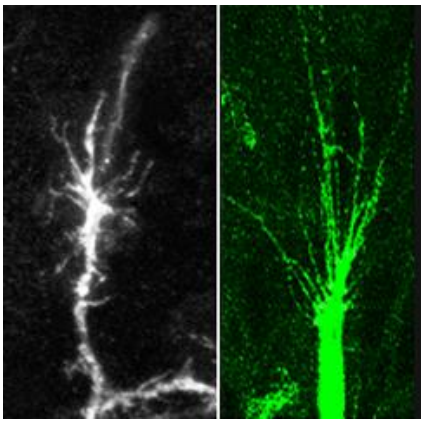

Figure 5-4 Morphological similarities between axonal growth cone and endothelial tip cell. Left; growth cone of fruit fly motor neuron (Sanchez-Soriano et al., 2007). Right; endothelial tip cell of mouse retina, visulaized with membrane markers.

5.1.2.2.1 Neurovascular guidance cues in angiogenesis

Netrin-DCC/Unc5 The laminin-related Netrin family consists of secreted matrix-bound proteins that interact with two canonical receptor families, the deleted colorectal carcinoma receptor (DCC) and the uncoordinated (UNC) 5 families. Among the Netrin receptors, UNC5B has been shown to express in arteries, capillaries and, in particular, strongly express in endothelial tip cells (Lu et al., 2004). Loss of UNC5B in mice causes embryonic lethality associated with excessive vessel branching and tip cell filopodia extension. Treatment with Netrin-1 causes tip cell filopodia retraction and this effect is abolished in

UNC5 knockout mice. In line with these findings, morpholino knockdown of either UNC5B or the ligand Netrin-1a, whose expression is strongest in the horizontal myoseptum midway along the the intersomitic vessel dorsal migration path, result in aberrant extension of tip cell filopodia and deviation from stereotyped path of the sprouting intersomitic vessels in zebrafish embryo (Lu et al., 2004). These evidences point to a role of UNC5B as a repulsive cue in endothelial sprouting, which is likely to act upon binding to its ligand Netrin-1. However, some studies have reported the function of Netrin-1 as a pro-angiogenic factor (Park et al., 2004; Wilson et al., 2006) via an unknown receptor. A possible explanation for the discrepancies between pro- and anti-angiogenic effects of Netrin-1 is the differential expression of its receptors as account for axon guidance. Besides, different mode of action of Netrin receptors depending on its ligation state has also been demonstrated (Eichmann et al., 2005; Nishiyama et al., 2003). Unligated UNC5B could induce vessel regression, while Netrin-1 stimulates EC survival and promotes angiogenesis by blocking its receptor proapoptotic activity (Castets et al., 2009).

Slit-Robo The vascular-specific Robo4 has been implicated in angiogenesis. Zebrafish embryos in which Robo4 is knocked down show defects in their intersomitic vessel sprouting and pathfinding (Bedell et al., 2005). These phenotypes are, however, not enough to pinpoint whether Robo4 mediates attractive or repulsive signals. Impaired sprouting may due to loss of an attractive cue, whereas misrouting of the sprouts may be a result of the absence of repulsive cues to direct their migration to the appropriate path. Several proteins important for actin nucleation were identified as Robo4 binding partners, in consistency with the suggested role of Robo4 in the regulation of filopodia formation in cultured endothelial cells (Sheldon et al., 2009). However, mice in which Robo4 is replaced with alkaline phosphatase reporter gene are viable and fertile with normal intersomitic and cephalic vessel patterning, suggesting that Robo4 is unlikely to be essential for developmental angiogenesis in mammals. Besides, expression of Robo4 which seems to be predominant in stalk cells in postnatal mouse retinas implies that this receptor is not required for vascular guidance (Jones et al., 2008a). Instead, Slit2 was shown to inhibit VEGF-induced EC migration *in vitro* and vascular hyperpermeability *in vivo*, and these effects were abolished in

absence of Robo4, suggesting a role of Robo4-Slit2 receptor-ligand pair in stabilizing the vasculature by counteracting with the angiogenic effects of VEGF (Jones et al., 2008a). By contrast, X-ray crystallography suggested that Robo4 does not bind Slit2 directly as it lacks many of the critical Slit2 binding residues (Morlot et al., 2007). Indeed, Robo4 has been shown to interact with Robo1, a potential receptor for Slit2 which is also express in endothelium (Sheldon et al., 2009). Interestingly, Slit2 binding to Robo1 has been reported to promote tumor angiogenesis (Wang et al., 2003). During axonal outgrowth, Robo3 and Robo1 heterodimerization inhibits Robo1 function (Sabatier et al., 2004). Therefore, while it is not yet clear which ligand is responsible for the anti-angiogenic function of Robo4, it is likely that this receptor inhibits the pro-angiogenic effects of Slit2-Robo1.

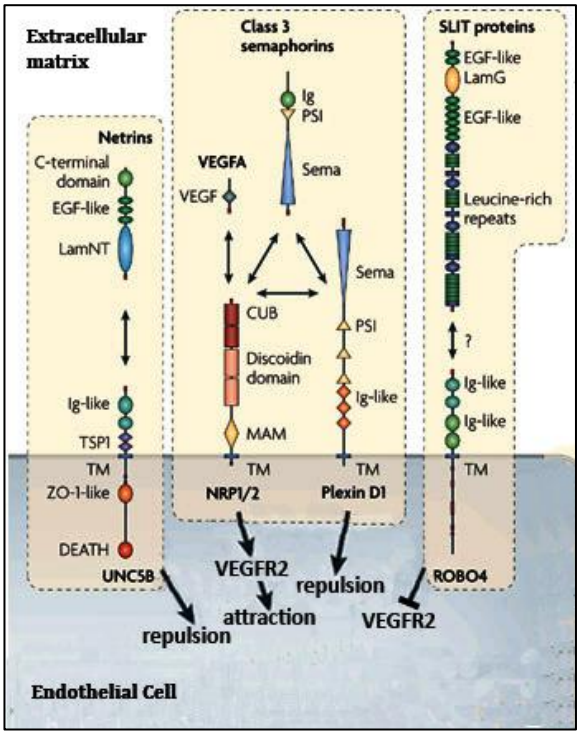

Figure 5-5 Common cues for neural and vascular guidances. Scheme is adapted from Adams and Alitalo, 2007

Semaphorin-Neuropilin/Plexin

Semaphorin (Sema) is a large family of secreted (class 3) proteins that are capable of long range diffusion and membrane-bound proteins that act at short distances. Semaphorins signal through two receptor families, Plexins (Plxn) and Neuropilins (Nrp). Membrane-bound Semaphorins directly bind Plexin, while the secreted class 3 Semaphorins bind to Neuropilins which signal through Plexins as co-receptors. Semaphorin 3E (Sema3E) which directly binds and signals through PlexinD1 (Plxnd1) is an exception to this rule (Carmeliet and Tessier-Lavigne, 2005). In zebrafish, Intersomitic vessels expressing Plxnd1 migrate through corridors between Sema3A-expressing somites. Knockdown of Plxnd1 results in irregular sprouting of intersegmental vessels from dorsal aorta and the growing sprouts do not track along the somite boundaries, suggesting that Plxnd1 mediates a

repulsive signal in the endothelium. The ligand that activates Plxnd1 in zebrafish is presumably Sema3a as implicated in the similar, albeit less severe, phenotypes in Sema3a knockout fish (Torres-Vazquez et al., 2004). In the mouse model, either global or endothelial-specific knockout of Plxnd1 causes perinatal lethality associated with severely disrupted vascular patterning (Gu et al., 2005; Zhang et al., 2009). The marked disorganization of intersomitic vessels which extend through the entire somites in Plxnd1-deficient mice confirms the role of Plxnd1 as a repulsive cue in vascular sprouting. The ligand that mediate this function in mice appears to be Sema3E which is strongly expressed in the caudal region of each somites and immediately adjacent to PlxnD1-expressing vessels. Loss of Sema3A results in the markedly similar phenotypes observed in Plxnd1 knockout mice, whereas Sema3A-deficient mice show a mild vascular branching defect (Gu et al., 2005; Serini et al., 2003). Importantly, Sema3E-Plxnd1 regulates vascular guidance independent of Neuropilins as double-mutant mice with loss of Sema3-binding site in Nrp-1 and complete loss of Nrp-2 have no vascular defect (Gu et al., 2005). Instead, the vascular function of Nrp1 receptor is depended on its binding to VEGF, possibly by acting as a co-receptor for VEGFR2 to mediate tip cell extension in guided vessel sprouting as revealed by genetic deletion of Nrp1 in mice and administration of the antibody that specifically blocks their VEGF binding site and complex formation with VEGFR2 (Gerhardt et al., 2004; Jones et al., 2008b).

5.1.2.3 Converting sprouts into vessels

Although the dynamic process of vessel sprout fusion has so far not been observed *in vivo*, the close proximity of endothelial tip cells that lead each new sprout and the filopodia-rich bridge-like structures frequently seen in the active sprouting area suggests that tip cells fuse together to give rise to new tubules (Roca and Adams, 2007). Given the motile and explorative behavior of tip cells, establishment of new vascular connections with other sprouts or existing capillaries requires strong adhesive forces along with the suppression of the tip cell invasive behavior. Indeed, the endothelial cell-specific transmembrane adhesion protein, vascular endothelial cadherin (VE-cadherin), which play a major role in the initiation of endothelial cell-cell contacts and establishment of adherens junctions, is also a known

suppressor of VEGFR2. VE-cadherin can form complex with VEGFR2 and negatively regulate its signaling properties by limiting its internalization (Lampugnani et al., 2006).

Establishment of blood flow in the newly formed interconnected vascular tubules requires lumen formation. Our current understanding of cellular and molecular mechanisms of vascular lumen formation is still modest. Two cellular mechanisms have been suggested to govern lumen formation in the vasculature; cord hollowing, by which central spaces are created inside cord of packed cells via cell flattening (Iruela-Arispe and Davis, 2009), and cell hollowing, in which intracellular vesicles generated in individual cells become exocytose and enable the interconnection of neighboring cells to form a multicellular lumen (Iruela-Arispe and Davis, 2009; Kamei et al., 2006). Integrins and several downstream partners have been demonstrated to have critical functions in lumenogenesis and tubular stabilization. Pharmacological inhibition of β1 integrins in chick embryo resulted in a complete loss of lumens in the aorta (Drake et al., 1992). EC-specific knockout of an integrin signaling molecule FAK (Focal adhesion) kinase shows defective tubular stabilization, while early vasculogenesis appears to be normal (Shen et al., 2005). Several in vitro studies reported the requirement of small GTPase proteins, Rac1 (RAS-related C3 botulinum substrate 1) and Cdc42 (cell division cycle 42), known regulators of cell cytoskeleton dynamics downstream of integrins, in the process of endothelial lumen formation (Davis and Bayless, 2003). The p21-activated kinase (PAK), a downstream effector of Rac1 and Cdc42 has recently been implicated in ECs lumen formation in an *in vitro* setting (Koh et al., 2008). In line with these in vitro studies, lumenogenesis during mouse and zebrafish embryonic development has been shown to be regulated by cerebral cavernous malformation (CCM) signaling proteins through Rho GTPase signaling (Kleaveland et al., 2009; Whitehead et al., 2009).

The generation of vascular lumens and initiation of blood flow, which subsequently leads to improvement of tissue perfusion, also contributes to the stabilization of new vascular connections. Decreased local expression of VEGF as a result of improved oxygen delivery, together with recruitment of pericytes and extracellular matrix proteins to the subendothelial basement membrane, promote maturation of vessels. Once the blood flow is established and oxygen supply meets local demands, some newly formed vascular

connections may undergo ‘prunning’, the process involving EC retraction or apoptosis to eliminate redundant vessels. Pruning may also occur during other stages of vessel development by alteration of factors that promote active angiogenesis and those that induce quiescent and maturation of vessels (Adams and Alitalo, 2007).

5.1.3 Intussusceptive angiogenesis

An alternative mode of angiogenesis remodeling with a clear distinction in the cellular mechanisms to the process of angiogenic sprouting has been reported in various tissues of several vertebrate species. In this alternative process, expansion and remodeling of the vascular networks proceed through the formation of transvascular pillars and subsequent vessel splitting, a mechanism called intussusception. Generation of the transcapillary pillars, the cylindrical tissue bridges enclosed by endothelial and mural cells occurs via establishment of transendothelial contacts of double layers of endothelium, which may take place within the same vessel after protrusion of the capillary walls into the lumen or between adjacent vessels. Although morphological evidences implicate the role of intussusception in the expansion of the capillary network and vascular pruning (Burri et al., 2004), our understanding of its physiological significance and molecular regulation is still very limited.

5.1.4 Arteriovenous differentiation

Arteries are wrapped extensively by extracellular matrix, elastic fibers, and vascular smooth muscle cells, to provide these vessels with the strength and flexibility necessary to absorb shear stress and high pressure from pulsatile flow produced by cardiac contractions. On the contrary, veins have less vascular smooth muscle coverage and contain valves to prevent backflow (fig. 5-6). In fact, not only areteries and veins are distinct in their morphological

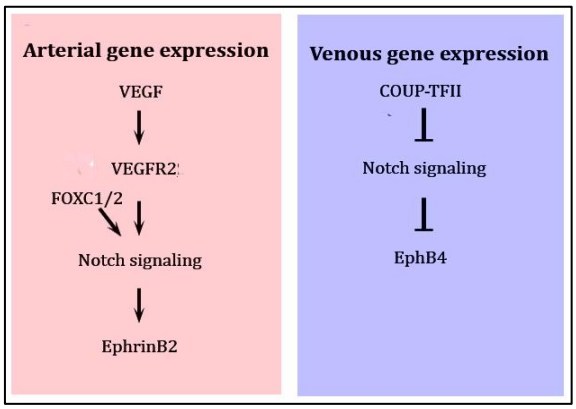

Figure 5-6 Molecular regulators of arterial and venous differentaion. Model is adapted from Adams and Alitalo, 2007

and functional properties, but also their respective endothelial cells are distinguished in their gene expression profiles. Several proteins have been found to express predominantly in either arterial or venous endothelial cells. One of the best known arterial markers is ephrinB2, and correspondingly one of its cognate receptor, EphB4, is largely confined to venous endothelial cells.

Two signaling pathways have been demonstrated to be involved in the regulation of ephrinB2 expression, VEGFR and Notch (Fig. 5-6). Stimulation of cultured endothelial cells by VEGF leads to increased expression of Dll4 ligand and subsequent activation of Notch signaling which, in turn directly controls an upregulation of ephrinB2 (Hainaud et al., 2006; Williams et al., 2006). *In vivo* VEGF secreted by peripheral nerves has also been demonstrated to promote arterial differentiation in mouse embryonic skin (Mukouyama et al., 2002). Knockdown of the zebrafish *gridlock* (*grl*), the ortholog of the mammalian Notch target genes *Hes1* and *Hey1* (see topic 5.1.2.1.1), causes loss of dorsal aorta and enlargement of axial vein, in association with reduced expression of arterial markers, including ephrinB2 and increase expression of venous markers. Conversely, overexpression of gridlock results in the reduction in size of axial vein, with no apparent increase of arteries. This suggests that gridlock functions rather as a suppressor of venous differentiation than an inducer of arterial fate (Zhong et al., 2001). Similarly, Hey1 and Hey2 double knockout mice show severe vascular defects and expression of arterial markers are largely absent (Fischer et al., 2004). The Forkhead transcription factor FoxC has also been shown to play a role in VEGF-induced Notch signaling pathways in the regulation of arterial fate by regulation of Hey2 and Dll4 expression (Hayashi and Kume, 2008). FoxC1 and FoxC2 double knockout mice show loss of arterial markers including Notch receptors and ligands, in association with arterio-venous shunts (Seo and Kume, 2006).

Several lines of evidences indicate that the nuclear receptor COUP-TFII, whose expression is limited to veins and lymphatic vessels, plays a key role in promoting venous endothelium differentiation. Veins show ectopic expression of arterial markers including Nrp1 and Notch1 in COUP-TFII null mice (Pereira et al., 1999; You et al., 2005), whereas EC-specific overexpression of the receptor suppresses arterial marker expression (You et al., 2005). Taken together, two different models have been proposed; 1) venous fate is a

default mode of EC differentiation and acquisition of arterial fate required activation of Notch signaling. 2) venous fate is acquired by COUP-TFII-mediated suppression of Notch-activated arterial fate (fig. 5-6).

In addition to genetic factors, the microenvironment within the vasculature is important in the regulation of arteriovenous differentiation. Changing of pulsatile, high-pressure arterial blood flow to low pressure venous flow in the yolk sac of chick embryos can suppress arterial differentiation as indicated by the lack of NRP1 and ephrinB2 expression (le Noble et al., 2004). Expression of ephrinB2 has also been shown to increase in adult neovascularization sites in physiological and pathological settings, reflecting the dynamic rather than fixed cell fate depending on local demand of angiogenic activity most likely through the alteration of VEGF levels (Gale et al., 2001).

5.1.5 Mouse retinal angiogenesis model

The post-natally developed highly organized vascular anatomy is the central attractiveness of the retina, which has been widely used to study developmental angiogenesis. Due to the well-defined temporal and spatial pattern of the retinal vasculature development, defects at different stages during angiogenic growth of these vessels can be easily recognized. Besides, initiation of vascular formation occurs after birth in mouse retinas and therefore it is possible to administer exogenous substances to examine their effects on vessel growth.

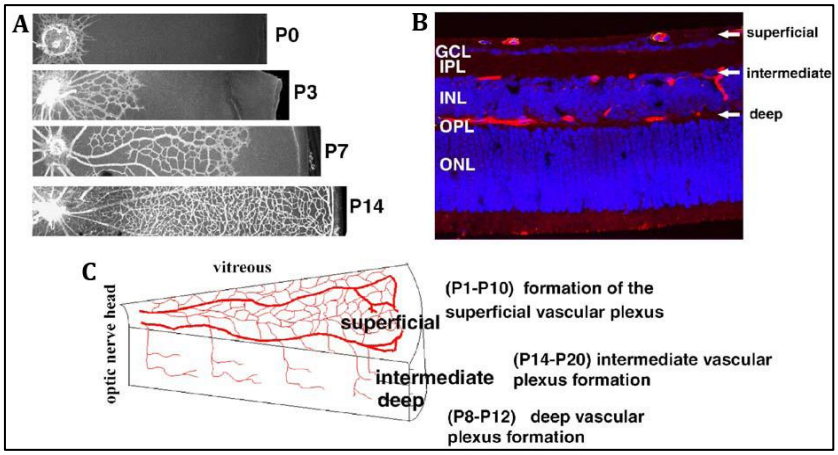

Figure 5-7 Development of the blood vessels of postnatal mouse retina (reproduced from Dorrell and Friedlander, 2006). A, The highly reproducible temporal and sptial pattern of superficial retina vessels formed after birth Vessels are visualized by collagen IV staining. B, Tranversal section of mouse retina stained with DAPI (blue) and CD31 (red). C, Model shows developmental time frames of each layer of retinal vasculatures.

During the first week of life in mice,

retinal vascularization begins within the retinal ganglion cell (RGC) layer, when a laminar network of vessels sprouts outward from the optic nerve head toward the retinal periphery. Around postnatal day (P) 8, when the superficial vascular plexus reaches the periphery, these vessels start to branch downward into the packed layer of amacrine, bipolar, and horizontal cells called inner nuclear layer (INL). First at the outer edge of the INL the deep vascular layer is developed, and later on during the third week after birth the intermediate vascular layer spreads throughout the inner edge of the INL (Fig. 5-7).

Interestingly, the developmental pattern of the superficial vascular plexus appears to precisely overlay the pre-existing astrocytic meshwork, which radiates from the optic nerve head and reaches the retinal periphery by birth. Consistent with this, endothelial tip cells filopodia are found to extend along the underlying processes of the astrocytes (Gariano and Gardner, 2005; Gerhardt et al., 2003). Retinal gial cells, including astrocytes and Mueller cells, produce VEGF in response to hypoxia (Dorrell and Friedlander, 2006; Stone et al., 1995). Adequate distributions of the different isoforms of the astrocyte-secreted VEGF, which remains on the cell surface and diffuses in the proximate extracellular surroundings, is crucial for vascular patterning (Carmeliet and Tessier-Lavigne, 2005; Gerhardt et al., 2003; Stalmans et al., 2002). Furthermore, Interaction between endothelial and gial processes mediated by adhesion molecule, R-cadherin, also play a role during the vessel guided migration events. Blockage of R-cadherin function results in underdeveloped retinal vasculature that fails to associate with the astrocytic network and migrates to normally avascular areas (Dorrell and Friedlander, 2006). These observations suggest a model in which initial interaction of VEGF produced by astrocytes and its receptor VEGFR2 expressed prominently on the filopodia processes of tip cells (Gerhardt et al., 2003) and subsequent R-cadherin mediated cell-cell adhesion are required to stabilize the filopodia contact to the astrocytic network and lead the migration of the the growing vessels (Dorrell and Friedlander, 2006; Gariano and Gardner, 2005).

5.2 Tumor angiogenesis

Like normal tissues, solid tumors require a functional vascular system which provides them with oxygen and nutrients as well as removes waste products to continue

their growth. Furthermore, the vasculature is the main route used by tumor cells for metastatic spread to remote tissues. Tumor vessels, on the other hand, develop apparent distinct characteristics from normal vascular system. These vessels, often dilated and tortuous, usually form chaotic branching patterns rather than organized into a hierarchical order of definitive arteries, veins, and capillaries as in normal vascular networks (Bergers and Benjamin, 2003). Endothelial cells lining tumor vessels often present in irregular shapes with uneven luminal membrane and loose intercellular contacts. These abnormalities in the endothelium, in association with the structurally atypical basement membrane and loose pericyte-endothelium connections, contribute to high permeability and even leakiness of the tumor vessels (Tozer et al., 2005). These abnormal features, often described as immature, reflect an imbalance in the control of the multistage neovascularization induced by tumors. Various pro-angiogenic factors are produced by tumor cells, including the most prominent factor, VEGF, which also seems to be the most ubiquitously expressed (Bergers and Benjamin, 2003; Folkman, 2007). Tumors may initially grow independently of the

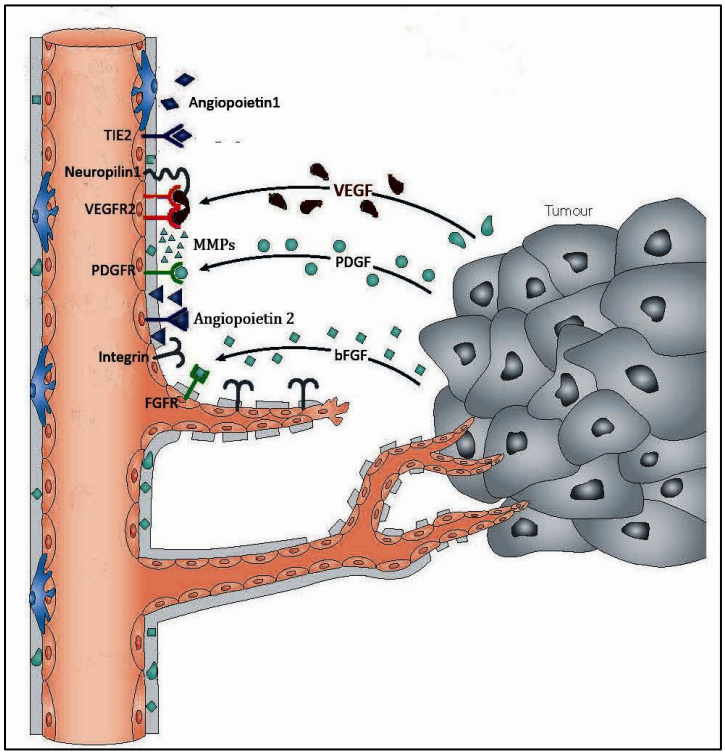

Figure 5-8 Tumor-induced angiogenic growth of blood vessels. Several growth factors such as basic fibroblast growth factors (bFGF), platelet-derived growth factor (PDGF), and most commonly VEGF are secreted from tumors to induce angiogenic responses through their cognate receptors expressed in the vascular endothelium. Matrix metalloproteinases (MMPs) are prodiced from VEGF-activated endothelial cells. Competitive binding of angiopoietin 2 secreted by some tumor cells which can sequester angiopoietin1 from the TIE2 receptor as well as signaling downstream of endothelial integrins might contribute to the pro-migratory stimuli. Scheme is adapted from Folkman, 2007.

vascular system or co-opt existing normal vessels for blood supply. Enlargement in size due to a rapid proliferation gives rise to necrotic and hypoxic areas inside the tumor mass, which demands increased nutrients and oxygen supply. As in normal tissue, oxygenation influences vessel growth through direct control of level and activity of the transcription factor HIF1α (Hypoxia-inducible factor 1, alpha subunit), a positive regulator of VEGF production (Carmeliet, 2003). Elevated levels of VEGF then induce the process of angiogenic sprouting of surrounding vessels into the tumors (Fig. 5-8). In addition to high levels of VEGF production, the potent angiogenesis inhibitor thrombospondin 1 (TSP1) has been shown to be down-regulated in tumor beds as a prerequisite for induction of tumor neovascularization and subsequent progression (Dameron et al., 1994; Rastinejad et al., 1989). The tightly regulated balance between pro- and anti-angiogenic factors during physiological angiogenesis is thus shifted during tumor-induced vessel formation. In normal vessel formation, pericyte coverage is important for acquisition of quiescent state of endothelial cells during the maturation of the newly formed vessels (Armulik et al., 2005). The defective pericyte coverage in tumor vessels therefore suggests that these vessels fail to become quiescent, enabling continuous induction of new vessel growth.

Given that tumor progression relies heavily on angiogenesis, several anti-angiogenic agents have been developed in an attempt to inhibit tumor growth. Numbers of agents have been generated to target VEGFR signaling mechanisms including neutralizing antibodies specific to VEGF or VEGFRs, soluble decoy VEGFRs, and inhibitors of tyrosine kinase with preference for VEGFRs. Various degrees of therapeutic benefits from these anti-angiogenic drugs are achieved in different cases owing to the complex nature of tumor cells, which may be able to overcome their angiogenic dependency. An increased vessel co-option was observed in a glioblastoma xenograft model after anti-VEGF treatment (Rubenstein et al., 2000). Tumor cells with an alteration in their gene expression which allow them to survive under hypoxic conditions after deprivation of blood supply may be selected for further progression as has been demonstrated in the mutation in *p53* gene (Yu et al., 2002). Furthermore, withdrawal of functional vascular system from tumors might trigger the more invasive behavior of tumor cells as a mechanism to escape from the area with low blood supply and subsequently metastasize to remote tissues (Bergers and Hanahan, 2008).

Combinatorial strategies to target both tumor cells themselves and the tumor vasculature are likely to be the most efficient approaches. New agents that act at different stages of angiogenesis as well as invasion of tumor cells are therefore of great necessity.

5.3 VEGF and their receptors (VEGFR)

5.3.1 General characteristics of VEGFs and VEGFRs

VEGF ligands Mammalian VEGF family consists of five members, VEGFA, VEGFB, VEGFC, VEGFD, and placenta growth factor (PlGF) (Ferrara et al., 2003). VEGFA (also referred to as VEGF) was firstly identified as an inducer of tumor microvascular permeability (Senger et al., 1983), and has been the focus of intensive studies in the field of vascular biology and cancer for almost 3 decades. Multiple isoforms of VEGFA generated from alternative splicing of an mRNA precursor (Robinson and Stringer, 2001) with strikingly different binding abilities and subsequent biological activities were described (Harper and Bates, 2008). Different spliced variants of VEGFA with pro-angiogenic activity detected in human were $VEGFA_{121}$, $VEGFA_{145}$, $VEGFA_{148}$, $VEGFA_{165}$, $VEGFA_{183}$, $VEGFA_{189}$, and $VEGFA_{206}$ owing to number of amino acids in the mature proteins. Recently, another spliced variant, $VEGFA_{165}$b with a difference in the last six amino acid residues at the C-Terminus has been identified (Harper and Bates, 2008). Interestingly, $VEGF_{165}$b was reported to have anti-angiogenic activity (Bates et al., 2002; Perrin et al., 2005). The smallest isoform, VEGFA121 is readily diffusible, whereas the bigger isoforms show binding affinity to heparan sulfate proteoglycan on the cell membrane and in the extracellular matrix.

VEGF receptors Secreted VEGF in dimeric form binds to VEGF receptor and activate its downstream signaling. Three structurally-related receptors, VEGFR1 (Flt-1), VEGFR2 (Flk-1), and VEGFR3 (Flt-4) are members of the receptor tyrosine kinase (RTK) superfamily. The extracellular region of VEGFR1 and VEGFR2 consists of seven immunoglobulin (Ig)-like domains, while disulfide bridge replaces the fifth domain in VEGFR2. All the three receptors possess a single transmembrane domain, two kinase domains, split by a kinase insert domain, and a C-Terminal tail (Fig. 5-9). Binding of VEGFRs to VEGF induces homo- and heterodimerization of the receptors and subsequent activation of tyrosine kinase activities

(Dixelius et al., 2003; Olsson et al., 2006). VEGFR1 binds to VEGFA, VEGFB, and PlGF, whereas VEGFR2 binds exclusively to VEGFA. VEGFR3 bind specifically to VEGFC and VEGFD. Proteolytic processed VEGFC and VEGFD are able to bind also to VEGFR2 (Holmes et al., 2007). Regulatory mechanisms and signaling downstream of the pivotal angiogenic mediator VEGFR2 is a focus of the work presented in this thesis and will be further described here in detail.

Regulation of VEGF/VEGFR activities A wide range of biological activities in response to the VEGF/VEGFR signaling is restrictively regulated by several mechanisms. The first to mention is the differential expression of the receptors and ligands depending on local requirement of active angiogenic activities. Hypoxia, a low oxygen supply condition commonly observed during development and typical in overgrowth tumors, has been shown to up-regulate expression of VEGFR (Ezhilarasan et al., 2007; Gerber et al., 1997; Nilsson et al., 2004) as well as the ligand VEGFA (Pugh and Ratcliffe, 2003). Notch signaling, on the contrary, enhances VEGFR1 expression while induces a down-regulation of VEGFR2 via unknown mechanism (Suchting et al., 2007).

In addition to the differential expression of both receptors and ligands, the existence of different spliced isoforms of VEGF with distinct binding abilities to the co-receptor neuropilin and heparan sulfate proteoglycans greatly affect the signal transduction upon their binding to VEGFRs. A clear example is $VEGFA_{165}b$ with an altered C-terminal tail, which is unable to bind neuropilin-1 (Kawamura et al., 2008) and has a reduced binding ability to heparin sulfate proteoglycans (Cebe Suarez et al., 2006) and rexerts anti-angiogenic activity upon binding to VEGFR2. Binding of VEGFA to heparan sulfate proteoglycan was previously reported to be essential to prolong and enhance signal transduction downstream of VEGFR2 (Jakobsson et al., 2006). Secreted variant of VEGFR1 and VEGFR2 generated by proteolytic processing were also reported (Ebos et al., 2004; Kendall and Thomas, 1993). With its higher binding affinity as compared to VEGFR2, secreted VEGFR1 can negatively regulated VEGFR2 signaling by competing with the VEGFR2 to bind to VEGFA (Hiratsuka et al., 1998). Different tyrosine phosphatases, for example T-cell protein tyrosine phosphatase (TCPTP) and high cell density-enhance PTP 1

(DEP-1), have been shown to dephosphorylate and thereby inhibit the signaling that required the kinase activity of VEGFR2 (Grazia Lampugnani et al., 2003; Mattila et al., 2008).

5.3.2 VEGFR2 signaling

The critical role of VEGFR2 in vascular development has been highlighted in the analysis of VEGFR2 null mice. Loss of VEGFR2 causes lethality of the mutant embryo as early as E8.5-9.0 due to defects in the formation of blood islands, indicating that the receptor is required from the very first step of vascular development (Shalaby et al., 1995). Haploid insufficiency of VEGF, as demonstrated in mice having only one allele of the ligand that phenocopied the defect found in VEGFR2 null mice (Carmeliet et al., 1996), underlined the crucial importance of VEGF/VEGFR2 signaling in vessel formation. Complex cascades of signaling mechanisms operated downstream of VEGFR2 serve to mediate the receptor stimulatory effects on a vast array of cellular activities ranging from cell proliferation, migration, survival, to vascular permeability.

Cell Proliferation Ligand binding triggers receptor dimerization and subsequent autophosphorylation of specific tyrosine residues in the receptors (Fig. 5-9), which thereby serve as docking sites for the recruitment of Src homology 2 (SH2) domain containing proteins. One of the few SH2 domain containing proteins that has been shown to interact with VEGFR2 is Phospholipase C-γ (PLC-γ). The importance of PLC-γ in normal development of blood vessels was demonstrated by the embryonic lethality of the PLC-γ knockout mice due to defective vasculogenesis (Ji et al., 1997). PLC-γ has been shown to be recruited to the phosphorylated Tyrosine (Tyr) 1175 of VEGFR2 (Takahashi et al., 2001). Subsequent phosphorylation of PLC-γ gives rise to its active form which mediates the hydrolysis of phosphatidylinositol-4,5-bisphosphate (PIP_2) to generate inositol-1,4,5-triphosphate (IP_3) and diacylglycerol (DAG). DAG and the increased intracellular calcium concentration by IP3, in turn, activate protein kinase C (PKC). Mitogen-activated protein kinase (MAPK) / extracellular-signal-regulated kinase-1/2 (ERK1/2) cascade which is

activated downstream of PKC can induce endothelial cell proliferation (Fig. 5-9) (Takahashi et al., 2001).

Migration Tyr1175 is a focal point of VEGFR2 signaling. Mutation of the tyrosine residue at this specific site to phenylalanine causes embryonic lethality in mice from a severe defect in vascular formation, resembling the phenotype of the VEGFR2 knockout mice (Sakurai et al., 2005). In addition to PLC-γ, the SH2 domain-containing protein B (Shb) (Holmqvist et al., 2003) and the Shc-related adaptor protein (Sck) (Warner et al., 2000) have also been shown to be recruited to VEGFR2 by binding to Tyr1175. Shb has been implicated in VEGFA-mediated cell migration via phosphoinositol 3-kinase (PI3K) (Holmqvist et al., 2003). PI3K mediated generation of phosphatidylinositol-3,4,5-trisphosphate is known to activate the Rho GTPase Rac which, in turn, trigger cell motility (Fig. 5-9) (Innocenti et al., 2003). The actin binding protein IQGAP1 might also play a role in VEGFR2-mediated activation of Rac (Yamaoka-Tojo et al., 2004). IQGAP1 can bind and activate Rac1 by inhibiting its intrinsic GTPase activity and thereby increases active (GTP-bound) Rac1 (Hart et al., 1996). In agreement with this model, VEGF stimulation has been shown to promote the association of Rac1 and IQGAP1 complex to phosphorylated VEGFR2 to facilitate endothelial cell migration in an *in vitro* setting (Fig. 5-9) (Yamaoka-Tojo et al., 2004).

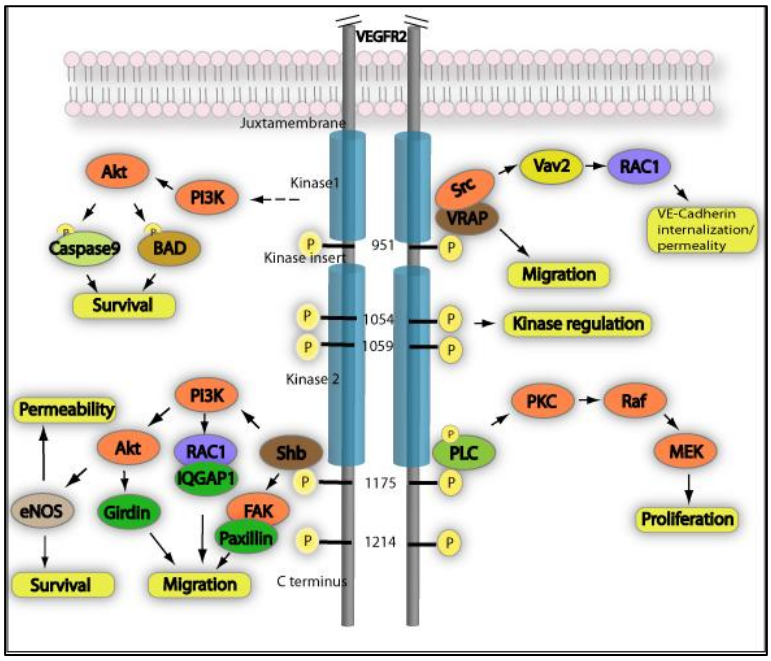

Figure 5-9 VEGFR2 signaling. Schemetic representation of some of the signaling pathways triggered upon VEGFA-stimulated activation of VEGFR2. Yellow circles marked with P represent phosphorylated tyrosines at the amino acid residues indicated with number of the human VEGFR2 homolog.

Activation of PI3K results in creation of the membrane bound PIP3 and subsequent membrane targeting and activation of protein kinase B (PKB/Akt) (Cantley, 2002). An Akt substrate actin-binding protein, Girdin (Girders of actin filament), has recently been shown to play an important role in angiogenesis by facilitating endothelial cell migration (Fig. 5-9). Mice lacking Girdin show severe defect in angiogenic sprouting of blood vessels in the retina model. *In vitro* Girdin knockdown endothelial cells are defective in lamellipodia formation and migration (Kitamura et al., 2008). In accord to the role of Akt in endothelial cell migration shown in this study, kinase-dead mutation of the p110α catalytic subunit of PI3K which is unable to phosphorylate Akt causes lethality of mouse embryos at mid-gestation from a severe defect in angiogenesis. Furthermore, endothelial cells from the mutant mice with no obvious alteration in proliferation or survival show strong migration defect, which interestingly could be rescued by overexpression of the small GTPase RhoA (Ras homolog gene family: member A), but not RhoB (Ras homolog gene family: member B) or Rac1 (Graupera et al., 2008).

Focal-adhesion kinase (FAK) was also reported to bind to Shb (Holmqvist et al., 2003). A signaling pathway involving VEGF-induced FAK phosphorylation and the recruitment of its substrate the actin anchoring protein paxillin might also be involved in VEGFR2 mediated cell migration (Holmqvist et al., 2003).

Two other phosphorylation sites, Tyr951 and Tyr1214, might also be involved in VEGF-mediated cell migration (Fig. 5-9). Tyr951 serves as a binding site for VEGF receptor-associated protein (VRAP, also known as Tsad, T-cell specific adaptor) (Matsumoto et al., 2005). VRAP knockout mice exhibit decreased tumor-induced angiogenesis and SiRNA-mediated VRAP knockdown cells show defective migratory response upon VEGF stimulation (Matsumoto et al., 2005). Phosphorylated Tyr1214 was reported to associate with the adaptor protein Nck (non-catalytic region of tyrosine kinase adaptor protein), which might facilitate actin remodeling through recruitment of the Src family protein Fyn to the site to activate cdc42 and MAPK (Lamalice et al., 2006).

Vascular permeability Although the first identified function of VEGF was the induction of vascular permeability (Senger et al., 1983), the precise mechanism is still elusive.

Generation of nitric oxide (NO) by endothelial nitric oxide synthase (eNOS) has been shown to be essential for VEGF induction of vascular permeability (Fukumura et al., 2001). Activation of eNOS requires Akt-dependent phosphorylation (Fig. 5-9) (Dimmeler et al., 1999; Fulton et al., 1999). The endothelial cell specific adhesion molecule VE-Cadherin is the key component of endothelium adherens junction that plays a main role in the control of vascular integrity and permeability (Carmeliet et al., 1999; Fukuhara et al., 2005). The tyrosine kinase Src recruited to VEGFR2 possibly via VRAP (Matsumoto et al., 2005) appears to be responsible for the disruption of VEGFR2/VE-Cadherin complex and increased vascular permeability upon VEGF stimulation (Eliceiri et al., 1999; Weis et al., 2004). The signaling cascade initiated by VEGFR2 activation involving Src-dependent phosphorylation of a Guanine nucleotide exchange factor (GEF) Vav2 and subsequent activation of Rac1 and its downstream effector the serine-threonine kinase PAK (p21-activated kinase), has been proposed. In this pathway serine phosphorylation of VE-Cadherin by PAK promotes its internalization into clathrin-coated vesicles and thereby triggers the disruption of intercellular junctions (Gavard and Gutkind, 2006) (Fig. 5-9). Alternatively, it has been proposed that phosphorylation of VE-Cadherin by VEGFR2 might recruit the phosphatase SHP-2 to dephosphorylate the VE-Cadherin-bound Src at its Tyr527 (Src internal regulatory phosphorylation site). Active Src could stimulate downstream Akt/eNOS signaling which results in endothelial cell junction disassembly (Ha et al., 2008).

Survival Akt signaling downstream of PI3K has been shown to be essential for endothelial cell survival (Fujio and Walsh, 1999). This might involve Akt-mediated phosphorylation of apoptotic proteins B-cell lymphoma 2 (Bcl-2)-associated death promoter (BAD) and caspase 9, which inhibits their apoptotic activities and thereby promotes cell survival (Brunet et al., 1999; Cardone et al., 1998).

5.4 Eph receptors and Ephrin ligands

5.4.1 General characteristic of Eph receptors and ephrin ligands

Structures and interactions Eph receptors (derived from erythropoietin-producing hepatocellular carcinoma cells from which their cDNAs was first cloned) represent the

largest family of RTKs. They are classified into two subclasses based on their extracellular sequence similarities and their binding affinities to thev two subclasses of their ligands. Thus far, ten A-class (EphA1-EphA10) and six B-class (EphB1-EphB6) of the receptors have been identified in vertebrates. The extracellular region of the Eph receptors consists of the ligand-binding globular domain, a cystein-rich region, and two fibronectin type-III repeats. The cytoplasmic part, containing the juxtamembrane region with two conserved tyrosine residues, a tyrosine-kinase domain, a sterile α-motif, and a PDZ (Postsynaptic density-95/discs large/zonula occludens-1)-binding motif, follows a single membrane spanning segment (Fig. 5-10). Their ligands, the ephrins (Eph receptor interacting proteins), are also divided into two subclasses. In vertebrates, six A-class (ephrinA1-ephrinA6) and three B-class Ephrins (ephrinB1-ephrinB3) are known to date. The two classes of ephrin ligands only share a similar extracellular Eph-receptor-binding domain. EphrinAs are tethered to the cell membrane by a glycosylphosphatidylinositol (GPI)-anchor. EphrinBs, on the other hand, are transmembrane proteins with a short cytoplasmic tail containing conserved tyrosine phosphorylation sites and a carboxy (C)-terminal PDZ-binding motif (Fig. 5-10) (Kullander and Klein, 2002; Pasquale, 2005).

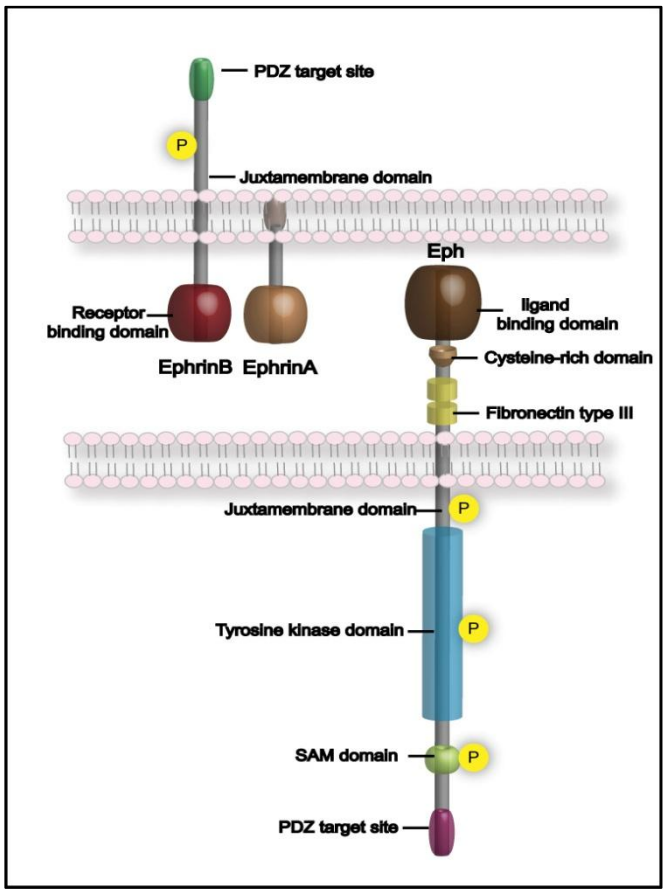

Figure 5-10 Eph receptors and ephrin ligands. Schemetic representation of structural organization of Ephs and ephrins. Yellow circles marked with P show region containing tyrosine phosphorylation sites.

Interactions between Eph receptors and ephrin ligands are promiscuous within each class. Although the binding affinities are varied among each couple, EphAs bind all ephrinAs

and EphB bind all ephrinBs. The exceptions to this class discrimination rule are ephrinA5, which can bind to EphB2 (Himanen et al., 2004) and EphA4, which binds to both classes of ephrins (Pasquale, 2004). Apart from the high affinity binding-interfaces, which is essential for initiation of receptor-ligand dimerization, regions that can mediate low-affinity homophilic binding have been identified in both Ephs and ephrins (Himanen and Nikolov, 2003; Pasquale, 2005). Aggregation of the Eph-ephrin complexes into high-order clusters is indeed a prerequisite for the induction of a robust signal transduction upon Eph-ephrin interactions (Pasquale, 2005). Signal strengths and outcomes of those signals are thought to rely heavily on the degree of clustering (Pasquale, 2008; Poliakov et al., 2004).

In addition to the formation of the “signaling cluster”, another unique characteristic of Eph-ephrin system that makes it standouts of all the RTKs is the ability to transduce the signal bidirectionally. Eph receptor “forward signaling” is mediated by either phosphorylation or association with various effector proteins. Ephrins, on the other hand, lack an intrinsic kinase activity and mediate their “reverse signaling” by recruitment of other kinases to the tyrosine phosphorylation sites as well as association of several effector molecules to the C-terminal PDZ-binding domain (Kullander and Klein, 2002).

Cis- vs trans-interaction Stimulation of the downstream signaling is best known to occur upon interaction of the Eph receptors and ephrin ligands on adjacent cells. Although there are some evidences of Ephs and ephrins interact in *cis* on the same cell surface, the functional relevance of *cis*-inteactions remains to be established. It has been reported that EphA3 and ephrinA5 co-expressed in axonal growth cone of retinal ganglion cells could interact in *cis*. Such interaction might prevent intercellular (*trans*) interaction and reduces Eph-mediated cellular responsiveness to ligands presented in *trans* (Carvalho et al., 2006; Egea and Klein, 2007). Ephs and their cognate ephrin ligands expressed in the same cells might not be able to interect *in cis* due their partitioning into separated membrane domains as demonstrated in the spinal cord motor neurons. EphA4 and ephrinA5 localized in different membrane domains of axonal growth cone do not interect and interestingly seem to mediate the opposite cellular response whereby EphA forward signaling induces repulsion and

ephrinA reverse signaling mediates attraction (Egea and Klein, 2007; Marquardt et al., 2005).

5.4.2 Eph forward signaling

Upon ligand engagement and subsequent formation of signaling clusters, each receptor undergoes trans-autophosphorylation by a partner receptor in the cluster (Kalo and Pasquale, 1999). It has been suggested that Eph receptors might as well be phosphorylated by Src-family kinases (Knoll and Drescher, 2004; Matsuoka et al., 2005; Pasquale, 2005). Phosphorylation of the two tyrosine residues within the juxtamembrane domain disrupts the intermolecular inhibitory interaction between the non-phosphorylated juxtamembrane domain and the kinase domain and thereby allows the kinase domain to convert into its fully active conformation (Wybenga-Groot et al., 2001; Zisch et al., 2000). Once activated, the receptors are able to interact with various adaptor molecules containing SH2 domains that often lack enzymatic activity and function as linkers that connect the receptors to further downstream signaling molecules (Kullander and Klein, 2002; Pawson and Scott, 1997). In addition, several interaction partners are recruited to the receptors independent of this autophosphorylation. These include several PDZ-domain-containing proteins as well as Rho-family guanine nucleotide-exchange factors (Rho-GEF) (fig. 5-11) (Noren and Pasquale, 2004).

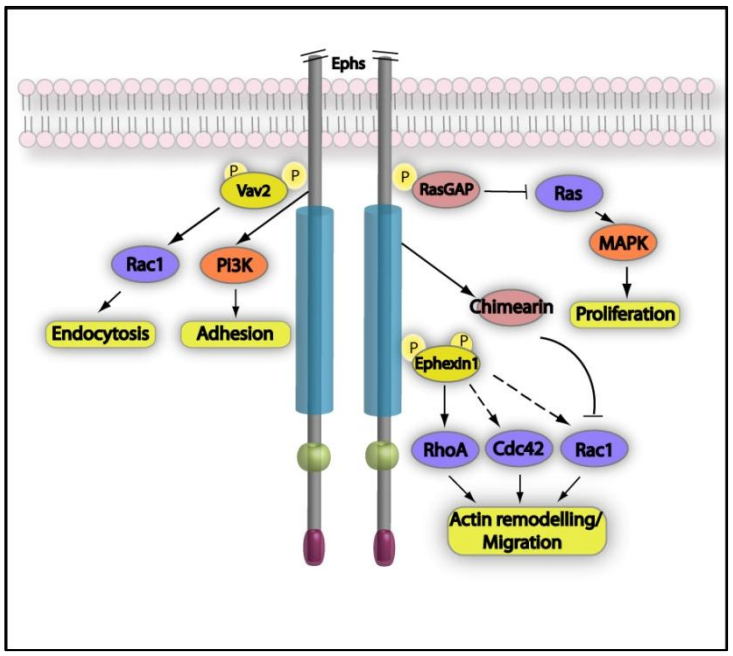

Figure 5-11 Eph receptor forward signaling. Schemetic representation of some of the signaling pathways triggered by Eph receptor activation. Blue cylinder, kinase domain; green circle, SAM domain; purple oval, PDZ-binding motif. Yellow circles marked with P represent phosphorylated tyrosines.

Among the broad ranges of diverse cellular activities mediated by signaling mechanisms downstream of Eph receptors, regulation of cell movements is probably the best characterized. Eph receptors are known to regulate cell movements by controlling the active state of Rho family GTPases that act directly at the actin rearrangement process (Noren and Pasquale, 2004). Activation of Rho GTPases is mediated by guanine nucleotide-exchange factors (GEFs) that promote the exchange of GDP for GTP. GTPase-activating proteins (GAPs), on the contrary, enhance the intrinsic GTPase activity of Rho proteins and thereby regulate their conversion to an inactive state (Heasman and Ridley, 2008; Rossman et al., 2005). Association of the Rho GEF ephexin 1 to unclustered (and thus non-phosphorylated) EphA is thought to activate Rac1, cdc42, and RhoA in parallel, leading to a balance of their GTPase activities required for axon outgrowth (Egea and Klein, 2007). Once Eph receptor is transphosphorylated, ephexin 1 recruited to the receptor is also phosphorylated, probably by Src (Knoll and Drescher, 2004), which shifts its preference toward RhoA leading to actin depolymerization and thereby growth cone retraction (Egea and Klein, 2007; Sahin et al., 2005). In addition to ephexin, the Rho GEF Vav2 has also been shown to play an important role in Eph-mediated growth cone retraction (Cowan et al., 2005). Vav2 seems to have a different mode of action as compared to ephexin 1. Firstly, Vav2 binds ephrin-activated Eph receptors of both classes in a phosphorylation-dependent manner. The tyrosine phosphorylation site at the juxtamembrane domain of Ephs and SH2 domain in Vav2 are required for this interaction. Once associated with Ephs, Vav2 becomes transiently phosphorylated to promote Rac1- dependent endocytosis of the Eph-ephrin complexes which leads the conversion of initial adhesion to repulsion during growth cone collapse (Cowan et al., 2005; Egea and Klein, 2007). Recently, a GAP specific for Rac1, α2-chimearin, has been identified as an EphA4 effector in the regulation of growth cone collapse and therefore essential for correct neuronal circuit formation (Beg et al., 2007; Iwasato et al., 2007; Shi et al., 2007; Wegmeyer et al., 2007). The adaptor protein Nck has been implicated as a linker for EphA4 and α2-chimearin interaction (Wegmeyer et al., 2007).

Other important molecular effectors such as PI3K and RasGAP are known to associate with Eph receptors and mediate a wide variety of cellular processes downstream

of the receptors including cell-matrix adhesion and mitogenesis (Kullander and Klein, 2002; Pasquale, 2008).

5.4.3 Ephrin reverse signaling

5.4.3.1 EphrinA reverse signaling

Although ephrinA-mediated signaling events have been implicated in several cellular activities, the mechanism by which these GPI-anchored proteins transduce their signals across the plasma membrane is poorly understood (Knoll and Drescher, 2002). EphrinAs have been proposed to interact in *cis* with other transmembrane proteins which therefore act as coreceptors to fulfill their signal transduction. There are increasing evidences in favor of this model including the ephrinA-mediated RGC axon repulsion during the development of thev retinotopic map through the p75 low-affinity nerve growth factor receptor (Lim et al., 2008). During the branching and synaptogenesis of these RGC axons the association of ephrinA and TrkB (Tropomycin-related kinase) B is required (Marler et al., 2008). Alternatively, Eph-stimulated ephrinA clusterings may possibly lead to changes in physical properties of lipid rafts in which ephrinAs are located and thereby cause the recruitment and activation of transmembrane proteins within the rafts (Davy et al., 1999).

5.4.3.2 EphrinB reverse signaling

EphrinBs can transduce their signals via their conserved tyrosine phosphorylation sites and the PDZ-binding motif on their cytoplasmic tails (fig. 5-12). EphB receptor binding and formation of the receptor-ligand clusters are likely to alter the ephrinB conformation in favor of the recruitment and phosphorylation of their tyrosine residues by Src family kinases (Palmer et al., 2002). Consequently, phosphorylated tyrosines of ephrinBs serve as docking sites for SH2-containing adaptor proteins. An example to this mode of action is the recruitment of Nck2 (also known as Grb4) to the EphB-stimulated phosphorylated ephrinB1 and activation of the signaling pathway that ultimately leads to changes in focal adhesion kinase (FAK) and the actin cytoskeleton (Cowan and Henkemeyer, 2001). Binding of Nck2 to ephrinBs, however, could potentially be mediated by the SH3 domain presented in Nck2 and its proline-rich binding site within the intracellular domain of ephrinBs. SH3-mediated

interaction of Nck2 to ephrinBs might allow the SH2 domain of Nck2 to recruit the G protein-coupled receptor kinase-interacting protein 1 (GIT1) to the signaling complex to promote spine maturation and synapse formation through the activation of the Rac GEF protein β-PIX (fig. 5-12) (Segura et al., 2007; Zhang et al., 2005). Protein tyrosine phosphatase BAS-like (PTP-BL), previously shown to bind to ephrinB by its PDZ motif (Lin et al., 1999), has been identified as a negative regulator of ephrinB tyrosine phosphorylation. PTP-BL is recruited to EphB-activated ephrins, with delayed kinetics as compared to their phosphorylation by Src, and dephosphorylates the tyrosine residues of ephrins (Palmer et al., 2002).

Several other PDZ motif-containing proteins have been shown to interact with ephrinBs. These include adaptor proteins that will recruit additional partners to the signaling complexes such as glutamate-receptor-interacting-proteins (GRIP) 1 and 2, and syntenin (Bruckner et al., 1999; Lin et al., 1999; Torres et al., 1998), or PDZ proteins with functional units like protein kinase C-interacting protein (Pick1), partitioning-defective protein 6 (PAR6), and PDZ-RGS3 (Lee et al., 2008; Lin et al., 1999; Lu et al., 2001; Torres et al., 1998). These interactions are essential for a wide variety of signal cascades involved in the modulation of cell-cell contacts (Lee et al., 2008), regulation of migratory signal of other receptors (Lu et al., 2001) as well as stabilization of other membrane proteins on the cell surface (Essmann et al., 2008). Association of ephrinB3 to PAR6 disrupts the binding of cdc42 to the ternary polarity complex of PAR6, PAR3, and atypical protein kinase

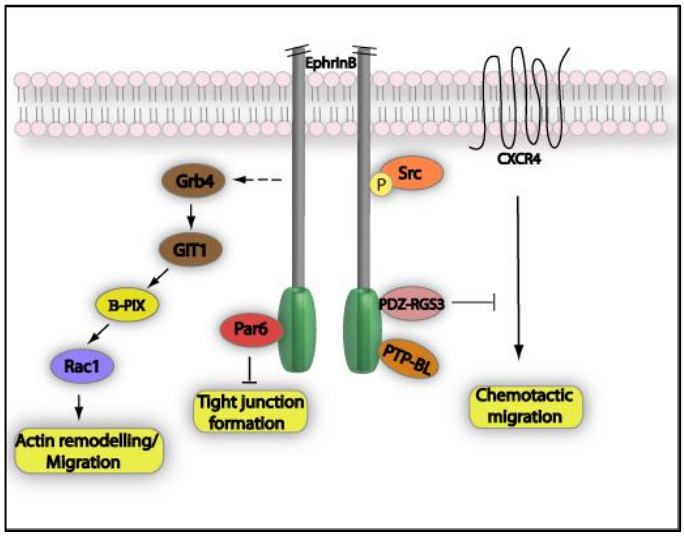

Figure 5-12 EphrinB reverse signaling. Schemetic representation of some signaling pathways mediated by recruitment of Src kinase to phosphorylate ephrinBs at specific tyrosines (yellow circle marked with P, one out of five conserved tyrosine phosphorylation sites is depicted here) and interactions of ephrinBs with PDZ proteins via the PDZ-binding site (green oval) at the end of their cytoplasmic tail.

C (aPKC) (Joberty et al., 2000; Lin et al., 2000) and thereby leads to inhibition of tight junction formation. Interestingly, phosphorylation of a certain tyrosine residue of ephrin results in loss of the ligand ability to interact with PAR6 (fig. 5-12) (Lee et al., 2008). Activation of ephrinB1 leads to recruitment of PDZ-RGS3 whose RGS domain acts as activator of intrinsic GTPase activity of the G protein α subunit (Gα) and therefore inactivates the GTP-bound form of the Gα and subsequent downstream signaling. This mode of action of ephrins has been shown to neutralize the G-protein coupled receptor CXCR4 attraction to the chemokine SDF1 during chemotactic cell migration in cerebral granular cells (fig. 5-12) (Lu et al., 2001).

5.4.4 Regulation of adhesion and repulsion

The complexity of the the Eph-ephrin signaling network is mirrored by a vast array of cellular effects. Regulation of cytoskeletal dynamics by both forward and reverse signal transduction through several downstream partners can lead to various outcomes ranging from repulsion to adhesion and attraction (Cowan and Henkemeyer, 2002; Pasquale, 2005). An apparent explanation to these diverse cellular responses is the distinct expression profiles of the receptors and ligands themselves as well as their downstream effectors in different cellular contexts. In certain settings, however, the same receptor and ligand couple could mediate both attractive and repulsive responses as demonstrated in the process of neural crest migration and axon outgrowth (Hansen et al., 2004; McLaughlin et al., 2003; Santiago and Erickson, 2002). Signaling strength, depending on levels of receptor and ligand expression and possibly degrees of their clustering, may contribute to these variable signaling outcomes (Pasquale, 2005; Poliakov et al., 2004; Stein et al., 1998).

Cleavage of ephrin ectodomain by the A-Disintegrin-And-Metalloprotease (ADAM) 10, the mammalian homolog of *Drosophila* Kuzbanian (KUZ), has been proposed as a possible molecular switch between adhesion and repulsion. KUZ was shown to associate with ephrinA2 and, upon complex formation with EphA3, mediate ephrin cleavage in *cis* to release the ligand from the cell surface and permit segregation of contacted cells. (Hattori et al., 2000). More recently, a different model whereby ADAM10 constitutively associated with EphA3 mediates *trans* cleavage of ephrinA5 presented on the surface of opposing cells

(Janes et al., 2005) has been proposed. Nonetheless, evidence supporting the existence of this non-cell-autonomous operation of ADAM10 in physiological setting is still missing.

Endocytosis of Eph-ephrin complexes might be an alternative mechanism for conversion of adhesive interaction to a repulsive signal. Interestingly, the endocytosed vesicles observed in both EphB and ephrinB expressing cells upon cell-cell interaction contain intact receptor-ligand complexes and plasma membrane fragments from both cells (Marston et al., 2003; Zimmer et al., 2003). This unusual mechanism is thought to imply a functional relevance in the exchange of Eph receptors, ephrin ligands, and possibly their associated proteins between cells for continued signaling in the intracellular compartments (Pasquale, 2008).

5.4.5 Eph-ephrin in vascular morphogenesis

Arterial-venous segregation Several Ephs and ephrins are expressed in the vascular system. Interestingly, EphB4 and its most preferred ligand ephrinB2 are differentially expressed in venous and arterial ECs, respectively. A Number of molecular regulators in the Notch and VEGFR signaling pathways, as well as hemodynamic factors have been shown to mediate this distinct expression pattern (see 5.1.4). Functional relevance of this arteriovenous-specific expression pattern has started to be revealed. In zebrafish, dorsal aorta and cardinal vein has recently been demonstrated to arise from a common precursor vessel rather than direct assembly of endothelial precursor cells into two independent vessels by vasculogenesis as previously thought. Venous-fated progenitors preferentially expressing EphB4 migrate ventrally from the common precursor vessel to form the cardinal vein, whereas ephrinB2 prominently expressed in the arterial-fated cells mediates repulsion of these cells from the ventral route to establish the dorsal aorta. EphrinB2ΔC (signaling deficient form) overexpressing cells transplanted into wild type zebrafish hosts show significant increased contribution to the cardinal vein, indicating that reverse signaling downstream of ephrinB2 is required for cellular repulsion during the ventral migration. Conversely, cells overexpressing ephrinB2 largely contributed to intersomitic vessels that sprout dorsally from the dorsal aorta, suggesting an increased repulsion of arterial

progenitors from the EphB4-presenting venous cells by elevated ephrinB2 signaling (Herbert et al., 2009).

Angiogenic remodeling Target deletion of the gene encoding ephrinB2 or EphB4 in mice clearly demonstrates the crucial requirement of these proteins in angiogenic remodeling. While the formation of primary plexus and dorsal aorta, occurred via vasculogenic assembly of endothelial precursor cells, appears to be normal, further development of these uniformed primitive vessels into the hierarchically organized network of functional vascular system through angiogenesis is severely defected. These defects lead to embryonic lethality in mice lacking either ephrinB2 or EphB4 (Adams et al., 1999; Gerety et al., 1999; Wang et al., 1998). Endothelial-cell-specific knockout (Gerety and Anderson, 2002) as well as a mutant lacking the cytoplasmic domain of ephrinB2 (ephrinB2ΔC) (Adams et al., 2001) recapitulate the vascular phenotypes of the ephrinB2 global knockout, suggesting the essential function of ephrinB2 reverse signaling in ECs.

Despite strong evidences that verify the essential functions of both ephrinB2 and EphB4 in blood vessel development, little is known about their molecular mechanisms. Stimulation of ECs with soluble pre-clustered ephrinB ligands or EphB receptors shows that both forward and reverse signaling promote *in vitro* angiogenic sprouting (Adams et al., 1999; Palmer et al., 2002). Activation of ephrinB1 reverse signaling has been shown to promote integrin-mediated EC attachment and migration and induce mouse corneal neovascularization (Huynh-Do et al., 2002). However, contradictory results on the inhibitory effects of EphB4 forward signaling in EC migration and proliferation have also been reported (Fuller et al., 2003; Hamada et al., 2003; Kim et al., 2002). A possible explanation for this might be the difference in concentration or clustering of soluble Ephs and ephrins (Kuijper et al., 2007). It has been shown that non-clustered forms of soluble Eph and ephrins are rather inhibitory than activating (Segura et al., 2007).

Mural cell recruitment Beside the vascular endothelium, ephrinB2 is expressed also in perivascular cells such as pericytes and vascular smooth muscle cells (Gale et al., 2001; Shin et al., 2001). Its functional relevance in these mural cells that provide structural stability

and elasticity to the vessel wall has been revealed through the conditional gene targeting approach to disrupt its expression selectively in these cells. Mural-cell-specific ephrinB2 knockout mice display perinatal lethality, edema, and extensive skin hemorrhage due to the inability of mural cells to appropriately incorporate into the blood vessel wall (Foo et al., 2006). *In vitro*, loss of ephrinB2 causes defective focal adhesion formation and cell spreading, and increased unpolarized motility of vascular smooth muscle cells. These effects have been proposed to be mediated by the Crk-family adaptor proteins and p130 Crk-associated substrate (CAS). Crk and CAS form complexes upon integrin activation and recruit several effector molecules to their SH2 domains to modulate actin dynamics through Rac1 activation (Chodniewicz and Klemke, 2004). EphrinB2 seems to be required for the tyrosine phosphorylation of CAS and thereby enable Crk-CAS binding (Foo et al., 2006).

Lymphatic development In newborn mice, the primitive plexus of the dermal lymphatic vessels expressing both ephrinB2 and EphB4 are actively remodeled by angiogenic sprouting that invade upper dermal layer to form a superficial capillary plexus. After the formation of the two vessel layers, the expression of ephrinB2 is only maintained in the valve-containing collecting lymphatic vessels, whereas EphB4 is detected throughout the lymphatic network (Makinen et al., 2005). The generation of two ephrinB2 signaling mutant mice lacking either the PDZ-binding motif (ephrinB2ΔV) or all the five conserved tyrosine residues (ephrinB25Y) has uncovered the critical role of the ligand in lymphatic vasculature remodeling. Homozygous ephrinB2ΔV mice die during the first postnatal week. While the initial formation of primitive plexus is unaffected, loss of PDZ-binding motif disturbs sprouting of lymphatic ECs and thus subsequent formation of superficial capillary networks. Collective lymphatic vessels of this mutant are devoid of valves. By contrast, ephrinB25Y mice display normal to very mild lymphatic phenotype, suggesting the requirement of PDZ interaction independent of tyrosine phosphorylation of ephrinB2 for the normal development of lymphatic vasculatures (Makinen et al., 2005).

Tumor angiogenesis Several Ephs and ephrins have been reported to be upregulated during tumor progression. Elevated levels of EphA2 expressed in active angiogenic tumor

vessels and its ligand ephrinA1 present in tumor cells as well as tumor endothelium has been linked to growth of many cancers (Brantley-Sieders and Chen, 2004; Ozawa et al., 2005; Pasquale, 2008). Knockout of EphA2 in mice or blocking EphA receptor activation with soluble recombinant proteins reduce tumor vascularization and thereby inhibit xenograft tumor growth (Brantley-Sieders and Chen, 2004; Fang et al., 2005; Kuijper et al., 2007). Truncated form of EphB4 lacking the cytoplasmic domain (EphB4ΔC) overexpressed in a breast cancer cell line could promote tumor growth associated with increased tumor vascularization, most likely via the activation of endothelium ephrinB2, in a xenograft model (Noren et al., 2004). However, it has also been reported that EphB4 might suppress angiogenic sprouting and therefore reduce branching, but enhance circumferential growth of blood vessels in brain tumors (Erber et al., 2006). These evidences together provide credible implication on the importance of Eph-ephrin signaling in tumor-induced neovascularization and tumor growth. Nevertheless, the exact biological role of Ephs and ephrins in tumors is unclear. The relevance of their interactions in the communication between tumor cells and ECs, the molecular mechanisms of their downstream signaling pathways, and the distinct cellular behaviors induced upon their signaling in specific cell types, all remain to be clarified to give access to therapeutic opportunities based on Ephs and ephrins targeting.

5.5 Receptor endocytosis

Diverse array of molecules are internalized from the cell surface and sorted into various internal membrane compartments via different endocytic pathways. Distinct molecular machineries are employed to mediate the common process of cargo selection, membrane budding and pinching off to form vesicular carriers, and subsequent trafficking of these vesicles to their targets. The best-characterized pathway is clathrin-mediated endocytosis (Fig. 5-13), which is responsible for internalization of virtually every signaling receptor and their associated ligands (Sorkin and von Zastrow, 2009). The key component of this pathway is the triskelion molecule clathrin which is able to assemble into a polyhedral lattice at the plasma membrane and function as a scaffold for membrane invagination (Conner and Schmid, 2003). Molecules destined to be endocytosed are recruited to the

clathrin-coated pits by interacting with adaptor molecules such as adaptor protein-2 (AP2) that binds directly to cargo proteins containing tyrosine or di-leucine-based motifs (Le Roy and Wrana, 2005). Other adaptors such as Epsin, its partner protein Epidermal growth factor receptor (EGFR)-pathway substrate-15 (EPS15), and Dishevelled (Dvl) have also been shown to facilitate endocytic complex assembly (Brett and Traub, 2006; Marmor and Yarden, 2004; Sorkin and von Zastrow, 2009; Yu et al., 2007). Ubiquitylation has been proposed to serve as targeting signal that directs ubiquitylated cargos into clathrin-coated pits as shown in the endocytosis process of several signaling receptors (Arevalo et al., 2006; Gupta-Rossi et al., 2004; Kazazic et al., 2009). Ubiquitin interaction motifs (UIM) that are presented in Epsin and EPS15 might mediate the binding of these adaptor proteins to ubiquitylated cargos (Sorkin and von Zastrow, 2009; Traub and Lukacs, 2007). In addition, interaction of epsin with phospholipids

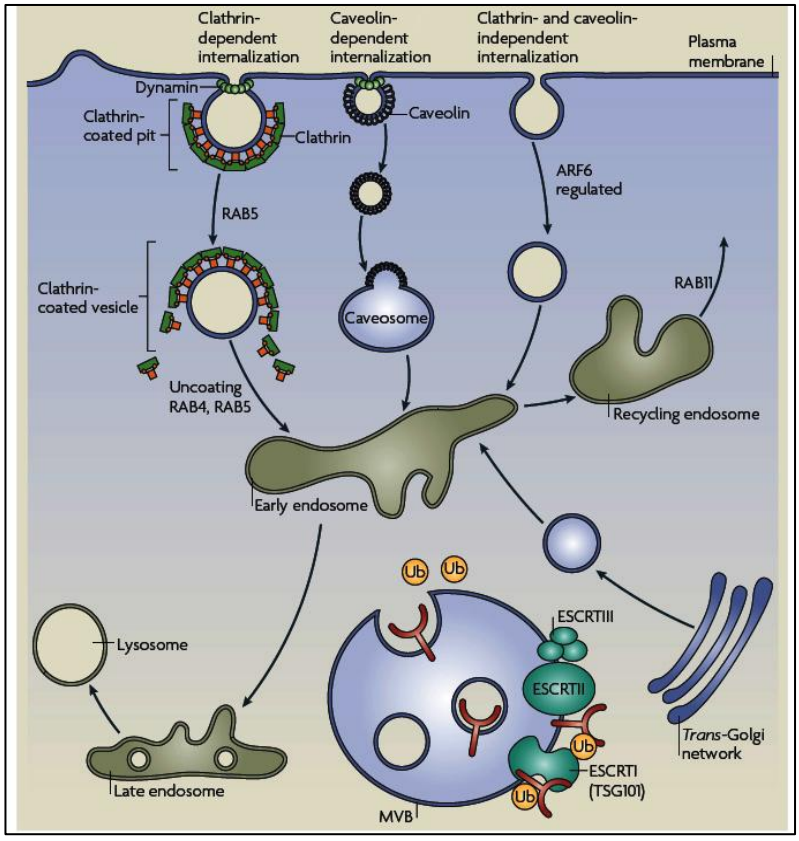

Figure 5-13 Endocytosis pathways. Surface receptors and other extracellular molecules are internalized intracellularly via several routes into early endosomes. Cargo can be rapidly recycled back to the plasma membrane in a Rab11-comtaining endosomal compartment or remained in the early endosomes that matured into late endosome and multivesicular body (MVB). Cargo destined for degration is sorted into intraluminal vesicle of MVB in a process that required ubiquitilation (Ub, Ubiquitin) and endosomal sorting complex required for transport (ESCRT). Further fusion of lysosome to MVB and late endosome results in protelytic degration of cargo. Model is reproduced from Gould and Lippincott-Schwartz, 2009.

such as phosphatidylinositol (PtdIns)-4,5-bisphosphate may also contribute to vesicle formation (Legendre-Guillemin et al., 2004). Once cargos are captured inside, the GTPase dynamin mediates the scission of the clathrin-coated pits from the cell membrane to form clathrin-coated vesicles (Sorkin and von Zastrow, 2009).

Although alternative routes of endocytosis that does not depend on clathrin have been shown to play an important role in the uptake of GPI-anchored proteins, toxins, pathogens, as well as some transmembrane proteins, the molecular nature of these pathway is largely unknown (Mayor and Pagano, 2007; Sigismund et al., 2008). These clathrin-independent endocytic routes are sensitive to cholesterol depletion. The enrichment of cholesterol in membrane rafts together with the observations that lipid rafts are depleted within clathrin-coated pits lead to the idea that these pathways are raft-dependent (Le Roy and Wrana, 2005; Nichols, 2003a; Nichols, 2003b). One of the clathrin-independent endocytosis pathways is characterized by the presence of caveolae, the plasma membrane invagination enriched in raft lipids (Fig. 5-13) (Rothberg et al., 1992). The raft-resident protein caveolin seems to be important for the formation of caveolae (Drab et al., 2001). A distinct mechanism which does not required clathrin, caveolin, or dynamin, but probably involve activities of the GTPase ARF6, a mediator of actin remodelling and phosphatidylinositol 4,5-bisphosphate formation, has also been described (Fig. 5-13) (D'Souza-Schorey and Chavrier, 2006; Naslavsky et al., 2004).

Endocytic vesicles derived from clathrin-dependent and clathrin-independent pathways are transported to early endosomes from where endocytosed proteins are further sorted into lysosomes for degradation or recycled back to the plasma membrane. Several GTPases of the Ras superfamily, Rab proteins, localized in distinct compartments of endosomes are known regulator of endosomal trafficking. Internalized proteins in Rab5-positive early endosomes can be directed to Rab11-positive recycling endosomes in a Rab4-dependent mechanism (Sorkin and von Zastrow, 2009). Proteins destined for degradation in lysosomes are kept in the endosomes that subsequently will mature to multivesicular bodies, where the endosomal sorting complex required for transport (ESCRT) mediates their sorting into intraluminal vesicles (Fig. 5-13) (Hurley and Emr, 2006; Le Roy and Wrana, 2005).

5.5.1 Endocytosis in control of signaling

It has become increasingly evident that endocytosis is not only a signal attenuation mechanism used by cells to remove signaling receptors from cell surface, but also an integral part of signaling that permits spatial and temporal regulation of signaling events. A cellular process that critically relies on strictly-regulated signal polarization is guided migration of cells or cellular extensions in response to extracellular cues. During *Drosophila* oogenesis border cells are guided by two RTKs, EGFR (Epidermal growth factor receptor) and PVR (PDGF/VEGF receptor) and migrate toward oocytes where their ligands are produced (Duchek and Rorth, 2001; Duchek et al., 2001). Endocytosis and recycling of these RTKs to the cell membrane are essential for spatial restriction of their downstream signaling and thereby ensure a localized cellular response required for directional migration of these cells (Jekely et al., 2005). In line with this finding, activation by RTKs of the pivotal regulator of actin remodeling and cell migration Rac requires Rab5-mediated clathrin-dependent endocytosis of Rac. Induced by mitogenic stimuli, Rac is endocytosed and transported to early endosomes where it becomes activated by the RacGEF Tiam1 (T-cell lymphoma invasion and metastasis 1). Subsequent recycling of activated Rac to specific regions of the plasma membrane ensures localized signaling which is required for the formation of polarized actin-based cellular protrusions that direct cell motility (Gould and Lippincott-Schwartz, 2009; Palamidessi et al., 2008). Similarly, regulation of melanoma cell polarity and directional movement by Wnt signaling requires internalization and intracellular translocation of the melanoma cell adhesion molecule (MCAM). In the presence of chemokine gradient, Wnt5A mediates intracellular assembly of membrane receptors MCAM and frizzled 3 (a Wnt receptor) with cytoskeletal proteins actin and myosin at the cell periphery in a polarized manner. This process is dependent on the endosomal recycling protein Rab4 and functions to trigger membrane retraction, thus influence direction of cell movement (Gould and Lippincott-Schwartz, 2009; Witze et al., 2008).

The mitogenic and survival signals mediated via MAPK/ERK downstream of different RTKs have been shown to depend on functional receptor endocytosis. Clathrin-mediated endocytosis of VEGFR2 is important for the activation of p44/42 MAPK and proliferation of ECs. Contact-mediated inhibition of the receptor internalization by the adheren junction

protein VE-Cadherin might allows dephosphorylation of the receptor by the junction-accociated phosphatase DEP-1 (density-enhanced phosphatase-1) and limit the receptor signaling (Lampugnani et al., 2006). Correspondingly, compelling evidences indicate the important role of clathrin-dependent endocytosis of EGFR to ensure the sufficient duration and signaling intensity of MAPK/ERK activation (Sigismund et al., 2008; Sorkin and von Zastrow, 2009; Vieira et al., 1996). In neurons, neurotrophins produced by post-synaptic cells activate the receptor TrkA expressed in the pre-synaptic axonal termini which results in endocytosis and transport of the activated TrkA along axonal microtubule network to the cell bodies where ERK5 activated by the receptor translocates into the nucleus to promote cell survival (Deinhardt et al., 2006; Howe et al., 2001; Watson et al., 2001; Wu et al., 2007). In addition to the signaling pathways mentioned here, endocytosis has also been shown to regulate different signaling cascades downstream of RTKs such as PI3K/Akt as well as several other receptor systems including transforming growth factor β receptors (TGFβ), G protein-coupled receptors (GPCR), and tumor necrosis factor receptor (TNFR) (Sorkin and von Zastrow, 2009).

5.6 The thesis project

Previous works have clearly demonstrated that ephrinB2 and its cognate receptor EphB4 are indispensable for appropriate development of the vascular system. Analysis of mutant mice lacking ephrinB2 or EphB4 showed that loss of either gene does not affect vasculogenesis since the formation of primitive plexus of uniformed vessels at the earlier stage of development appeared normal. However, further expansion and remodeling of the primary vessels to achieve the complex hierarchical functional vascular networks by angiogenesis in both mutant mice is almost completely diminished. Further molecular insights come from the analysis of mutant mice in which the cytoplasmic tail of ephrinB2 is removed (ephrinB2ΔC). Defects in vascular development of the ephrinB2 signaling-deficient mice that resemble the complete knockout of ephrinB2 indicate the importance of reverse signaling downstream of ephrinB2 for its vascular function. Two signaling mutant mice, ephrinB25Y in which all five conserved tyrosine residues of ephrinB2 were mutated and ephrinB2ΔV with deletion of the PDZ-binding motif at the end of its cytoplasmic tail, have

been generated. While defective lymphangenesis found in ephrinB2ΔV but not ephrinB25Y mice suggests the importance of PDZ interaction downstream of ephrinB2 in this process, the implication of this pathway in the development of blood vasculature is still unclear.

The project presented in this dissertation was therefore set out to elucidate the unanswered questions, namely the exact role of ephrinB2 in the multifaceted development of the blood vasculature and the precise molecular mechanisms underlying ephrinB2 function. By employing the mouse retina model, this work identified the process of endothelial tip cell filopodial extension during guided migration of growing retinal vessels along the astrocyte network to be regulated by ephrinB2 through its PDZ-dependent signaling. The molecular linkage between ephrinB2 and the pivotal angiogenesis regulator VEGFR2, demonstrated for the first time in this study, provides a mechanistic insight of how ephrinB2 might accomplish this task. The novel finding that ephrinB2 regulates VEGFR2 endocytosis which thereby allow sustained signaling downstream of VEGFR2 in intracellular compartments, implies a possible mechanism that endothelial tip cells might use to ensure spatial resolution of the receptor signaling required for localized control of actin dynamics during the directional migration of developing blood vessel. Angiogenesis is an essential process for tumor growth and metastasis. Another aim of this study was thus to address the importance of ephrinB2 in progression of tumors. This led to the finding that tumor-induced angiogenesis and consequently tumor growth rely on PDZ-interaction downstream of ephrinB2, resembling the mechanism governing developmental angiogenesis. This uncovered role of ephrinB2 might provide an alternative for anti-angiogenic treatment in tumor therapy.

6. Results

6.1. EphrinB2 PDZ-signaling controls endothelial tip cell filopodial extension during sprouting angiogenesis

In order to study the role of ephrinB2 reverse signaling in angiogenesis *in vivo*, two different signaling mutant mouse lines were employed. The tyrosine phosphorylation-deficient *ephrinB2*$^{5Y/5Y}$ mice bearing targeted mutation of all five conserved tyrosine residues, whereas the PDZ-signaling-deficient *ephrinB2*$^{\Delta V/\Delta V}$ mice lacking a C-terminal valine residue within the PDZ-interaction site, have been generated as previously described (Makinen et al., 2005). The latter showed impairment of lymphatic vasculature remodeling (Makinen et al., 2005). The development of the vascular system of these two signaling mouse mutants was analyzed in the retina model where the growth of the vasculature tree occurs exclusively by angiogenic sprouting in a highly reproducible pattern (Dorrell and Friedlander, 2006).

6.1.1. EphrinB2 reverse signaling through PDZ-interaction is indispensable for developmental angiogenesis

During the first postnatal week the retinal vasculature sprouts from the optic nerve head along the astrocytic scaffold toward the non-vascularized hypoxic area. A superficial vascular network forms in one plane and later on sprouts toward the deeper layers of the retina to form intermediate and deep vascular plexus. To visualize superficial vascular plexus whole-mounted retinas were stained with FITC conjugated lectin from *Bandeiraea simplicifolia.* Analysis of the retina vasculatures of newborn mice in C57Bl/6 background revealed that in homozygous *ephrinB2*$^{\Delta V/\Delta V}$ (eB2ΔV/ΔV) mice the extension of the superficial retinal vascular plexus was severely impaired compared with wild type littermates (control) (Fig. 6-1). The significantly reduced migration of endothelial cells toward the retinal periphery, assessed by radial length of the vascular bed (Fig. 6-1a, c), as well as lateral branching (Fig. 6-1b), ultimately resulted in a great reduction in the retinal blood vasculature density of the *ephrinB2*$^{\Delta V/\Delta V}$ mice (Fig. 6-1d).

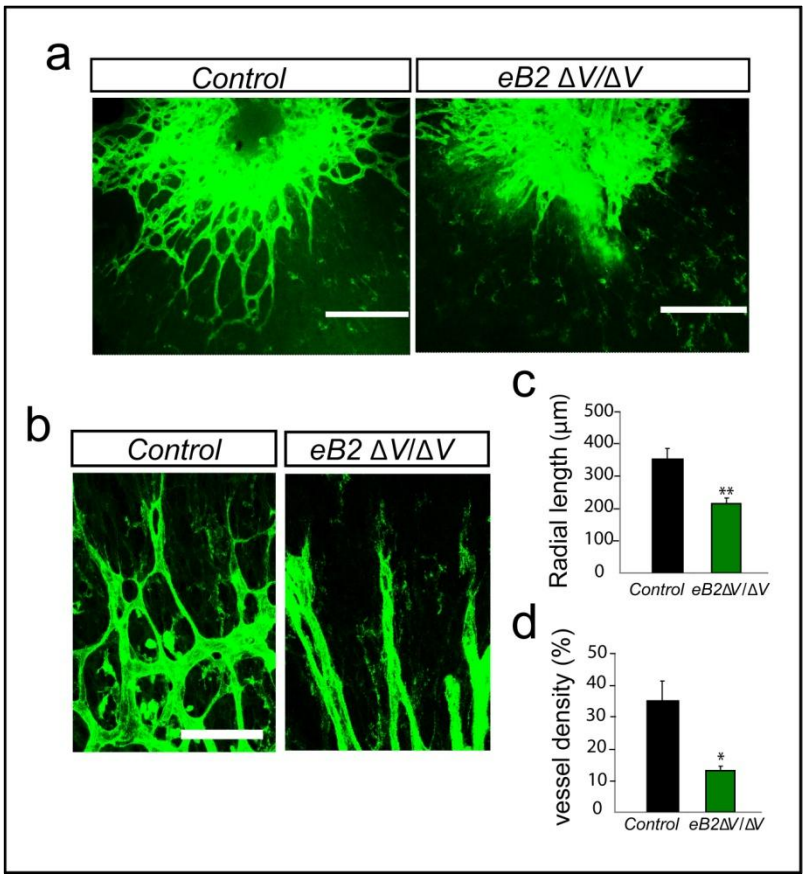

Figure 6-1 EphrinB2 PDZ interactions are required for expansion of superficial retinal vasculature in new born mice. Retinas from C57/BL6 wild type (control), and *ephrinB2*$^{\Delta V/\Delta V}$ mutant (eB2 ΔV/ΔV) mice were stained with isolectin-B4, flat-mounted and visualized by confocal microscopy. Removal of the PDZ-interaction domain (eB2 ΔV/ΔV) results in impairment of angiogenic sprouting and formation of primitive capillary plexus as observed in the expansion of the vascular bed shown in P1 retinas, **a**, and vascular branching as shown in the closed up image at the sprouting front of P2 retinas, **b**. Scale bars: 150 µm (**a**) and 75 µm (**b**). **c**, Quantification of the extension of the capillary bed based on the radial length from the optic nerve to the periphery *ephrinB2*$^{\Delta V/\Delta V}$ mutant retinas (eB2 ΔV/ΔV). **d**, Vessel density quantified as percentage of retina area covered with vessels was, in average, 35.21±6.17% and 13.11±1.38% in wild type and mutant retinas, repectively. Error bars represent standard error of the means (SEM). Statistical analysis was performed by two-tailed t-test, n=4 wild type and 4 *ephrinB2*$^{\Delta V/\Delta V}$ mice, * P< 0.05, ** P < 0.01.

Due to early postnatal lethality of *ephrinB2*$^{\Delta V/\Delta V}$ mice in the C57Bl/6 background, detailed analysis of retina vessels at later developmental stages was done in CD1 mice that survived the requirement of ephrinB2 PDZ-dependent signaling during development and showed normal fertility. At postnatal day (P) 7 when the leading front of the vascular bed is about to reach the retinal periphery and the morphology of arteries and veins is clearly distinguishable, analysis of the vasculature in arterial zones revealed 25-27% decrease in branching and density of the vascular bed in *ephrinB2*$^{\Delta V/\Delta V}$ mice compared with wild type littermates (Fig. 6-2a, b, c). Likewise, formation of vascular sprouts quantified by the number of filopodia bursts within the developing vascular plexus was significantly reduced in the *ephrinB2*$^{\Delta V/\Delta V}$ mutant mice (Fig. 6-2d).

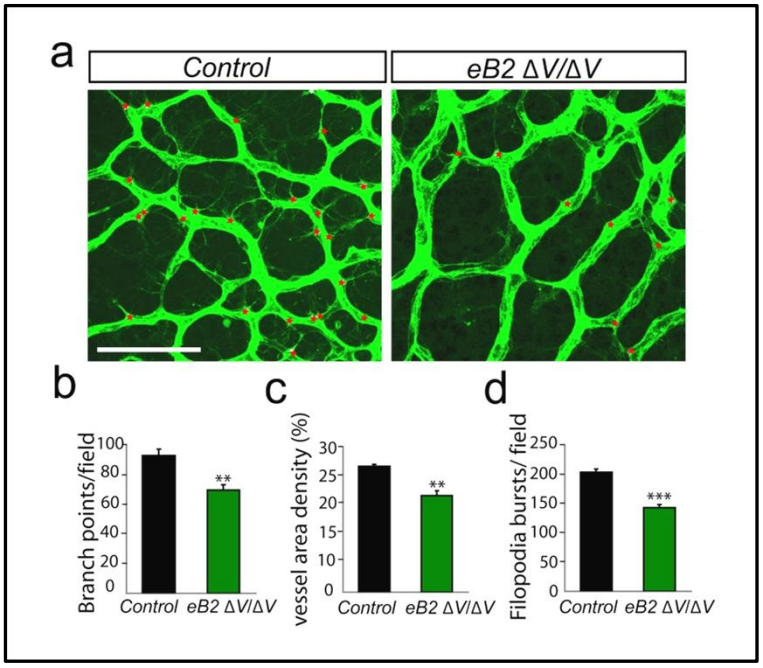

Figure 6-2 Vascular branching and formation of vascular sprouts are impaired in absence of ephrinB2 PDZ-dependent signaling. a, Decreased vessel branching and tip cell sprouting (tip cells are indicated by red asterisks) in *ephrinB2*$^{\Delta V/\Delta V}$ mice (eB2 ΔV/ΔV) compared with wild type littermates (control) in CD1 background was observed in P7 retinas. Scale bar is 75 µm. **b**, Quantification of vessel branching showed a significant decrease from an average of 92.84±4.36 to 69.39±3.60 branch points per 0.1 mm^2 microscopic field in wild type and *ephrinB2*$^{\Delta V/\Delta V}$ retinas, respectively. **c**, Vessel density measured as percentage of retina area covered with vessels in wild type retinas was 26.03±0.36% in average as compared with 19.92±1.05% in the mutant retinas. **d**, Defective vascular sprouting activity of *ephrinB2*$^{\Delta V/\Delta V}$ mice was evidenced from the reduction in number of filopodial bursts counted at 193.41±5.20 and 155.03±5.5 per 0.1 mm^2 microscopic field on average in wild type and *ephrinB2*$^{\Delta V/\Delta V}$ mutant retinas, respectively. Error bars represent SEM. Two-tailed t-test, n=4 wild type and 4 *ephrinB2*$^{\Delta V/\Delta V}$ mice, * P< 0.05, ** P < 0.01, *** P < 0.001.

To further verify that the vascular phenotypes observed in ephrinB2$^{\Delta V/\Delta V}$ mice are not transient and could be caught up during later stages of development, retinal vasculature in adult mice (12-15 weeks old) was analyzed. Vessels were labeled with cardiac injection of high-molecular weight FITC-dextran and vascular density was assessed in the deep retinal layer. Similar reduction in the density of the vasculature in the deep plexus of adult *ephrinB2*$^{\Delta V/\Delta V}$ mice compared with wild type littermates (Fig. 6-3) confirmed that the phenotypes observed in these mice during the first postnatal week are not due to a delay in vascular development.

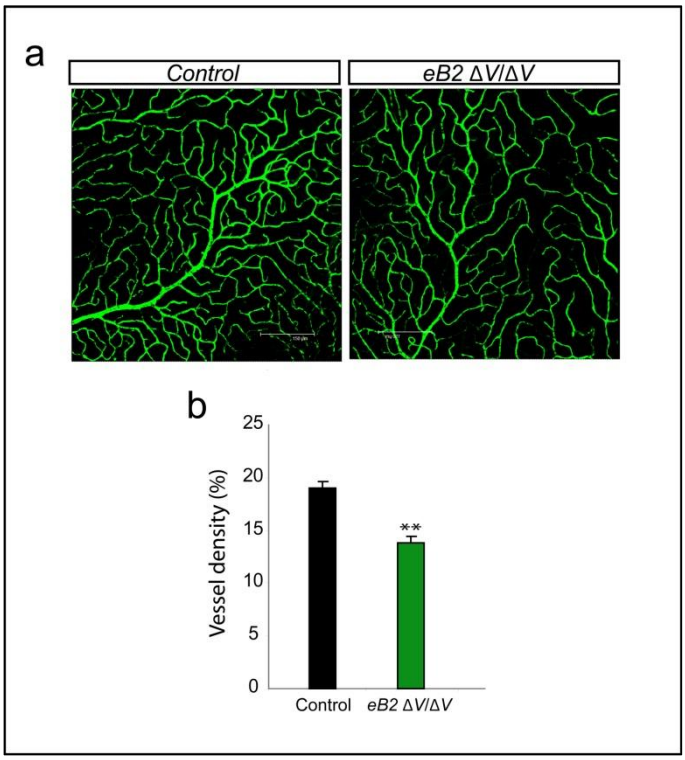

Figure 6-3 The vascular phenotypes caused by loss of ephrinB2 PDZ-interactions are persisted in adult mice. a, Following perfusion with FITC-dextran, retinas from adult *ephrinB2*$^{\Delta V/\Delta V}$ (eB2 ΔV/ΔV) mice and wild type littermates (control) were flat-mounted and vascularization in the deep retinal plexus was analyzed by confocal microscopy. Scale bar is 150 µm. **b**, Vascular density based on percentage of retina area covered with vessels was measured 13.78±0.68% in *ephrinB2*$^{\Delta V/\Delta V}$ retinas and 19.02±0.61% in wild type retinas. Error bar represents SEM, Two-tailed t-test, n=3 wild type and 3 *ephrinB2*$^{\Delta V/\Delta V}$ mice, ** P< 0.01.

6.1.2. Angiogenic growth of blood vessels is unaffected in the absence of ephrinB2 tyrosine phosphorylation

In contrast to the disruption of PDZ-dependent signaling downstream of ephrinB2, impairment of ephrinB2 tysosine phosphorylation has no apparent effect on retinal vasculature development. Expansion of the superficial vascular plexus observed in newborn *ephrinB2*$^{5Y/5Y}$ homozygous mutant mice in C57Bl/6 background appeared normal compared with control wild type littermates (Fig. 6-4a). These mice are also viable and fertile. Detailed analysis of the developing vessels at the age of P7 in CD1 background showed the undistinguished vessel branching, density of vascular bed, as well as formation of new vessel sprouts in homologous *ephrinB2*$^{5Y/5Y}$ mice compared with wild type littermates (Fig. 6-4b, c, d, e).

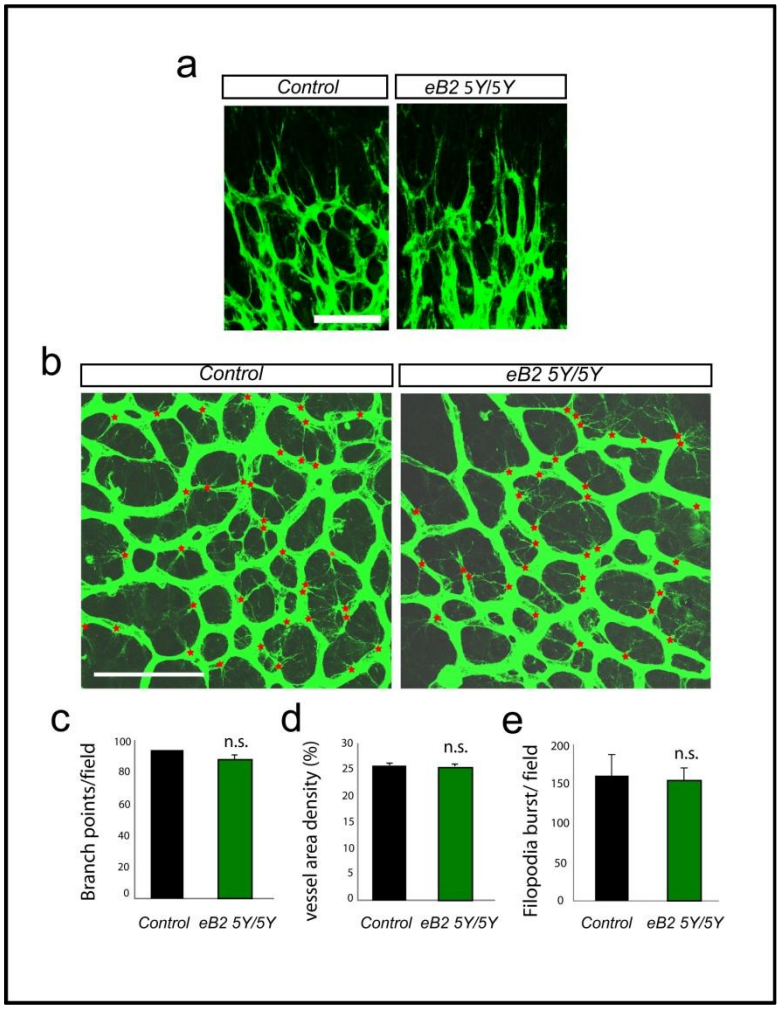

Figure 6-4 EphrinB2 phosphotyrosine dependent signaling is dispensable for *in vivo* retinal angiogenesis. **a**, Extension of superficial retinal vascular network of P2 *ephrinB2*$^{5Y/5Y}$ mice (eB2 5Y/5Y) in C57Bl/6 background was indistinguishable from wild type littermates (control). **b**, Vessel branching and tip cell sprouting (tip cells are indicated by red asterisks) in the developing retinal vasculatures of P7 *ephrinB2*$^{5Y/5Y}$ mutants in CD1 background were unaffected. Scale bar is 75 µm in both **a** and **c**. **c,** Vessel branching quantified by number of branch points per 0.1 mm^2 microscopic field was not significantly different between wild type (95.08±4.10) and *ephrinB2*$^{5Y/5Y}$ (92.84±4.36) mutant retinas. **d**, Similar vessel density, assessed by percentage of retina area covered with vessels, was observed in wild type (25.67±0.27%) and *ephrinB2*$^{5Y/5Y}$ mice (25.26±0.34%). **e**, Number of filopodia bursts within the vascular bed was counted, on average, 160.44±26.83 and 154.17±15.91 per 0.1 mm^2 microscopic field in wild type and *ephrinB2*$^{5Y/5Y}$ mice, respectively, reflecting unaltered sprouting activity of the mutant vessels. Two-tailed t-test, n=3 wild type mice and 3 *ephrinB2*$^{5Y/5Y}$ mice, n.s. not significant.

Together, these results indicate the crucial role of ephrinB2 reverse signaling through PDZ-interactions, which is independent of its tysosine phosphorylation, in angiogenic sprouting of the retinal blood vasculature.

6.1.3. The requirement of ephrinB2 PDZ-signaling in angiogenic growth of blood vessels is widespread throughout the central nervous system

During development, the vasculature of the central nervous system develops exclusively via angiogenesis as opposed to *de novo* vasculogenesis taking place in several other tissues. In addition to the retinas, different vascular beds within several regions of the *ephrinB2*$\Delta V/\Delta V$ mutant brains were examined. In agreement with the importance of ephrinB2 PDZ-dependent signaling in angiogenic sprouting of the retinal vasculatures, pronounced vascularization defects were observed in the cortex, thalamus, and striatum of adult *ephrinB2*$\Delta V/\Delta V$ mutants with a general reduction in vessel density of 20-30% compared with wild type littermates (Fig. 6-5). This observation implies that ephrinB2 via its PDZ signaling may represent a general regulator of sprouting angiogenesis.

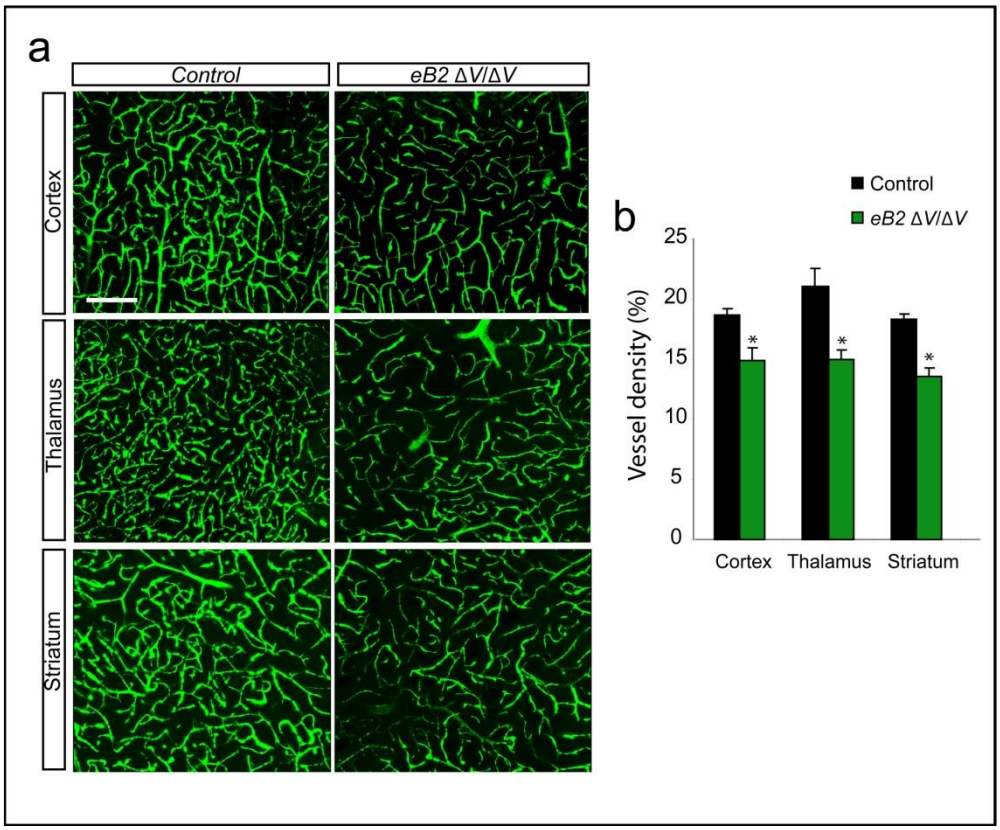

Figure 6-5 *EphrinB2*$^{\Delta V/\Delta V}$ mice show vascular defects throughout the central nervous system. **a**, Adult (12-15 weeks old) CD1 *ephrinB2*$^{\Delta V/\Delta V}$ mice (eB2 ΔV/ΔV) and wild type littermates (control) were injected with high molecular weight FITC-dextran. Blood vessels in the cortex, thalamus and striatum were visualized by confocal microscopy. Scale bar: 150 µm. **b**, Similar reduction in the vascularization of *ephrinB2*$^{\Delta V/\Delta V}$ mutant brains was observed in different regions. Vascular density of wild type as compared with *ephrinB2*$^{\Delta V/\Delta V}$ mice was, in average, 18.63±0.60% versus 14.92±0.99%, 21.01±1.54% versus 14.95±0.80%, and 18.34±0.44% versus 13.52±0.77%, in the cortex, thalamus, and striatum, respectively. Error bars represent SEM. Two-tailed t-test, n=3 wild type and 3 *ephrinB2*$^{\Delta V/\Delta V}$ mice, * $P < 0.05$.

6.1.4. Lack of ephrinB2 PDZ-signaling specifically affects filopodial extension in endothelial tip cells, without alteration of cell proliferation

Bidirectional signaling of Eph receptors and their ephrin ligands represents one of the most important guidance cues that directs the axonal growth cones at the distal end of

growing axons to their appropriated targets. Emerging evidences suggest that axonal growth cones and capillary tip cells share several repulsive and attractive cues in their environment that ultimately determine their directional migration. To address the question whether the exact cellular mechanism regulated by ephrinB2 during sprouting angiogenesis would be the guidance of vascular sprouts, endothelial tip cells at the leading front of the growing vascular network were investigated. Extension of filopodial processes, a hallmark of endothelial tip cells that reflects their highly explorative and invasive behavior, was found to be clearly affected by the lack of ephrinB2 PDZ target site. A striking reduction of up to 56.7% of filopodial density was observed in *ephrinB2*$^{\Delta V/\Delta V}$ mice compared with wild type littermates (Fig. 6-6) and implicated the importance of ephrinB2 PDZ-signaling in the formation or stabilization of the filopodia structure required for guided migration of sprouting endothelial tip cells.

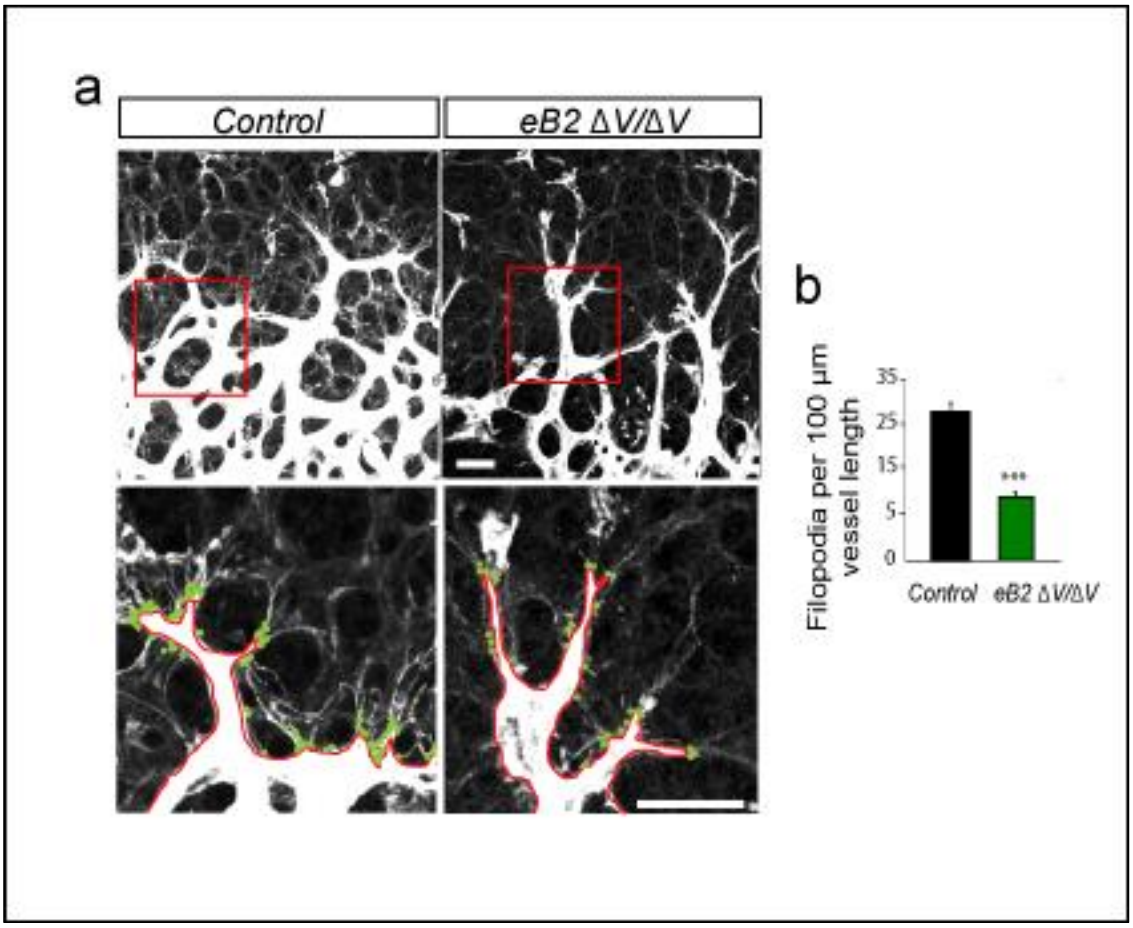

Figure 6-6 Disruption of ephrinB2 PDZ-dependent signaling causes severe defect in endothelial tip cell filopodia extension. a, Developing retinal vasculatures of CD1 P7 *EphrinB2*$^{\Delta V/\Delta V}$ mice (eB2 ΔV/ΔV) and wild type littermates (control) were visualized by isolectin-B4. Lower panel are closed up images of the vascular front areas as indicated by the red box. Filopodial extensions (green dots) were quantified along the length of the vessel front (red line). Scale bars represent 25 µm. **b**, *ephrinB2*$^{\Delta V/\Delta V}$ mutant retina vessels exhibited a drastic decrease in filopodia extension at the sprouting front counted 12.48±0.88 as compared with 28.84±1.71 filopodia per 100 µm vessel length (in average) in wild type retinas. Error bar represent SEM. Two-tailed t-test, n=6 wild type and 5 *ephrinB2*$^{\Delta V/\Delta V}$ mice, *** P<0.001.

Reduction in vessel coverage could also be attributed to a decreased endothelial cell proliferation. To examine this possibility, proliferating cells in the developing mouse retina were labeled with Bromodioxyuridine (BrdU) and number of BrdU positive cells per vascular area was quantified. *EphrinB2*$^{\Delta V/\Delta V}$ mutants and wild types littermates showed no difference in the proliferation of endothelial cells at the vascular front (Fig. 6-7), suggesting that reduced sprouting activity rather than endothelial proliferation account for the decreased vessel density caused by loss of ephrinB2 PDZ-signaling.

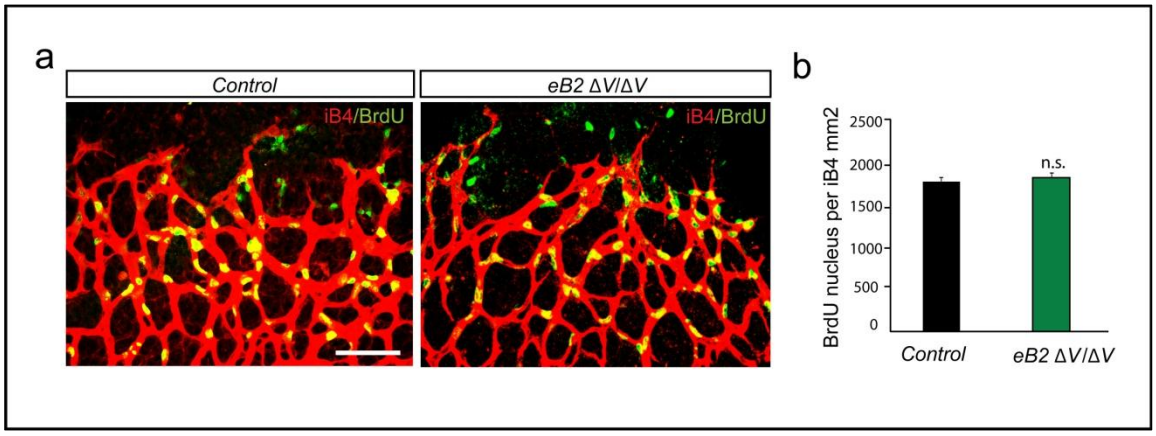

Figure 6-7 Endothelial cell proliferation is not affected in *ephrinB2*$^{\Delta V/\Delta V}$ mutant retinas. a, Isolectin B4 (red) and BrdU (green) staining of whole-mounted wild type (control) and *ephrinB2*$^{\Delta V/\Delta V}$ (eB2 ΔV/ΔV) mouse retinas at the age of P7 showed indistinguishable endothelial cell proliferative activity at the vascular front. Scale bar is 50 µm. **b**, Quantification of BrdU positive cells per isolectin-B4-positive vessel area confirmed indifferent number of proliferating endothelial cells between wild type (1806.92±83.87 cells per mm^2) and *ephrinB2*$^{\Delta V/\Delta V}$ (1854.56±87.58 cells per mm^2). Error bar represent SEM. Two-tailed t-test, n=3 wild type and 3 *ephrinB2*$^{\Delta V/\Delta V}$ mice, n.s. not significant.

6.1.5. Complementary expression of ephrinB2 in sprouting retinal vessels and EphB receptors in the scaffolding astrocytic network

For the detection of ephrinB2 whole-mounted retinas were stained with the recombinant protein consisting of EphB4 ectodomain and the Fc fraction of the human immunoglobulin G (EphB4-Fc). EphB4-Fc preferentially binds to ephrinB2 and thereby allows the detection of ephrinB2 localization by fluorochrome-conjugated anti-Fc. In the actively sprouting retinal vascular network, ephrinB2 was found to be expressed in all microvessels and arteries as well as mural cells sparsely covering the entire vascular bed, but largely absent in matured veins (fig. 6-8a-c). At the sprouting fronts, both endothelial tip cells and stalk cells were positive for ephrinB2 (Fig. 6-8d). In agreement with the function of ephrinB2 at the tip cells, clusters of ephrinB2 were also present in the filopodia structures of the tip cells (Fig.6-8e-f). During retinal vasculature development astrocytes secrete VEGF that, though the signaling of its receptor VEGFR2 predominantly expressed in tip cells and localized to filopodia, guides the extension of tip cell filopodia and subsequent migration of endothelial sprouts along the astrocytic scaffold. Interestingly, staining of whole-mounted retinas with ephrinB2 extracellular domain fused with human Fc (ephrinB2-Fc) revealed the high expression of EphB receptors in the astrocytic meshwork (Fig. 6-8g-i), suggesting the potential role of astrocytes to provide a source of ephrinB2 activation in vascular endothelium.

Figure 6-8 EphrinB2 is expressed throughout the developing retinal vascular network and its receptors EphB are abundant in the astrocytic scaffold. a-c, Double staining of whole-mounted P4 retinas with isolectin-B4 to mark the entire vascular bed (green) and EphB4-Fc that labeled ephrinB2 (red) showed the expression of ephrinB2 all over the actively sprouting vascular network including arteries (white circles) and all microvessels with the exception of veins (white asterisks). Perivascular cells including pericytes and smooth muscle cells are also positive for ephrinB2. **d,** At the vascular front the expression of ephrinB2 was detected in both tip and stalk cells. **e** and **f**, high magnification images which focus on an endothelial tip cell as indicated by the white box in **d** showed clusters of ephrinB2 localized at the tip cell filopodia (white arrowheads in **e**). **g-i**, Whole-mounted retina staining with an antibody specific for the astrocyte marker GFAP and ephrinB2-Fc fusion protein showed the expression of EphB receptors (green) in astrocytic network (red). **h** and **i** are high magnification images of the area indicated by the white box in **g**. Scale bars: **a,** 150 µm, **d** and **g**, 25 µm, **e** and **h**, 10 µm.

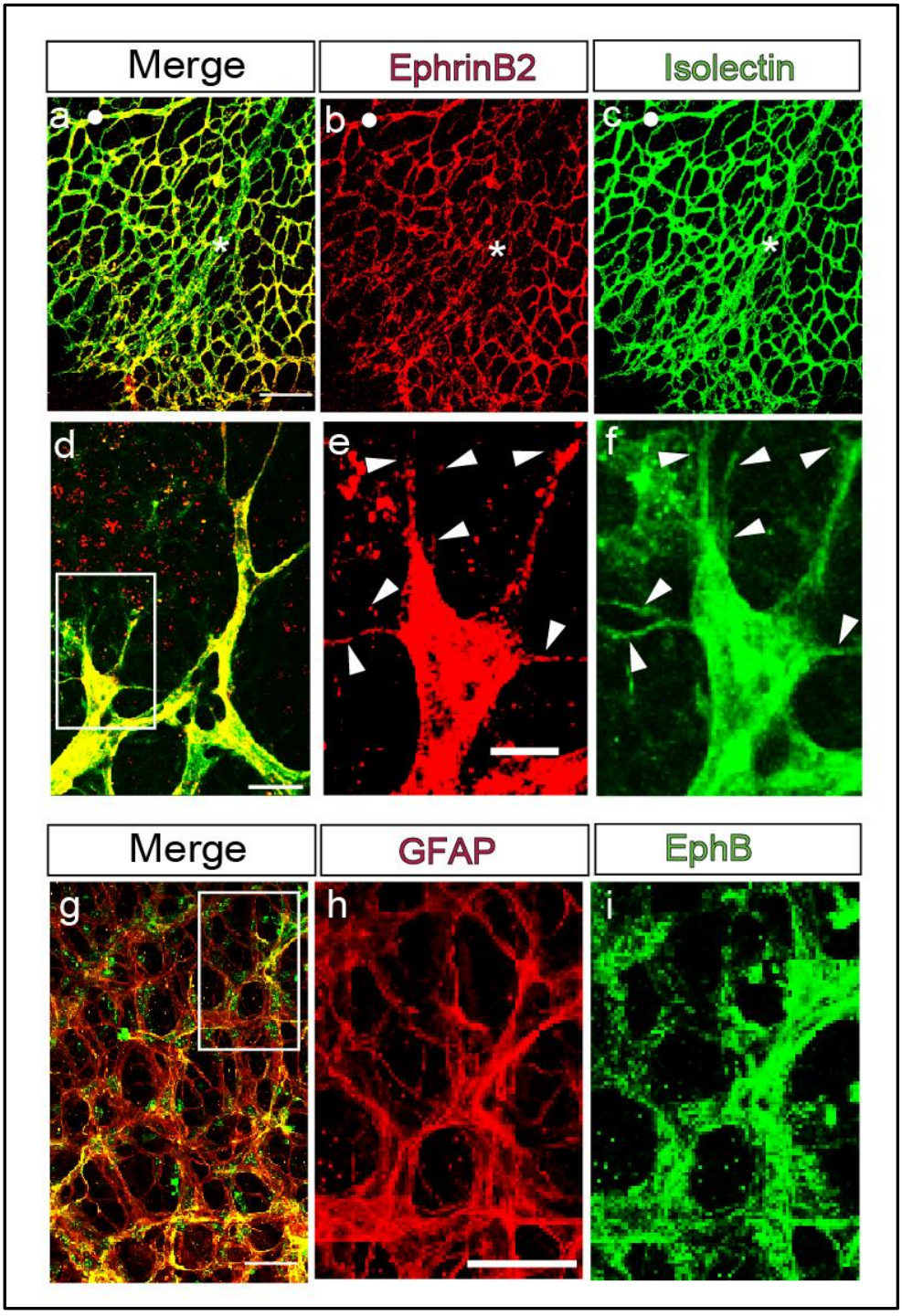
Merge
EphrinB2
Isolectin
a
b
c
d
e
f
Merge
GFAP
EphB
g
h
i

6.1.6. EphrinB2 gain-of-function promotes filopodial protrusion in cultured endothelial cells

To further confirm the direct effect of ephrinB2 on filopodial dynamics in endothelial cells, *YFP-ephrinB2* fusion gene or only *YFP* were introduced into primary mouse lung endothelial cells (MECs) by electroporation. Eletroporated cells were seeded onto 2-dimentional matrix consisting of fibronectin and gelatin. Numbers and cumulative lengths of filopodial protrusions in these cells were quantified. In comparison to MECs overexpressing only YFP, cells overexpressing YFP-ephrinB2 showed excessive extension of filopodia during their spreading on the 2-dimensional matrix (Fig. 6-9a, b). In consistence with this observation, MECs overexpressing YFP-ephrinB2 exhibited highly dynamic extension and retraction of filopodia that facilitated cell movement in 3-dimentional matrigel (Fig. 6-9c, movie S1).

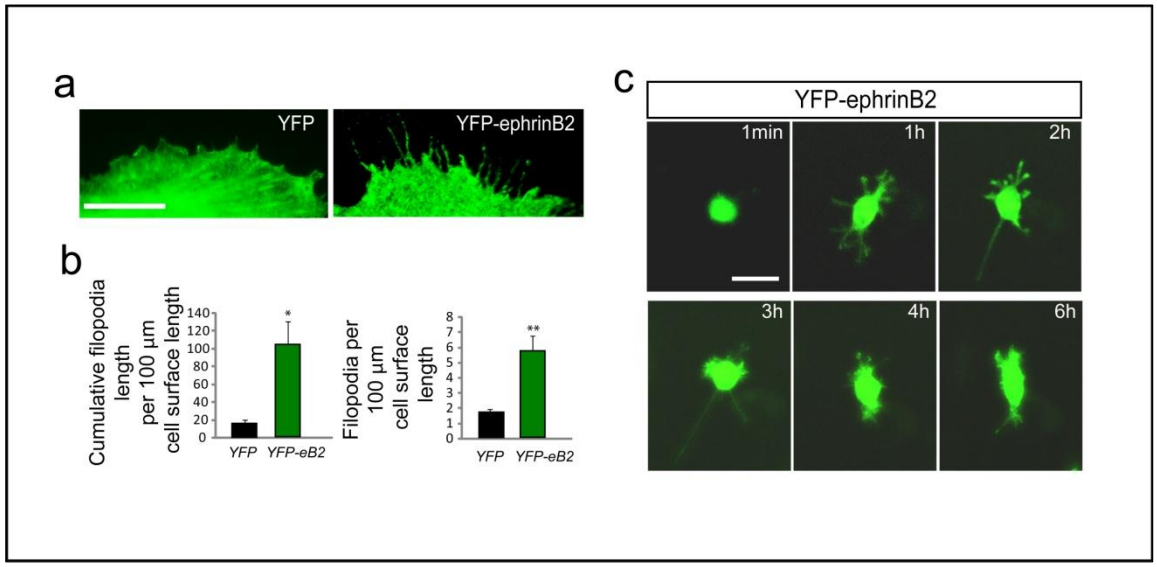

Figure 6-9 Overexpression of ephrinB2 induces filopodial dynamics in endothelial cells. Primary mouse endothelial cells overexpressing YFP-ephrinB2 showed numerous filopodial extensions after 6h of cell spreading on 2-dimensional matrix (**a**), counted up to 5.81±0.95 filopodia per 100 µm of cell surface length (in average) as compared with 1.74±0.21 per 100 µm of cell surface length in cells overexpressing only YFP (**b**). Increase in cumulative filopodial lengths was also evident comparing 17.23±3.23 and 106.36±24.85 µm per 100 µm of cell surface length (in average) in the YFP and the YFP-ephrinB2 overexpressing cells, respectively. (**b**). **c**, Six consecutive time points from the supplementary time lapse movie 1 showed active sprouting activity of YFP-ephrinB2 overexpressing cells seeded in 3-dimensional matrigel. Scale bars: **a,** 100 µm, **c,** 25 µm. Error bar represent SEM. Two-tailed t-test, n=14 cells per condition, * P<0.05, ** P<0.01.

6.1.7. EphrinB2 PDZ-interaction confers contact-mediated repulsive activity to endothelial cells

Matrigel, the mixture of basement membrane proteins and growth factors secreted from a mouse sarcoma cell line that resembles the complex extracellular environments of several tissues, has been used extensively to study endothelial cell behavior during their organization into a three-dimensional branching network. Once seeded onto matrigel, endothelial cells extend cellular processes and migrate toward nearby cells to establish cell-cell contacts. The cellular assembly and elongation subsequently give rise to the capillary-like structures containing intercellular or lumen-like spaces. In agreement with ephrinB2 gain-of-function that resulted in excessive filopodia extensions (Fig. 6-9), overexpression of YFP-ephrinB2 in endothelial cells whose endogenous *ephrinB2* has been knocked out (Fig. 6-10) conferred highly invasive behavior as well as cell-cell contact-mediated repulsive activity to these cells. This consequently prevented their inclusion into the tubular endothelial network formed on matrigel (Fig. 6-11a and movie S2).

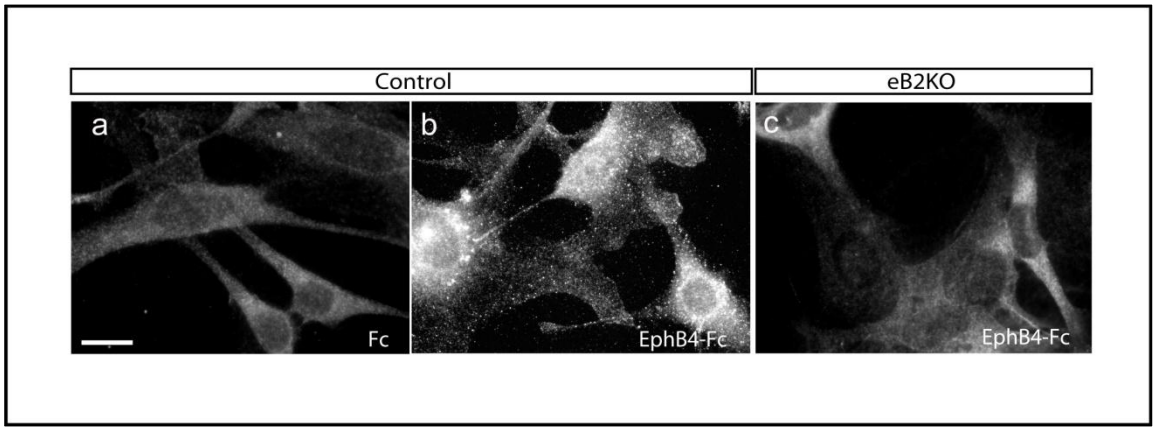

Figure 6-10 Characterization of ephrinB2 knockout endothelial cells. a-c, Loss of ephrinB2 expression was confirmed by an immunofluorescence assay in which ephrinB2-clustering was induced by stimulation with the extracellular domain of the ephrinB2-preferential receptor EphB4 fused with human Fc (EphB4-fc), previously pre-clustered by coupling with anti-Fc antibody. Non-stimulated cells (treated with pre-clustered Fc) showed no ephrinB2 staining (**a**). EphrinB2 clusters were observed in control *ephrinB2*$^{lox/lox}$ endothelial cells (**b**) but absent in ephrinB2 knockout cells (eB2KO) derived from *ephrinB2*$^{lox/lox}$ cells after Cre recombination (**c**). Scale bar is 25 µm.

This repulsive phenotype was in an evident contrast to the ephrinB2 knockout cells that have lost the contact-dependent repulsion and tightly integrated into the tubular structures (Fig. 6-11b and movie S3). The induction of cellular repulsion in endothelial cells by ephrinB2 depends on its PDZ signaling. Re-introduction of the ephrinB2 expression construct in which all the tyrtosine phosphorylation sites are mutated while the PDZ-binding motif still present (ephrinB25Y), but not the construct with a targeted deletion of the PDZ-interaction site (ephrinB2ΔV), could rescue the repulsive phenotype in ephrinB2 knockout cells (Fig. 6-11c-e, Fig. 6-12, and movie S4-6).

These observations are consistent with an intercellular repulsive activity regulated by Eph-ephrin contacts observed in other cell types (Mellitzer et al., 1999; Zimmer et al., 2003) that might be involved in initial destabilizing forces possibly required for the budding of the selected sprouting endothelial cells (tip cells) from a tightly-arranged endothelial cell layer lining the vascular wall.

Figure 6-11 EphrinB2 reverse signaling mediates repulsive activity in endothelial cells. a, MECs whose endogenous *ephrinB2* had been knocked out were electroporated with *YFP-ephrinB2* (green cells) and seeded on matrigel. Overexpression of YFP-ephrinB2 induced contact-mediated cellular repulsion and subsequent exclusion of the endothelial cells from the cord-like structures. Three different time points of the supplementary time-lapse movie 2 are shown. **b,** endothelial cells lacking ephrinB2 stably integrated in endothelial tubes. EphrinB2KO endothelial cells (green cells) were infected with adenovirus encoding *GFP* and seeded on matrigel. Three consecutive time points of the supplementary time-lapse movie 3 are shown. **c,** The repulsive phenotype conferred by ephrinB2 is reverse signaling dependent. Overexpression of YFP-ephrinB2ΔC in MECs lacking endogenous ephrinB2 (green cells) resulted in stable integration of these cells into the tubular structures. Three different time points of the supplementary time-lapse movie 4 are shown. **d**, PDZ-interactions are required to trigger the repulsive behavior in endothelial cells. EphrinB2KO MECs overexpressing YFP-ephrinB2ΔV (green cells) were stably integrated in the tubular network when seeded in matrigel. Three different time points of the supplementary time-lapse movie 5 are shown. **e**, Tyrosine-dependent signaling is dispensable for the repulsive action of ephrinB2 in endothelial cells. EphrinB2KO MECs overexpressing YFP-ephrinB25Y (green cells) were repulsed from other cells that assembled to form tubular structures in matrigel, similar to the behavior observed in the overexpression of full-length ephrinB2. Three different time points of the supplementary time-lapse movie 6 are shown. Red arrows indicate some of the cells that were integrated (b,c, and d) or non-integrated (a and e) in the capillary-like structures. Scale bar is 50 μm.

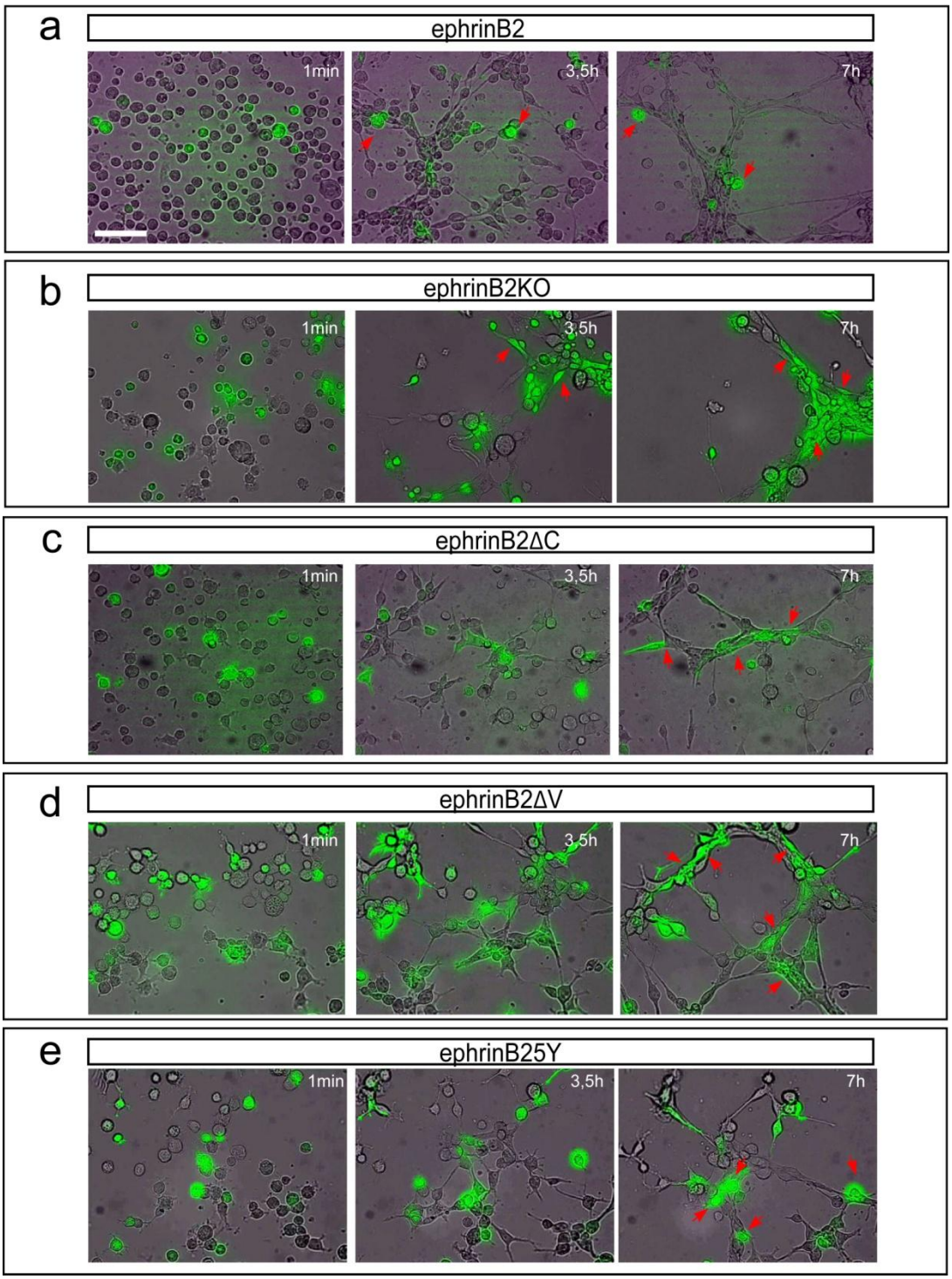
a
ephrinB2
1min
3,5h
7h
b
ephrinB2KO
1min
3,5h
7h
c
ephrinB2ΔC
1min
3,5h
7h
d
ephrinB2ΔV
1min
3,5h
7h
e
ephrinB25Y
1min
3,5h
7h

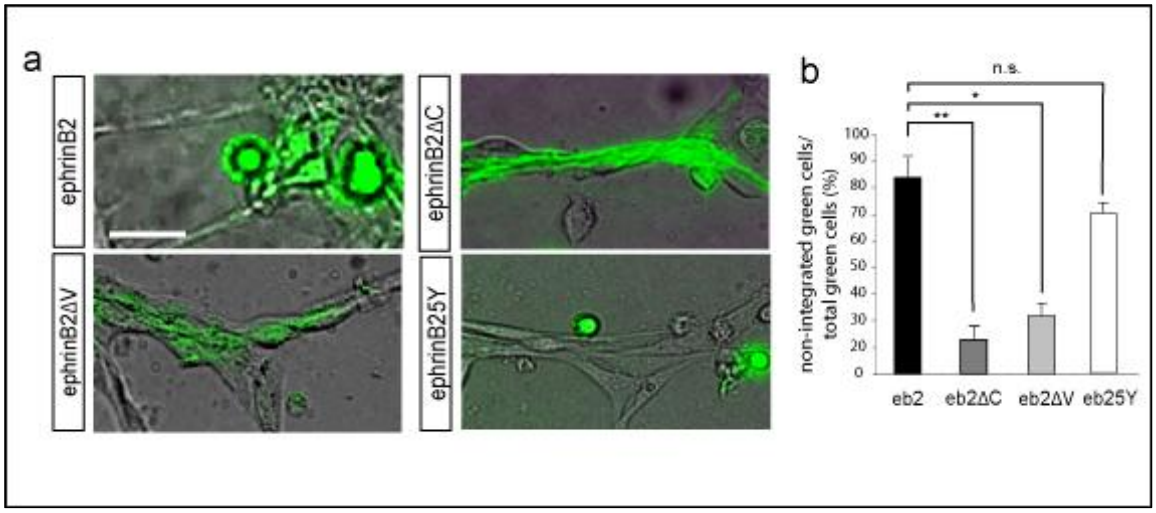

Figure 6-12 Contact-mediated repulsion of endothelial cells requires ephrinB2 PDZ-interaction, but not tyrosine phosphorylation. **a**, High magnification pictures of the tubular structures formed in matrigel by endothelial cells lacking ephrinB2 some of which were expressing YFP-ephrinB2, YFP-ephrinB2ΔC, YFP-ephrinB2ΔV or YFP-ephrinB25Y (all in green). Introduction of *ephrinB2* wild type and *ephrinB25Y*, but not *ephrinB2ΔC* and *ephrinB2ΔV*, was sufficient to restore the repulsive phenotype in endothelial cells. **b**, Quantification of green cells that were excluded from the tubes is shown as percentage of all green cells in each condition. 83.33±9.62%, 22.51±6.34%, 34.26±4.90%, and 70.36±3.55% of all cells overexpressing YFP-ephrinB2 (eb2), YFP-ephrinB2ΔC (eb2ΔC), YFP-ephrinB2ΔV (eb2ΔV), and YFP-ephrinB25Y (eb25Y), respectively, were unable to integrated into the endothelial tubes. Scale bar is 25 µm. Error bars represent SEM. Two-tailed t-test, n=3 movies of YFP-ephrinB2, 3 movies of YFP-ephrinB2ΔV, 4 movies of YFP-ephrinB2ΔC, and 4 movies of YFP-ephrinB25Y, * P<0.05, ** P < 0.01, n.s. not significant).

6.1.8. Supplementary information on CD-Rom

Movie 1. Endothelial cells overexpressing YFP-ephrinB2 extended numerous dynamic filopodia which facilitated cell migration in the extracellular matrix. The movie is 8 h long with 96 frames at 5 min intervals.

Movie 2. EphrinB2 confers a repulsive phenotype in endothelial cells. Dynamic filopodial processes protruded from YFP-ephrinB2 overexpressing cells (green) were, upon contact with neighboring cells, rapidly retracted which consequently led to the exclusion of these cells from the capillary-like structures. The movie is 7 h long with 84 frames at 5 min intervals.

Movie 3. Endothelial cells lacking ephrinB2 (green) lost their contact-dependent repulsion and invasive migratory behavior. These cells tightly assembled into capillary-like structures. The movie is 7 h long with 84 frames at 5 min intervals.

Movie 4. Deletion of the cytoplasmic tail results in the loss of function of ephrinB2. EphrinB2 knockout endothelial cells in which *YFP-ephrinB2ΔC* was re-introduced (green) behaved indifferent from other knockout cells. These cells lost the repulsive phenotype and integrated into the tubular network, suggesting the significance of reverse signaling downstream of ephrinB2 in the regulation of endothelial cell contact-mediated repulsion. The movie is 8 h long with 96 frames at 5 min intervals.

Movie 5. PDZ-interactions are necessary for the repulsive activity conferred by ephrinB2. Expression of YFP-ephrinB2ΔV (green) in the ephrinB2 deficient cells was unable to rescue the repulsive and invasive behavior observed upon the expression of wild type ephrinB2. These YFP-ephrinB2ΔV expressing cells were readily integrated into the tubular network. The movie is 8 h long with 96 frames at 5 min intervals.

Movie 6. Tyrosine phosphorylation is dispensable for the repulsive phenotype. EphrinB2 knockout endothelial cells in which YFP-ephrinB25Y was re-introduced (green) behaved similar to those expressing wild type ephrinB2. These cells exhibited high motility and were excluded from the endothelial tubes. The movie is 8 h long with 96 frames at 5 min intervals.

Together, these results indicate that ephrinB2 reverse signaling through PDZ-interactions controls vascular sprouting by promoting tip cell filopodial extension during developmental angiogenesis. EphrinB2 might also be important in the modulation of endothelial cell invasive behavior which could be involved in the regulation of cellular contact between endothelial cells.

6.2. EphrinB2 PDZ-interaction is crucial for VEGFR2 internalization and signal transduction

Interaction between VEGF secreted from astrocytes and localized in the extracellular matrix within the close proximity to the astrocyte surface, and its receptor VEGFR2 located on the endothelial tip cell filopodia has been suggested to provide the initial establishment of

astrocyte-endothelial contacts that mediate endothelial cell guidance along the pre-existing astrocytic scaffold during the vascularization of the retina (Gerhardt et al., 2003). Therefore, the next question to be addressed is if the impairment of filopodial extensions in *ephrinB2*$^{\Delta V/\Delta V}$ mutant tip cells could be a result of misregulated VEGFR2 function indicating a molecular crosstalk between ephrinB2 reverse and VEGFR2 signaling.

6.2.1. VEGF-induced endocytosis of VEGFR2 requires PDZ interactions downstream of ephrinB2

Intracellular compartmentalization of signaling receptors has been supported by several compelling evidences to represent a critical mechanism that cells use to strictly regulate signal transduction temporally and spatially. Rather than being removed from the cell surface and en route directly to the proteolytic degradation machinery only to dampen cellular response to extracellular signals as previously thought, several receptors endocytosed and sorted into different endosomal compartments are now recognized to continue their signaling as is the case for EGF and NGF receptors. Indeed, activation of some signaling pathways downstream of these receptors has been clearly demonstrated to rely on receptor endocytosis (Howe et al., 2001; Sigismund et al., 2008). Internalization of VEGFR2 has also been shown to promote its phosphorylation and mitogenic signaling (Lampugnani et al., 2006). Conversely, at the cellular surface VEGFR2 is dephosphorylated and inactivated by membrane-associated phosphatases such as CD148 (Lampugnani et al., 2006) or VE-PTP (Mellberg et al., 2009).

To test whether ephrinB2 might have a role in the VEGFR2 trafficking, endocytosis of VEGFR2 in primary endothelial cells isolated from ephrinB2 signaling mutant mice was assessed by using the immunofluorescence-based, antibody feeding assay. Briefly, cell surface VEGFR2 was labeled with an antibody raised against its ectodomain prior to stimulation of the receptor internalization. VEGFR2 internalization was activated by stimulation with VEGF. After cell fixation, remaining surface receptor was firstly detected with a fluorochrome-conjugated secondary antibody. Then cells were permeabilized and internalized receptor was detected with another secondary antibody conjugated with different fluorochrome. *EphrinB2*$^{lox/lox}$ MECs (control) robustly internalized surface VEGFR2

in response to stimulation with VEGF, whereas ephrinB2 knockout (eB2KO) as well as PDZ-signaling-deficient (eB2ΔV) MECs failed to do so. Disruption of ephrinB2 tyrosine phosphorylation does not seem to affect VEGFR2 internalization. Phosphotyrosine-deficient cells (eB25Y) exhibited comparable level of internalized VEGFR2 to control cells (Fig. 6-13).

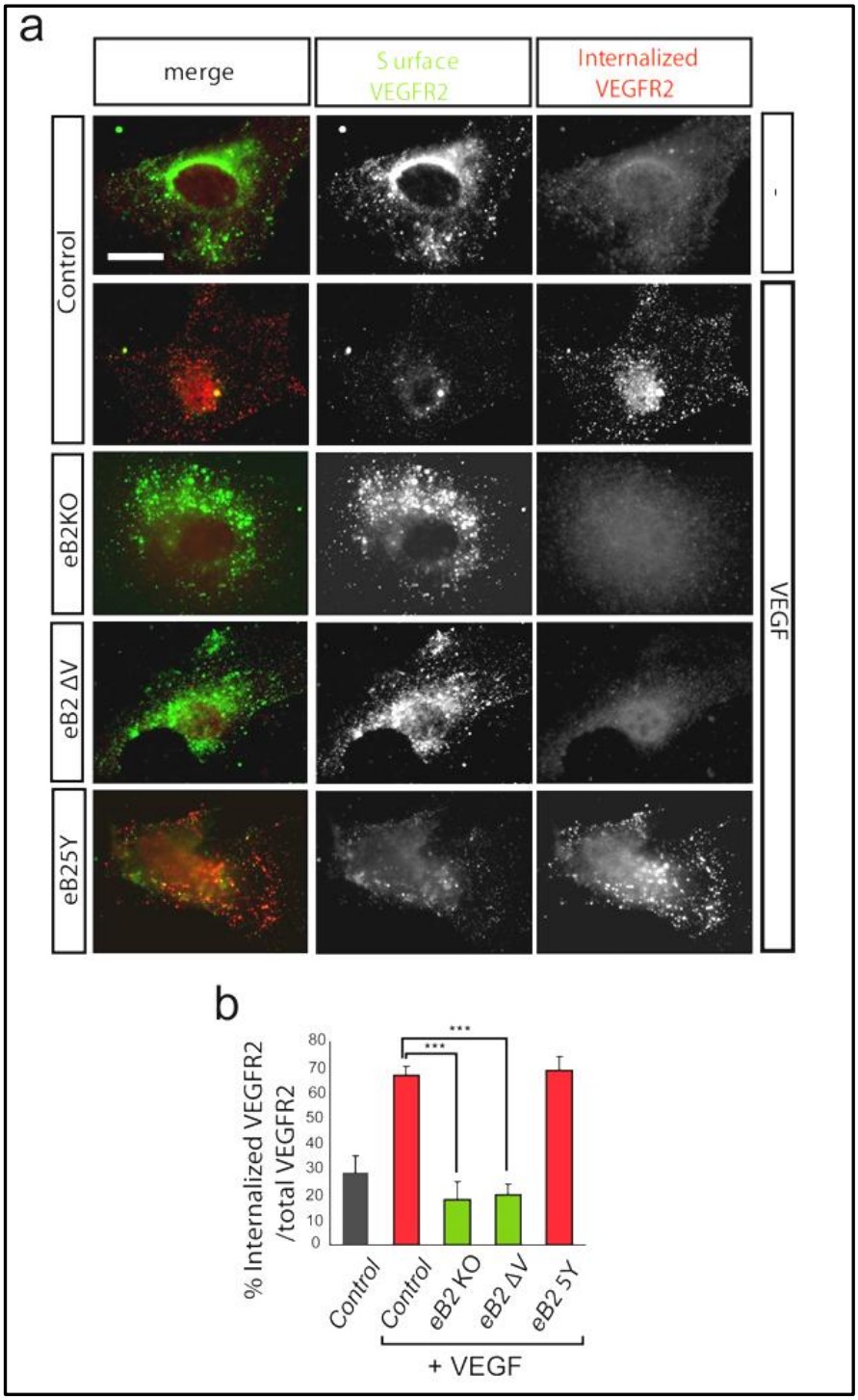

Figure 6-13. EphrinB2 PDZ-signaling is necessary for VEGFR2 internalization. **a**, Endocytosis of VEGFR2 was visualized by the antibody feeding assay. *EphrinB2*$^{lox/lox}$ primary endothelial cells (control), ephrinB2-deficient cells derived from these cells by viral-transduction of Cre-recombinase (*ephrinB2*$^{lox/lox}$*; Cre*$^{+}$, eB2 KO), ephrinB2 PDZ signaling-deficient cells (*ephrinB2*$^{\Delta V/\Delta V}$, eB2ΔV), and ephrinB2 phosphotyrosine-signaling deficient cells (*ephrinB2*$^{5Y/5Y}$, eB25Y) were stimulated for 30 min with VEGF. VEGFR2 that remained at the plasma membrane was labeled in green, while internalized receptor was marked in red. Scale bar is 25 µm. **b**, Quantification of VEGFR2 internalization based on fluorescence intensities, shown as average percentage of internalized VEGFR2 (red) versus total VEGFR2 (red + green). In control cells the basal level of VEGFR2 internalization measured 28.67±7.75% (grey bar) increased up to 66.67±3.67% after VEGF-stimulation. EphrinB2 knockout and *ephrinB2*$^{\Delta V/\Delta V}$ MECs were unable to respond to VEGF-stimulation as only 17.80±7.04% and 19.67±4.29% of VEGFR2, respectively, were internalized. On the contrary, up to 68.83±5.44% of VEGFR2 internalization was observed in *EphrinB2*$^{5Y/5Y}$ mutant cells. Error bars represent SEM. Two-tailed t-test, n=4 independent experiments, *** P<0.001.

6.2.2. Expression levels of ephrinB2, VEGFRs, and NICD are unaltered in *ephrinB2*$^{\Delta V/\Delta V}$ mutant mice and endothelial cells

To verify that the vascular defects and the impairment of VEGFR2 internalization observed in *ephrinB2*$^{\Delta V/\Delta V}$ mice and primary endothelial cells are not the consequence of a reduction in the expression levels of ephrinB2 or VEGF receptors, *ephrinB2*$^{\Delta V/\Delta V}$ and wild type MECS were subjected to western blot analysis. In comparison to wild type cells, no significant change in the expression levels of EphrinB2, VEGFR2 and VEGFR3 (another receptor in VEGF family that is essential for lymphangiogenesis and also plays an important role in angiogenic growth of blood vessels during development) could be detected in the *ephrinB2*$^{\Delta V/\Delta V}$ cells (Fig. 6-14a).

Notch signaling is a known modulator of ephrinB2 expression and therefore of the acquisition of arterial identity of endothelial cells (Roca and Adams, 2007). Signaling pathways activated downstream of Notch and VEGFR2 are intertwined within a negative feedback loop that permits a strict regulation of their signal outcomes. VEGF functions upstream of Notch signaling by acting as an inducer of the Notch ligand DLL4 expression that consequently leads to *trans*-activation of Notch. On the other hand, VEGFR2 has also been shown to be downregulated once Notch downstream signal is activated (Suchting et al., 2007). Moreover, deregulated VEGFR2 has been suggested to be responsible for

excessive filopodial sprouting in developing mouse retinal vessels following disruption of Notch signaling (Hellstrom et al., 2007; Suchting et al., 2007). To examine the possibility that Notch signaling might be involved in the vascular function of ephrinB2, the levels of activated Notch1 (NICD, Notch intracellular domain) in *ephrinB2*$^{\Delta V/\Delta V}$ mutant mice and control wild type littermates were assessed by western blot analysis. Comparable levels of NICD detected in the mutant and the control brain tissues (Fig. 6-14b) suggest that the vascular defects as well as impaired VEGFR2 endocytosis caused by disruption of ephrinB2 PDZ-signaling are not a consequence of deregulated Notch signaling.

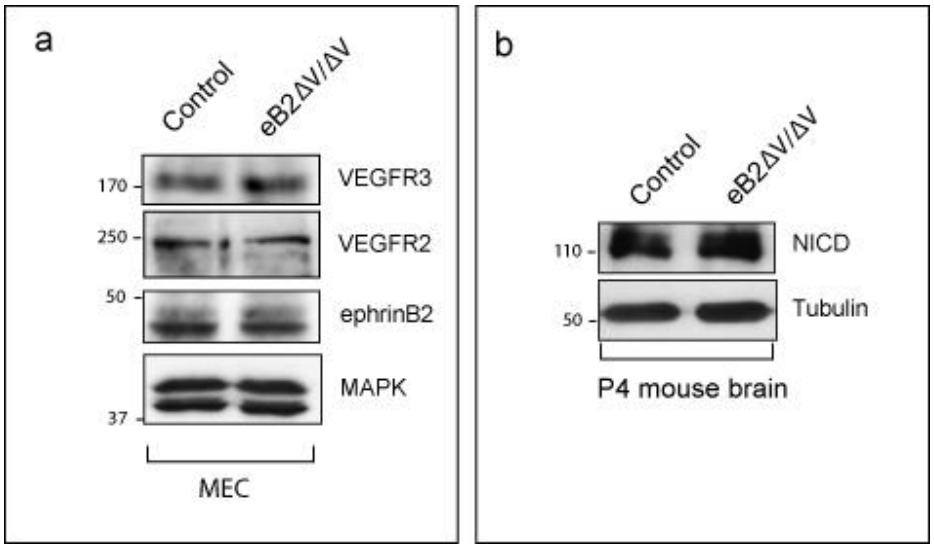

Figure 6-14 Characterization of *ephrinB2*$^{\Delta V/\Delta V}$ mutant mice and endothelial cells. a, Endothelial cells isolated from *ephrinB2*$^{\Delta V/\Delta V}$ (eB2ΔV/ΔV) and wild type mice (control) were characterized with respect to the expression of ephrinB2, VEGFR2 and VEGFR3. Level of MAPK was used as loading control. All protein levels were equal in mutant and wild type cells. **b,** Notch signaling is not affected in ephrinB2 PDZ-mutant mice. *EphrinB2*$^{\Delta V/\Delta V}$ mutants and control wild type littermates show equal levels of activated Notch1 assessed by the levels of Notch1 intracellular domain (NICD). Tubulin protein level was used as loading control. Data shown in **a** was generated by Essmann C.L.

6.2.3. Activation of ephrinB2 induces VEGFR2 internalization

To functionally corroborate the control of VEGFR2 endocytosis by ephrinB2 reverse signaling, MECs were treated with soluble EphB4-Fc fusion protein pre-clustered with anti-

hFc. The treatment of pre-clustered EphB-Fc has been previously shown to activate tyrosine phosphorylation as well as the recruitment of PDZ containing proteins to the cytoplasmic tails of ephrinB ligands (Palmer et al., 2002). Internalization of VEGFR2 upon EphB4-Fc stimulation in different ephrinB2 signaling mutant endothelial cells was assessed by the antibody feeding assay. Similar to VEGF-stimulation, MECs isolated from *ephrinB2*$^{lox/lox}$ mice without Cre recombination that were used as control showed significantly increased internalization of VEGFR2 following EphB4-Fc stimulation (Fig. 6-15). Loss of ephrinB2 as well as absence of ephrinB2 PDZ-dependent signaling resulted in severe impairment in VEGFR2 trafficking upon EphB4-Fc treatment as evident in the low levels of internalized VEGFR2 nearly at the baseline level of non-stimulated control cells in the *ephrinB2*$^{lox/lox}$*; Cre*$^{+}$ and *ephrinB2*$^{\Delta V/\Delta V}$ MECs, respectively. By contrast, lack of ephrinB2 tysosine-phosphorylation has no apparent effect on the ability of endothelial cells to internalize VEGFR2. *EphrinB2*$^{5Y/5Y}$ cells exhibited robust internalization of VEGFR2 upon EphB4-Fc stimulation to the level similar to that observed in control cells (Fig. 6-15).

Figure 6-15. Stimulation of ephrinB2 reverse signaling by EphB4-Fc is sufficient to induce VEGFR2 internalization. **a**, *EphrinB2*$^{lox/lox}$ (control), ephrinB2 knockout (*ephrinB2*$^{lox/lox}$*; Cre*$^{+}$, eB2KO), *ephrinB2*$^{\Delta V/\Delta V}$ (eB2ΔV), or *ephrinB2*$^{5Y/5Y}$ (eB25Y) primary endothelial cells were stimulated with the pre-clustered soluble EphB4 receptor (EphB4-Fc) for 30 min. VEGFR2 internalization was analyzed by antibody feeding assay. Remaining surface VEGFR2 was labeled in green and internalized receptor was marked in red. Scale bar is 25 µm. **b,** Quantification of VEGFR2 internalization based on fluorescence intensities, shown as average percentages of internalized VEGFR2 (red) from total VEGFR2 (red + green). Activation of ephrinB2 signaling upon EphB4-Fc treatment in control cells resulted in a robust internalization up to 73.46±4.18% of total VEGFR2, whereas in the ephrinB2-deficient cells only 18.13±7.83% of the receptor was internalized. In comparison to the control cells, significant reduction in the level of internalized VEGFR2 reaching only 33.35±5.43% upon EphB4-Fc treatment was observed in *ephrinB2*$^{\Delta V/\Delta V}$ mutant cells. On the contrary, in the EphB4-Fc stimulated *ephrinB2*$^{5Y/5Y}$ mutant cells up to 66.64±4.75% of VEGFR2 was internalized following EphB4-Fc treatment. Error bars represent SEM. Two-tailed t-test, n=4 independent experiments, ** P<0.01, *** P<0.001).

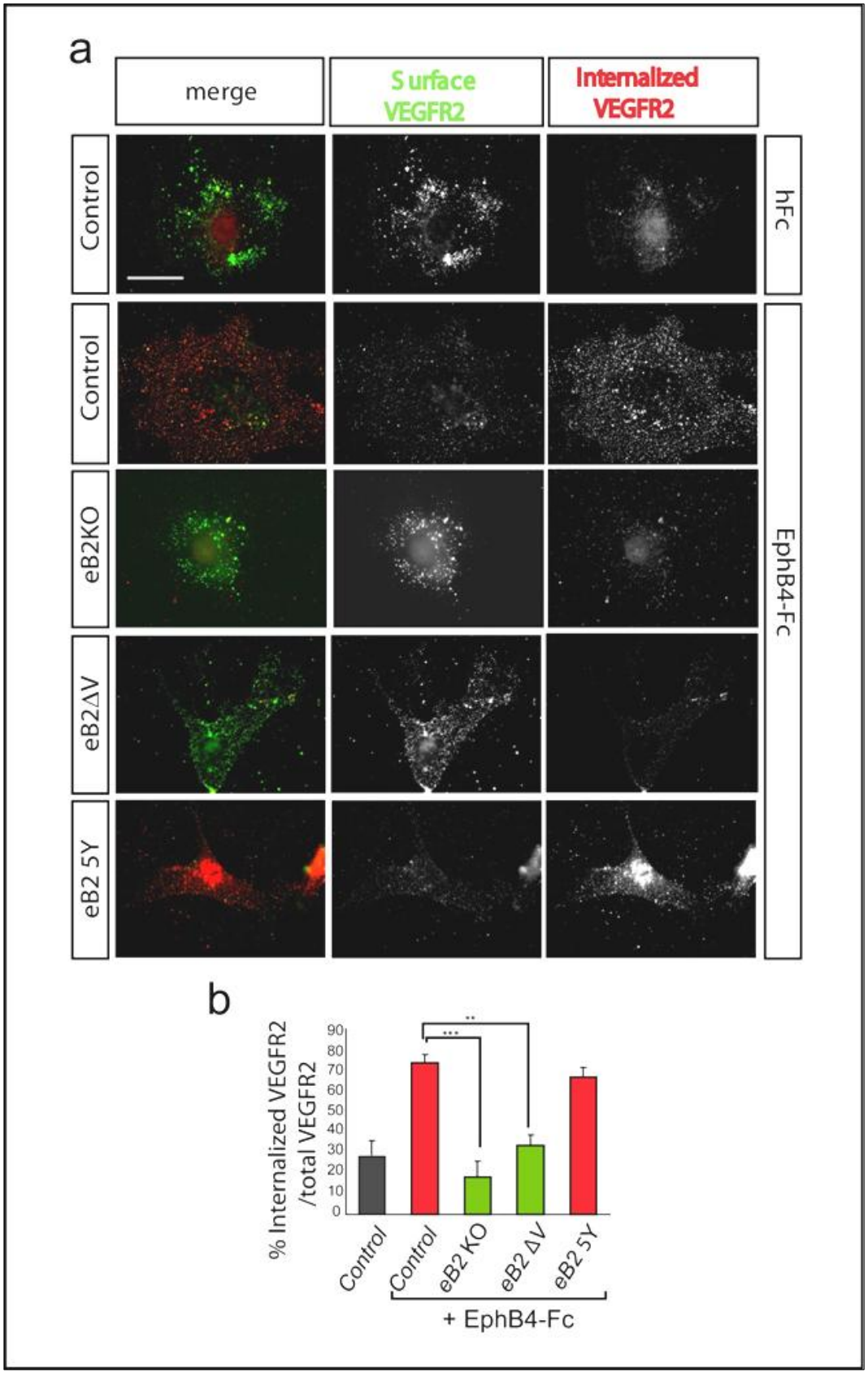
a
merge
Surface VEGFR2
Internalized VEGFR2
Control
Control
eB2KO
eB2ΔV
eB2 5Y
hFc
EphB4-Fc
b
% Internalized VEGFR2 /total VEGFR2
90
80
70
60
50
40
30
20
10
0
**
***
Control
Control
eB2 KO
eB2 ΔV
eB2 5Y
+ EphB4-Fc

Induction of VEGFR2 internalization by EphB4-Fc-mediated ephrinB2 activation was further confirmed using surface biotinylation assay developed to assess internalization of surface receptors in live tissues. Briefly, mouse cortical slices were kept alive in artificial cerebro-spinal fluid buffer and surface proteins were labeled with biotin prior to stimulation with pre-clustered EphB4-Fc or hFc as a control. Remaining cell surface-bound biotin was stripped off before preparation of tissue lysates. Biotinylated proteins endocytosed intracellularly were pulled down with Neutravidin sepharose and levels of internalized VEGFR2 were detected with immunoblot analysis. Following EphB4-Fc stimulation a substantial increase in the amount of internalized VEGFR2, as compared with only hFc treatment, was observed in wild type control tissues. The effect of ephrinB2 activation on VEGFR2 internalization was completely inhibited in *ephrinB2*$^{\Delta V/\Delta V}$ mutant (Fig. 6-16). Unaltered level of Tie2, a receptor tyrosine kinase that is also important for vascular development, upon EphB4-Fc stimulation in both wild type and *ephrinB2*$^{\Delta V/\Delta V}$ mutant (Fig. 6-16) suggests that ephrinB2 specifically induces internalization of VEGFR2 but not of other angiogenic receptors.

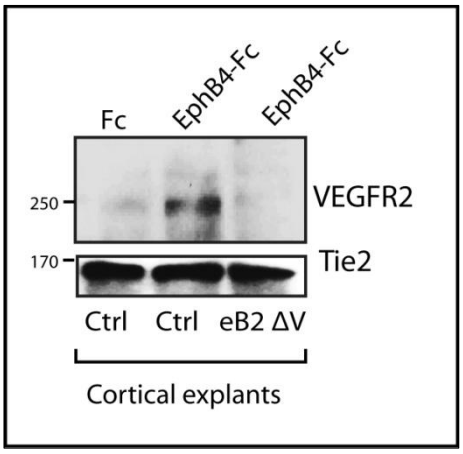

Figure 6-16. The effect of ephrinB2 activation on VEGFR2 trafficking was confirmed in live tissue. An *ex vivo* surface biotinylation assay was employed to examine the capability of activated ephrinB2 to trigger internalization of VEGFR2 in lived tissues. Biotinylated internalized receptors from *ephrinB2*$^{\Delta V/\Delta V}$ (eB2ΔV) and wild type littermate (ctrl) cortical slices, prepared from newborn (P7-9) pups, were pulled down with Neutravidin beads following EphB4-Fc or only Fc stimulation. Levels of internalized VEGFR2 and Tie2 were assessed by western blot. VEGFR2 was not internalized in the *ephrinB2*$^{\Delta V/\Delta V}$ mutant tissue and Tie-2 receptor trafficking was not affected by EphB4-Fc stimulation.

6.2.4. Kinetics of ephrinB2-induced VEGFR2 internalization

Kinetics of VEGFR2 internalization following activation of ephrinB2 by EphB4-Fc was studied by using surface biotinylation assay in MECs. VEGFR2 was robustly endocytosed only after 10 min in the presence of EphB4-Fc (Fig. 6-17). Gradual reduction in the levels of endocytosed receptor could be observed at 30 min and 60 min after EphB4-stimulation (Fig. 6-17). This is most likely due to receptor degradation as has previously been reported (Lampugnani et al., 2006). In consistence with the cortical slice biotinylation, internalization level of Tie2 in endothelial cells was not altered by EphB4-Fc stimulation (Fig. 6-17). The impairment of VEGFR2 internalization previously seen in *ephrinB2*$^{\Delta V/\Delta V}$ mouse brain tissues (Fig. 6-16) was as well consistently observed in the mutant primary endothelial cells. The unaltered level of internalized VEGFR2 in *ephrinB2*$^{\Delta V/\Delta V}$ cells following 30 min-treatment with EphB4-Fc, as compared with hFc treatment (Fig. 6-17), indicates that in absence of its PDZ target site ephrinB2 is unable to trigger endocytosis of VEGFR2.

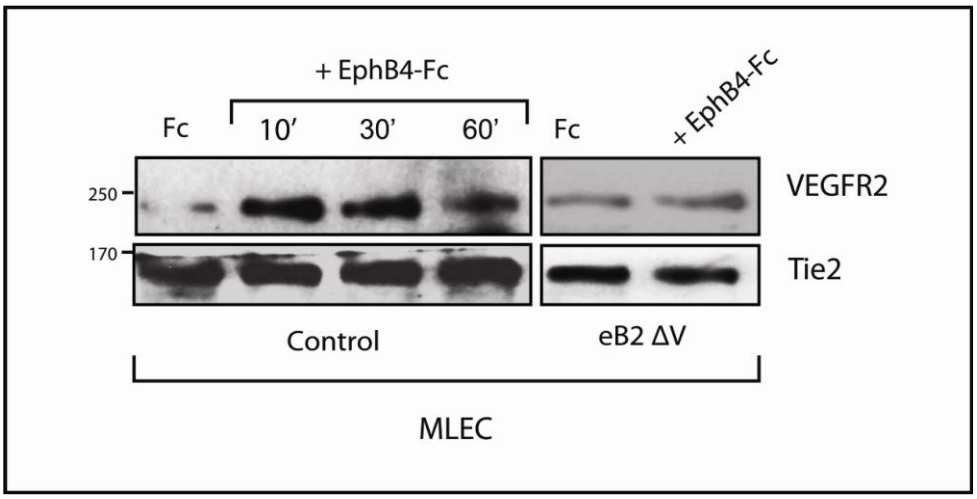

Figure 6-17 Kinetics of VEGFR2 internalization following ephrinB2 activation in endothelial cells. Internalization of VEGFR2 in primary endothelial cells after ephrinB2 activation by EphB4-Fc was assessed using a cell surface biotinylation assay. MECs from wild type (control) or *ephrinB2*$^{\Delta V/\Delta V}$ (eB2ΔV) mice were stimulated at different time points as indicated. Tie-2 receptor trafficking was not affected by ephrinB2 activation. VEGFR2 internalization was not induced by EphB4-Fc treatment in *ephrinB2*$^{\Delta V/\Delta V}$ endothelial cells.

6.2.5. VEGFR2 and ephrinB2 are potential interaction partners

In line with the direct control of VEGFR2 endocytosis by ephrinB2, clusters of activated ephrinB2 were largely co-localized with VEGFR2 at the plasma membrane pf primary endothelial cells following stimulation with VEGF (Fig. 6-18a). EphrinB2 at the cell surface was visualized with EphB4-Fc and fluorochrome-conjugated anti-human Fc antibody. Surface VEGFR2 was labeled with an antibody raised against the receptor extracellular domain. Furthermore, ephrinB2 and VEGFR2 in new born mouse brains were co-immunoprecipitated (Fig. 6-18b). Together, these results suggest that VEGFR2 and ephrinB2 form signaling complex to exert their collaborated function in endothelial cells.

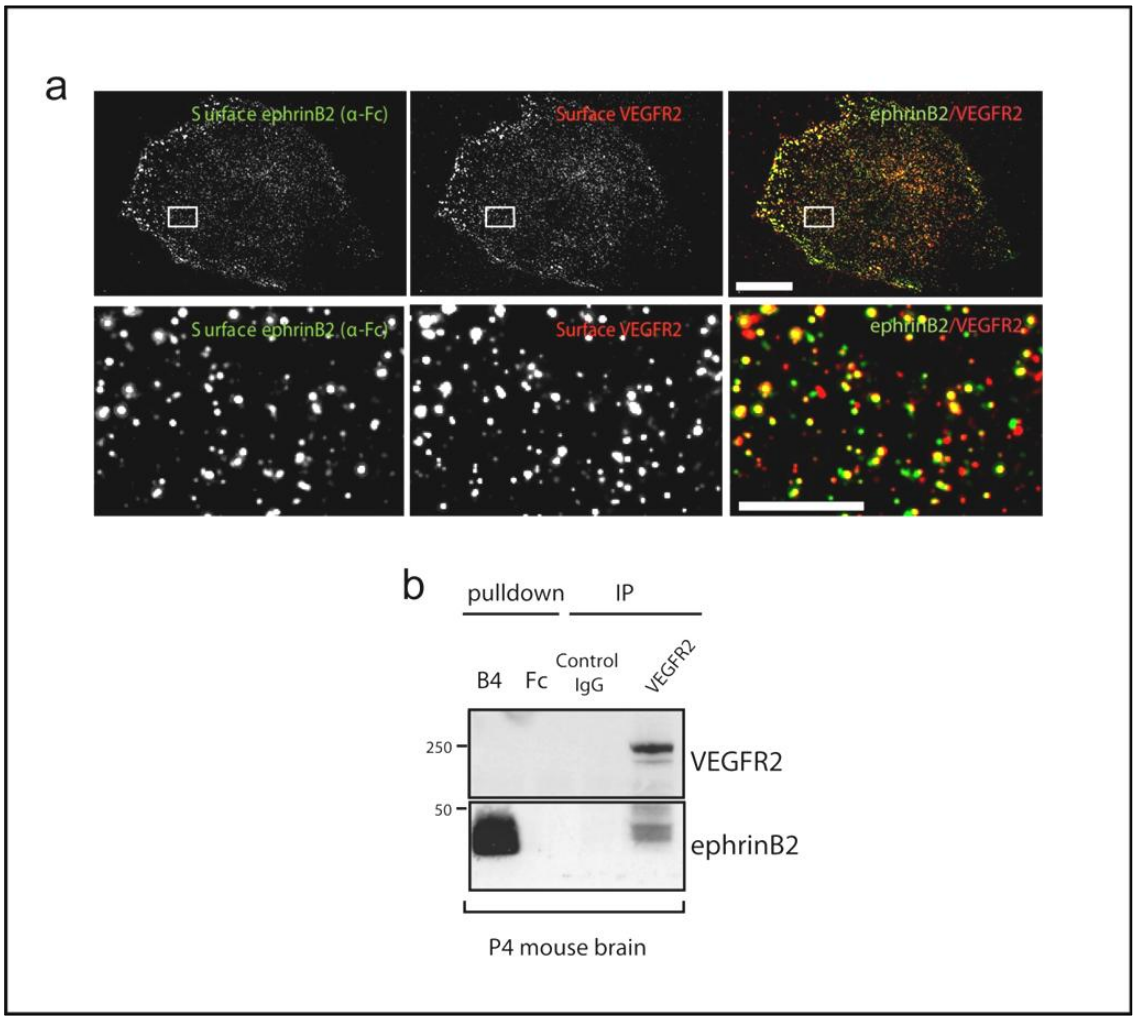

Figure 6-18 EphrinB2 and VEGFR2 co-localized at the cell membrane and co-immunoprecipitated. a, Primary endothelial cells were stimulated with VEGF for 10 min. After fixation, cell surface ephrinB2 stained with EphB4-Fc is shown in green and cell surface VEGFR2 detected with VEGFR2 extracellular domain-specific antibody is shown in red. Higher magnifications figures from the areas indicated with white box are shown in the lower panel. Scale bars: 25 µm in upper panels and 10 µm in lower panels. **b,** VEGFR2 and ephrinB2 form complex *in vivo*. P4 mouse brain lysates were immunoprecipitated with anti-VEGFR2 antibodies or an unrelated antibody as a control and analyzed for co-immunoprecipitated ephrinB2. As a positive control ephrinB2 was pulled down with EphB4-Fc. Data shown in **b** was generated by Essmann C.L.

Taken together the results presented indicate that ephrinB2, acting through its PDZ-dependent signaling, is a potent regulator of VEGFR2 trafficking. The next question to be addressed is whether this function of ephrinB2 PDZ-interactions to trigger the internalization of VEGFR2 from the endothelial cell surface would be relevant for the activation and downstream signaling of the receptor, which might also explain the vascular phenotypes observed before in the *ephrinB2*$^{\Delta V/\Delta V}$ mutant mice.

6.2.6. VEGFR2 activation is compromised in absence of ephrinB2 PDZ-interactions

Upon ligand binding, VEGFR2 is dimerized and initiate *trans* auto-phosphorylation. Several tyrosine phosphorylation sites in the intracellular domain of the receptor serve as docking sites for the recruitment of various effector molecules to transduce receptor signaling. Tyrosine 1175 is known as the focal point of VEGFR2 signaling considering various downstream pathways that mediate diverse cellular responses upon the receptor activation initiated at this site. Therefore, phosphorylation at the tyrosine 1175 of VEGFR2 in endothelial cells lacking ephrinB2 or those bearing different ephrinB2 signaling-deficient mutation was firstly examined by immunofluorescence using an antibody specific for this phosphorylated tyrosine residue. Stimulation of control *ephrinB2*$^{lox/lox}$ MECs with VEGF induced a substantial increase tyrosine 1175 phosphorylation within only 10 min. Of interest, the phosphorylation level of tyrosine 1175 in the control cells is sustained until 30 min after VEGF-stimulation (Fig 6-19). EphrinB2 knockout MECs, by contrast, showed barely

detectable level of VEGFR2 phosphorylation at both time points observed. Phosphorylation at this particular tyrosine residue in the cells bearing mutation in the PDZ-target site of *ephrinB2* was reduced to the same extent as the cells lacking ephrinB2, whereas ephrinB2 phosphotyrosine-deficient cells showed similar level of VEGFR2 phosphorylation as the control cells (Fig. 6-19).

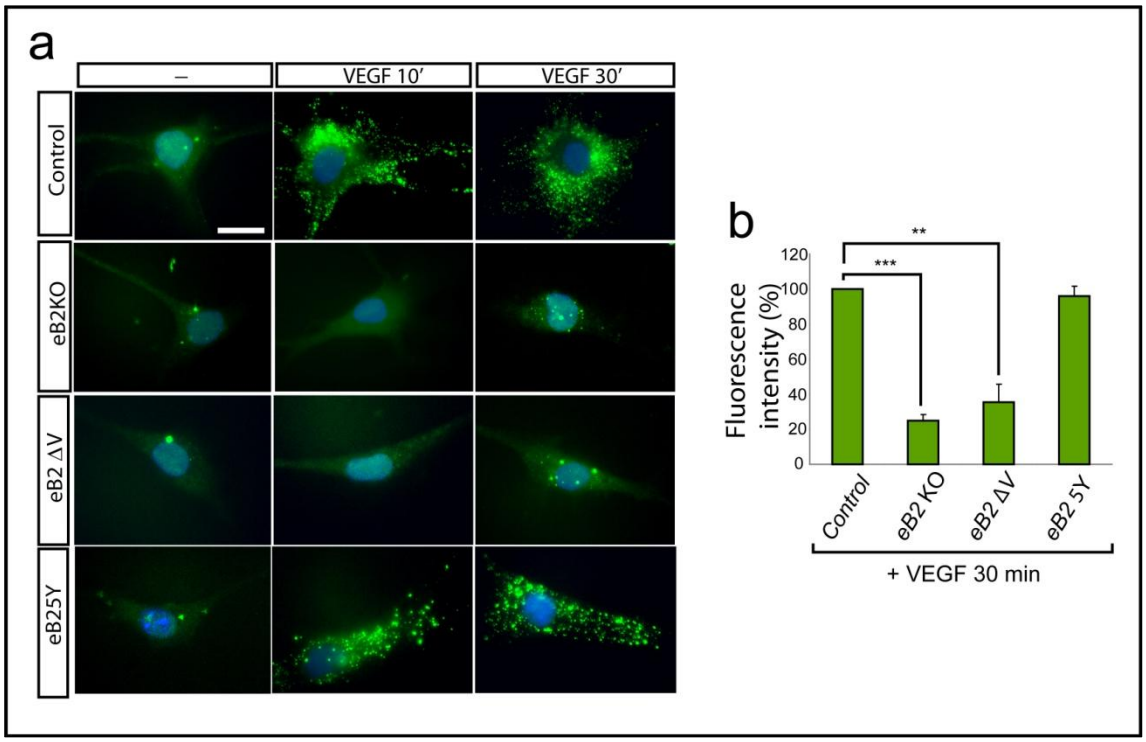

Figure 6-19. VEGF-stimulated phosphorylation of VEGFR2 is compromised in *ephrinB2*$^{\Delta V/\Delta V}$ endothelial cells. **a**, EphrinB2$^{lox/lox}$ (control), ephrinB2 knockout (*ephrinB2*$^{lox/lox}$*; Cre*$^{+}$, eB2 KO), *ephrinB2*$^{\Delta V/\Delta V}$ (eB2ΔV) and *ephrinB2*$^{5Y/5Y}$ (eB25Y) primary endothelial cells were stimulated for 10 and 30 min with VEGF and the levels of VEGFR2 phosphorylation were visualized by immunofluorescence with specific antibodies against the phosphorylated Tyr1175 in VEGFR2. Scale bar is 25 µm. **b**, Quantification of VEGFR2 Tyr1175 phosphorylation based on fluorescence intensities is shown as percentage of phosphorylation in each mutant compared with control cells after 30 min of VEGF treatment. EphrinB2 knockout and *ephrinB2*$^{\Delta V/\Delta V}$ cells showed severely reduced VEGFR2 phosphorylation reaching only 24.92±3.42% and 35.59±10.03% of control cells, respectively. *EphrinB2*$^{5Y/5Y}$ mutant cells displayed up to 95.94±5.58% of VEGFR2 phosphorylation seen in control cells. Error bar represent SEM. Two-tailed t-test, n=3 independent experiments, ** P<0.01, *** P<0.001.

Different auto-phosphorylation sites of VEGFR2 are also involved in distinct cellular mechanisms regulated by the receptor (see chapter 5.3.2). To examine the importance of ephrinB2 on the activation of VEGFR2 and subsequent initiation of signaling cascades at different auto-phosphorylation sites as well as to validate the results observed in cultured cells in an *in vivo* system, phosphorylation levels of tyrosine 1054, 1175, and 1212 were assessed in *ephrinB2*$^{\Delta V/\Delta V}$ mutant mice and wild type littermates. Whole brain lysates from newborn mice were immunoprecipitated with limiting amount of anti-VEGFR2 antibody to avoid unequal amounts of the receptor being pulled out due to less vascular density in the mutant mice. Levels of phosphorylation at tyrosine 1054 located within the receptor kinase domain (Fig. 6-20a), tyrosine 1175 (Fig. 6-20b) and 1214 (Fig. 6-20c) at its carboxy-terminus were assessed by antibodies specific for corresponding phosphorylated tyrosine residues. *EphrinB2*$^{\Delta V/\Delta V}$ mice showed severe reduction in the tyrosine phosphorylation of VEGFR2 at all the sites observed, indicating that in these mutant mice that fail to efficiently internalize VEGFR2, activation of the receptor is also impaired.

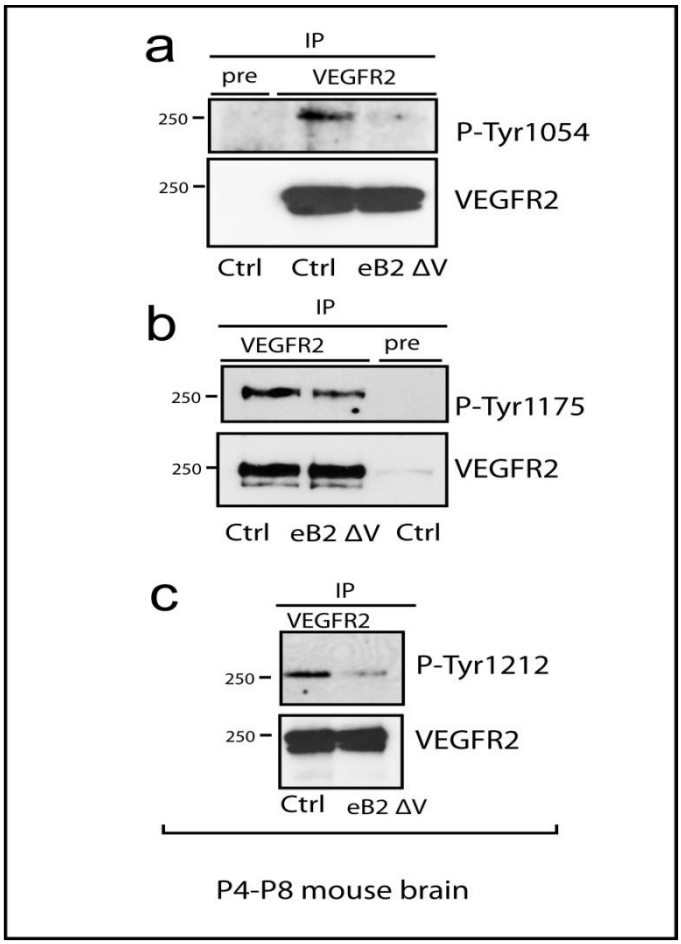

Figure 6-20. *EphrinB2*$^{\Delta V/\Delta V}$ mutant mice show general impairment of VEGFR2 phosphorylation at different tyrosine residues. Newborn mouse brain tissue lysates were immunoprecipitated with anti-VEGFR2 antibody or pre-immune serum as a control and analyzed by western blot with antibodies specific for phosphorylated VEGFR2 on Tyr1054, Tyr1175 or Tyr1212 as indicated. Western blot using anti-VEGFR2 antibody confirmed the equal level total VEGFR2 in the immunoprecipitated fractions. Data shown in **a** and **c** were generated by Essmann C.L.

6.2.7. Endocytosis is essential for VEGFR2 downstream signaling

The data obtained from both *in vitro* and *in vivo* settings shown here provide the proof that ephrinB2 PDZ-dependent signaling is crucial for internalization as well as activation of VEGFR2. The next experiments were therefore aimed to examine the possible functional relevance of VEGFR2 endocytosis for its signal transduction. The potent inhibitor of dynamin-dependent endocytosis, dynasore, was administered to primary endothelial cells prior to stimulation with VEGF. Activation of VEGFR2 was subsequently evaluated by the receptor phosphorylation levels in western blot analysis of the anti-VEGFR2 immunoprecipitated fractions. Co-treatment of VEGF with dynasore resulted in a striking reduction of the VEGFR2 activation assessed at different auto-phosphorylated tyrosine residues as compared with treatment with VEGF alone (Fig 6-21 and Fig. 6-22). These data, consistent with previous report (Lampugnani et al., 2006), suggest the requirement of endocytosis for the activation of downstream signaling of VEGFR2.

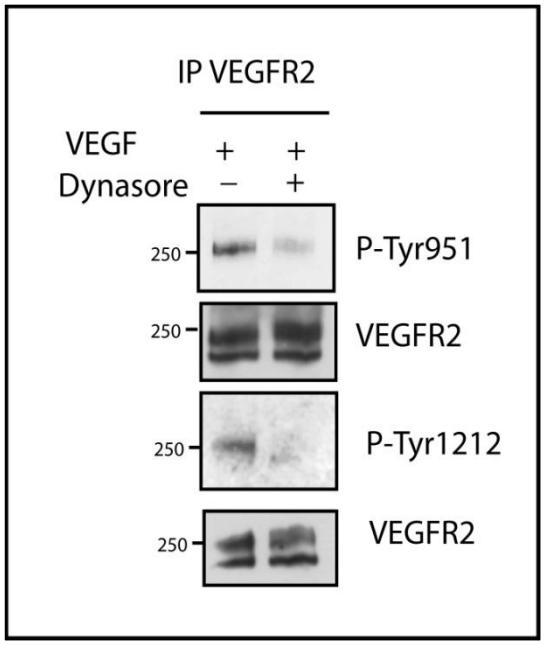

Figure 6-21. Endocytic trafficking is necessary for VEGF-stimulated VEGFR2 phosphorylation. MECs were left untreated or pre-treated for 2 h with dynasore and subsequently stimulated for 30 min with VEGF. Activation of the receptor was assessed by immunoprecipitation of VEGFR2 from the cell lysates and western blot analysis of phosphorylation on Tyr951 and Tyr 1212 using antibodies specific to the corresponding phophorylated tyrosine residue of VEGFR2. Western blot using anti-VEGFR2 antibody confirmed equal level of total VEGFR2 in the immunoprecipitated fractions. Data was generated by Essmann C.L.

6.2.8. VEGFR2 signaling intensity and duration depend on endocytosis of the receptor

Compartmentalization of EGF receptor into endosomes has previously been reported to be essential for its signal transduction by prolonging the duration of signaling with no apparent alteration on signal intensity (Sigismund et al., 2008). To gain more insight into how endocytosis influences the downstream signaling of VEGFR2, its signaling kinetics was examined. The prominent signaling effector of VEGFR2, Akt, is known to play important roles in different molecular pathways involving in proliferative and migratory signals downstream of VEGFR2. The role of endocytosis in the activation of Akt upon VEGF stimulation was therefore investigated. In primary endothelial cells, VEGFR2 phosphorylation (assessed at the tyrosine 1175) robustly occurred within only 5 min following VEGF stimulation. Although phosphorylation level gradually decreased after 5 min, certain level could still be detected 30 min after stimulation. By contrast, in the presence of dynasore drastically a lower level of the receptor phosphorylation was observed 5 min after stimulation and the level was severely reduced until barely detectable very shortly afterwards (Fig 6-22a). Stimulation with VEGF resulted in elevated activation of Akt (assessed by an antibody specific for phosphorylated Akt) reaching its peak at 30 min during the 30 min observation period. In line with the VEGFR2 phosphorylation, both the level of Akt phosphorylation and its activation time-span were greatly reduced in the cells that had been treated with dynasore (Fig. 6-22a). Importantly, *ephrinB2*$^{\Delta V/\Delta V}$ endothelial cells also showed impairment in VEGF-stimulated Akt phosphosphorylation compared with control wild type cells (fig. 6-22b).

These results strongly suggest the crucial role of endocytosis to promote the transition of VEGFR2 to its fully activated state as well as to facilitate sustained signaling downstream of the receptor over a prolonged period. EphrinB2 through its PDZ-interaction motif most likely works as a molecular linker that bridges VEGFR2 to the endocytic machinery and thereby makes possible the transduction of its signal to cellular responses.

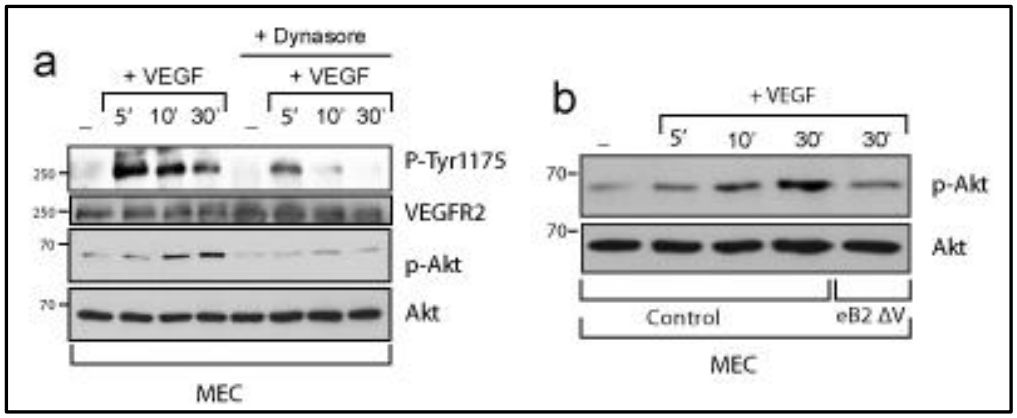

Figure 6-22. Activation and prolongation of signaling downstream of VEGFR2 require receptor endocytosis. a, MECs were left untreated or pre-treated for 2 h with Dynasore and subsequently stimulated for the indicated times with VEGF. Activation of the receptor was assessed by phosphorylation on Tyr1175 in total cell lysates. VEGFR2 downstream signaling was assessed by level of Akt phosphorylation. Inhibition of endocytosis causes a drastic decrease of VEGFR2 phosphorylation and impairment of its signal transduction, affecting both intensity and duration of the signaling. **b,** VEGFR2 signaling is defective in *ephrinB2*$^{\Delta V/\Delta V}$ endothelial cells. MECs isolated from *ephrinB2*$^{\Delta V/\Delta V}$ (eB2ΔV) or control wild type mice were left untreated or stimulated with VEGF for the indicated times. VEGFR2 downstream signalling was assessed by Akt phosphorylation. Total levels of VEGFR2 and Akt in the lysates were used as loading control. Data generated by Essmann C.L.

6.3. EphrinB2 regulates endothelial tip cell filopodial extension by triggering VEGFR2 internalization

The finding of the novel role of ephrinB2 to mediate internalization of VEGFR2 together with the reported function of VEGFR2 in control of tip cell sprouting activity urge an appealing assumption that the regulation of filopodial extension by ephrinB2 might involve its capability to trigger VEGFR2 endocytosis and downstream signaling. To test this, a short-term culture system of explanted retinas was developed. Briefly, retinas were dissected from P4-5 pups and flat-mounted onto hydrophilic membrane filter with the nerve fiber layer facing the membrane. Cultured medium was layered under the filter. Retina explants were incubated for 2-4 h for recovery. Stimulation of acute tip cell responses was carried out for 4h by addition of exogenous stimulators and/or inhibitor into the medium.

6.3.1. VEGF-induced extension of endothelial tip cell filopodia requires receptor endocytosis

Explanted retinas robustly responded to stimulation with VEGF as evidenced by the drastic increase in number of filopodial extensions at the sprouting front of vascular bed (Fig. 6-23). This observation confirms the cellular function of VEGFR2 as a pivotal regulator of actin dynamic and guided migration of endothelial tip cells. Simultaneous treatment of explanted retinas with VEGF and dynasore dampened the stimulatory effect of VEGF and caused the reduction in number of filopodial extensions to almost the basal level when no stimulant was presented (Fig. 6-23), demonstrating the crucial requirement of endocytosis for VEGFR2 function at the endothelial tip cell.

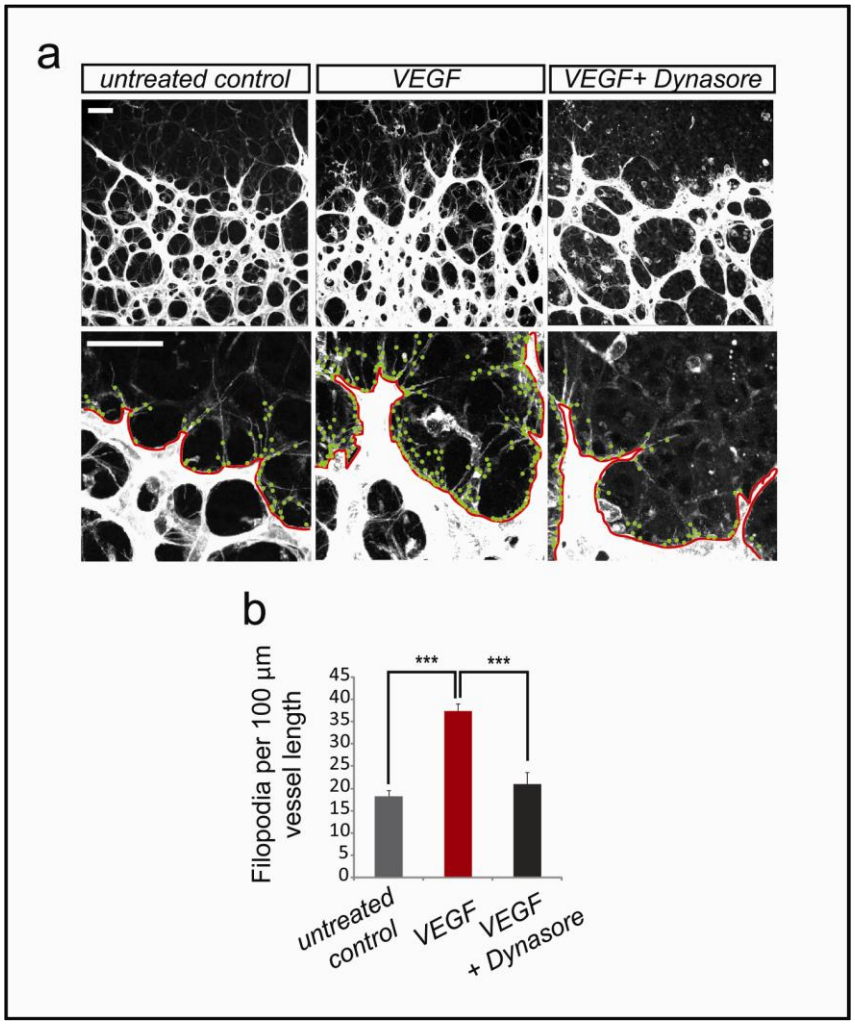

Figure 6-23 Acute stimulation of explanted retina with VEGF induces tip cell filopodial extension in an endocytosis-dependent manner. a, P4 retina explants were stimulated with VEGF or simultaneously treated with VEGF and Dynasore for 4 h. Vessels were stained with isolectin-B4 and filopodial extension along the length of the sprouting front was analyzed. In the lower panels are high magnification pictures of the same vascular beds shown in the upper panels. Green dots indicate filopodia and red lines show the length of vascular front. Scale bars represent 25 µm. **b**, Quantification of filopodial extension per vessel length revealed an average of 18.21±1.34 filopodia per 100 µm of vessel length in the untreated control which was increased up to 37.39±1.6334 filopodia per 100 µm of vessels after VEGF-stimulation. In the presence of Dynasore, VEGF-stimulation failed to promote filopodial extension. Only 20.99±2.69 filopodia per 100 µm vessel length (in average) was observed following the co-treatment of Dynasore and VEGF. Error bars represent SEM. Two-tailed t-test, n=10-12 retinas in each condition, *** P<0.001.

6.3.2. Activation of ephrinB2 signaling is sufficient to rescue compromised filopodial extension caused by VEGF deprivation

In agreement with the evidences presented above that point out to a crucial requirement of ephrinB2 PDZ-interactions for VEGFR2 endocytosis and activation of its downstream signaling, stimulation of ephrinB2 reverse signaling in explanted retinas with EphB4-Fc resulted in a significant increase in the extension of filopodial structures at the leading front of vascular network (Fig. 6-24). The effect following EphB4-Fc stimulation was similar to the cellular response observed upon VEGF-stimulation (Fig. 6-23). To further verify the entwined relation between VEGFR2 and ephrinB2 signaling cascades and the dependency of the former on the latter to exert its function particularly in the endothelial tip cells, the ability of ephrinB2 to trigger activation of VEGFR2 signaling and consequently rescue the cellular outcome of inactivated VEGFR2 was examined.

Figure 6-24. Activation of ephrinB2 induces tip cell filopodial extension in explanted retinas. **a**, P4 retina explants were stimulated with pre-clustered EphB4-Fc or hFc for 4h. Vessels were stained with isolectin-B4 and filopodial extension at the sprouting front was analyzed. In the lower panel are high magnification pictures of the upper panel. Green dots indicate filopodia and red lines show the length of vascular front. Scale bars represent 25 µm. **b**, In the control condition in which only Fc was presented, retina explants exhibited 19.27±3.13 filopodia per 100 µm of vessel length (in average). Upon stimulation with EphB4-Fc, filopodia extension was increased up to an average of 29.83±1.81 per 100 µm of vessels. Error bars represent SEM. Two-tailed t-test, n=10-12 retinas in each conditions, ** P<0.001.

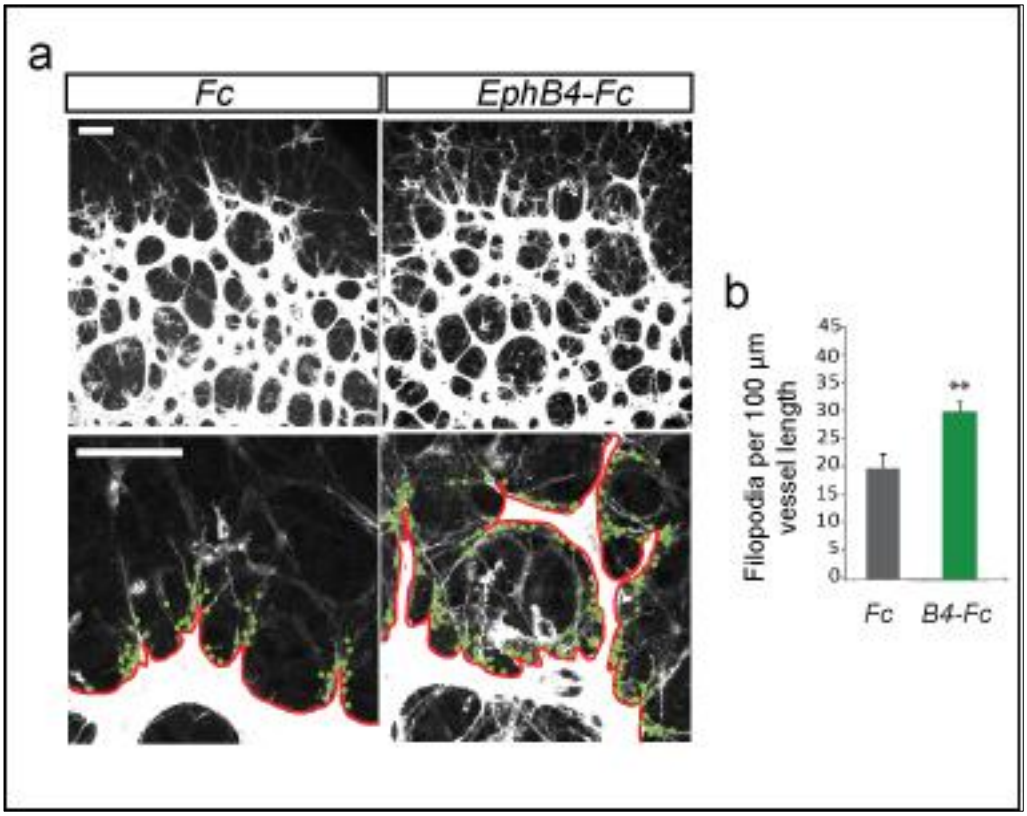

Soluble VEGFR1 extracellular domain-Fc fusion protein (sFlt1) has previously been shown to efficiently inhibit VEGFR2 activation. The mode of action of this inhibitor is based on its higher VEGF-binding affinity as compared with VEGFR2, which therefore make it an efficient competitor to bind and seclude VEGF from VEGFR2. Intraoccular injection of sFlt1 has previously been reported to cause a complete retraction of endothelial tip cell filopodia at the sprouting front of retinal vasculature (Gerhardt et al., 2003). Similarly, deprivation of VEGF and thus inhibition of VEGFR2 activation by sFlt1 treatment abrogated extension of filopodia in explanted retina vessels (Fig. 6-25). Importantly, co-treatment of sFlt1 with EphB4-Fc to activate ephrinB2 reverse signaling was able to diminish the inhibitory effect of sFlt1 and rescue filopodial extension in the explants (Fig. 6-25), underscore the credible role of ephrinB2 as a prime regulator of VEGFR2 internalization and activation of its downstream signaling to control the active sprouting activity of endothelial tip cells.

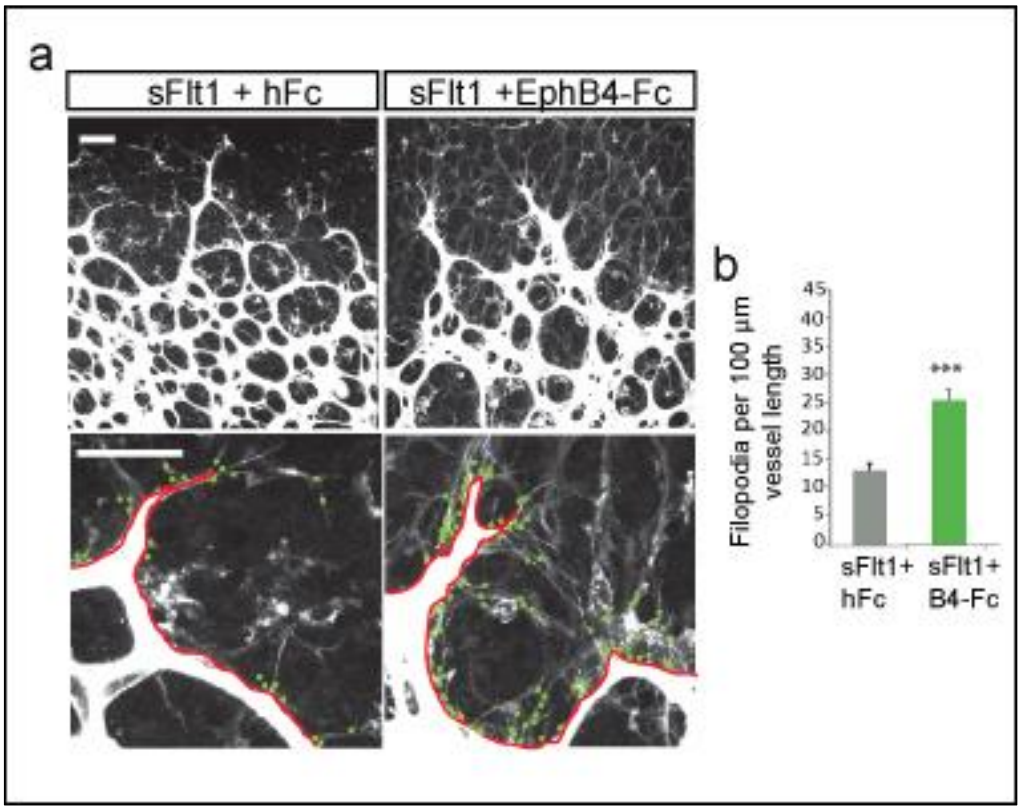

Figure 6-25 EphrinB2 activation rescues tip cell filopodial dynamics following VEGF sequestering. a, P4 retina explants were simultaneously treated with soluble Flt-1 (sFlt1) and hFc or sFlt1 and EphB4-Fc for 4h. Vessels were visualized by isolectin-B2 staining and filopodial extension at the sprouting front was analyzed. In the lower panels are high magnification pictures of the same vascular beds shown in upper panels. Green dots indicate filopodia and red lines show the length of vascular front. Scale bars represent 25 µm. **b**, Quantification of number of filopodial processes per vessel length is shown in average values. Retinal explants treated with sFlt1 and hFc showed 13.01±1.33 filopodia per 100 µm of vessels. In the presence of EphB4-Fc number of filopodia was increased to 25.46±1.92 per 100 µm of vessels. Error bars represent SEM. Two-tailed t-test, n=10-12 retinas in each conditions, *** P<0.0001.

6.4. EphrinB2 PDZ-signaling in endothelial cells influences tumor growth by regulating tumor angiogenesis

Tumors are long known to trigger angiogenic growth of blood vessels in host organs in order to attain oxygen and nutrients sufficient to supply rapid growth of tumor masses as well as to gain access to remote tissue by intravasation into the blood stream through these

abnormally developed hyperdilated vessels. Secretion of VEGF as evident in a number of different tumor types is the well-known mechanism by which tumors induce vessel sprouting. VEGF production is also dependent on oxygen levels in the microenvironments. Under hypoxic conditions such as the ones found when tumor masses are overgrown and oxygen supply from the existing vascular system cannot compensate for such rapid growth rate, VEGF expression is upregulated to attract vessel outgrowth toward the hypoxic areas by acting through VEGFR2 abundantly expressed in the vascular endothelium. Since our previous data has identified ephrinB2 PDZ-dependent signaling in collaboration with VEGFR2 to control the extension of tip cell filopodia during guided migration of developing vessels, it is appealing to speculate that similar signaling mechanism downstream of ephrinB2 might also be involved in VEGFR2 function during tumor angiogenesis.

6.4.1. Blockade of ephrinB2 PDZ-signaling decreases brain tumor growth and reduces angiogenic sprouting of tumor vasculature

To address the role of ephrinB2 reverse signaling via PDZ-interactions on tumor progression, an orthotopic glioma tumor model was employed. Firstly, the high grade syngenic astrocytomas were generated according to a previous report where this tumor model has been proved to be a successful tool to reveal the functional significance of HIF and VEGF in tumor angiogenesis and progression (Blouw et al., 2003). In brief, astrocytes isolated from new born mice were immortalized by stable transfection with SV40 large T antigen. The immortalized astrocytes were subsequently transformed into astrocytomas by viral transduction of constitutively active H-ras (V-12H-ras). Colonies that grew in selective media were checked for expression of SV40 large T antigen and V-12H-ras by western blot analysis (Fig. 6-26).

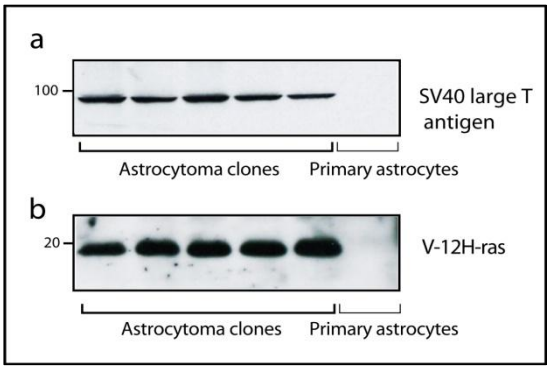

Figure 6-26 Characterization of high grade astrocytomas. Expression of SV40 large T antigen (**a**) and V-12H-ras (**b**) in syngenic astrocytomas was analyzed by western blot using corresponding antibodies. High levels SV40 large T antigen and V12H-ras were detected in all the astrocytoma clones, but not in the primary astrocytes which were used as negative control.

A pool of several astrocytoma clones expressing high level of SV40 large T antigen and V12H-ras were injected intracranially into *ephrinB2*$^{\Delta V/\Delta V}$ mice and wild type littermates of the same crossing generation as those mice from which the cells were generated to preserve the same genetic background and avoid an immune rejection. Intracranial tumor growth in *ephrinB2*$^{\Delta V/\Delta V}$ mutant mice was severely reduced reaching less than 25% of control tumors grown in wild type littermates (Fig. 6-27).

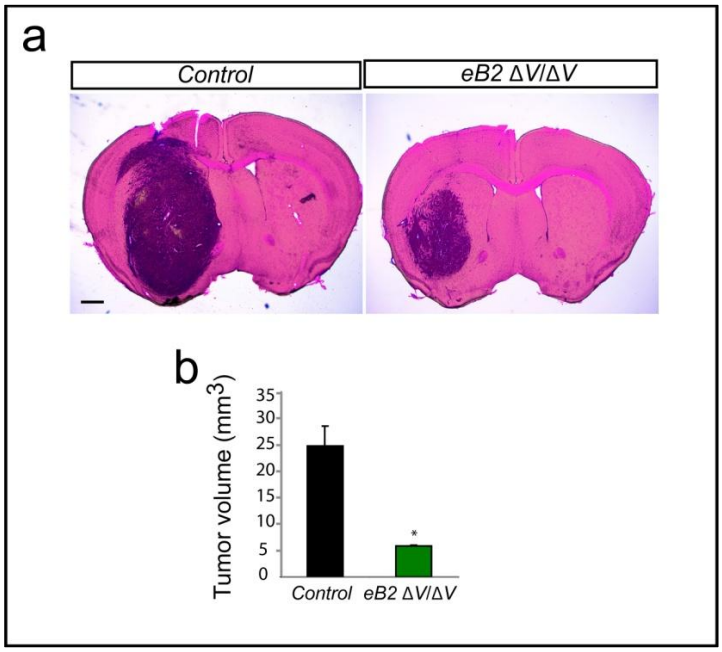

Figure 6-27 Intracranial astrocytoma growth is reduced in *ephrinB2*$^{\Delta V/\Delta V}$ mice compared with wild type littermates. a, Tumors grown in *ephrinB2*$^{\Delta V/\Delta V}$ (eB2 ΔV/ΔV) mutant mice or wild type littermates (control) were stained with hematoxylin-eosin (HE). Scale bar represent 1 mm. **b**, Quantification using a semi-automated stereological system revealed an average tumor volume of 24.38±4.61 mm^3 in control animals and 5.82±0.19 mm^3 in *ephrinB2*$^{\Delta V/\Delta V}$ mutants. Error bars represent SEM. Two-tailed t-test, n=7-11 tumors from each genotype, * P<0.05. Astrocytomas injection and analysis of tumor volumes were performed by Siedel S.

The stunted tumor growth in *ephrinB2*$^{\Delta V/\Delta V}$ mice was associated with striking reduction of tumor vascularization as reflected by quantification of the vascular density from the endothelial marker CD34-positive areas within tumor beds (Fig. 6-28c). Similar reduction in the perfused vascular area (marked by intravascular lectin) revealed that functional vessels in tumors grown in *ephrinB2*$^{\Delta V/\Delta V}$ mice were as well decreased (data not shown). Morphologically, the vasculature of control tumors was hyperdilated and torturous (Fig. 6-28a), reflecting the unusual high level of pro-angiogenic stimulants that shift the balance in the angiogenesis program in favor of vessel expansion and therefore hinder maturation processes. Vascular sprouts and filopodial extensions were readily detectable on these tumor vessels (Fig. 6-28b). By contrast, the vasculature of tumors grown in *ephrinB2*$^{\Delta V/\Delta V}$ mice was less torturous and resembled the normal brain vessels found under physiological conditions (Fig. 6-28a). Importantly, similar to the angiogenic sprouting defects observed in *ephrinB2*$^{\Delta V/\Delta V}$ mutant retinas, the filopodia-rich newly formed vascular sprouts were barely detectable in these tumors (Fig. 6-28b). This data points out the important role of ephrinB2 PDZ-dependent signaling in tumor-induced angiogenic sprouting and tumor growth.

Figure 6-28 Angiogenic sprouting of intracranial astrocytomas grown in *ephrinB2*$^{\Delta V/\Delta V}$ mice is impaired. **a**, Vascularization of astrocytomas grown in *ephrinB2*$^{\Delta V/\Delta V}$ (eB2 ΔV/ΔV) mutant mice and wild type littermates (control) were assessed by CD34 staining. **b**, Higher magnification images of tumor vessels show vascular sprouts. Arrows point to filopodial extensions in the tumor vessels. Note the smooth and normalized vessels in the *ephrinB2*$^{\Delta V/\Delta V}$ mutants. Scale bars represent 100 µm in **a** and 25 µm in **b**. **c**, Quantification of vessel density is based on the area covered by vessel staining and shown in average percentages. Control tumors showed 12.78±0.77% vessel density, whereas *ephrinB2*$^{\Delta V/\Delta V}$ mutant tumors had only 7.64±0.65% of vascularized area. Error bars represent SEM, Two-tailed t-test, n=7-11 tumors from each genotype, * P<0.05. Data generated by Siedel S.

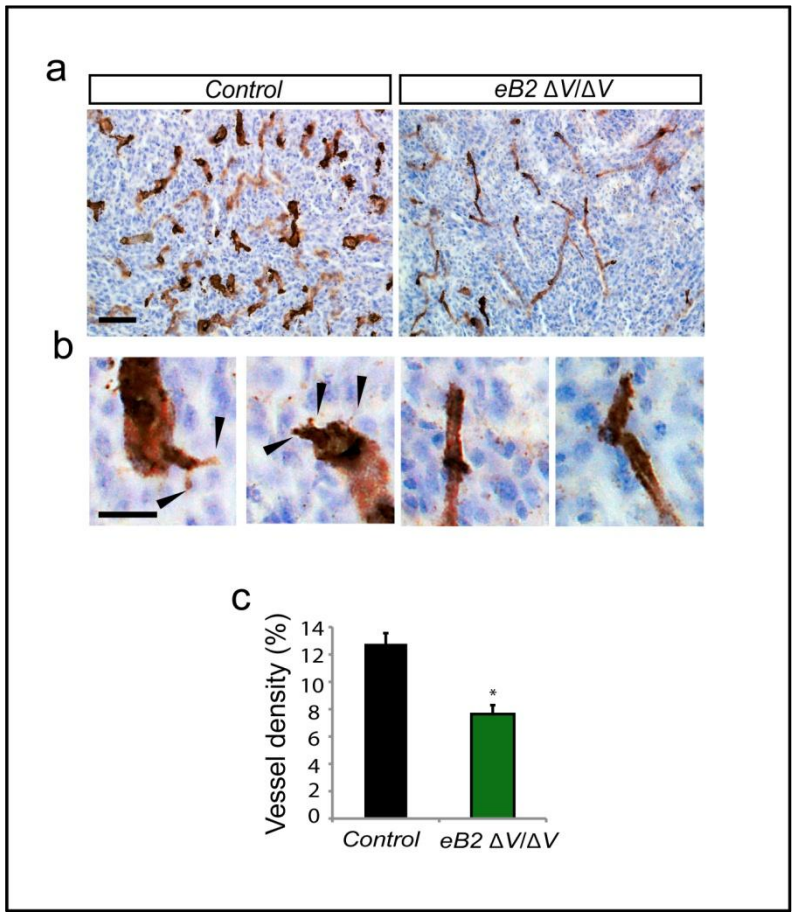

6.4.2. Endothelial-specific loss of ephrinB2 is sufficient to inhibit tumor angiogenesis

Given the global expression of ephrinB2ΔV protein in the mutant mice, the effects on tumor growth and vascularization could not yet be pinpointed to reflect a direct role of ephrinB2 in endothelial cells. To assess tumor growth in the context of endothelial specific ephrinB2 deficiency Gl261 astrocytomas were injected intracranially in the tamoxifen-inducible endothelial specific ephrinB2 knockout mice (tamoxifen-treated *ephrinB2*$^{loxP/loxP}$*; VE-Cadherin-CreER2*$^{+}$, *ephrinB2*$^{i\Delta EC}$) and control littermates (*ephrinB2*$^{WT/loxP}$*; VE-Cadherin-CreER2*$^{-}$ treated with tamoxifen). The severe reduction of tumor growth in the *ephrinB2*$^{\Delta V/\Delta V}$ mutant mice was reproducible in the endothelial-specific ephrinB2 deficient mice (Fig. 6-29).

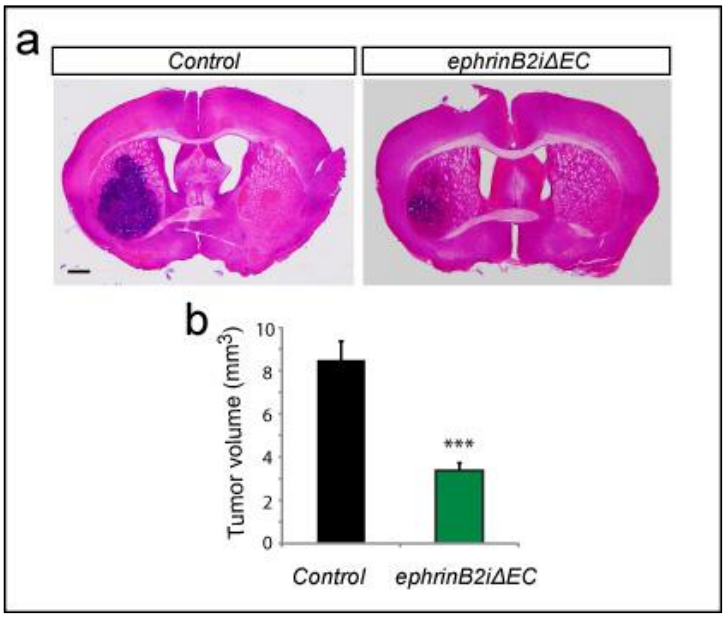

Figure 6-29 Endothelial-specific *ephrinB2* knockout mice show arrested intracranial tumor growth. **a**, Intracranial growth of Gl261 astrocytomas was reduced in mice with an endothelial-specific tamoxifen-inducible ephrinB2 loss-of-function (*ephrinB2*$^{i\Delta EC}$) as compared with tumors grown in control littermates. Tumors were stained with hematoxylin-eosin (HE). Scale bar represent 1 mm. **b**, Quantification of tumor volumes revealed a substantial reduction from an average of 8.48±0.89 mm^3 in control mice to 3.37±0.36 mm^3 in *ephrinB2*$^{i\Delta EC}$ mice. Error bars represent SEM, Two-tailed t-test, n=8-9 tumors from each genotype, *** P<0.001. Tumor injection and analysis of tumor volumes were performed by Siedel S.

Moreover, in consistent with the impairment in angiogenic sprouting of the tumor vasculature seen in *ephrinB2*$^{\Delta V/\Delta V}$ mice, a drastic reduction in tumor vascular density (Fig. 6-30c) as well as morphologically similar vessels which were smooth and devoid of sprouts (Fig. 6-30a, b) were also observed in tumors grown in endothelial-specific ephrinB2 knockout mice. These results suggest the cell-autonomous endothelial-specific function of ephrinB2 in the regulation of tumor angiogenesis.

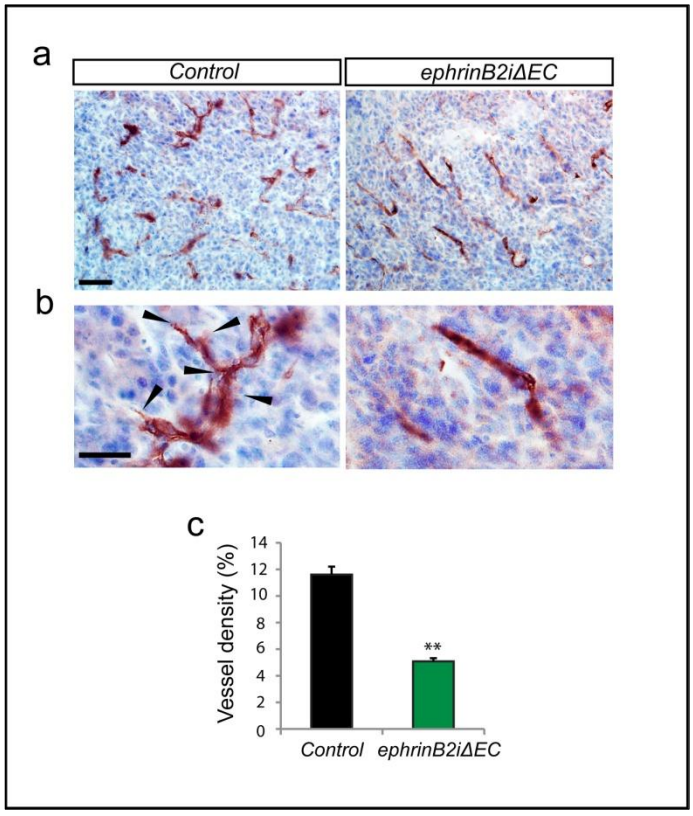

Figure 6-30 EphrinB2 function during pathological sprouting angiogenesis is endothelial cell specific. a, Vascularization of intracranial tumors grown in endothelial-specific ephrinB2 knockout mice (*ephrinB2*$^{i\Delta EC}$) and control littermates was examined by immunostaining with CD34. **b**, High magnification images show detailed morphology and spouting activity of tumor vessels readily observed by the extension filopodial processes (indicated with black arrowheads). Scale bars represent 100 µm. **c**, Quantification of vessel density based on area of tumor masses covered by vessel staining revealed an average of 11.61±0.60% and 5.08±0.24% of vessel coverage in control and *ephrinB2*$^{i\Delta EC}$ tumors, respectively. Error bars represent SEM. Two-tailed t-test, n=5 tumors from each genotype, ** P<0.01. Data generated by Siedel S.

6.4.3. Pathological angiogenesis in different vascular beds are commonly controlled by ephrinB2

The effect of the disruption of ephrinB2 PDZ-signaling on tumor angiogenesis was also observed in different vascular beds as evidenced in the analysis of a heterotopic tumor model. Astrocytomas subcutaneously injected in *ephrinB2*$^{\Delta V/\Delta V}$ mice formed substantially smaller tumors as compared with tumors grown in wild type littermates (Fig. 6-31).

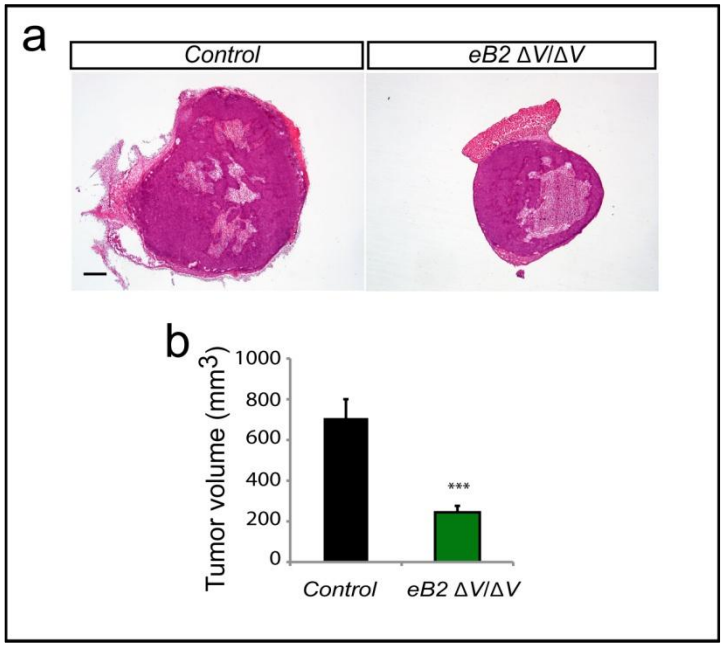

Figure 6-31 Subcutaneous tumor growth is reduced in *ephrinB2*$^{\Delta V/\Delta V}$ mice compared with wild type littermates. a, Astrocytomas grown in *ephrinB2*$^{\Delta V/\Delta V}$ (eB2 ΔV/ΔV) mice and wild type littermates (control) were stained with hematoxylin-eosin (HE). Scale bar represent 100 µm. **b**, Quantification of tumor volume by a semi-automated stereological system showed that tumors in *ephrinB2*$^{\Delta V/\Delta V}$ mutant mice only grew up to 244.42±31.69 mm^3, whereas tumors grown in control animals reached the size of 707.50±92.87 mm^3 (in averages). Error bars represent SEM. Two-tailed t-test, n=15-17 tumors from each genotype, *** P<0.001. Tumor injection and analysis of tumor volumes were performed by Siedel S.

Concurrently, analysis of tumor vascularization revealed decrease in vessel density in the tumors grown under the skin of *ephrinB2*$^{\Delta V/\Delta V}$ mutant mice (Fig. 6-32c). Tumor vessels in these mutant mice were also less tortuous and lacked the filopodia-extending vascular sprouts (Fig. 6-32a, b).

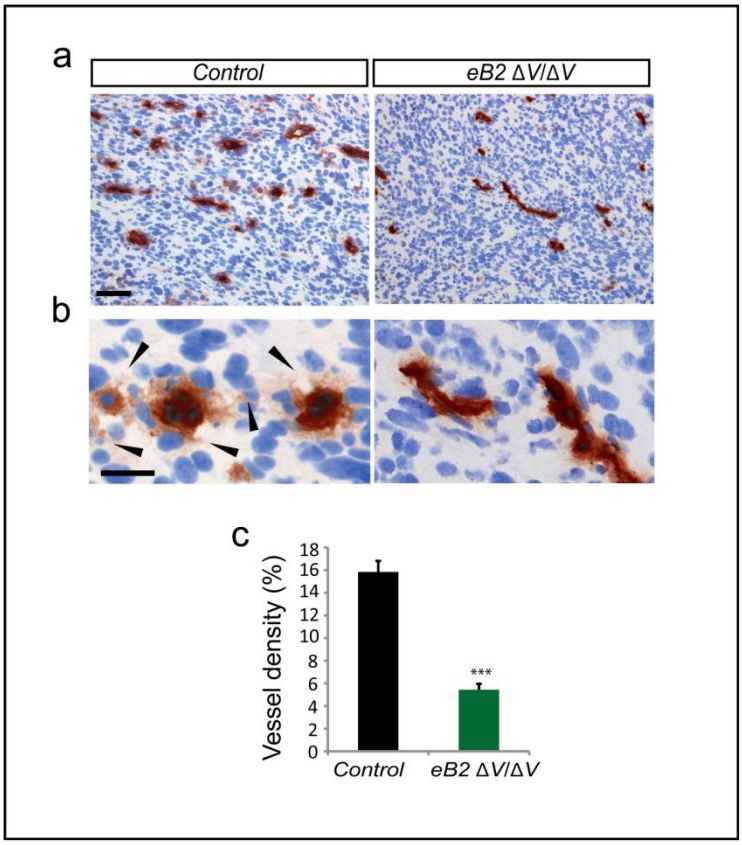

Figure 6-32 Angiogenesis is impaired in tumors developed subcutaneously in *ephrinB2*$^{\Delta V/\Delta V}$ mutant mice. **a**, Vasculature of subcutaneous tumors grown in *ephrinB2*$^{\Delta V/\Delta V}$ (eB2 ΔV/ΔV) mutant mice and wild type littermates (control) were labeled by CD34 staining. **b**, Higher magnification images showed active filopodial sprouting as indicated by black arrowheads, observed in control but not *ephrinB2*$^{\Delta V/\Delta V}$ mutant tumors. Scales bars: **a**, 100 µm and **b**, 25 µm. **c**, Quantification of vessel density is based on area of tumor masses covered by vessel staining. Tumors of control animals showed an average of 15.85±0.97% vascular coverage, in comparison to tumors grown in *ephrinB2*$^{\Delta V/\Delta V}$ mutant animals in which only 5.45±0.52% of tumor area was vascularized. Error bars represent SEM. Two-tailed t-test, n=8 tumors from each genotype, *** P<0.001. Data generated by Siedel S.

These data demonstrate the significant function of ephrinB2 through PDZ-dependent signaling as a potent regulator of active angiogenic sprouting not only in normal development, but also in tumor-induced pathological growth of blood vessels and thereby influencing tumor progression.

7. Discussion

Eph/ephrin bi-directional signaling has been widely appreciated as one of the most important guidance cue in charge of directing axonal growth cones to their appropriate targets during the wiring of the complex neural circuits. The work presented in this dissertation has identified a novel function of ephrinB2 reverse signaling via PDZ-interactions in the control of endothelial tip cells sprouting activity during angiogenic growth of blood vessels in both physiological and pathological settings. Molecularly, ephrinB2 exerts its function in concert with the pivotal angiogenesis regulator VEGFR2 by controlling the receptor endocytosis and its subsequent signal transduction.

Directional migration guided by receptors -localized at the surface of migrating cells- and their cognate ligands presented in the extracellular matrix or guidepost cells along the migration routes is tightly regulated by receptor endocytosis (Jekely et al., 2005; Palamidessi et al., 2008). Intracellular compartmentalization and recycling of surface RTKs has been proposed to ensure localized intracellular responses to guidance cues by spatially restricting signaling activation (Jekely et al., 2005; Palamidessi et al., 2008). The results presented here reinforce such a model of RTK-mediated guidance event during the outgrowth of newly formed vascular sprouts. Activation of ephrinB2 promotes VEGFR2 endocytosis which allows the proper spatial activation and signaling downstream of the receptor at the endothelial tip cell filopodia (Fig 7-1). The appropriately localized activation of VEGFR2 at

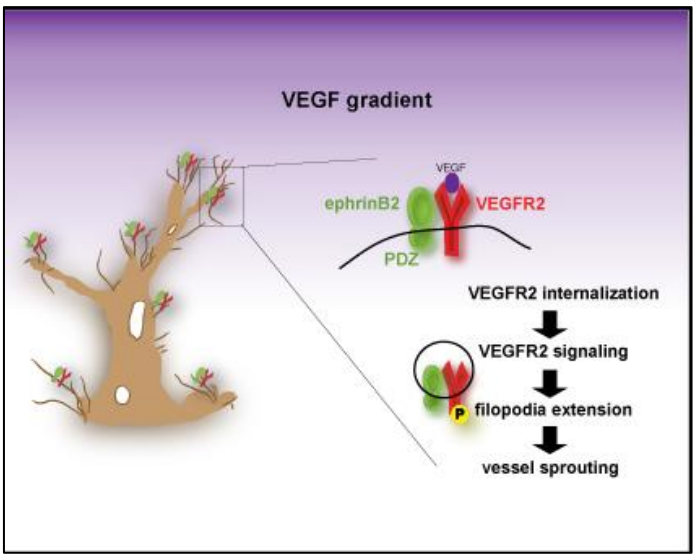

Figure 7-1 Role of ephrinB2 in endothelial tip cell. EphrinB2 expressed at the tip cell filopodia regulates endocytosis and signaling to control filopodia extension and guided migration of vascular sprouts. Black line; plasma membrane; black circle, endocytic vesicle; yellow circle marked with P, phosphorylated tyrosines at the intracellular domain of VEGFR2.

the tip cell filopodia might stabilize the contact to perivascular cells such as astrocytes and help to direct the oriented migration of endothelial cells.

The finding of the defective angiogenesis in tumors injected in mice with disrupted ephrinB2 PDZ-signaling suggests a general mechanism by which ephrinB2 plays a key role to control VEGFR2 function during normal development as well as pathological conditions. In addition, the function of ephrinB2 as a regulator of VEGFR trafficking might not be restricted only to VEGFR2. VEGFR3, the major regulator of lymphangiogenesis whose role in active angiogenesis of blood vasculatures in both developmental and pathological settings has recently been revealed (Tammela et al., 2008), has been shown to internalized from the plasma membrane in an ephrinB2-dependent manner (Wang et al.).

Blockade of ephrinB2 signaling to simultaneously interfere both with VEGFR2 and VEGFR3 functions might therefore represent an intriguing alternative of anti-angiogenic treatment for tumor therapy.

7.1. VEGFR2 internalization is required for the full activation of downstream signaling

The concept that cell surface receptors could activate their downstream signaling intracellularly has been supported by continuously growing evidences from various receptor/ligand systems. Internalization of VEGFR2 was previously believed to only direct the surface receptor to the intracellular degradation machinery and thereby serve as a desensitizing mechanism to control cellular responses to VEGF stimulation. In contrast to this earlier dogma, Lampugnani et al. has shown that internalized VEGFR2 remained activated and its signaling activity, as assessed by activation of p44/42 MAPK, was sustained. Furthermore, association of VEGFR2 with the adherens junction protein VE-Cadherin inhibits VEGFR2 internalization and reduces its downstream mitogenic signaling activity (Lampugnani et al., 2006). In accord to this study, Lee et al. reported an endogenous VEGF signaling pathway that is crucial for vascular homeostasis. Genetic deletion of *VEGF* specifically in endothelial cells causes increased cell death leading to catastrophic circulatory collapse and death of these mutant mice. Exogenous VEGF is unable to compensate for the absence of autocrine endothelial VEGF. In addition, phosphorylation of

VEGFR2 is suppressed by a small molecule antagonist that can freely enter the cell, but not by an extracellular VEGF inhibitor, suggesting that activation of the receptor is likely to occur intracellular (Lee et al., 2007). The data presented in this dissertation not only underscore the crucial role of endocytosis in VEGFR2 signaling, but also provide for the first time an evidence of the control of the receptor migratory signal by endocytosis during the angiogenic sprouting process. Moreover, ephrinB2 is identified here as a key player in the regulatory mechanism that controls VEGFR2 endocytosis.

The results presented here demonstrate the striking reduction of VEGFR2 phosphorylation observed in all the major autophosphorylation sites when the receptor endocytosis is inhibited by the dynamin inhibitor, dynasore, as well as in mutant mice lacking ephrinB2 PDZ-dependent signaling. Activation of Akt, a well-known downstream effector of VEGFR2, is also suppressed in a similar manner. These results point out the crucial importance of endocytosis for the full activation of VEGFR2 and its downstream signals. It has previously been proposed that retaining of VEGFR2 at the cell surface makes the receptor accessible to protein tyrosine phosphatases and therefore leads to the dephosphorylation of the receptor and inhibition of its downstream signaling (Lampugnani et al., 2006; Mattila et al., 2008). Two tyrosine phosphatases have been implicated in the VEGFR2 dephosphorylation. The transmembrane phosphatase DEP-1 (Density-enhanced phosphatase 1, also known as CD148) is associated with VE-Cadherin and VEGFR2 complex at the cell-cell junctions (Borges et al., 1996; Carmeliet et al., 1999). DEP-1 regulates VE-Cadherin-mediated contact inhibition of endothelial cell proliferation via the dephosphorylation of VEGFR2 (Lampugnani et al., 2002). *In vivo*, *DEP-1* knockout mice exhibit early lethality due to defective vascular development associated with increased endothelial cell proliferation (Takahashi et al., 2003). It will be very interesting to study, using the conditional deletion of DEP-1, to which extent this phosphatase is regulating the function of VEGFR2 during sprouting angiogenesis in the retina and in tumor settings. Another phosphatase, T-cell protein tyrosine phosphatase (TCPTP) that, despite its name, is widely expressed in several cell types (Alonso et al., 2004) has also been shown to involve in control of VEGFR2 signaling. In response to α1β1 integrin-mediated cell adhesion to collagenous matrix TCPTP is translocated from the nucleus to the cytoplasm (Mattila et al.,

2005). Overexpression of constitutively active TCPTP could bind to and dephosphorylate VEGFR2 and prevent its internalization in an *in vitro* model. Activation of TCPTP by the cytoplasmic tail of collagen-binding integrin α1 inhibited endothelial cell migration (Mattila et al., 2008). This inhibitory function of TCPTP has been proposed to be important for the maturation of newly developed vessels. Activation TCPTP by intergrin α1β1 upon binding to collagen-rich newly generated endothelium basement membrane could possibly inhibit VEGFR2 activation and thereby attenuate the invasive activity of endothelial cells (Mattila et al., 2008). TCPTP-deficient mice die shortly after birth from an inflammatory phenotype due to impaired immune system (You-Ten et al., 1997). The survival of these mice over the course of embyogenesis suggests that TCPTP is not crucial for vasculogenesis. Its involvement in angiogenesis is, however, have not yet been examined *in vivo*,

Interestingly, DEP-1 has been shown to target specifically the tyrosine residues within the kinase activation loop of VEGFR2, Tyr1054/1059, but not other autophosphorylation sites (Chabot et al., 2009). These phosphorylation sites have also been reported to be substrates of TCPTP (Mattila et al., 2008). Phosphorylation at these tyrosine residues seems to be required for maximal level of the receptor kinase activity (Kawamura et al., 2008). The observations on decreased internalization of VEGFR2 in the presence of DEP-1 and constitutively active TCPTP as well as the previous report of the delay VEGF-induced receptor internalization upon heterotropic expression of VEGFR2 in which tyrosine 1054 and 1059 were mutated to phenylalanine (Dougher and Terman, 1999), suggest that certain level of VEGFR2 phosphorylation at least at the tyrosine residues in its kinase activation loop might be a prerequisite for the initiation of receptor internalization. Once endocytosed into the intracellular compartments, VEGFR2 is fully activated and signaling effectors are recruited to transducer its signal to various cellular responses.

7.2. Endocytosis and spatial distribution of VEGFR2 during guided migration

Growing evidences support that endocytosis provides an intracellular platform to control signal specificity, amplitude, and timing. Endocytosis not only regulates the intracellular signaling components availability to surface receptors (Murphy et al., 2009;

Sadowski et al., 2009) but also restricts spatially certain signaling events as evidenced for example in the *Drosophila* PDGF/VEGF receptor- and Rac1-mediated cell migration (Jekely et al., 2005; Palamidessi et al., 2008). These previously reported data together with the result presented here urge a model of space-restricted signaling of VEGFR2 and other RTKs that is operated by the endocytic machinery (Fig. 7-2). In the presence of its ligand along the migration routes, VEGFR2 is initially activated and internalized into endocytic vesicles. Remaining surface receptors are inactivated by membrane-associated phosphatases, whereas endocytosed receptors become fully activated. Subsequent recycling of the endocytic vesicles allow relocalization and generation of localized pools of active receptors to specific regions where signaling is required. Interaction with downstream signaling adaptors specifically located in diverse endocytic vesicles might control the restricted spatial activation of certain signaling cascades which will result in diverse cellular responses.

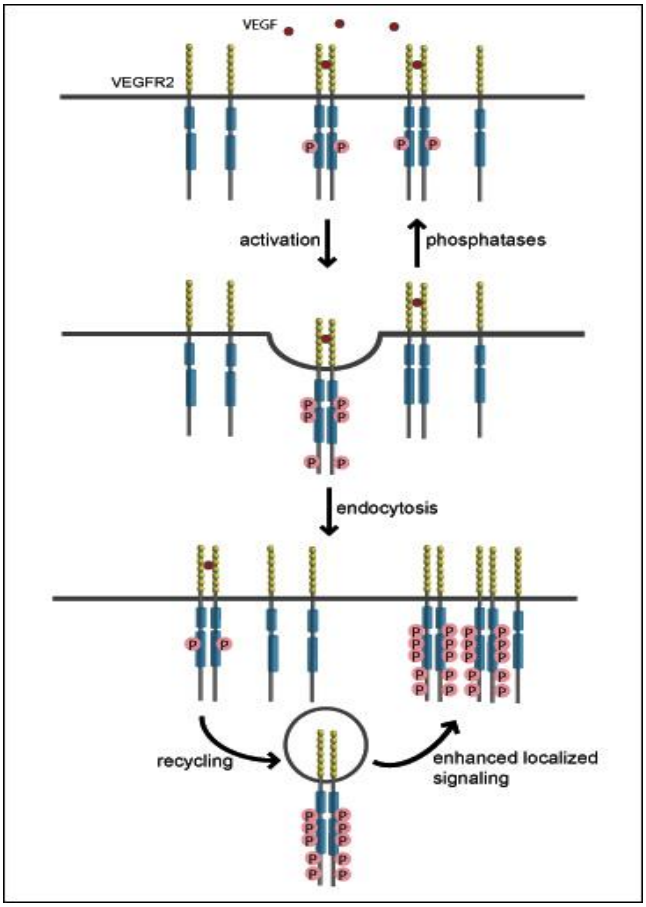

Figure 7-2 Possible role of endocytosis in control of localization and intensity of VEGFR2 signaling. VEGFR2 localized at the cell surface are activated upon VEGF binding. Receptors remained at the plasma membrane are deactivated by phosphatases, whereas those internalized into intracellular compartments become fully activated. Recycling of activated receptors in the endocytic vesicles back to the cell surface might facilitate relocation of the receptors to specified regions as well as enhancement of signaling strengths. Pink circles marked with P represent phosphorylated tyrosines.

7.3. EphrinB2 and VEGFR2 in control of tip cell filopodial extension

The long and thin plasma membrane protrusion, supported by paralleled actin bundles, of the filopodial process has generally been described as an antennae used by cells to probe their microenvironment. The best known fundamental role of filopodia is to direct cellular orientation during guided migration. Diverse signaling receptors for different extracellular matrix molecules are found in filopodia, supporting its role as a signal transduction site where cell surface receptors transfer signaling information from the cell surrounding to activate cellular responses required for migration (Mattila and Lappalainen, 2008). Filopodial processes extended from endothelial tip cells at the sprouting front of the developing retinal vasculature are enriched with VEGFR2. This has been proposed to function as a molecular sensor for VEGF gradients secreted from the astrocytic network into the surrounding matrix and lead to the migration of endothelial sprouts towards the avascular area (Gerhardt et al., 2003). The retina explant assay developed in this study is proven a very useful tool to investigate acute responses of endothelial tip cells at the sprouting front of the vascular bed, following exposure to different stimuli. This, of course, allows further insights into the molecular mechanisms involved in the filopodial sprouting function of VEGFR2. Numerous filopodia are sprouted out from the vascular front of explanted retinas upon treatment with VEGF. VEGF sequestering, by contrast, results in a severe impairment of filopodial extension, an effect which can be mimicked by blockade of dynamin-dependent endocytosis. Similar to VEGF administration, stimulation of ephrinB2 signaling can also promote filopodial sprouting and activated ephrinB2 is able to rescue the sprouting activity of explanted retina vessels following VEGF blockade. These data, and several other evidences provided in this study, demonstrate for the first time the crucial importance of endocytosis in the regulation of VEGFR2-mediated sprouting activity of endothelial tip cells and furthermore indentify ephrinB2 as an indispensable molecular linkage between these events. The next question to be clarified is what signaling events operated downstream of VEGFR2 upon its endocytosis from the cell surface is in charge of the filopodial extension process. For example, possible targets for VEGFR2 activation could be the convergence of F-actin during the formation of filopodial core actin bundles as well as signaling events controlling the adhesion of filopodial protrusions to the extracellular matrix.

Regulation of actin dynamic by VEGFR2 signaling Several molecules activated downstream of VEGFR2 upon VEGF binding have been shown to directly modulate cell migration by affecting actin cytoskeleton dynamics. IQGAP1, whose name derives from the presence of calmodulin-binding IQ motifs and a region with sequences similarity to Ras GTPase activating proteins (GAPs), is an actin-binding protein which represents a prime candidate for VEGFR2-modulation of migratory behavior. IQGAP1 has a well established function as an activator of Cdc42 and Rac1 by inhibiting their GTPase activity and thereby stabilizing their active GTP-bound form (Hart et al., 1996; Noritake et al., 2004). A potent-actin assembling machinery involving the diaphanous formin (Dia), which is known to promote the formation of linear actin filaments through possessive barbed-end elongation (Goode and Eck, 2007), might require binding of Dia1 to IQGAP1 to release Dia1 from its autoinhibitory conformation (Brandt and Grosse, 2007). In agreement with this notion, activation of cdc42 by IQGAP1 has been shown to induce formation of filopodia (Swart-Mataraza et al., 2002). It has been reported that VEGF stimulation induced physical interaction between IQGAP1 and phosphorylated VEGFR2. This association leads to tyrosine phosphorylation of IQGAP1 and induction of migratory and mitogenic responses in endothelial cells (Yamaoka-Tojo et al., 2004). The data presented here demonstrate the importance of endocytosis for the full activation of VEGFR2. Inhibition of dynamin-dependent endocytosis which results in a severe reduction of VEGFR2 phosphorylation at all the major autophosphorylation sites might as well disrupts the recruitment and activation of IQGAP1 and thereby causes the defect in actin filament assembly required for filopodia formation.

Integrins and elongation of filopodia protrusions Cell-adhesion molecules such as integrins and cadherins are often found at the filopodia tips or along the shafts (Galbraith et al., 2007; Steketee and Tosney, 2002; Vasioukhin et al., 2000). Integrins in an unligated but activated state have been reported to accumulate at the tip of filopodia processes to probe the extracellular matrix and form initial adhesion sites that facilitate cell migration (Galbraith et al., 2007). Stabilization of filopodial structures to the surrounding matrix by integrins, translocated to filopodia tips by the actin-based motor protein myosin, is necessary for

subsequent elongation of the filopodial processes (Zhang et al., 2004). Interestingly, myosin can bind to phosphatidylinositol phosphates which aid its targeting to clathrin-coated structures and might contribute to its function during filopodial formation (Mattila and Lappalainen, 2008; Spudich et al., 2007). Transient fibronectin deposition in astrocytes and localization of fibronectin-type integrins at the tips of endothelial tip cell filopodia enriched with VEGFR2 has also been reported in postnatal retinas (Gerhardt et al., 2003). Different fibronectin- and laminin-binding integrins are known to exert their function in collaboration with VEGFR2 through complex formation of both proteins. Phosphorylation and activation of integrins, following induction of VEGFR2 signal transduction that involves Src kinases and PI3K-Akt signaling, play an important role in VEGF-stimulated angiogenic responses (Avraamides et al., 2008; Byzova et al., 2000; Somanath et al., 2009). Indeed, the reciprocal nature of integrin-VEGFR2 cross-talk that is important not only for activation of integrins, but also for prolonged and full activation of VEGFR2 signaling cascades has been demonstrated (Somanath et al., 2009; Wijelath et al., 2006). Similar to several RTKs, endocytic trafficking is an important mechanism controlling the biological activities of integrins (Caswell et al., 2009; Jones et al., 2006; Pellinen and Ivaska, 2006). Moreover, engagement of integrins can influence intracellular trafficking and signaling downstream of other receptors as evidenced in the enhancement of EGF receptor autophosphorylation and mobilization of the active receptor. This involves associated recycling of the EGF receptor and integrin α5β1 towards cellular protrusions at the migrating front to drive Akt-mediated invasive migration (Caswell et al., 2008). Given the pivotal role of β1 integrins in developmental and pathological angiogenesis as well as its ability to modulate VEGFR2 signaling (Avraamides et al., 2008; Wijelath et al., 2006), it is tempting to speculate that the coordinated intracellular trafficking of integrin β1-VEGFR2 might as well exist to regulate spatial distribution of the associated receptor signaling complex at the matrix-filopodia adhesive sites. Such mechanism might be necessary for the attachment of endothelial tip cell filopodia to the surrounding matrix and activation of other migratory signals downstream of the receptors during guided angiogenic sprouting.

7.4. Triggering VEGFR2 signaling: A team effort of VEGF and ephrinB2

Endocytosis of VEGFR2 assessed by antibody feeding assay presented here shows similar levels of internalized receptor in endothelial cells treated with VEGF or only pre-clustered EphB4-Fc. VEGF and ephrinB2 most likely work simultaneously in physiological conditions to induce VEGFR2 activation and internalization. To confirm this notion, VEGFR2 internalization upon combinatorial stimulation with both VEGF and EphB4-Fc was investigated. However, no significant difference between combinatorial and single agent stimulation could be observed (data not shown). This is probably due to the saturation of the system. Up to 70% of VEGFR2 was found to be internalized upon treatment with either VEGF or EphB4-Fc. Alternatively, one would hypothesize that activation of ephrinB2 by EphB4-Fc might be sufficient to induce internalization of VEGFR2 in absence of VEGF. Endothelial cells are able to produce VEGF (Maharaj et al., 2006), evaluation of VEGF-independent ephrinB2 function in VEGFR2 internalization would therefore require endothelial cells without endogenous *VEGF*. In the experiments presented here, the possibility of the presence of endothelial VEGF could not be ruled out. The examination filopodial extension in retina explants, which represents a functional readout of VEGFR2 internalization and activation, on the other hand, pointed to a co-operative effect of VEGF and ephrinB2. Extension of endothelial tip cell filopodia was more efficiently induced by VEGF than by EphB4-Fc. Importantly, under VEGF-deprived condition following treatment with s-Flt1, activation of ephrinB2 signaling by EphB4-Fc partially rescued the vascular defect of explanted retinas, suggesting a co-operative rather than independent effect. Low levels of VEGF which most likely are still available for tip cells after VEGF sequestering by s-Flt1 might allow the cells, in which ephrinB2 signaling is highly activated, to efficiently induce VEGFR2 internalization and function.

7.5. Interaction between VEGFR2 and ephrinB2

Two evidences presented here, the co-localization of ephrinB2 and VEGFR2 on the same membrane domains in cultured endothelial cells and the co-immunoprecipitation of the two molecules from neonatal mouse brain, suggest that ephrinB2 and VEGFR2 interact to exert their biological activities. However, at this stage it cannot be pinpointed whether these

two interacting partners can directly associate or other bridging molecules are required to mediate such interaction. Several SH2 and/or SH3 adaptor molecules are involved in signal transduction of activated VEGFR2 through various pathways. An interesting example among the known VEGFR2 adaptor proteins is Nck2 (also known as Nckβ or Grb4) that contains three N-terminal juxtaposed SH3 domains and a C-terminal SH2 domain. Nck2 has been shown to be recruited to activated VEGFR2 seemingly via its SH2 domain and enable the activation of c-jun N-terminal kinase (JNK) and ERK presumably by association with the upstream effectors of these proteins via its SH3 domain to promote endothelial cell proliferation (Wang et al., 2007). Interestingly, the putative SH3-binding motif presented in the cytoplasmic tail of ephrinBs has also been proposed to mediate their binding to Nck2 which links them to multiple downstream regulators and promotes dendrite morphogenesis (Segura et al., 2007; Xu and Henkemeyer, 2009). Therefore, Nck2 may represent a plausible linker between VEGFR2 and ephrinB2. Direct physical interaction between the VEGFR2 and ephrinB2 via their extracellular regions as well cannot be neglected. Future studies will aim to identify the interaction domains of both proteins and other putative scaffolding molecules that control ephrinB2-VEGFR2 interaction. This might lead to the identification of new therapeutic strategies to inhibit angiogenesis by interfering with the association of ephrinB2 and VEGFR2 molecules.

7.6. Molecular mechanism underlying ephrinB2 function in the endocytosis of VEGFR2

The work presented here demonstrates the critical role of PDZ-dependent reverse signaling downstream of ephrinB2 in the regulation of VEGFR2 endocytosis and function required for angiogenic sprouting in both physiological and pathological conditions. Further insight into the molecular mechanism employed by ephrinB2 to mediate this function seems to be an obvious next query. Among PDZ proteins that have been described to be expressed in blood vessels and to bind to ephrinB ligands (Makinen et al., 2005), PICK1 (protein interacting with C-kinase1) and Dvl2 (Dishevelled2) are appealing candidates as ephrinB2 effector molecules owing to their reported roles in the regulation of signaling receptor endocytosis.

PICK1 is well-known as a key modulator in the trafficking of the neurotransmitter receptor AMPAR (α-amino-3-hydroxy-5-methylisoxazole-4-propionic acid receptor) which is a fundamental mechanism for the regulation of synaptic strength (Hanley, 2008). The two functional domains, PDZ and BAR (Bin/amphiphysin/Rvs), present in PICK1 confer the ability to interact with a number of signaling molecules involved in different cellular processes including actin polymerization and phospholipid membrane curvature. The PDZ domain of PICK1 shows specificity to a diverse array of ligands such as different subunits of AMPAR, ephrinBs, Ephs and other RTKs (Dev, 2007). The ability of BAR domain to associate with negatively charged phosphoinositides and to contribute to the invagination of the lipid bi-layer membrane suggests that PICK1-lipid association might play an essential role in receptor endocytosis and trafficking of intracellular membrane compartments (Jin et al., 2006; McMahon and Gallop, 2005; Peter et al., 2004). Moreover, PICK1 BAR domain has also been shown to associate with and inhibit the activity of the major catalyst of branched actin network Arp2/3 complex and allow AMPAR endocytosis to proceed possibly by locally lowering membrane tension (Rocca et al., 2008). Interestingly, there is a predicted binding site for PICK1 in the C-terminal domain of VEGFR2 (Dev, 2007) and given the ability of PICK1 to form homoligomer presenting two available PDZ motifs (Xia et al., 1999) it would be interesting to investigate whether PICK1 is a bridging molecule that might act as a transducer of ephrinB2 signaling to trigger the internalization of VEGFR2 from plasma membrane.

Dvl has been reported to participate in a wide array of molecular machineries underlying several different cellular processes ranging from cell fate decision, migration, dendritogenesis, to planar polarity (Gao and Chen). The three members of Dvl proteins identified in human and mice possess three conserved domains, an N-terminal DIX (Dishevelled, Axin) domain required for their polymerization (Schwarz-Romond et al., 2007; Wharton, 2003), a central PDZ domain that mediate their interactions with membrane receptors and various intracellular effectors, and a C-terminal DEP (Dvl, Egl-10, Pleckstrin) domain that is essential for their binding to membrane lipids (Simons et al., 2009) and also a number of signaling partners (Gao and Chen). The role of Dvl in endocytosis is well-established in Wnt (derived from *Drosophila* Wingless (Wg) and its mammalian homolog

Integration sites (Int) signaling pathways). Upon Wnt5a stimulation, Dvl2 is recruited to the activated Wnt receptor Frizzled4 in the cell membrane and brings β-arrestin2 to the receptor complexes to promote receptor sorting into clathrin-coated pits for internalization (Chen et al., 2003). Association of Dvl2, through its DEP domain, with a subunit of the clathrin adaptor protein AP-2 has also been shown to be essential for Frizzled4 internalization (Yu et al., 2007). The role of β-arrestin2 in clathrin-dependent endocytosis is not only limited to G protein-coupled receptors but also known to be involved in the internalization of other signaling receptors and adhesion molecules including TGF-β receptor, EGFR, and VE-Cadherin (Chen et al., 2003; Gavard and Gutkind, 2006; Maudsley et al., 2000). Further work will be required to address the possible role of Dvl2 in EphrinB2-mediated VEGFR2 endocytosis.

Identification of other possible interaction partners of ephrinB2 among all the PDZ proteins encoded from mouse genome would be of great interest and will require high-throughput approaches such as protein arrays and mass spectrometry.

7.7. Control of ephrinB2 expression by Notch signaling and tip cell function of ephrinB2

An emerging role of Notch signaling pathway during the development of the vascular system is the regulation of the endothelial tip/stalk cell specification. Notch exerts this function via the well-known mechanism of lateral inhibition, which is, at least partially, coupled to the VEGF pathway. The initial migratory response of endothelial cells during active angiogenic sprouting is induced by gradients of VEGF highly expressed in hypoxic regions in absence of functional oxygen-delivering blood vessels. Activation of VEGFR2 by VEGF has been shown to upregulate expression of the Notch ligand *Dll4* (Liu et al., 2003; Lobov et al., 2007). *Trans*-activation of Notch signaling by Dll4 in adjacent cells suppresses sprouting phenotypes and allows only a fraction of endothelial cells to become tip cells (Hellstrom et al., 2007; Siekmann and Lawson, 2007). The molecular mechanism underlying the tip cell suppression by Notch is not fully understood. Differential regulation of VEGF receptor expression in subpopulations of endothelial cells at the sprouting front of growing vessels by Notch signaling is thus far the only mechanistic insight that has been described.

Several lines of evidences demonstrate that Notch can negatively regulate VEGFR2 expression possibly through the transcriptional regulator Hey1, whose expression is directly controlled by Notch (Henderson et al., 2001; Holderfield et al., 2006; Suchting et al., 2007; Williams et al., 2006).Conversely, the VEGF decoy receptor VEGFR1, which can antagonize VEGFR2 pro-angiogenic activities, is upregulated by Notch (Harrington et al., 2008). Based on these findings, the current model is a negative-feedback loop, in which Dll4 upregulated upon VEGF stimulation activates Notch signaling in adjacent cells to suppress VEGFR2 expression and thereby dampen their angiogenic response (Phng and Gerhardt, 2009). Another ligand of Notch, Jagged1, also contributes to lower the Notch activity in the tip cells by antagonizing Dll4 expressed in stalk cells (Benedito et al., 2009).

EphrinB2 has been reported to be a direct downstream target of Notch signaling. Binding of NICD-RBPJ complex to *ephrinB2* gene transiently activates its expression (Grego-Bessa et al., 2007). According to the novel function of ephrinB2 in the regulation of endothelial tip cell filopodial extension by modulating VEGFR2 internalization discovered in this study, one might wonder how ephrinB2 exerts its function in tip cell when Notch activity is seemingly low. Indeed, tip and stalk cells are not stable cell fates. Their specification instead represents a dynamic process of cells receiving stimulus of similar strength at the sprouting front and constantly battling for the tip cell position at the level of Dll4 and VEGFR2 signaling output. Imaging of sprouting zebrafish vessels has shown that tip cells can rapidly switch their invasive migratory behavior to become quiescent and integrate into nearby vessels (Leslie et al., 2007; Torres-Vazquez et al., 2004). This illustrates the dynamic changes of Notch activity once cells encounter a new microenvironment and different neighbors. The oscillating expression of Notch signaling components mediated by differential protein stability and timing of transcription and translation has been demonstrated to control spatial patterning of somitogenesis (Lewis, 2008). Such synchronous oscillation might explain the heterogenous expression pattern of NICD and Dll4 which are highly expressed, but not only restricted to, stalk and tip cells, respectively (Roca and Adams, 2007). Furthermore, expression of Dll4 can be regulated not only by VEGF/VEGFR2 signaling but also other pathways including Notch (Carlson et al., 2005; Shawber et al., 2003). The possibility that Notch and its signaling compartments are activated transiently

leading to an upregulation of DLL4 as well as ephrinB2 before cells commit to tip cell fate cannot be excluded. Staining of retina vessels by EphB4-Fc shows the general expression of ephrinB2 in arterial endothelium and all over capillary beds. Both, tip and stalk cells, are found positive for ephrinB2, suggesting the stable expression of ephrinB2 protein upon transient downregulation of Notch signaling when some endothelial cells are selected to become tip cells. Once tip cells are specified, modulation of Dll4 by Notch signaling as well as downregulation of *Hes/Hey* transcription by their own translational products (Lewis, 2008) may provide a negative feedback mechanism that potentially could contribute to the oscillation of Notch activity in tip cells by the transiently enhanced Dll4 expression in stalk cells and allow sustained ephrinB2 expression sufficient to induce migratory response in collaboration with VEGFR2. In addition, ephrinB2 expression in tip cells might also be regulated independently of VEGFR2 and Notch activities.

7.8. Different roles of ephrinB2 during angiogenic growth of blood vessels

Overexpression of full-length or tyrosine phosphorylation-deficient ephrinB2 in primary endothelial cells causes contact-mediated repulsion which prevents these cells from integrating into the capillary-like structures formed on 3D matrigel. The PDZ-truncated form of ephrinB2, on the other hand, is unable to reproduce such a repulsive phenotype and allows strong cellular contacts between endothelial cells during tubular assembly. These findings raise an intriguing assumption that ephrinB2 function in vascular development might not be limited only to the control of VEGFR2 endocytosis and migratory signal in endothelial tip cells, but also be involved in the earlier step when cells selected to become tip cells attain invasive phenotypes. Endothelial cells lining the vessel wall in the quiescent condition or during maturation of newly formed vessels establish adherens and tight junctions to maintain stable cell-cell contacts and keep the integrity of the entire vascular structure which must support high-pressure blood flows. Upon exposure to angiogenic stimuli, a subset of endothelial cells with changes in their expression profile that is sufficient to overcome the suppression mechanism of the invasive phenotype (mainly through Notch signaling as mentioned above) will be selected to become tip cells. The cellular contacts between these

selected cells and their neighbors need to be accordingly altered to allow a cell polarity shifting before the cells sprouting out from an intact vessel (Adams and Alitalo, 2007).

Eph/ephrin signaling has a well-established function in cell repulsion (Marston et al., 2003; Zimmer et al., 2003), which is particularly important for axon guidance and formation of tissue boundaries during embryogenesis (Palmer et al., 2002). Endocytosis of intact Eph/ephrin signaling complex and proteolytic cleavage of the receptor or ligand extracellular portions, which results in the removal of Eph/ephrin adhesive complex from cell surface, have been shown to convert initial adhesion via ligand/receptor binding to cell repulsion (Egea and Klein, 2007). Moreover, the direct control of tight junction formation by ephrinB has also been reported. The Par (partitioning defective) polarity complex protein Par-6 is a major scaffold molecule that couples the small GTPase Cdc42 to the activation of the atypical protein kinase C (aPKC) required for actin rearrangement during the formation of tight junctions to establish and maintain cell-cell contacts (Joberty et al., 2000; Lee et al., 2008). It has been shown that ephrinB1 can compete with Cdc42 for Par-6 binding and thereby interrupts the activation of Par/cdc42 complex that consequently causes the loss of epithelial tight junctions during early *Xenopus leavis* embryogenesis. Overexpression of ephrinB1 in blastomere embryos results in effective competition of ephrinB1 over Cdc42 for Par-6 interaction and thereby shows disrupt tight junction formation. Tyrosine phosphorylation of ephrinB1, on the contrary, interferes with the association of ephrinB1 and Par-6 (Lee et al., 2008). Binding of Cdc42 to Par-6 has previously been demonstrated to mediate by the semi-CRIB-PDZ domain of Par-6 (Gao and Macara, 2004; Yamanaka et al., 2001). Although the PDZ-binding motif of ephrinB1 might not be essential for its binding to Par-6 (Lee et al., 2008), its importance for the disruption of Cdc42/Par-6 association remains to be clarified. Whether a similar mechanism regulated by ephrinB2 applies to the control of endothelial cell adhesion and a transient upregulation of ephrinB2 might be operated to alter the tight association between these cells for the initiation of sprouting activity are open questions that require further investigation.

7.9. Eph/ephrin signaling in tumor progression: angiogenesis and beyond

The critical role of ephrinB2 PDZ-dependent signaling in tumor-induced neovascularization, which is a crucially process required for tumor growth, is clearly demonstrated in this study. The angiogenic response of host blood vessels induced by astrocytoma tumors and mediated by ephrinB2appears to be endothelial cell-autonomous and generic in different tumor microenvironments. Several EphB receptors, expressed in astrocytes (Wang et al., 2005) or astrocytoma tumors (Bian et al., 2006; Nakada et al., 2004), could potentially represent a source of ephrinB2 activation in the endothelium. Moreover, various Eph receptors and ephrin ligands have been reported to be widely expressed in tumor cells and tumor stromas and their intriguing expression levels correlated with cancer progression and metastasis (Pasquale). These facts attract a large number of researchers that aim to clarify the functional relevance of Eph and ephrins in these processes.

Depending on the cellular context and/or stages of tumor progression several Eph receptors are found to be upregulated or silenced. Similar to the divergence in their abundances, both tumor-promoting and tumor-suppressing functions of Eph receptor forward signaling by controlling diverse cellular processes including proliferation, survival, and invasive migration have been described (Merlos-Suarez and Batlle, 2008; Pasquale). Interactions between EphB recptor presented in cororectal cancer cells and ephrinB2 expressed in villus cells limits the expansion of the cancer cells outside the villus cavity by a mechanism involving E-cadherin-mediated cancer cell adhesion (Cortina et al., 2007). Recent studies implicate that different signaling outcomes might be achieved from the conventional ephrin-mediated Eph receptor tyrosine kinase activities and the ligand-independent crosstalk between Eph receptor and other oncogenic pathways. EphB4-mediated downregulation of β1-integrin levels and cell-substrate adhesion independently of ephrinB ligands has been shown to inhibit migration of some tumor types (Noren et al., 2009), whereas EphB2-dependent decreased cell adhesion can also promote invasion of other tumors (Nakada et al., 2005). Crosstalk between EphA2 and Akt seems to promote tumor invasiveness independent of EphA2 kinase activity. Stimulation of the receptor with

ephrinB1, by contrast, counteracts the effect of Akt and inhibits tumor cell migration (Miao et al., 2009).

Several evidences have demonstrated that reverse signaling downstream of ephrin ligands is also involved in multiple mechanisms within tumor cells that modulate tumor progression. Rac1 activation and secretion of matrix metalloproteinase (MMP) have been proposed to be regulated by ephrinB signaling in many tumor types (Jiang et al., 2008; Nakada et al., 2006; Tanaka et al., 2007). Moreover, ephrinB reverse signaling may also influence tumor transformation and invasiveness at the transcriptional level by modulating the signal transducer and activator of transcription 3 (STAT3) (Bong et al., 2007).

Given the abundance of different Ephs and ephrins in tumor cells and tumor blood vessels, interactions between the receptors and ligands on the surfaces of these cells, which are in close proximity within the tumor microenvironment, might have other roles in the tumor endothelium in addition to its key function in tumor angiogenesis. EphrinB2 expressed in the tumor endothelium is able to stimulate EphB4-mediated upregulation of the adhesion molecule selectin to promote the recruitment of bone-marrow derived endothelial progenitor cells which participate in tumor neovascularization (Foubert et al., 2007). It will be interesting to investigate whether EphB-expressing tumor cells might employ similar mechanism to intravasate into the blood stream during their metastasis to distant tissues.

8. Materials and Methods

8.1. Materials

8.1.1. Chemicals, enzymes and commercial kits

Chemicals were purchased from the companies Merck, Serva, Sigma, Fluka and Roth. Water used to prepare all solutions was filtered with the “Milli-Q-Water System” (Millipore). Restrictions enzymes were purchased from New England Biolabs (NEB). Plasmid preparations, PCR purifications or gel-extractions were done using the Qiagen Plasmid Mini/Maxi kit or PCR Purification kit, respectively. Special supplies and kits are mentioned in detail with the according method.

8.1.2. Bacteria

DH5α (Invitrogen)

TOP10 (Invitrogen)

8.1.3. Cell lines

Phoenix A: Retroviral packaging line created by introducing gag-pol and viral envelope protein expression constructs into 293T cells (a human embryonic kidney line transformed with adenovirus E1a).

8.1.4. Primary Cells

MLEC: Endothelial cells isolated from lungs of new born C57BL/6 mice.

ASCT: Central nervous system tumor cells which have been transformed from mouse astrocytes by the introduction of H-RasV12 and SV40-large T antigen oncogenes.

8.1.5. Media and dissection buffers

8.1.5.1. Media and antibiotics for bacterial culture

Luria-Bertani (LB) medium

Bacto-Tryptone	10 g
Bacto-Yeast extract	5 g
NaCl	5 g

Distilled water was added to the final volume of 1l. The pH is 7.5. Solution was sterilized by autoclaving and stored at RT.

LB plates

LB media	1 l
Bacto-Agar	15 g

Autoclaved and stored at 4°C.

Antibiotics (1000x stocks)

Ampicillin	100 mg/ml
Kanamycin monosulfate	50 mg/ml

8.1.5.2. Media for cell lines (500 ml)

DMEM+GlutaMAX™-I+4.5 mg/l D-glucose (Gibco)	450 ml
Penicillin-streptomycin	5 ml

(100 U/ml penicillin and 100 µg/ml streptomycin in final concentration)

Fetal bovine serum 10%	50 ml

8.1.5.3. Media for primary cell culture

Sterilization by filtration was done with 0.22 µm filter. All media can be kept at 4ºC maximally for 2 months.

8.1.5.3.1 Endothelial cell dissection

Dissection buffer (500 ml)

Hank's buffered salt solution (HBSS)	450 ml
FBS 10%	50 ml

Collagenase (2500 units/ml)

Collagenase type II from *Clostridium histolyticum*	
(Biochrom AG, 325units/mg)	100 mg
D-PBS	13 ml

Collagenase was dissolved in PBS, filtered and aliquoted in small amount and stored at 20ºC.

1% Gelatin

Gelatin from bovine skin type B	10 g
D-PBS	1 l

Solution was sterilized by autoclaving and stored at RT. Filtration before use is required.

Coupling buffer (50ml)

HBSS	50 ml
BSA 2%	1 g

BSA was dissolved in HBSS and sterilized by filtration.

8.1.5.3.2 Endothelial cell culture

Endothelial cell growth medium (500 ml)

DMEM+GlutaMAX™-I+4.5 mg/l D-glucose (Gibco)	390 ml
Penicillin-streptomycin	5 ml

(100 U/ml penicillin and 100 µg/ml streptomycin in final concentration)

Fetal bovine serum 20%	100 ml
Endothelial cell growth supplement/Heparin (PAA)	2 ml
Amphotericin B (Fungizone 250 Units/20 ml, Sigma)	3 ml

Note: fetal bovine serum used for endothelial cell culture need to be tested not to promote cell differentiation and support cell growth for many passages. The serum used for embryonic stem cell culture usually worked well with endothelial cells.

8.1.5.3.3 Angiogenesis assay

Tube formation assay (starving medium, 50 ml)

DMEM+GlutaMAX™-I+4.5 mg/l D-glucose (Gibco)	49.5 ml
Fetal bovine serum 1%	0.5 ml

8.1.5.3.3 Dissection medium for primary astrocyte isolation

10x HBSS	50 ml
1M HEPES	5 ml
7.5% (w/v) $NaHCO_3$ pH 7.35	2.5 ml

Sterile water was added to fill up the volume to 500 ml.

8.1.5.3.4 Astrocyte and astrocytoma culture media (500 ml)

Basal Medium Eagle (BME)	422 ml
20% Glucose in BME	15 ml
100 mM Sodium Pyruvate	5 ml
HEPES	5 ml
Horse serum (HS, without heat-inactivation)	50 ml
MITO serum Extender (BD Biosciences)	500 µl
Penicillin-Streptomycin	2.5 ml

(50 U/ml penicillin and 50 µg/ml streptomycin in final concentration)

8.1.6. Plasmids

YFP-ephrinB2

The construct for expression of the YFP-fusion ephrinB2 gene were generated as previously described (Zimmer et al., 2003). Mouse ephrinB2 gene was cloned to the C-terminus of the eYFP gene in the vector pEYFP-N1 (Clontech).

YFP-ephrinB2ΔC

YFP-ephrinB2ΔC was generated by replacing the CFP gene from pJK42 (Lauterbach and Klein, 2006) with the YFP gene from pEYFP-N1 at the *Sal*I and *Bsr*GI cloning sites. Most of the cytoplasmic domain of ephrinB2 was removed. The remaining cytoplasmic tail contains only the amino acid sequence RKHSPQHTTT.

YFP-ephrinB2ΔV

Generation of YFP-ephrinB2ΔV was done by site directed mutagenesis (Stratagene) to remove the C-terminal valine from the ephrinB2 gene in the YFP-ephrinB2 plasmid.

YFP-ephrinB25Y

To generate YFP-ephrinB25Y, the *Bbs*I-*Eco*RV fragment encoding the C-terminal part of ephrinB2 in the YFP-ephrinB2 plasmid was replaced by a fragment in which five conserved tyrosine residues of ephrinB2 were mutated as previously described (Makinen et al., 2005).

8.1.7. Oligonucleotides

All small oligonucleotides were synthesized by MWG (www.mwg-biotech.com) and purified with HPSF.

EphrinB2KI_for: 5'-CGG AGT GCG CAG AAC TGG-3'

EphrinB2KI_rev: 5'-GAT TTG GCT TCA CAA AGG GAC T-3'

Elf-2-S1: 5'-CTC TGT GTG GAA GTA CTG TTG-3'

Wtas4: 5'-CCG CCA ATG TGT GTC TGT AGC-3'

LacZ_F: 5'-CCA GCT GGC GTA ATA GCG AA-3'

LacZ_R: 5'-CGC CCG TTG CAC AGA TG-3'

8.1.8. Solutions and buffers

8.1.8.1 Standard solutions

Phosphate-buffered saline (PBS)

137 mM NaCl	NaCl 8 g
2.7 mM KCl	KCl 0.2 g
8 mM Na_2HPO_4	Na_2HPO_4 1.15 g
1.5 mM KH_2PO_4	KH_2PO_4 0.24 g

All ingredients were dissolved in 800 ml of distilled water. pH was adjusted to 7.4 with HCl and final volume were adjusted to 1 l. Solution was sterilized by autoclaving and stored at RT.

10× PBS

1.37 M NaCl	NaCl 80 g
27 mM KCl	KCl 2 g
81 mM Na_2HPO_4	Na_2HPO_4 11.5 g
15 mM KH_2PO_4	KH_2PO_4 2.4 g

All ingredients were dissolved in 800 ml of distilled water. pH was adjusted to 7.4 with HCl and final volume were adjusted to 1 l. Solution was sterilized by autoclaving and stored at RT.

4% Paraformaldehyde (PFA)

PFA 4% (w/v)	20 g

D-PBS	500 ml
5N NaOH	200 µl
HCl min. 37%	75 µl

PBS was pre-heated to 70°C before PFA powder was added and stirred at high speed. NaOH was then added for a completely dissolve PFA. HCl min. 37% was finally added to adjust pH to 7.3. Solution was stored in aliquots at -20°C.

8.1.8.2 Solutions for agarose gel electrophoresis

50x TAE

Tris Base	242 g
0.5 M EDTA pH 8.0	100 ml
Acetic Acid 100%	57.1 ml

Tris base was dissolved in 600 ml of distilled water with magnet stirrer. EDTA and acetic Acid were then added. Final volume was adjusted to 1 L with distilled water. Solution was stored at room temperature.

Final concentration of the solution:

2M Tris acetate

50mM EDTA

Gel loading buffer

Glycerol	25 ml
50x TAE	1 ml
Orange G	0.1 g
H_2O	4 ml

8.1.8.3 Solutions and buffers for western blot analysis

Lysis buffer

50 mM Tris pH 7.5	1M Tris pH 7.5	25 ml
150 mM NaCl	5M NaCl	15 ml
0.5% Nonidet P40 (NP-40)	NP-40	2.5 ml
10% Glycerol	Glycerol (87%)	57.5 ml

Distilled water was added to final volume 500 ml. Solution was stored at 4°C.

Added freshly to 50 ml:

Protease inhibitor cocktail tablet (complete) 1 tablet

20 mM NaF	NaF	0.042 g
10 mM NaPPi	NaPPi	0.223 g
1 mM vanadate	100 mM Na_3VO_4	300 µl

SDS PAGE separating gel 7.5% (10 ml)

H_2O	4.85 ml
1.5M Tris pH 8.8, 0.4% SDS	2.6 ml
30% w/v Acrylamind/bisacrylamid	2.5 ml
10% APS	50 µl
TEMED	5 µl

SDS PAGE stacking gel 4% (5 ml)

H_2O	3.05 ml
1.5M Tris pH 6.8, 0.4% SDS	1.3 ml
30% w/v Acrylamind/bisacrylamid	65 ml
10% APS	50 µl
TEMED	5 µl

6x Sample buffer for reducing conditions

12% SDS	SDS 3.6 g
300 mM Tris-HCl, pH 6.8	1.5M Tris 6 ml
600 mM DTT	DTT 2.77 g
0.6% BPB	BPB 0.18 g
60% Glycerol	Glycerol 18 ml

Distilled water was added to 30 ml. Buffer was stored in 0.5 ml aliquots at -20°C. Add 50 µl β-mercaptoethanol in 1 ml of 4x buffer.

5x Electrophoresis buffer

Tris base	154.5 g
Glycine	721 g
SDS	50 g

Distilled water was added to 10 l. Buffer was stored at RT.

Protein transfer buffer

Tris base 31.04 g

Glycine 144.13 g

Approximately 9 l of distilled water were added. Mixed to dissolve and made up to a final volume of 10 l. This 10X buffer was stored at RT.

Freshly before use:

35 ml of distilled water was added to 5 ml of the 10x buffer. 10 ml of Methanol was added to yield 50 ml 1X buffer.

Final concentration of the 1x transfer buffer:

25 mM Tris base

192 mM Glycine

20% Methanol

0.1M Sodium phosphate buffer, pH 7.2

1) 0.2 M $NaH_2PO_4 \cdot H_2O$ 69.0 g

2) 0.2 M $Na_2HPO_4 \cdot 7H_2O$ 134.1 g

70 ml of solution 1 was mixed with 180 ml of solution 2. Distilled water was added to mark 500 ml. pH of the mixture should be 7.2.

PBS-Tween (PBST)

1x PBS

0.1% Tween®20

Solution was kept at RT.

Blocking solution

5% skim milk skim milk 0.5 g

PBST 10 ml

Solution was prepared freshly just before use.

Stripping buffer

5 mM Sodium Phosphate buffer, pH 7-7.4

2% SDS

Freshly before use, 10 µl of β-Mercaptoethanol was added to 50 ml of the buffer.

8.1.8.4 Solutions for embedding of vibratome sections

0.1M Acetate buffer, pH 6.5

1M Sodium acetate	99 ml
1M Acetic acid	960 µl

pH adjusted and made up to a final volume of 1 l. Stored at RT.

Embedding solution

1) Ovalbumin

Ovalbumin (Sigma, A-S253)	90 g
0.1M Acetate buffer	200 ml

Albumin was dissolved in acetate buffer by stiring o/n at RT. The solution was filtered through a gaze and undissolved albumin or air bubbles were removed.

2) Gelatin

Gelatin	1.5 g
0.1M Acetate buffer	100 ml

Gelatin was dissolved in warm acetate buffer. After gelatin solution cooled down, it was carefully mixed with ovalbumin solution without producing bubbles. The mixed solution was aliquoted and stored at -20°C.

8.1.8.5 Solutions for lacZ staining

1M MgCl2

MgCl2	50.83 g
H2O	250 ml

0.1M Phosphate Buffer pH 7.3

0.1M NaH_2PO_4	115 ml
0.1M Na2HPO4	385 ml

The 2 phosphate buffers were mixed at the amount indicated to yield 500 ml buffer with pH approximately 7.3

Fixation solution

25% glutaraldehyde	0.4 ml
100 mM EGTA pH 7.3	2.5 ml
1M MgCl2	0.1 ml
0.1M sodium phosphate pH 7.3	47 ml

All ingredients were mixed freshly before use to yield 50 ml solution.

Wash buffer

1M MgCl2	2 ml
deoxycholate (DOC)	0.1 g
NP-40	0.2 ml

0.1M sodium phosphate pH 7.3 was added to the final volume of 1 l. Solution was stored at RT.

X-Gal Staining solution

1) Staining solution

potassium ferrocyanide (Sigma P-9378)	0.106 g
potassium ferricyanide (Sigma P-8131)	0.082 g
wash buffer	50.0 ml

Solution was kept in the dark at 4ºC.

2) X-Gal

X-Gal	200 mg
N-N-dimetylformamide.	2 ml

X-Gal solution at the final concentration 100mg/ml was aliquoted and stored at -20ºC.

0.5 ml of X-Gal solution was added freshly before use to 50 ml staining solution.

8.1.8.6 Solutions for retina staining

Isolectin B4

FITC conjugated lectin from *Bandeiraea simplicifolia* (Isolectin B4, Sigma-Aldrich) was dissolved in Dulbecco's phosphate buffer saline (D-PBS, Sigma) to a final concentration of 1mg/ml, aliquoted and stored at 4ºC in the dark.

Lectin blocking buffer

D-PBS containing 0.5% Triton X-100.

BSA was added to the buffer freshly before use to the final concentration of 0.2% (w/v).

Lectin staining buffer (PBlec)

D-PBS containing 1% Triton X-100.

8.1.8.7 Solutions for tumor vessel staining

TE buffer (10 mM Tris, 1 mM EDTA), pH 8.0

1) 0.5 M EDTA, pH 8.0

186.1 g of $Na_2EDTA{\cdot}2H_20$ was dissolved in 700 ml distilled water. After adjusting pH to 8.0 by adding approximately 50 ml of 10N NaOH, distilled water was added to bring up the volume to 1 l.

2) 1 M Tris-HCl

121.1 g Tris Base (TRIZMA) was dissolved in 700 ml distilled water. Concentrated HCl was added to desired pH:

pH 7.4: 70 ml

pH 8.0: 42 ml

pH 9.0: ~8 ml

Distilled water was added to mark 1 L.

2 ml of 1 M Tris-HCl, pH 8.0 was mixed with 0.4 ml of 0.5 M EDTA, pH 8.0, and 197.6 ml of distilled water was add to mark 200 ml. Solution was sterilized by filtration and stored at RT.

0.6 % H_2O_2

10 ml of concentrated H_2O_2 (30%) was mixed with 400 ml of PBS to yield 500 ml solution.

Blocking solution

PBS containing 0.01% triton X-100 and 20% normal goat serum (NGS).

Antibody staining solution

PBS containing 0.01% triton X-100 and 10% NGS.

8.1.9. Antibodies

Table 8-1 Primary antibodies

Antibody	Species	Company	Dilution	Application
PECAM-1 (MEC13.3)	mouse monoclonal	BD Pharmingen	1:25	EC isolation
external Flk-1	goat polyclonal	R&D Systems	1:40 4 µg:40 µl bead	Antibody feeding IP
internal Flk-1 (A-3)	mouse monoclonal	Santa Cruz Biotechnology	1:200	WB
Tyr1175	rabbit polyclonal	Cell Signaling Technology	1:1000	WB
Tyr1212	rabbit polyclonal	Cell Signaling Technology	1:1000	WB
Tyr1059	rabbit polyclonal	Cell Signaling Technology	1:1000	WB
Tyr951	rabbit polyclonal	Cell Signaling Technology	1:1000	WB
Neuropilin (H-286)	rabbit polyclonal	Santa Cruz	1:200	WB
Akt	rabbit polyclonal	Cell Signaling Technology	1:1000	WB
Phospho-Akt (Ser473)	rabbit polyclonal	Cell Signaling Technology	1:2000	WB

Cleaved Notch1 (Val1744)	rabbit polyclonal	Cell Signaling Technology	1:1000	WB
SV-40 T antigen (PAb416)	mouse monoclonal	Calbiochem	1:100	WB
c-H-Ras (F235-1.7.1)	mouse monoclonal	Calbiochem	1:50	WB
Tie2	rat monoclonal	R&D Systems	1:500	WB
GFAP	rabbit polyclonal	DAKO	1:70	IHC
CD34 (MEC14.7)	rat monoclonal	Abcam	1:100	IHC
BrdU	rat monoclonal	AbD Serotec	1:200	IHC
Histone H3	rabbit polyclonal	Cell Signaling Technology	1:50	IHC

Table 8-2 Secondary antibodies

Antibody	Species	Company	Dilution	Application
anti-mouse-HRP	goat polyclonal	Jackson Immunoresearch	1:5000	WB
anti-rabbit-HRP	goat polyclonal	Jackson Immunoresearch	1:5000	WB

anti-goat-Cy2	donkey polyclonal	Jackson Immunoresearch	1:200	IC
anti-goat-Cy3	donkey polyclonal	Jackson Immunoresearch	1:200	IC
anti-hFc-488	donkey polyclonal	Jackson Immunoresearch	1:100	IC
anti-hFc-Txred	goat polyclonal	Jackson Immunoresearch	1:100	IC
anti-hFc-Cy5	donkey polyclonal	Jackson Immunoresearch	1:100	IC
anti-rabbit-488	donkey polyclonal	Molecular Probes	1:400	IC
anti-rat-HRP	goat polyclonal	Jackson Immunoresearch	1:100	IHC

6.1.10. Mouse lines

EphrinB2$^{lox/lox}$ conditional knockout mice were generated by introduction of the construct containing the second exon of mouse *ephrinB2* gene flanked by *loxP* sites into the endogenous *ephrinB2* locus by homologous recombination. *Neo* cassette flanked by *FRP* sites was removed by crossing to trangenic mice expressing flp recombinase (Grunwald et al., 2004). The line has been maintained in C57Bl/6 background and used for isolation of primary ECs. After isolation viral-encoding cre was introduced to the ECs to generate *ephrinB2 KO* ECs.

EphrinB2$^{\Delta V/\Delta V}$ knock-in mice were generated by George Wilkinson in collaboration with Ralf Adams (Makinen et al., 2005) by replacing the first exon of the endogenous mouse *ephrinB2* gene with the cDNA lacking the codon encoding valine amino acid at the end of the C-

terminus. ORF of the cDNA was fused in frame to exon 1. Germline mutant mice were generated with standard protocols. Subsequently, *neomycin* cassette downstream of the cDNA was removed by Cre-mediated excision. The line was kept on a genetic background enriched for CD1 (due to lethality in newborn homozygous mice on C57Bl/6 background). The deficiency of the ephrinB2∆V to interact with PDZ protein was validated by syntenin1 pull down and EphB4-stimulated syntenin1 and ephrinB2 colocalization experiments.

***EphrinB2*$^{5Y/5Y}$** knock-in mice were generated by George Wilkinson (Makinen et al., 2005) and maintained on a genetic background enriched for CD1. cDNA encoding ephrinB2 in which 5 conserved tyrosine residues were replaced with 4 phenylalanine and a leucine residues was inserted into the first exon of the endogenous *ephrinB2* gene. *EphrinB2*$^{5Y/5Y}$ mutant embryos showed a severe reduction in the tyrosine phosphorylation level (assessed by anti-4G10).

***EphrinB2*$^{lacZ/+}$** mice were generated by insertion of the construct encoding tau-lacZ fusion protein into the first exon of the endogenous *ephrinB2* locus. *Tau-lacZ* was fused in frame after the initiation codon (ATG) of exon 1. Intronic sequence 3′ to exon 1 was replaced by *PGKneo* (Wang et al., 1998). The line was maintained on C57Bl/6 background.

Note: Fusion of bovine tau, a microtubule binding protein, to *E. coli* lacZ is aimed for lebelling of the entire cellular extent including filopodia extensions as shown in the study on axon lebelling (Callahan and Thomas, 1994).

8.2 METHODS

8.2.1 Molecular Biology

8.2.1.1. Preparation of plasmid DNA

Plasmid DNA was purified from small-scale (5 ml, minipreparation) or from large-scale (200 ml, maxipreparation) bacterial cultures. Single colonies of transformed bacteria or from a bacterial glycerol stock were picked each into LB medium containing 100 µg/ml ampicillin or kanamycin and grown for 14-18 h at 37°C with vigorous shaking. Mini- and

maxipreparation of plasmid DNA were carried out according to the QIAGEN protocol using lysis of the cells and binding of the plasmid DNA to a special resin. After washing, elution and precipitation the plasmid DNA was redissolved in a suitable volume of buffer EB (QIAGEN) for minipreparation or buffer TE pH 8.0 (QIAGEN) for maxipreparation. DNA concentration was measured in a UV spectrometer at 260 nm. The following formula was used: dsDNA: OD × 50 × dilution factor = X µg/ml

8.2.1.2. Enzymatic treatment of DNA

Cleavage of plasmid DNA: Approximate 15-20 µg of DNA was cut in with 15-20 units (U) of restriction enzymes in 50 µl of the appropriate buffer. The incubation temperatures were as indicated for optimal activity of each enzyme.

Dephosphorylation of DNA fragments: 10×buffer, deionized water and 1 U (1 µl) of calf intestine alkaline phosphatase (Roche) were added to the restriction enzyme reaction to get a total reaction volume of 100µl, incubated for 20 min at 37°C and heat-inactivated at 75°C for 15 min. Subsequently the dephosphorylated DNA fragments were purified from the reaction mix with the QIAquick Nucleotide Removal Kit (QIAGEN) according manufacturer's protocol. The DNA was eluted in 15 µl of buffer EB.

Ligating vector and target DNA fragments: A 10 µl reaction containing purified linearized vector and DNA fragments in 1:5 molar ratio, 1 µl of 10x ligation buffer (NEB), and 1 µl of T4 DNA ligase (NEB) was incubated O/N at 16°C or at RT for 2 h, followed by 30 min at 37°C for sticky end ligations. Approximately 2-5 µl of the reaction was used to transform competent bacteria.

8.2.1.3. Agarose gel electrophoresis and DNA purification

According to the DNA sizes, 0.8-2% agarose gel was prepared by microwave melting agarose in TAE buffer. After the agarose solution cooled down to ~45°C, ethidium bromide was added (6 µl is required for 100 ml agarose gel) and the solution was poured into a gel chamber. When the gel solidified DNA solution mixed with loading buffer in 10:1 volume ratio were loaded onto the gel and run for 30-35 min at 180-200 V. DNA was visualized and photographed under UV light using a gel documentation system (BioRad).

For purification of DNA, the appropriated DNA band (according to its size) was excised from the agarose gel with a scalpel and purified by the QIAquick Gel Extraction Kit (QIAGEN) as recommended by the manufacturer. The DNA was eluted in 15 µl of buffer EB.

8.2.1.4 Preparation of competent *E.coli*

An o/n culture of DH5α cells was inoculated at 1:100 volume ratio in 1 l of LB medium. The bacteria culture was grown at 37°C with vigorous shaking until the optical density measured with 600 nm wavelength reached 0.5-0.8. The culture was chilled on ice for 30 min followed by centrifuged at 4000xg at 4°C. The pellet was resuspended in 1 l of cold sterile water and centrifuged again. 0.5 l of sterile water was used for the second resuspension. After centrifugation and harvesting the clean bacteria pellet, 20 ml of 10% glycerol was added for resuspension. The bacteria suspension was then centrifuged as above and resuspended in 3 ml of 10% glycerol. Aliquots of 50 µl were frozen in liquid nitrogen and stored at -80°C.

8.1.2.5 Transformation of competent *E.coli* by electroporation

50 µl of competent bacteria was thawed on ice and 0.5 µl of plasmid DNA or 1-5 µl of ligation product was added. The mixture was transferred into a sterile, pre-chilled 0.2 cm cuvette without making bubbles. The gene pulser apparatus was set to 25 µF and 2.5 kV; the pulse controller to 200 Ω. The dried cuvette was placed into the chamber slide and pulsed once. Immediately, 200 µl of SOC or LB medium without antibiotic was added to the cells, which were then transferred to a 12 ml bacteria culture tube and shaken 60 min at 37ºC. Subsequently, the bacteria were spread on LB plates containing selective antibiotic and grown o/n at 37°C.

8.2.1.6 PCR Genotyping

Dissolving DNA: Tail samples (1-3 mm) were taken from mice at weaning age (~ 3 weeks). To dissolve DNA, tail samples were heated at 95°C for 30 min in 100 µl 50 mM NaOH and vortexed thoroughly. Heating step could be repeated once when necessary. Once the

samples were well digested, the mixture was neutralized with 10 µl of 1.5 M Tris-HCl (pH 8.8) and processed with PCR or stored at 4°C.

PCR: 1-2 µl of DNA was used as template in the PCR reaction containing 200 µM dNTPs (25 mM of each dNTP in dNTPs mix stock), 20-50 pmol of each primers to amplify a sequence of genomic DNA specific for a given allele, 1x PCR buffer (500mM KCl, 15mM MgCl2, 100mM Tris·HCl, pH 8.8, 0.8% Nonidet, NEB) and 0.3-0.5 µl of Taq polymerase (NEB). The PCR was carried out in a total volume of 50 µl. Agarose gel electrophoresis was used to separate PCR products.

8.2.2. Cell culture

8.2.2.1. Propagation and freezing of mammalian cell lines

Cells were grown at 37°C in a humidified incubator supplied with 5% CO_2 on non-coated polystyrene culture dishes (Falcon). Confluent 100 mm dishes were washed once with warm PBS, and incubated with 2 ml Trypsin/EDTA (Invitrogen) for ~2 min to detach cells from the dish. Growth medium containing FBS was added to stop trypsin enzymatic activity. Cells were usually seeded in a 1:10 ratio for experiments in the following day. Confluency has no observable effect on Phoenix A cell or astrocytoma growth. The cells thus could be seeded at very low confluency for long-term culture.

Phoenix A and astrocytoma cells were frozen in 46.25 % growth medium, 46.25 % FBS, and 7.5 % DMSO. Cells from a 100 mm confluent plate were aliquot into 3 cryotubes (2 ml) which were quickly transferred into an isopropanol container and stored at -80°C. Once the cells were frozen they were removed from the isopropanol container and stored at -80°C or transferred to liquid nitrogen tank for long-term storage. To recover frozen cells, cells were thawed slowly on ice, resuspended in growth medium, pelleted to remove DMSO and seeded.

8.2.2.2. Transfection of cell lines using Lipofectamine

One day before transfection, $3.5x10^6$ cells were plated onto polystyrene culture dish (Falcon) with normal growth medium. On the day of transfection, cells (~70-80% confluence) were washed once with PBS and medium was changed to growth medium without

antibiotics (exposure to antibiotics during transfection will cause cell death). 24 µg of plasmid DNA was mixed with 1 ml of basal medium without serum (D-MEM). In a separate tube 30 µl of lipofectamine was gently mixed with 1 ml of the basal medium. After 5 min incubation at RT, DNA and lipofectamine diluents were mixed and gently and incubated at RT for 20 min. The mixture was then added to the cells drop-wise and mixed gently by rocking the plate back and forth. Cells were incubated at 37°C in 5% CO_2 and transfection efficiency could be assessed after 16 h.

8.2.2.3. Primary endothelial cell isolation and culture condition

The generation of conditional knockout mice *ephrinB2*$^{lox/lox}$ has been described (Grunwald et al., 2004). P1-10 mice were sacrificed. Lungs and brains were removed into dissection buffer and minced into small pieces. The tissues were then treated with collagenase type II (260 units/ml for lung tissues and 130 units/ml for brain tissues) at 37°C in a humidified incubator supplied with 5% CO_2 for 30 min with occasional shaking. 0.5 ml of collagenase is required per tissue from one mouse. The digested tissues were passed through 40 µm disposable cell strainer to remove tissue debris and cell clumps that were not well-digested and centrifuged at 1,100 rpm for 5 min at 4°C. Lung tissue pellets were collected and resuspended in the dissection buffer. Brain tissue pellets were mixed with 25% BSA in PBS and centrifuge at 2,600 rpm for 20 min at 4°C to remove myelin before resuspension with dissection buffer. To wash out remaining collagenase and BSA tissue suspensions were centrifuged at 1,100 rpm for 5 min at 4°C, pellets were collected and resuspended in fresh dissection buffer. After 2 washes, tissue pellets were resuspended in 2 ml dissection buffer and incubated with anti rat IgG coated magnetic beads (Invitrogen, $8x10^7$ beads per 1 brain or lung) o/n pre-coupled with rat anti-mouse PECAM-1 (MEC13.3 BD Pharmingen, 7 µg per one brain or lung) at 4°C for 1 h with gentle rotation. The beads were washed 5 times by placing the tube to a magnet (Dynal Biotech), aspirating the supernatant, and refilling with dissection buffer. The washed beads were resuspended in endothelial cell growth medium and plated onto 1% gelatin-coated plate. The magnetic beads were detached from the cells by trypsinization in the first passage.

Mouse lung endothelial cells has higher growth rate as compare to brain endothelial cells. The lung cells could be passage for 14-16 times without any obvious change in their angiogenic activities whereas the brain cells have reduced proliferation rate after ~10 passages. Confluency of the culture plays an important role in survival, proliferation, and angiogenic activities of the primary endothelial cells. The confluent cultures, which grow in monolayer and display cobble stone-like morphology, should be propagated at 1:4 or not less than 1:6 ratio. Very sparse cultures result in cell death. Cells should be propagated a day before angiogenesis assays to a sub-confluent culture ($1.8x10^5$ cells in 60 mm plate, ~60% confluency).

8.2.2.4 Generation of ephrinB2 knock out endothelial cells

Endothelial cells isolated from *ephrinB2*$^{lox/lox}$ mice were infected with adenovirus encoding Cre recombinase (Vector Biolabs) at Moi 200 (200 phage forming units/ cell). After o/n incubation, medium containing virus was changed to fresh growing medium. The virally infected cells were cultured for 1 week before use.

8.2.2.5 Endothelial cell transfection and stimulation

The ephrinB2 expression constructs were introduced into primary mouse endothelial cells by electroporation using basic endothelial nucleofector kit (Amaxa) according to manufacturer's recommended protocol. $2x10^5$ cells were seeded onto 60 mm culture dish 3 days before transfection. On the day of transfection cells at ~70-80% confluency were trypsinized and cell suspension was centrifuged at 1000 rpm for 5 min. Supernatant was removed and 500 µl of fresh growth medium was added to resuspend cell pellet. The cells were counted to determine cell density and $4\text{-}5x10^5$ cells were aliquot into new tube. After centrifugation and discarding supernatant, 100 µl of basic nucleofactor solution (without supplement provided in the kit) was added to resuspend cell pellet and 1-3 µg of plasmid DNA (in less than 5 µl) was added to the suspension. The suspension was transferred into a cuvette provided in the kit without making bubbles. The cuvette was placed into the holder in

the nucleofactor machine. Cells were electroporated with program T-23. Immediately after electroporation finished 500 µl of warm growth medium was added to the cuvette and cells suspension was transferred into a gelatin-coated 60 mm culture dish filled with 3.5 ml of growth medium. Plastic pipette provided in the kit is recommended for the transferring the cells from the cuvette after electroporation to prevent cell damage. The whole process after the nucleofactor solution was added should not take longer than 20 min as this reduce cell viability. Transfection efficiency could be assessed after 16 h.

Recombinant mouse EphB4-Fc and ephrinB2-Fc chimeras (R&D) were clustered by incubation with the antibody against human Fc (Jackson ImmunoResearch) at a 15:1 w/v concentration ratio for 1 h at RT. The pre-clustered recombinant proteins at a final concentration of 4 µg/ml in serum-reduced medium were used for stimulation of the primary endothelial cells.

8.2.2.6. Primary astrocyte dissection

Brains were removed from new born mice (P2-5) and transferred into a 60 mm culture dish filled with ice cold dissection buffer. Meninges was totally removed from the brain and cerebral hemispheres were transferred into a 15 ml plastic tube filled with cold dissection buffer. Subsequently dissection buffer was removed and 2 ml of 1X trypsin-EDTA (2.5 g/L of Trypsin, 0.38 g/L EDTA•4Na in HBSS without $CaCl_2$, $MgCl_2$, Invitrogen) was incubated with the brain for 25 min at 37°C in a humidified incubator supplied with 5% CO_2. Trypsin enzymatic activity was inhibited by addition of 5 ml of growth medium and brain tissues were triturated with fire-polished Pasteur pipette until a homogeneous tissue suspension was observed. The suspension was centrifuged for 5 min at 80g and supernanant was discarded. Cells were resuspended in 10 ml of growth medium and plated in 75 cm^2 polystyrene culture flask (Nunc) (1 brain/1 flask). Medium was changed after 2-3 days.

To remove oligodendrocytes which could grow on top of astrocyte monolayer, primary cells cultured for 1 week after isolation were washed with PBS and fresh growth

medium was added. To prevent contamination culture flask cap was wrapped with parafilm and the flask was put in a latex glove and sealed tightly before the flask was shaked at 250 rpm, at 37°C in a bacteria incubator. Cells were washed with PBS and medium with detached cells was changed twice every 24 h. Purity of the astrocyte culture was assessed by staining with anti-GFAP antibody.

8.2.2.7 Generation of murine astrocytomas

Immortalization

pOT vector harboring SV40 Large-T antigen (gift from T. Acker) was linearized at *Sal*I restriction site for stable transfection. As pOT vector has no mammalian selectable marker, eYFP-N1 (Clontech) harboring *neoR* was to co-transfected with pOT. eYFP-N1 was linealized by *Dra*III digestion. Both linealized vectors were purified by PCR purification column and dissolved in small volumes of elution buffer. On the day of transfection primary astrocytes (from 70-80% confluent plate) were harvested and 1-2x10^6 cells were suspended in 100 µl basic endothelial cell nucleofactor solution. 5 µg of pOT and 1.5 µg of eYFP-N1 (>3:1 ratio) in less than 5 µl in total were added to the cell suspension. Astrocytes were electroporated with Amaxa nucleofactor machine with program T-20. 48-64 h posttransfection, stably transfected cells were selected in astrocyte growth medium containing 300µg/ml geneticin (Gibco) for 3 weeks. Resistant colonies were pooled and proceed with H-Ras viral infection.

H-RasV12 virus production

pBABE-Hygro retroviral vector (Addgene) harboring *H-RasV12* was introduced into Phoenix A cells by lipofectamin transfection as described. Medium was changed at 24 h after transfection (8 ml/100 mm diameter plate). Transfected cells were cultured for another 24 h and 48 h when supernatant containing virus particles was collected and filtered through a 0.45 µm filter to remove detached cells. Supernatant was aliquoted in 2-4 ml volumes and kept at -80°C. Note: Medium used throughout the process contained no antibiotic.

Viral infection

Immortalized astrocytes were passaged a day before infection at $3x10^5$ cells in a 100 mm culture dish. On the day of infection (cells should reach 40-50% confluency) cell were washed once with PBS and 4 ml of virus supernatant mixed with 4 µg/ml polybrene (Sigma) and 4 ml of growth medium was added to the cells. 48 h postinfection, 2 µg/ml puromycin (Sigma-Aldrich) was added to growth medium to select for stably transfected cells. Colonies grew after 3 weeks of selection were pooled and expression of SV-40 Large T antigen and H-RasV12 proteins was confirmed by immunoblot analysis.

8.2.3. Angiogenesis assay with primary endothelial cells

8.2.3.1. Tube formation assay

Matrigel, a solubilized basement membrane matrix extracted from Engel-Holm-Swarm (EHS) mouse sarcomas (BD Biosciences) has been used in the endothelial cell capillary-like structure formation. In fact, it has been shown that some other cell types such as fibroblasts were able to from a similar network structure when seeded onto the matrigel. Matrigel is mainly consisted of laminin with some other membrane matrix protein including collagen IV and heparin sulfate proteoglycans. It also contains fibroblast growth factor (bFGF), TGF-β and other growth factors naturally produced by EHS tumors. As matrigel was extracted from sarcomas, different production batches could be varied in the compositions. Matrigel is in liquid form when temperature is lower than 4°C and polymerized at RT. For the formation assay in a 48-well manner, 150 µl of ice-cold matrigel was added to layer each well of a plate pre-cooled on ice. The gel was left to polymerize at RT for 5 min. Endothelial cells from sub-confluent culture were detached from plate with accutase (PAA), resuspended in starving medium containing 1% fetal bovine serum, and plated onto the matrigel-layered well. $1.5x10^4$ cells were required for each well. The plate was incubated at 37°C in a humidified incubator supplied with 5% CO_2 for 6-8 hours.

Quantitative measurement of the tubular network based on the percentage of area covered with capillary structures was done by using ImageJ (NIH). EphrinB2KO cells were

still able to form tubular structures although these tubes showed a 2.4 fold increase in tube disruption. However ephrinB2KO tubes were suitable for re-introduction of wild type and signaling mutants to study the repulsive activity conferred by ephrinB2 signaling. For the quantification of percentage of non-integrated cells, all YFP-expressing cells were identified at the beginning of each movie and their movements were followed until the tubular network was formed at end of the movie. Cells that died or exit from the frame were excluded from the quantification. The percentage of cells that were not integrated into the tubular structures compared to the total number of green cells, remained in the frame at the end of the movie was calculated.

8.2.2.2. Time lapse imaging

Live-cell imaging of primary endothelial cells seeded on matrigel was performed using a Zeiss Axiovert 200M microscope equipped with a temperature controlled CO_2-incubation chamber. Temperature was set to 37°C and CO2 level to 5%. The chamber was humidified by passing CO2 gas though a water container and sponge soaked in sterile water. Images were acquired using a 20x objective with a CoolSNAP-fx camera at a rate of one frame per 40 seconds or one minute. Images were processed using MetaMorph software (Molecular Devices).

8.2.4. Immunocytochemistry

8.2.4.1. Antibody Feeding Assay

Sub-confluent culture of primary mouse endothelial cells was split a day before the assay. 40,000 cells were seeded onto 1% gelatin-coated 13 mm glass cover slip in each well of a 24-well culture plated. Cells were blocked at 37°C for 10 min in blocking solution consisted of DMEM, 2% (w/v) bovine serum albumin and 4% (v/v) goat serum (Jackson ImmunoResearch). Anti-Flk1 primary antibody (R&D, 1:40) in the blocking solution was incubated with cells at 37°C for 20 min. After 2 washes with warm D-PBS + Ca^{2+}/Mg^{2+} cells were stimulated with recombinant human $VEGF_{165}$, pre-clustered EphB4-Fc or human Fc in

endothelial growth medium at 37°C for 30 min, and fixed with 4% PFA in PBS at 4°C for 30 min. After incubation with 50 mM NH_4Cl for 10 min at RT, cover slips were washed once with PBS and transferred onto a dark humidified tray. Surface receptors were detected by incubation with Cy2- conjugated secondary antibodies (Jackson ImmunoResearch, 1:200) in blocking solution (PBS containing 2% (w/v) bovine serum albumin and 4% (v/v) donkey serum) without permeabilization for 2 h at room temperature. After 3 washes with PBS, cells were permeabilized for 30 min with ice cold blocking solution containing 0.25% (v/v) Triton X-100 and Cy3-conjugated secondary antibody (Jackson ImmunoResearch, 1:200) was incubated with the cells for 1 h at room temperature to visualize internalized receptors.

A digital camera (SpotRT; Diagnostic Instruments) attached to an epifluorescence microscope (Zeiss) equipped with a 63x objective (Plan-Apochromat; Zeiss) was used for imaging. Quantitative measurements based on fluorescent intensities were performed using MetaMorph software (Molecular Devices). Percentages of internalized receptors (red fluorescent) as compared to total amount of receptors (green fluorescent + red fluorescent) were calculated from at least 10 endothelial cells from each group, 4 independent experiments were performed. Depending on the equality of variances between the tested populations examined by F-test, type-one or type-two Student's *t* tests were used to assess statistical significance of their differences. n=number of experiments.

8.2.4.2. Staining of surface ephrinB2 with recombinant protein EphB4-Fc

Sub-confluent culture of endothelial cells was seeded on gelatin-coated cover slip in 24-well plate and Recombinant EphB4-Fc was pre-clustered as described. A final concentration of 4 µg/ml of clustered EphB4-Fc in a starving medium containing 2% FBS without growth supplement was used to stimulate endothelial cells at 37°C for 15 min. 200 µl of medium is required for each well. After stimulation, endothelial cells were fixed in 4% PFA in PBS at 4°C for 30 min. Following washing of PFA with PBS, cells were incubated with 50 mM NH_4Cl (to reduce auto-fluorescent) for 10 min at room temperature then washed once with PBS. Cover slips were transferred to a dark humidified tray. 100 µl of blocking solution

(PBS containing 2% (w/v) bovine serum albumin and 4% (v/v) donkey serum) was gently overlaid each cover slip and incubated for 1 h at RT. 0.25% Triton X-100 was added to the blocking solution when permeabilization is required. Next, blocking solution was removed and fluorochrome-conjugated antibody raised against human Fc (Jackson Immunoresearch) in blocking solution at 1:200 volume ratio was incubated with cells for 1 h at RT. Cells were washed for 3 times with PBS and cover slips were mounted with vectashield mounting medium containing DAPI. Slides was kept in the dark o/n, sealed with nail polish and kept at 4°C. Note that pipeting during solution changing and washing steps should be done gently but quick enough not to let the cover slip dried as buffer precipitates causes background.

8.2.5. Biochemistry

9.2.5.1. Tissue lysis and protein immunoprecipitation

Lysis: Neonatal mouse brains were lysed with 3X volume to weight of cold NP-40 lysis buffer in a glass Teflon dounce homogenizer. Tissue lysate was transferred into 2 ml eppendorf tubes and further lysed at 4°C on a rotating wheel for 30 min. Insoluble material was removed by centrifugation for 15 min at 13000 rpm at 4°C. Supernatants were collected and protein concentrations were measured using the DC Protein Assay (BioRad). Supernatants were used immediately or frozen in liquid nitrogen and stored at -80°C.

Immunoprecipitation: To lower the amount of non-specific proteins 1-2 mg of tissue protein samples each was incubated with 45 µl protein G-Sepharose beads (for mouse monoclonal or goat polyclonal antibodies, Amersham) or protein A-Sepharose beads (for rabbit polyclonal antibodies, Amersham), which were pre-cleaned from methanol by washing with PBS, on a rotating wheel for 30 min at 4°C. Beads were removed by centrifugation at 4,000 rpm for 5 min and supernatant was incubated with 45 µl methanol-free beads pre-bound with 4 µg anti-flk1 antibody (R&D systems) for 2 h at 4°C. The supernatants were then discarded and the beads were washed three times with lysis buffer to remove uncoupled proteins. 12 µl of 6x SDS sample buffer was added to the beads and the samples denatured by boiling at 95°C for 3 min before loading on a polyacrylamide gel.

8.2.5.2. Immunoblotting

Protein samples were separated in 7.5% SDS-PAGE and transferred to 0.45 µm nitrocellulose membranes (Schleicher & Schuell) by semi-dry blotting (1 mA per cm^2 of membrane for 45-120 min according to protein sizes). Membrane was incubated with blocking solution (5% BSA or 5% non-fat milk in PBST) for 1 h and primary antibody diluted in PBST was incubated with the membrane for 1 h at RT (or diluted in blocking solution and incubated o/n at 4°C) with continuous rocking. After 3 washings for 5 min with PBST secondary antibody diluted in PBST was applied to the membrane and incubated for 1 h at RT. Subsequently, antibody solution was removed and the membrane was washed for 3 times with PBST. Finally, the membrane was incubated with 1 ml of ECL solution (Amersham) and exposed to X-ray films (Kodak, Biomax) to visualize signals. If subsequent detection of another protein was necessary the membrane was incubated with stripping buffer (PBS containing 2% SDS and 0.02% β-mercaptoethanol) for 30 min at 65°C and re-blotted as described above.

8.2.6. Analysis of postnatal retinal angiogenesis

8.2.6.1. Retina dissection

Neonatal mice from P1 to P7 were sacrificed. Eyes were removed and fixed with 4% PFA at 4°C o/n. Eyes were washed with PBS and put in a culture dish filled with PBS. Under a stereo microscope equipped with internal light source, eye was hold with a blunt forceps at tissue surrounding the eye ball and a small cut was made above the eye lens. Len and iris were extracted with fine forceps. Retina was subsequently extracted from the eye cup by inserting blunt end forceps between retina and eyecup and then shearing eye cup and forceps in opposite directions. Vitreous body and hyaloids vessels were totally removed from retina with sharp end forceps without touching the retina tissue. Retinas were processed for vessel staining or passed through a series of continuous increased concentrations of methanol diluted in PBS (25%, 50%, 75%, and 100%) for dehydration and stored at -20°C in 100% methanol.

8.2.6.3. Retina vessel staining

Visualization of retinal vessels was done as described (Gerhardt et al., 2003) with minor modifications. Briefly, retinas dissected from neonatal mice were permeabilized and stained with 40 µg/ml FITC conjugated lectin from *Bandeiraea simplicifolia* (Isolectin B4, Sigma-Aldrich) at 4°C overnight. After 5 washes with PBS, retinas were post-fixed in 4% paraformaldehyde (PFA) and flat mounted with Vectashield mounting medium containing DAPI (Vector Laboratories).

8.2.6.3. Retina whole mount LacZ staining

Retinas were dissected from eye cups and fixed in freshly made glutathione fixative for 1h at RT, washed 3 times 10 min each in wash buffer and incubated in X-Gal staining solution (X-Gal 1 mg/ml as a final concentration) at 37 °C in the dark for 1-2 h. Retinas were washed 3 times for 10 min in wash buffer and postfixed in 4% PFA at RT for 30 m. After washing once with PBS retinas were flat-mounted with Vectashield mounting medium.

8.2.6.4. Retina endothelial cell proliferation assay

P7 pups were injected with BrdU (100 µg/ g body weight) intraperitoneally 2 h prior to eye dissection. Following an o/n 4% PFA fixation retinas were stained with isolectinB4 as described. Subsequently, retinas were post fixed for 1 h at RT with 4% PFA, washed 3 times with PBS and incubated with PBS containing 6 M HCl and 0.1% Triton X-100 for 1 h at RT. After 5 washes in PBS with 0.1 % Triton X-100, retinas were incubated o/n sequentially with BrdU antibody (AbD Serotec, 1:100) and Alexa Fluor-coupled secondary antibody. Retinas were washed 3 times for 1 h and flat-mounted on glass slices with Vectashield mounting medium.

8.2.6.5 Quantification of retinal angiogenesis

Quantification of retinal angiogenesis in CD1 mice was done in P7 retinas. Number of branch points and filopodia bursts in randomly defined fields in arterial zones were counted manually. The values were normalized with field sizes. Filopodia per tip cell were counted from at least 30 tip cells (inside the vascular beds) in each mouse. Filopodia extension at the sprouting fronts was quantified based on number of filopodia per 100 µm of vessel length (measured from lines drew along the border of vascular fronts). Vascular density measurement was done by calculation of areas covered with vessel in at least five arterial zones in each retina using ImageJ. For the P2 C57/Bl6 mouse retinas, the radial length of the vascular network was measured from the average length of at least 3 lines drawn from the center of the retina in the optic disc to the edge of the network. Vascular density was measured from the vascular areas in 300x300 µm fields next to the optic discs. Endothelial cell proliferation was assessed based on number of BrdU positive cells per vascular area. 6-8 retinas from each genotype were used for all quantifications. Filopodia protrusions at the vascular front were analyzed from 20 microscopic fields picked from 10-12 retinas per group for *ephrinB2*$^{\Delta V/\Delta V}$ and control littermates and quantified using MetaMorph software (Molecular Devices). Depending on the equality of variances between the tested populations examined by F-test, type-one or type-two Student's *t* tests were used to assess statistical significance of their differences.

8.2.7 Acute retina explantation

Eyes were enucleated from new born pups (P4-5) and transferred to FBS free DMEM medium. Retinas were dissected from eye cups and vitreous bodies were totally removed. Retinas were flat-mounted onto the hydrophilic polytetrafluoroethylene (PTFE) membrane of Millicell inserts (Millipore) with photoreceptor layer on top and nerve fiber layer attached to the membrane. DMEM with 10% FBS was layered underneath the membrane and dropped on retinas to prevent dryness. Retina explants were incubated at 35°C in a humidified incubator with 5% CO_2 for 2-4 h before stimulation. For stimulation of retina endothelial tip cells all factors diluted in DMEM with 3% FBS were layered underneath the insert membrane and dropped on the explants. Concentrations of VEGF164 and EphB4Fc

or hFc used were 1 µg/ml and 10 µg/ml, respectively. Soluble Flt-1 at a concentration of 1 µg/ml and 0.32 mM of dynasore were added to the medium when required. Stimulation were carried out at 35°C in a humidified incubator with 5% CO_2 for 4 h. Explants were fixed with 4% PFA at 35°C for 4h and proceeded for isolectin staining of vessels as described.

8.2.8 Surface biotinylation assay in cortical slices

Acute cortical slices (400 µm thick) were prepared from brains of P8-9 mice using custom made slicer. Slices were kept in artificial cerebrospinal fluid (ACSF: 124 mM NaCl, 3 mM KCl, 1.25 mM KH_2PO_4, 2.5 mM $CaCl_2$, 2 mM $MgSO_4$, 26 mM $NaHCO_3$, 10 mM glucose, saturated with 95% O2 and 5% CO_2) for 1-2 h at room temperature. To label surface proteins slices were incubated on ice with EZlink-NHS-SS-Biotin (Pierce, Rockford, Illinois) at a concentration of 0.5 mg/ml ACSF for 1 h. After 2 washes with ACSF, 10 µg/ml EphB4Fc or control hFc proteins were applied to the slices. Stimulations were carried out for 1-1.5 h at room temperature. Remaining surface biotin was stripped out by incubation with 2.3 g/ml reduced L-Glutathione (Sigma) for 30 min on ice. Glutathione was subsequently neutralized by incubation with Ethanolamide (0.9 µl/ml ACSF) on ice for 30 min. Slices were washed twice with ACSF and cells were lysed with NP-40 lysis buffer (see immunoprecipitation). Equal amounts of proteins from each sample were incubated with Neutravidin sepharose (Pierce, Rockford, Ilinois) on a rotating wheel overnight at 4°C. Beads were washed for 3 times with lysis buffer and boiled at 95°C in SDS sample buffer before proceed for western blot analysis.

8.2.9. Histology

8.2.9.1 Cardiac injection of FITC-Dextran

Mice were anesthetized with an intraperitoneal injection of chloralhydrate (8% chloralhydrate, 0.9% NaCl in H_2O). 1.5 ml of 50 mg/ml fluorescein isothiocyanate dextran, molecular weight $2x10^6$ (Sigma-Aldrich), in PBS were injected intracardially. Brains and eyes were dissected and fixed with 4% PFA at 4°C overnight. 60 µm coronal brain sections were

obtained with a vibratome and mounted with Vectashield mounting medium containing DAPI. Retinas were dissected and flat-mounted as described. Confocal images of brain and retina vessels were used to analyze vessel density based on areas of the brain or retina tissues covered with vessels by ImageJ. Four mice from each genotype were used for quantification. Depending on the equality of variances between the tested populations examined by F-test, type-one or type-two Student's *t* tests were used to assess statistical significance of their differences.

8.2.9.2 Whole mount retina staining

Retinas dissected from eyes fixed overnight in 4% PFA were blocked in D-PBS containing 0.5 % Triton X-100, 2 % (w/v) BSA and 4 % (v/v) donkey or goat serum (depend on species of secondary antibody) for 2 h at RT. Subsequently, retinas were incubated with primary antibody (and isolectin when vessel staining in required) for 64 h at 4°C with gentle rocking. A volume of 0.4 ml in 24-well plate is suitable for 2-4 retinas. Concentration of primary antibody and recombinant proteins used: rabbit anti-GFAP (DAKO) 1:70, EphB4-Fc (R&D) 1:20, EphrinB2-Fc (R&D) 1:20. Primary antibody adhered non-specifically to the retina tissue was washed out with PBS 3 times for 1 h. Retinas were incubated with secondary antibody in blocking buffer o/n at 4°C, washed 5 times for 1 h, and post-fixed for 30 m with 4 % PFA before flat-mounted with Vectashield mounting medium (Vector Laboratories, Burlingames, CA). Note: secondary antibody Cy5-conjugated goat anti hFc (Jackson Immunoresearch) was used at a concentration of 1:100. To prevent any precipitates from PFA and serum in blocking buffer to adhere to the tissue and cause background, PFA and blocking buffer were filtered through 0.45 µm filter before use. Fixation time can be crucial to the staining. For some epitopes, eyes could be fixed with 4 % PFA on ice for 4-6 h prior to retina dissection and staining.

8.2.9.3. Vibratome sections

Perfused and postfixed brains were embedded in a gelatine-albumin (gel/alb) mixture (0.5g gelatine in 100ml PBS, then dissolved 30g egg albumin in this solution). A layer of 2ml gel/alb vigorously mixed with 100 µl 25% glutaraldehyde was poured into a small plastic mould and left to polymerize for 2-5 min. Brain was placed on top and 3ml gel/alb with 150 µl glutaraldehyde was poured into the mould to cover it. The mould was left to set for 5minutes at RT and submersed in cold PBS for 1-2 h to ensure complete polymerization. The gel/alb block was trimmed and glued to the vibratome platform and placed into the vibratome chamber filled with cold PBS. Generally, 40-80 µm coronal sections (for immunofluorescense) were cut at low speed and high vibration frequency.

8.2.9.4 Tumor transplantation

CD1 ephrinB2$^{\Delta V/\Delta V}$ and control littermate or C57B/BL6 ephrinB2i∆EC and control littermate (ephrinB2WT/loxPCre^{-} treated with Tamoxifen) mice were anesthetized and placed into a stereotactic apparatus (Kopf instruments). A burr hole was made 2 mm left of the sagittal suture and 0.5 mm anterior to the bregma using a dental drill 0.7 mm in diameter. For transplantation 5x10^4 CD1 astrocytoma cells (see above) or C57B/BL6-Gl261 astrocytoma cells were resuspended in cold, CO_2-independent medium and slowly injected at a depth of 3.5 mm from the dura using a 2.5 µl Hamilton microsyringe with an unbeveled 33G needle. Mice were maintained until the development of neurological symptoms. Two separate transplantation experiments were performed with independently generated astrocytoma lines in a total of 18 animals (11 controls and 7 ephrinB2∆V). Tumor bearing mice were injected with 100 µg biotinylated tomato lectin (Vector Laboratories, Burlingame, CA, USA) retrobulbarly, 5 minutes prior to cardiac perfusion with 4% PFA in PBS. Tumor volume was determined by tracing the tumor area using the semi-automated stereological system Stereo Investigator 4.34 (MicroBrightField Inc., Williston, VT, USA) and a Zeiss Axiophot microscope (Carl Zeiss, Jena, Germany), equipped with a Hitachi HV-C20A (Hitachi) camera. Series of every twelfth section (480 µm interval) throughout the brain were analyzed. For subcutaneous tumor injections CD1 ephrinB2∆V and control littermate were anesthetized, shaved and 2x10^6 CD1 astrocytoma cells resuspended in PBS/Matrigel were injected in a total volume of 200µl into either flank of the mice. Tumor bearing animals were

maintained for 21 days until tumors exceeded a volume of 800 mm^3. Tumors were frozen in TissueTek for further histological analysis. Statistical comparisons of the measurements were made using type-one or type-two Student`s t-test depending on the equality of their variances examined by F-test.

8.2.9.5. Antibody staining of brain tumor sections

Tumor samples were frozen and cut into 40 µm (intracranial tumor) or 8 µm (subcutaneous tumor) thick sections. For hematoxylin-eosin (HE) staining, they were first stained with Mayer´s hematoxylin (10 min) and then counterstained with alcoholic eosin for 2 minutes. For immunohistochemical studies, free-floating (intracranial tumor) or mounted (subcutaneous tumor) sections were washed in PBS. Endogenous peroxidase was neutralized with 0.6 % H_2O_2 in PBS for 30 min. After washing again in PBS, sections were mounted on microscope slides and dried for 3 h at room temperature (intracranial tumor). Antigen retrieval was performed for 10 minutes in Tris-EDTA (TE) buffer, pH 8.0, in a steamer. Sections were blocked with 20 % normal goat serum (NGS)/0.01 % Triton in PBS for 1 h. For CD34 staining sections were blocked with 5% bovine serum albumin (BSA)/0.01% Triton for 1 h. Subsequently a second blocking step was performed using 20% NGS/0.01% Triton in PBS for 1.5 h. The sections were then treated overnight at 4 °C with CD34 primary antibody (1:100, clone MEC14.7, Abcam) in 10% NGS/0.01% Triton in PBS. After washing in PBS, sections were incubated with secondary antibody peroxidase-conjugated goat anti rat IgG, diluted 1:100 in 10% NGS/0.01% Triton in PBS for 1 h. After a PBS wash, visualization was performed using the CSA II, Biotin-Free Catalyzed Amplification System (Dako, Glostrup, Denmark) according to the manufacturer's instructions. After washing in PBS, sections were counterstained in hematoxylin for 8 min and mounted in Aquatex (Merck, Darmstadt, Germany). Vessel density was quantified by measuring blood vessels area stained with CD34 in 10 randomly chosen optical fields per tumor. Depending on the equality of variances between the tested populations examined by F-test, type-one or type-two Student's *t* tests were used to assess statistical significance of their differences.

10. Bibliography

Adams, R.H., and Alitalo, K. (2007). Molecular regulation of angiogenesis and lymphangiogenesis. Nat Rev Mol Cell Biol *8*, 464-478.

Adams, R.H., Diella, F., Hennig, S., Helmbacher, F., Deutsch, U., and Klein, R. (2001). The cytoplasmic domain of the ligand ephrinB2 is required for vascular morphogenesis but not cranial neural crest migration. Cell *104*, 57-69.

Adams, R.H., Wilkinson, G.A., Weiss, C., Diella, F., Gale, N.W., Deutsch, U., Risau, W., and Klein, R. (1999). Roles of ephrinB ligands and EphB receptors in cardiovascular development: demarcation of arterial/venous domains, vascular morphogenesis, and sprouting angiogenesis. Genes Dev *13*, 295-306.

Alonso, A., Sasin, J., Bottini, N., Friedberg, I., Osterman, A., Godzik, A., Hunter, T., Dixon, J., and Mustelin, T. (2004). Protein tyrosine phosphatases in the human genome. Cell *117*, 699-711.

Ambler, C.A., Nowicki, J.L., Burke, A.C., and Bautch, V.L. (2001). Assembly of trunk and limb blood vessels involves extensive migration and vasculogenesis of somite-derived angioblasts. Dev Biol *234*, 352-364.

Arevalo, J.C., Waite, J., Rajagopal, R., Beyna, M., Chen, Z.Y., Lee, F.S., and Chao, M.V. (2006). Cell survival through Trk neurotrophin receptors is differentially regulated by ubiquitination. Neuron *50*, 549-559.

Armulik, A., Abramsson, A., and Betsholtz, C. (2005). Endothelial/pericyte interactions. Circ Res *97*, 512-523.

Avraamides, C.J., Garmy-Susini, B., and Varner, J.A. (2008). Integrins in angiogenesis and lymphangiogenesis. Nat Rev Cancer *8*, 604-617.

Bates, D.O., Cui, T.G., Doughty, J.M., Winkler, M., Sugiono, M., Shields, J.D., Peat, D., Gillatt, D., and Harper, S.J. (2002). VEGF165b, an inhibitory splice variant of vascular endothelial growth factor, is down-regulated in renal cell carcinoma. Cancer Res *62*, 4123-4131.

Bedell, V.M., Yeo, S.Y., Park, K.W., Chung, J., Seth, P., Shivalingappa, V., Zhao, J., Obara, T., Sukhatme, V.P., Drummond, I.A.*, et al.* (2005). roundabout4 is essential for angiogenesis in vivo. Proc Natl Acad Sci U S A *102*, 6373-6378.

Beg, A.A., Sommer, J.E., Martin, J.H., and Scheiffele, P. (2007). alpha2-Chimaerin is an essential EphA4 effector in the assembly of neuronal locomotor circuits. Neuron *55*, 768-778.

Benedito, R., Roca, C., Sorensen, I., Adams, S., Gossler, A., Fruttiger, M., and Adams, R.H. (2009). The notch ligands Dll4 and Jagged1 have opposing effects on angiogenesis. Cell *137*, 1124-1135.

Bergers, G., and Benjamin, L.E. (2003). Tumorigenesis and the angiogenic switch. Nat Rev Cancer *3*, 401-410.

Bergers, G., and Hanahan, D. (2008). Modes of resistance to anti-angiogenic therapy. Nat Rev Cancer *8*, 592-603.

Bertolini, F., Shaked, Y., Mancuso, P., and Kerbel, R.S. (2006). The multifaceted circulating endothelial cell in cancer: towards marker and target identification. Nat Rev Cancer *6*, 835-845.

Bian, X.W., Wang, Q.L., Xiao, H.L., and Wang, J.M. (2006). Tumor microvascular architecture phenotype (T-MAP) as a new concept for studies of angiogenesis and oncology. J Neurooncol *80*, 211-213.

Blann, A.D., Woywodt, A., Bertolini, F., Bull, T.M., Buyon, J.P., Clancy, R.M., Haubitz, M., Hebbel, R.P., Lip, G.Y., Mancuso, P.*, et al.* (2005). Circulating endothelial cells. Biomarker of vascular disease. Thromb Haemost *93*, 228-235.

Blouw, B., Song, H., Tihan, T., Bosze, J., Ferrara, N., Gerber, H.P., Johnson, R.S., and Bergers, G. (2003). The hypoxic response of tumors is dependent on their microenvironment. Cancer Cell *4*, 133-146.

Bong, Y.S., Lee, H.S., Carim-Todd, L., Mood, K., Nishanian, T.G., Tessarollo, L., and Daar, I.O. (2007). ephrinB1 signals from the cell surface to the nucleus by recruitment of STAT3. Proc Natl Acad Sci U S A *104*, 17305-17310.

Borges, L.G., Seifert, R.A., Grant, F.J., Hart, C.E., Disteche, C.M., Edelhoff, S., Solca, F.F., Lieberman, M.A., Lindner, V., Fischer, E.H*., et al.* (1996). Cloning and characterization of rat density-enhanced phosphatase-1, a protein tyrosine phosphatase expressed by vascular cells. Circ Res *79*, 570-580.

Brandt, D.T., and Grosse, R. (2007). Get to grips: steering local actin dynamics with IQGAPs. EMBO Rep *8*, 1019-1023.

Brantley-Sieders, D.M., and Chen, J. (2004). Eph receptor tyrosine kinases in angiogenesis: from development to disease. Angiogenesis *7*, 17-28.

Brett, T.J., and Traub, L.M. (2006). Molecular structures of coat and coat-associated proteins: function follows form. Curr Opin Cell Biol *18*, 395-406.

Bruckner, K., Pablo Labrador, J., Scheiffele, P., Herb, A., Seeburg, P.H., and Klein, R. (1999). EphrinB ligands recruit GRIP family PDZ adaptor proteins into raft membrane microdomains. Neuron *22*, 511-524.

Brunet, A., Bonni, A., Zigmond, M.J., Lin, M.Z., Juo, P., Hu, L.S., Anderson, M.J., Arden, K.C., Blenis, J., and Greenberg, M.E. (1999). Akt promotes cell survival by phosphorylating and inhibiting a Forkhead transcription factor. Cell *96*, 857-868.

Burri, P.H., Hlushchuk, R., and Djonov, V. (2004). Intussusceptive angiogenesis: its emergence, its characteristics, and its significance. Dev Dyn *231*, 474-488.

Byzova, T.V., Goldman, C.K., Pampori, N., Thomas, K.A., Bett, A., Shattil, S.J., and Plow, E.F. (2000). A mechanism for modulation of cellular responses to VEGF: activation of the integrins. Mol Cell *6*, 851-860.

Callahan, C.A., and Thomas, J.B. (1994). Tau-beta-galactosidase, an axon-targeted fusion protein. Proc Natl Acad Sci U S A *91*, 5972-5976.

Cantley, L.C. (2002). The phosphoinositide 3-kinase pathway. Science *296*, 1655-1657.

Cardone, M.H., Roy, N., Stennicke, H.R., Salvesen, G.S., Franke, T.F., Stanbridge, E., Frisch, S., and Reed, J.C. (1998). Regulation of cell death protease caspase-9 by phosphorylation. Science *282*, 1318-1321.

Carlson, T.R., Yan, Y., Wu, X., Lam, M.T., Tang, G.L., Beverly, L.J., Messina, L.M., Capobianco, A.J., Werb, Z., and Wang, R. (2005). Endothelial expression of constitutively active Notch4 elicits reversible arteriovenous malformations in adult mice. Proc Natl Acad Sci U S A *102*, 9884-9889.

Carmeliet, P. (2003). Angiogenesis in health and disease. Nat Med *9*, 653-660.

Carmeliet, P., Ferreira, V., Breier, G., Pollefeyt, S., Kieckens, L., Gertsenstein, M., Fahrig, M., Vandenhoeck, A., Harpal, K., Eberhardt, C*., et al.* (1996). Abnormal blood vessel development and lethality in embryos lacking a single VEGF allele. Nature *380*, 435-439.

Carmeliet, P., and Jain, R.K. (2000). Angiogenesis in cancer and other diseases. Nature *407*, 249-257.

Carmeliet, P., Lampugnani, M.G., Moons, L., Breviario, F., Compernolle, V., Bono, F., Balconi, G., Spagnuolo, R., Oosthuyse, B., Dewerchin, M*., et al.* (1999). Targeted deficiency or cytosolic truncation of the VE-cadherin gene in mice impairs VEGF-mediated endothelial survival and angiogenesis. Cell *98*, 147-157.

Carmeliet, P., and Tessier-Lavigne, M. (2005). Common mechanisms of nerve and blood vessel wiring. Nature *436*, 193-200.

Carvalho, R.F., Beutler, M., Marler, K.J., Knoll, B., Becker-Barroso, E., Heintzmann, R., Ng, T., and Drescher, U. (2006). Silencing of EphA3 through a cis interaction with ephrinA5. Nat Neurosci *9*, 322-330.

Castets, M., Coissieux, M.M., Delloye-Bourgeois, C., Bernard, L., Delcros, J.G., Bernet, A., Laudet, V., and Mehlen, P. (2009). Inhibition of endothelial cell apoptosis by netrin-1 during angiogenesis. Dev Cell *16*, 614-620.

Caswell, P.T., Chan, M., Lindsay, A.J., McCaffrey, M.W., Boettiger, D., and Norman, J.C. (2008). Rab-coupling protein coordinates recycling of alpha5beta1 integrin and EGFR1 to promote cell migration in 3D microenvironments. J Cell Biol *183*, 143-155.

Caswell, P.T., Vadrevu, S., and Norman, J.C. (2009). Integrins: masters and slaves of endocytic transport. Nat Rev Mol Cell Biol *10*, 843-853.

Cebe Suarez, S., Pieren, M., Cariolato, L., Arn, S., Hoffmann, U., Bogucki, A., Manlius, C., Wood, J., and Ballmer-Hofer, K. (2006). A VEGF-A splice variant defective for heparan sulfate and neuropilin-1 binding shows attenuated signaling through VEGFR-2. Cell Mol Life Sci *63*, 2067-2077.

Chabot, C., Spring, K., Gratton, J.P., Elchebly, M., and Royal, I. (2009). New role for the protein tyrosine phosphatase DEP-1 in Akt activation and endothelial cell survival. Mol Cell Biol *29*, 241-253.

Chen, M.J., Yokomizo, T., Zeigler, B.M., Dzierzak, E., and Speck, N.A. (2009). Runx1 is required for the endothelial to haematopoietic cell transition but not thereafter. Nature *457*, 887-891.

Chen, W., ten Berge, D., Brown, J., Ahn, S., Hu, L.A., Miller, W.E., Caron, M.G., Barak, L.S., Nusse, R., and Lefkowitz, R.J. (2003). Dishevelled 2 recruits beta-arrestin 2 to mediate Wnt5A-stimulated endocytosis of Frizzled 4. Science *301*, 1391-1394.

Chodniewicz, D., and Klemke, R.L. (2004). Regulation of integrin-mediated cellular responses through assembly of a CAS/Crk scaffold. Biochim Biophys Acta *1692*, 63-76.

Choi, K., Kennedy, M., Kazarov, A., Papadimitriou, J.C., and Keller, G. (1998). A common precursor for hematopoietic and endothelial cells. Development *125*, 725-732.

Conner, S.D., and Schmid, S.L. (2003). Regulated portals of entry into the cell. Nature *422*, 37-44.

Cortina, C., Palomo-Ponce, S., Iglesias, M., Fernandez-Masip, J.L., Vivancos, A., Whissell, G., Huma, M., Peiro, N., Gallego, L., Jonkheer, S.*, et al.* (2007). EphB-ephrin-B interactions suppress colorectal cancer progression by compartmentalizing tumor cells. Nat Genet *39*, 1376-1383.

Coultas, L., Chawengsaksophak, K., and Rossant, J. (2005). Endothelial cells and VEGF in vascular development. Nature *438*, 937-945.

Cowan, C.A., and Henkemeyer, M. (2001). The SH2/SH3 adaptor Grb4 transduces B-ephrin reverse signals. Nature *413*, 174-179.

Cowan, C.A., and Henkemeyer, M. (2002). Ephrins in reverse, park and drive. Trends Cell Biol *12*, 339-346.

Cowan, C.W., Shao, Y.R., Sahin, M., Shamah, S.M., Lin, M.Z., Greer, P.L., Gao, S., Griffith, E.C., Brugge, J.S., and Greenberg, M.E. (2005). Vav family GEFs link activated Ephs to endocytosis and axon guidance. Neuron *46*, 205-217.

D'Souza-Schorey, C., and Chavrier, P. (2006). ARF proteins: roles in membrane traffic and beyond. Nat Rev Mol Cell Biol *7*, 347-358.

Dameron, K.M., Volpert, O.V., Tainsky, M.A., and Bouck, N. (1994). Control of angiogenesis in fibroblasts by p53 regulation of thrombospondin-1. Science *265*, 1582-1584.

Davis, G.E., and Bayless, K.J. (2003). An integrin and Rho GTPase-dependent pinocytic vacuole mechanism controls capillary lumen formation in collagen and fibrin matrices. Microcirculation *10*, 27-44.

Davy, A., Gale, N.W., Murray, E.W., Klinghoffer, R.A., Soriano, P., Feuerstein, C., and Robbins, S.M. (1999). Compartmentalized signaling by GPI-anchored ephrin-A5 requires the Fyn tyrosine kinase to regulate cellular adhesion. Genes Dev *13*, 3125-3135.

De Palma, M., Venneri, M.A., Galli, R., Sergi Sergi, L., Politi, L.S., Sampaolesi, M., and Naldini, L. (2005). Tie2 identifies a hematopoietic lineage of proangiogenic monocytes required for tumor vessel formation and a mesenchymal population of pericyte progenitors. Cancer Cell *8*, 211-226.

Deinhardt, K., Salinas, S., Verastegui, C., Watson, R., Worth, D., Hanrahan, S., Bucci, C., and Schiavo, G. (2006). Rab5 and Rab7 control endocytic sorting along the axonal retrograde transport pathway. Neuron *52*, 293-305.

Dev, K.K. (2007). PDZ domain protein-protein interactions: a case study with PICK1. Curr Top Med Chem *7*, 3-20.

Dimmeler, S., Fleming, I., Fisslthaler, B., Hermann, C., Busse, R., and Zeiher, A.M. (1999). Activation of nitric oxide synthase in endothelial cells by Akt-dependent phosphorylation. Nature *399*, 601-605.

Dixelius, J., Makinen, T., Wirzenius, M., Karkkainen, M.J., Wernstedt, C., Alitalo, K., and Claesson-Welsh, L. (2003). Ligand-induced vascular endothelial growth factor receptor-3 (VEGFR-3) heterodimerization with VEGFR-2 in primary lymphatic endothelial cells regulates tyrosine phosphorylation sites. J Biol Chem *278*, 40973-40979.

Djonov, V.G., Kurz, H., and Burri, P.H. (2002). Optimality in the developing vascular system: branching remodeling by means of intussusception as an efficient adaptation mechanism. Dev Dyn *224*, 391-402.

Dorrell, M.I., and Friedlander, M. (2006). Mechanisms of endothelial cell guidance and vascular patterning in the developing mouse retina. Prog Retin Eye Res *25*, 277-295.

Dougher, M., and Terman, B.I. (1999). Autophosphorylation of KDR in the kinase domain is required for maximal VEGF-stimulated kinase activity and receptor internalization. Oncogene *18*, 1619-1627.

Drab, M., Verkade, P., Elger, M., Kasper, M., Lohn, M., Lauterbach, B., Menne, J., Lindschau, C., Mende, F., Luft, F.C.*, et al.* (2001). Loss of caveolae, vascular dysfunction, and pulmonary defects in caveolin-1 gene-disrupted mice. Science *293*, 2449-2452.

Drake, C.J., Davis, L.A., and Little, C.D. (1992). Antibodies to beta 1-integrins cause alterations of aortic vasculogenesis, in vivo. Dev Dyn *193*, 83-91.

Duchek, P., and Rorth, P. (2001). Guidance of cell migration by EGF receptor signaling during Drosophila oogenesis. Science *291*, 131-133.

Duchek, P., Somogyi, K., Jekely, G., Beccari, S., and Rorth, P. (2001). Guidance of cell migration by the Drosophila PDGF/VEGF receptor. Cell *107*, 17-26.

Ebos, J.M., Bocci, G., Man, S., Thorpe, P.E., Hicklin, D.J., Zhou, D., Jia, X., and Kerbel, R.S. (2004). A naturally occurring soluble form of vascular endothelial growth factor receptor 2 detected in mouse and human plasma. Mol Cancer Res *2*, 315-326.

Egea, J., and Klein, R. (2007). Bidirectional Eph-ephrin signaling during axon guidance. Trends Cell Biol *17*, 230-238.

Eichmann, A., Le Noble, F., Autiero, M., and Carmeliet, P. (2005). Guidance of vascular and neural network formation. Curr Opin Neurobiol *15*, 108-115.

Eilken, H.M., Nishikawa, S., and Schroeder, T. (2009). Continuous single-cell imaging of blood generation from haemogenic endothelium. Nature *457*, 896-900.

Eliceiri, B.P., Paul, R., Schwartzberg, P.L., Hood, J.D., Leng, J., and Cheresh, D.A. (1999). Selective requirement for Src kinases during VEGF-induced angiogenesis and vascular permeability. Mol Cell *4*, 915-924.

Erber, R., Eichelsbacher, U., Powajbo, V., Korn, T., Djonov, V., Lin, J., Hammes, H.P., Grobholz, R., Ullrich, A., and Vajkoczy, P. (2006). EphB4 controls blood vascular morphogenesis during postnatal angiogenesis. EMBO J *25*, 628-641.

Essmann, C.L., Martinez, E., Geiger, J.C., Zimmer, M., Traut, M.H., Stein, V., Klein, R., and Acker-Palmer, A. (2008). Serine phosphorylation of ephrinB2 regulates trafficking of synaptic AMPA receptors. Nat Neurosci.

Ezhilarasan, R., Mohanam, I., Govindarajan, K., and Mohanam, S. (2007). Glioma cells suppress hypoxia-induced endothelial cell apoptosis and promote the angiogenic process. Int J Oncol *30*, 701-707.

Fang, W.B., Brantley-Sieders, D.M., Parker, M.A., Reith, A.D., and Chen, J. (2005). A kinase-dependent role for EphA2 receptor in promoting tumor growth and metastasis. Oncogene *24*, 7859-7868.

Ferrara, N., Gerber, H.P., and LeCouter, J. (2003). The biology of VEGF and its receptors. Nat Med *9*, 669-676.

Fischer, A., Schumacher, N., Maier, M., Sendtner, M., and Gessler, M. (2004). The Notch target genes Hey1 and Hey2 are required for embryonic vascular development. Genes Dev *18*, 901-911.

Folkman, J. (2007). Angiogenesis: an organizing principle for drug discovery? Nat Rev Drug Discov *6*, 273-286.

Foo, S.S., Turner, C.J., Adams, S., Compagni, A., Aubyn, D., Kogata, N., Lindblom, P., Shani, M., Zicha, D., and Adams, R.H. (2006). Ephrin-B2 controls cell motility and adhesion during blood-vessel-wall assembly. Cell *124*, 161-173.

Foubert, P., Silvestre, J.S., Souttou, B., Barateau, V., Martin, C., Ebrahimian, T.G., Lere-Dean, C., Contreres, J.O., Sulpice, E., Levy, B.I.*, et al.* (2007). PSGL-1-mediated activation of EphB4 increases the proangiogenic potential of endothelial progenitor cells. J Clin Invest *117*, 1527-1537.

Fujio, Y., and Walsh, K. (1999). Akt mediates cytoprotection of endothelial cells by vascular endothelial growth factor in an anchorage-dependent manner. J Biol Chem *274*, 16349-16354.

Fukuhara, S., Sakurai, A., Sano, H., Yamagishi, A., Somekawa, S., Takakura, N., Saito, Y., Kangawa, K., and Mochizuki, N. (2005). Cyclic AMP potentiates vascular endothelial cadherin-mediated cell-cell contact to enhance endothelial barrier function through an Epac-Rap1 signaling pathway. Mol Cell Biol *25*, 136-146.

Fukumura, D., Gohongi, T., Kadambi, A., Izumi, Y., Ang, J., Yun, C.O., Buerk, D.G., Huang, P.L., and Jain, R.K. (2001). Predominant role of endothelial nitric oxide synthase in vascular endothelial growth factor-induced angiogenesis and vascular permeability. Proc Natl Acad Sci U S A *98*, 2604-2609.

Fuller, T., Korff, T., Kilian, A., Dandekar, G., and Augustin, H.G. (2003). Forward EphB4 signaling in endothelial cells controls cellular repulsion and segregation from ephrinB2 positive cells. J Cell Sci *116*, 2461-2470.

Fulton, D., Gratton, J.P., McCabe, T.J., Fontana, J., Fujio, Y., Walsh, K., Franke, T.F., Papapetropoulos, A., and Sessa, W.C. (1999). Regulation of endothelium-derived nitric oxide production by the protein kinase Akt. Nature *399*, 597-601.

Galbraith, C.G., Yamada, K.M., and Galbraith, J.A. (2007). Polymerizing actin fibers position integrins primed to probe for adhesion sites. Science *315*, 992-995.

Gale, N.W., Baluk, P., Pan, L., Kwan, M., Holash, J., DeChiara, T.M., McDonald, D.M., and Yancopoulos, G.D. (2001). Ephrin-B2 selectively marks arterial vessels and neovascularization sites in the adult, with expression in both endothelial and smooth-muscle cells. Dev Biol *230*, 151-160.

Gao, C., and Chen, Y.G. Dishevelled: The hub of Wnt signaling. Cell Signal *22*, 717-727.

Gao, L., and Macara, I.G. (2004). Isoforms of the polarity protein par6 have distinct functions. J Biol Chem *279*, 41557-41562.

Gariano, R.F., and Gardner, T.W. (2005). Retinal angiogenesis in development and disease. Nature *438*, 960-966.

Gavard, J., and Gutkind, J.S. (2006). VEGF controls endothelial-cell permeability by promoting the beta-arrestin-dependent endocytosis of VE-cadherin. Nat Cell Biol *8*, 1223-1234.

Gerber, H.P., Condorelli, F., Park, J., and Ferrara, N. (1997). Differential transcriptional regulation of the two vascular endothelial growth factor receptor genes. Flt-1, but not Flk-1/KDR, is up-regulated by hypoxia. J Biol Chem *272*, 23659-23667.

Gerety, S.S., and Anderson, D.J. (2002). Cardiovascular ephrinB2 function is essential for embryonic angiogenesis. Development *129*, 1397-1410.

Gerety, S.S., Wang, H.U., Chen, Z.F., and Anderson, D.J. (1999). Symmetrical mutant phenotypes of the receptor EphB4 and its specific transmembrane ligand ephrin-B2 in cardiovascular development. Mol Cell *4*, 403-414.

Gerhardt, H., Golding, M., Fruttiger, M., Ruhrberg, C., Lundkvist, A., Abramsson, A., Jeltsch, M., Mitchell, C., Alitalo, K., Shima, D.*, et al.* (2003). VEGF guides angiogenic sprouting utilizing endothelial tip cell filopodia. J Cell Biol *161*, 1163-1177.

Gerhardt, H., Ruhrberg, C., Abramsson, A., Fujisawa, H., Shima, D., and Betsholtz, C. (2004). Neuropilin-1 is required for endothelial tip cell guidance in the developing central nervous system. Dev Dyn *231*, 503-509.

Goode, B.L., and Eck, M.J. (2007). Mechanism and function of formins in the control of actin assembly. Annu Rev Biochem *76*, 593-627.

Gould, G.W., and Lippincott-Schwartz, J. (2009). New roles for endosomes: from vesicular carriers to multi-purpose platforms. Nat Rev Mol Cell Biol *10*, 287-292.

Graupera, M., Guillermet-Guibert, J., Foukas, L.C., Phng, L.K., Cain, R.J., Salpekar, A., Pearce, W., Meek, S., Millan, J., Cutillas, P.R.*, et al.* (2008). Angiogenesis selectively requires the p110alpha isoform of PI3K to control endothelial cell migration. Nature *453*, 662-666.

Grazia Lampugnani, M., Zanetti, A., Corada, M., Takahashi, T., Balconi, G., Breviario, F., Orsenigo, F., Cattelino, A., Kemler, R., Daniel, T.O.*, et al.* (2003). Contact inhibition of VEGF-induced proliferation requires vascular endothelial cadherin, beta-catenin, and the phosphatase DEP-1/CD148. J Cell Biol *161*, 793-804.

Grego-Bessa, J., Luna-Zurita, L., del Monte, G., Bolos, V., Melgar, P., Arandilla, A., Garratt, A.N., Zang, H., Mukouyama, Y.S., Chen, H.*, et al.* (2007). Notch signaling is essential for ventricular chamber development. Dev Cell *12*, 415-429.

Grunewald, M., Avraham, I., Dor, Y., Bachar-Lustig, E., Itin, A., Jung, S., Chimenti, S., Landsman, L., Abramovitch, R., and Keshet, E. (2006). VEGF-induced adult neovascularization: recruitment, retention, and role of accessory cells. Cell *124*, 175-189.

Grunwald, I.C., Korte, M., Adelmann, G., Plueck, A., Kullander, K., Adams, R.H., Frotscher, M., Bonhoeffer, T., and Klein, R. (2004). Hippocampal plasticity requires postsynaptic ephrinBs. Nat Neurosci *7*, 33-40.

Gu, C., Yoshida, Y., Livet, J., Reimert, D.V., Mann, F., Merte, J., Henderson, C.E., Jessell, T.M., Kolodkin, A.L., and Ginty, D.D. (2005). Semaphorin 3E and plexin-D1 control vascular pattern independently of neuropilins. Science *307*, 265-268.

Gupta-Rossi, N., Six, E., LeBail, O., Logeat, F., Chastagner, P., Olry, A., Israel, A., and Brou, C. (2004). Monoubiquitination and endocytosis direct gamma-secretase cleavage of activated Notch receptor. J Cell Biol *166*, 73-83.

Ha, C.H., Bennett, A.M., and Jin, Z.G. (2008). A novel role of vascular endothelial cadherin in modulating c-Src activation and downstream signaling of vascular endothelial growth factor. J Biol Chem *283*, 7261-7270.

Hainaud, P., Contreres, J.O., Villemain, A., Liu, L.X., Plouet, J., Tobelem, G., and Dupuy, E. (2006). The role of the vascular endothelial growth factor-Delta-like 4 ligand/Notch4-ephrin B2 cascade in tumor vessel remodeling and endothelial cell functions. Cancer Res *66*, 8501-8510.

Hamada, K., Oike, Y., Ito, Y., Maekawa, H., Miyata, K., Shimomura, T., and Suda, T. (2003). Distinct roles of ephrin-B2 forward and EphB4 reverse signaling in endothelial cells. Arterioscler Thromb Vasc Biol *23*, 190-197.

Hanley, J.G. (2008). PICK1: a multi-talented modulator of AMPA receptor trafficking. Pharmacol Ther *118*, 152-160.

Hansen, M.J., Dallal, G.E., and Flanagan, J.G. (2004). Retinal axon response to ephrin-as shows a graded, concentration-dependent transition from growth promotion to inhibition. Neuron *42*, 717-730.

Harper, S.J., and Bates, D.O. (2008). VEGF-A splicing: the key to anti-angiogenic therapeutics? Nat Rev Cancer *8*, 880-887.

Harrington, L.S., Sainson, R.C., Williams, C.K., Taylor, J.M., Shi, W., Li, J.L., and Harris, A.L. (2008). Regulation of multiple angiogenic pathways by Dll4 and Notch in human umbilical vein endothelial cells. Microvasc Res *75*, 144-154.

Hart, M.J., Callow, M.G., Souza, B., and Polakis, P. (1996). IQGAP1, a calmodulin-binding protein with a rasGAP-related domain, is a potential effector for cdc42Hs. EMBO J *15*, 2997-3005.

Hattori, M., Osterfield, M., and Flanagan, J.G. (2000). Regulated cleavage of a contact-mediated axon repellent. Science *289*, 1360-1365.

Hayashi, H., and Kume, T. (2008). Foxc transcription factors directly regulate Dll4 and Hey2 expression by interacting with the VEGF-Notch signaling pathways in endothelial cells. PLoS One *3*, e2401.

Heasman, S.J., and Ridley, A.J. (2008). Mammalian Rho GTPases: new insights into their functions from in vivo studies. Nat Rev Mol Cell Biol *9*, 690-701.

Hellstrom, M., Phng, L.K., Hofmann, J.J., Wallgard, E., Coultas, L., Lindblom, P., Alva, J., Nilsson, A.K., Karlsson, L., Gaiano, N.*, et al.* (2007). Dll4 signalling through Notch1 regulates formation of tip cells during angiogenesis. Nature *445*, 776-780.

Henderson, A.M., Wang, S.J., Taylor, A.C., Aitkenhead, M., and Hughes, C.C. (2001). The basic helix-loop-helix transcription factor HESR1 regulates endothelial cell tube formation. J Biol Chem *276*, 6169-6176.

Herbert, S.P., Huisken, J., Kim, T.N., Feldman, M.E., Houseman, B.T., Wang, R.A., Shokat, K.M., and Stainier, D.Y. (2009). Arterial-venous segregation by selective cell sprouting: an alternative mode of blood vessel formation. Science *326*, 294-298.

Himanen, J.P., Chumley, M.J., Lackmann, M., Li, C., Barton, W.A., Jeffrey, P.D., Vearing, C., Geleick, D., Feldheim, D.A., Boyd, A.W.*, et al.* (2004). Repelling class discrimination: ephrin-A5 binds to and activates EphB2 receptor signaling. Nat Neurosci *7*, 501-509.

Himanen, J.P., and Nikolov, D.B. (2003). Eph signaling: a structural view. Trends Neurosci *26*, 46-51.

Hiratsuka, S., Minowa, O., Kuno, J., Noda, T., and Shibuya, M. (1998). Flt-1 lacking the tyrosine kinase domain is sufficient for normal development and angiogenesis in mice. Proc Natl Acad Sci U S A *95*, 9349-9354.

Hofmann, J.J., and Iruela-Arispe, M.L. (2007). Notch signaling in blood vessels: who is talking to whom about what? Circ Res *100*, 1556-1568.

Holderfield, M.T., Henderson Anderson, A.M., Kokubo, H., Chin, M.T., Johnson, R.L., and Hughes, C.C. (2006). HESR1/CHF2 suppresses VEGFR2 transcription independent of binding to E-boxes. Biochem Biophys Res Commun *346*, 637-648.

Holmes, K., Roberts, O.L., Thomas, A.M., and Cross, M.J. (2007). Vascular endothelial growth factor receptor-2: structure, function, intracellular signalling and therapeutic inhibition. Cell Signal *19*, 2003-2012.

Holmqvist, K., Cross, M., Riley, D., and Welsh, M. (2003). The Shb adaptor protein causes Src-dependent cell spreading and activation of focal adhesion kinase in murine brain endothelial cells. Cell Signal *15*, 171-179.

Howe, C.L., Valletta, J.S., Rusnak, A.S., and Mobley, W.C. (2001). NGF signaling from clathrin-coated vesicles: evidence that signaling endosomes serve as a platform for the Ras-MAPK pathway. Neuron *32*, 801-814.

Hurley, J.H., and Emr, S.D. (2006). The ESCRT complexes: structure and mechanism of a membrane-trafficking network. Annu Rev Biophys Biomol Struct *35*, 277-298.

Huynh-Do, U., Vindis, C., Liu, H., Cerretti, D.P., McGrew, J.T., Enriquez, M., Chen, J., and Daniel, T.O. (2002). Ephrin-B1 transduces signals to activate integrin-mediated migration, attachment and angiogenesis. J Cell Sci *115*, 3073-3081.

Innocenti, M., Frittoli, E., Ponzanelli, I., Falck, J.R., Brachmann, S.M., Di Fiore, P.P., and Scita, G. (2003). Phosphoinositide 3-kinase activates Rac by entering in a complex with Eps8, Abi1, and Sos-1. J Cell Biol *160*, 17-23.

Iruela-Arispe, M.L., and Davis, G.E. (2009). Cellular and molecular mechanisms of vascular lumen formation. Dev Cell *16*, 222-231.

Iwasato, T., Katoh, H., Nishimaru, H., Ishikawa, Y., Inoue, H., Saito, Y.M., Ando, R., Iwama, M., Takahashi, R., Negishi, M.*, et al.* (2007). Rac-GAP alpha-chimerin regulates motor-circuit formation as a key mediator of EphrinB3/EphA4 forward signaling. Cell *130*, 742-753.

Jakobsson, L., Kreuger, J., Holmborn, K., Lundin, L., Eriksson, I., Kjellen, L., and Claesson-Welsh, L. (2006). Heparan sulfate in trans potentiates VEGFR-mediated angiogenesis. Dev Cell *10*, 625-634.

Janes, P.W., Saha, N., Barton, W.A., Kolev, M.V., Wimmer-Kleikamp, S.H., Nievergall, E., Blobel, C.P., Himanen, J.P., Lackmann, M., and Nikolov, D.B. (2005). Adam meets Eph: an ADAM substrate recognition module acts as a molecular switch for ephrin cleavage in trans. Cell *123*, 291-304.

Jekely, G., Sung, H.H., Luque, C.M., and Rorth, P. (2005). Regulators of endocytosis maintain localized receptor tyrosine kinase signaling in guided migration. Dev Cell *9*, 197-207.

Ji, Q.S., Winnier, G.E., Niswender, K.D., Horstman, D., Wisdom, R., Magnuson, M.A., and Carpenter, G. (1997). Essential role of the tyrosine kinase substrate phospholipase C-gamma1 in mammalian growth and development. Proc Natl Acad Sci U S A *94*, 2999-3003.

Jiang, G., Freywald, T., Webster, J., Kozan, D., Geyer, R., DeCoteau, J., Narendran, A., and Freywald, A. (2008). In human leukemia cells ephrin-B-induced invasive activity is supported by Lck and is associated with reassembling of lipid raft signaling complexes. Mol Cancer Res *6*, 291-305.

Jin, W., Ge, W.P., Xu, J., Cao, M., Peng, L., Yung, W., Liao, D., Duan, S., Zhang, M., and Xia, J. (2006). Lipid binding regulates synaptic targeting of PICK1, AMPA receptor trafficking, and synaptic plasticity. J Neurosci *26*, 2380-2390.

Joberty, G., Petersen, C., Gao, L., and Macara, I.G. (2000). The cell-polarity protein Par6 links Par3 and atypical protein kinase C to Cdc42. Nat Cell Biol *2*, 531-539.

Jones, C.A., London, N.R., Chen, H., Park, K.W., Sauvaget, D., Stockton, R.A., Wythe, J.D., Suh, W., Larrieu-Lahargue, F., Mukouyama, Y.S.*, et al.* (2008a). Robo4 stabilizes the vascular network by inhibiting pathologic angiogenesis and endothelial hyperpermeability. Nat Med *14*, 448-453.

Jones, E.A., Yuan, L., Breant, C., Watts, R.J., and Eichmann, A. (2008b). Separating genetic and hemodynamic defects in neuropilin 1 knockout embryos. Development *135*, 2479-2488.

Jones, M.C., Caswell, P.T., and Norman, J.C. (2006). Endocytic recycling pathways: emerging regulators of cell migration. Curr Opin Cell Biol *18*, 549-557.

Kalo, M.S., and Pasquale, E.B. (1999). Multiple in vivo tyrosine phosphorylation sites in EphB receptors. Biochemistry *38*, 14396-14408.

Kamei, M., Saunders, W.B., Bayless, K.J., Dye, L., Davis, G.E., and Weinstein, B.M. (2006). Endothelial tubes assemble from intracellular vacuoles in vivo. Nature *442*, 453-456.

Kawamura, H., Li, X., Harper, S.J., Bates, D.O., and Claesson-Welsh, L. (2008). Vascular endothelial growth factor (VEGF)-A165b is a weak in vitro agonist for VEGF receptor-2 due to lack of coreceptor binding and deficient regulation of kinase activity. Cancer Res *68*, 4683-4692.

Kazazic, M., Bertelsen, V., Pedersen, K.W., Vuong, T.T., Grandal, M.V., Rodland, M.S., Traub, L.M., Stang, E., and Madshus, I.H. (2009). Epsin 1 is involved in recruitment of ubiquitinated EGF receptors into clathrin-coated pits. Traffic *10*, 235-245.

Kendall, R.L., and Thomas, K.A. (1993). Inhibition of vascular endothelial cell growth factor activity by an endogenously encoded soluble receptor. Proc Natl Acad Sci U S A *90*, 10705-10709.

Kim, I., Ryu, Y.S., Kwak, H.J., Ahn, S.Y., Oh, J.L., Yancopoulos, G.D., Gale, N.W., and Koh, G.Y. (2002). EphB ligand, ephrinB2, suppresses the VEGF- and angiopoietin 1-induced Ras/mitogen-activated protein kinase pathway in venous endothelial cells. FASEB J *16*, 1126-1128.

Kitamura, T., Asai, N., Enomoto, A., Maeda, K., Kato, T., Ishida, M., Jiang, P., Watanabe, T., Usukura, J., Kondo, T.*, et al.* (2008). Regulation of VEGF-mediated angiogenesis by the Akt/PKB substrate Girdin. Nat Cell Biol *10*, 329-337.

Kleaveland, B., Zheng, X., Liu, J.J., Blum, Y., Tung, J.J., Zou, Z., Sweeney, S.M., Chen, M., Guo, L., Lu, M.M.*, et al.* (2009). Regulation of cardiovascular development and integrity by the heart of glass-cerebral cavernous malformation protein pathway. Nat Med *15*, 169-176.

Knoll, B., and Drescher, U. (2002). Ephrin-As as receptors in topographic projections. Trends Neurosci *25*, 145-149.

Knoll, B., and Drescher, U. (2004). Src family kinases are involved in EphA receptor-mediated retinal axon guidance. J Neurosci *24*, 6248-6257.

Koh, W., Mahan, R.D., and Davis, G.E. (2008). Cdc42- and Rac1-mediated endothelial lumen formation requires Pak2, Pak4 and Par3, and PKC-dependent signaling. J Cell Sci *121*, 989-1001.

Kuijper, S., Turner, C.J., and Adams, R.H. (2007). Regulation of angiogenesis by Eph-ephrin interactions. Trends Cardiovasc Med *17*, 145-151.

Kullander, K., and Klein, R. (2002). Mechanisms and functions of Eph and ephrin signalling. Nat Rev Mol Cell Biol *3*, 475-486.

Lamalice, L., Houle, F., and Huot, J. (2006). Phosphorylation of Tyr1214 within VEGFR-2 triggers the recruitment of Nck and activation of Fyn leading to SAPK2/p38 activation and endothelial cell migration in response to VEGF. J Biol Chem *281*, 34009-34020.

Lampugnani, M.G., Orsenigo, F., Gagliani, M.C., Tacchetti, C., and Dejana, E. (2006). Vascular endothelial cadherin controls VEGFR-2 internalization and signaling from intracellular compartments. J Cell Biol *174*, 593-604.

Lampugnani, M.G., Zanetti, A., Breviario, F., Balconi, G., Orsenigo, F., Corada, M., Spagnuolo, R., Betson, M., Braga, V., and Dejana, E. (2002). VE-cadherin regulates endothelial actin activating Rac and increasing membrane association of Tiam. Mol Biol Cell *13*, 1175-1189.

Lancrin, C., Sroczynska, P., Stephenson, C., Allen, T., Kouskoff, V., and Lacaud, G. (2009). The haemangioblast generates haematopoietic cells through a haemogenic endothelium stage. Nature *457*, 892-895.

Lauterbach, J., and Klein, R. (2006). Release of full-length EphB2 receptors from hippocampal neurons to cocultured glial cells. J Neurosci *26*, 11575-11581.

le Noble, F., Moyon, D., Pardanaud, L., Yuan, L., Djonov, V., Matthijsen, R., Breant, C., Fleury, V., and Eichmann, A. (2004). Flow regulates arterial-venous differentiation in the chick embryo yolk sac. Development *131*, 361-375.

Le Roy, C., and Wrana, J.L. (2005). Clathrin- and non-clathrin-mediated endocytic regulation of cell signalling. Nat Rev Mol Cell Biol *6*, 112-126.

Lee, H.S., Nishanian, T.G., Mood, K., Bong, Y.S., and Daar, I.O. (2008). EphrinB1 controls cell-cell junctions through the Par polarity complex. Nat Cell Biol *10*, 979-986.

Lee, S., Chen, T.T., Barber, C.L., Jordan, M.C., Murdock, J., Desai, S., Ferrara, N., Nagy, A., Roos, K.P., and Iruela-Arispe, M.L. (2007). Autocrine VEGF signaling is required for vascular homeostasis. Cell *130*, 691-703.

Legendre-Guillemin, V., Wasiak, S., Hussain, N.K., Angers, A., and McPherson, P.S. (2004). ENTH/ANTH proteins and clathrin-mediated membrane budding. J Cell Sci *117*, 9-18.

Leslie, J.D., Ariza-McNaughton, L., Bermange, A.L., McAdow, R., Johnson, S.L., and Lewis, J. (2007). Endothelial signalling by the Notch ligand Delta-like 4 restricts angiogenesis. Development *134*, 839-844.

Lewis, J. (2008). From signals to patterns: space, time, and mathematics in developmental biology. Science *322*, 399-403.

Lim, Y.S., McLaughlin, T., Sung, T.C., Santiago, A., Lee, K.F., and O'Leary, D.D. (2008). p75(NTR) mediates ephrin-A reverse signaling required for axon repulsion and mapping. Neuron *59*, 746-758.

Lin, D., Edwards, A.S., Fawcett, J.P., Mbamalu, G., Scott, J.D., and Pawson, T. (2000). A mammalian PAR-3-PAR-6 complex implicated in Cdc42/Rac1 and aPKC signalling and cell polarity. Nat Cell Biol *2*, 540-547.

Lin, D., Gish, G.D., Songyang, Z., and Pawson, T. (1999). The carboxyl terminus of B class ephrins constitutes a PDZ domain binding motif. J Biol Chem *274*, 3726-3733.

Liu, Z.J., Shirakawa, T., Li, Y., Soma, A., Oka, M., Dotto, G.P., Fairman, R.M., Velazquez, O.C., and Herlyn, M. (2003). Regulation of Notch1 and Dll4 by vascular endothelial growth factor in arterial endothelial cells: implications for modulating arteriogenesis and angiogenesis. Mol Cell Biol *23*, 14-25.

Lobov, I.B., Renard, R.A., Papadopoulos, N., Gale, N.W., Thurston, G., Yancopoulos, G.D., and Wiegand, S.J. (2007). Delta-like ligand 4 (Dll4) is induced by VEGF as a negative regulator of angiogenic sprouting. Proc Natl Acad Sci U S A *104*, 3219-3224.

Lu, Q., Sun, E.E., Klein, R.S., and Flanagan, J.G. (2001). Ephrin-B reverse signaling is mediated by a novel PDZ-RGS protein and selectively inhibits G protein-coupled chemoattraction. Cell *105*, 69-79.

Lu, X., Le Noble, F., Yuan, L., Jiang, Q., De Lafarge, B., Sugiyama, D., Breant, C., Claes, F., De Smet, F., Thomas, J.L.*, et al.* (2004). The netrin receptor UNC5B mediates guidance events controlling morphogenesis of the vascular system. Nature *432*, 179-186.

Maharaj, A.S., Saint-Geniez, M., Maldonado, A.E., and D'Amore, P.A. (2006). Vascular endothelial growth factor localization in the adult. Am J Pathol *168*, 639-648.

Makinen, T., Adams, R.H., Bailey, J., Lu, Q., Ziemiecki, A., Alitalo, K., Klein, R., and Wilkinson, G.A. (2005). PDZ interaction site in ephrinB2 is required for the remodeling of lymphatic vasculature. Genes Dev *19*, 397-410.

Marler, K.J., Becker-Barroso, E., Martinez, A., Llovera, M., Wentzel, C., Poopalasundaram, S., Hindges, R., Soriano, E., Comella, J., and Drescher, U. (2008). A TrkB/EphrinA interaction controls retinal axon branching and synaptogenesis. J Neurosci *28*, 12700-12712.

Marmor, M.D., and Yarden, Y. (2004). Role of protein ubiquitylation in regulating endocytosis of receptor tyrosine kinases. Oncogene *23*, 2057-2070.

Marquardt, T., Shirasaki, R., Ghosh, S., Andrews, S.E., Carter, N., Hunter, T., and Pfaff, S.L. (2005). Coexpressed EphA receptors and ephrin-A ligands mediate opposing actions on growth cone navigation from distinct membrane domains. Cell *121*, 127-139.

Marston, D.J., Dickinson, S., and Nobes, C.D. (2003). Rac-dependent trans-endocytosis of ephrinBs regulates Eph-ephrin contact repulsion. Nat Cell Biol *5*, 879-888.

Matsumoto, T., Bohman, S., Dixelius, J., Berge, T., Dimberg, A., Magnusson, P., Wang, L., Wikner, C., Qi, J.H., Wernstedt, C.*, et al.* (2005). VEGF receptor-2 Y951 signaling and a role for the adapter molecule TSAd in tumor angiogenesis. EMBO J *24*, 2342-2353.

Matsuoka, H., Obama, H., Kelly, M.L., Matsui, T., and Nakamoto, M. (2005). Biphasic functions of the kinase-defective Ephb6 receptor in cell adhesion and migration. J Biol Chem *280*, 29355-29363.

Mattila, E., Auvinen, K., Salmi, M., and Ivaska, J. (2008). The protein tyrosine phosphatase TCPTP controls VEGFR2 signalling. J Cell Sci *121*, 3570-3580.

Mattila, E., Pellinen, T., Nevo, J., Vuoriluoto, K., Arjonen, A., and Ivaska, J. (2005). Negative regulation of EGFR signalling through integrin-alpha1beta1-mediated activation of protein tyrosine phosphatase TCPTP. Nat Cell Biol *7*, 78-85.

Mattila, P.K., and Lappalainen, P. (2008). Filopodia: molecular architecture and cellular functions. Nat Rev Mol Cell Biol *9*, 446-454.

Maudsley, S., Pierce, K.L., Zamah, A.M., Miller, W.E., Ahn, S., Daaka, Y., Lefkowitz, R.J., and Luttrell, L.M. (2000). The beta(2)-adrenergic receptor mediates extracellular signal-regulated kinase activation via assembly of a multi-receptor complex with the epidermal growth factor receptor. J Biol Chem *275*, 9572-9580.

Mayor, S., and Pagano, R.E. (2007). Pathways of clathrin-independent endocytosis. Nat Rev Mol Cell Biol *8*, 603-612.

McLaughlin, T., Hindges, R., Yates, P.A., and O'Leary, D.D. (2003). Bifunctional action of ephrin-B1 as a repellent and attractant to control bidirectional branch extension in dorsal-ventral retinotopic mapping. Development *130*, 2407-2418.

McMahon, H.T., and Gallop, J.L. (2005). Membrane curvature and mechanisms of dynamic cell membrane remodelling. Nature *438*, 590-596.

Mellberg, S., Dimberg, A., Bahram, F., Hayashi, M., Rennel, E., Ameur, A., Westholm, J.O., Larsson, E., Lindahl, P., Cross, M.J.*, et al.* (2009). Transcriptional profiling reveals a critical role for tyrosine phosphatase VE-PTP in regulation of VEGFR2 activity and endothelial cell morphogenesis. FASEB J *23*, 1490-1502.

Mellitzer, G., Xu, Q., and Wilkinson, D.G. (1999). Eph receptors and ephrins restrict cell intermingling and communication. Nature *400*, 77-81.

Merlos-Suarez, A., and Batlle, E. (2008). Eph-ephrin signalling in adult tissues and cancer. Curr Opin Cell Biol *20*, 194-200.

Miao, H., Li, D.Q., Mukherjee, A., Guo, H., Petty, A., Cutter, J., Basilion, J.P., Sedor, J., Wu, J., Danielpour, D.*, et al.* (2009). EphA2 mediates ligand-dependent inhibition and ligand-independent promotion of cell migration and invasion via a reciprocal regulatory loop with Akt. Cancer Cell *16*, 9-20.

Morlot, C., Thielens, N.M., Ravelli, R.B., Hemrika, W., Romijn, R.A., Gros, P., Cusack, S., and McCarthy, A.A. (2007). Structural insights into the Slit-Robo complex. Proc Natl Acad Sci U S A *104*, 14923-14928.

Mukouyama, Y.S., Shin, D., Britsch, S., Taniguchi, M., and Anderson, D.J. (2002). Sensory nerves determine the pattern of arterial differentiation and blood vessel branching in the skin. Cell *109*, 693-705.

Murphy, J.E., Padilla, B.E., Hasdemir, B., Cottrell, G.S., and Bunnett, N.W. (2009). Endosomes: a legitimate platform for the signaling train. Proc Natl Acad Sci U S A *106*, 17615-17622.

Nakada, M., Drake, K.L., Nakada, S., Niska, J.A., and Berens, M.E. (2006). Ephrin-B3 ligand promotes glioma invasion through activation of Rac1. Cancer Res *66*, 8492-8500.

Nakada, M., Niska, J.A., Miyamori, H., McDonough, W.S., Wu, J., Sato, H., and Berens, M.E. (2004). The phosphorylation of EphB2 receptor regulates migration and invasion of human glioma cells. Cancer Res *64*, 3179-3185.

Nakada, M., Niska, J.A., Tran, N.L., McDonough, W.S., and Berens, M.E. (2005). EphB2/R-Ras signaling regulates glioma cell adhesion, growth, and invasion. Am J Pathol *167*, 565-576.

Naslavsky, N., Weigert, R., and Donaldson, J.G. (2004). Characterization of a nonclathrin endocytic pathway: membrane cargo and lipid requirements. Mol Biol Cell *15*, 3542-3552.

Nichols, B. (2003a). Caveosomes and endocytosis of lipid rafts. J Cell Sci *116*, 4707-4714.

Nichols, B.J. (2003b). GM1-containing lipid rafts are depleted within clathrin-coated pits. Curr Biol *13*, 686-690.

Nilsson, I., Rolny, C., Wu, Y., Pytowski, B., Hicklin, D., Alitalo, K., Claesson-Welsh, L., and Wennstrom, S. (2004). Vascular endothelial growth factor receptor-3 in hypoxia-induced vascular development. FASEB J *18*, 1507-1515.

Nishiyama, M., Hoshino, A., Tsai, L., Henley, J.R., Goshima, Y., Tessier-Lavigne, M., Poo, M.M., and Hong, K. (2003). Cyclic AMP/GMP-dependent modulation of Ca2+ channels sets the polarity of nerve growth-cone turning. Nature *423*, 990-995.

Noren, N.K., Lu, M., Freeman, A.L., Koolpe, M., and Pasquale, E.B. (2004). Interplay between EphB4 on tumor cells and vascular ephrin-B2 regulates tumor growth. Proc Natl Acad Sci U S A *101*, 5583-5588.

Noren, N.K., and Pasquale, E.B. (2004). Eph receptor-ephrin bidirectional signals that target Ras and Rho proteins. Cell Signal *16*, 655-666.

Noren, N.K., Yang, N.Y., Silldorff, M., Mutyala, R., and Pasquale, E.B. (2009). Ephrin-independent regulation of cell substrate adhesion by the EphB4 receptor. Biochem J *422*, 433-442.

Noritake, J., Fukata, M., Sato, K., Nakagawa, M., Watanabe, T., Izumi, N., Wang, S., Fukata, Y., and Kaibuchi, K. (2004). Positive role of IQGAP1, an effector of Rac1, in actin-meshwork formation at sites of cell-cell contact. Mol Biol Cell *15*, 1065-1076.

Olsson, A.K., Dimberg, A., Kreuger, J., and Claesson-Welsh, L. (2006). VEGF receptor signalling - in control of vascular function. Nat Rev Mol Cell Biol *7*, 359-371.

Ozawa, M.G., Yao, V.J., Chanthery, Y.H., Troncoso, P., Uemura, A., Varner, A.S., Kasman, I.M., Pasqualini, R., Arap, W., and McDonald, D.M. (2005). Angiogenesis with pericyte abnormalities in a transgenic model of prostate carcinoma. Cancer *104*, 2104-2115.

Palamidessi, A., Frittoli, E., Garre, M., Faretta, M., Mione, M., Testa, I., Diaspro, A., Lanzetti, L., Scita, G., and Di Fiore, P.P. (2008). Endocytic trafficking of Rac is required for the spatial restriction of signaling in cell migration. Cell *134*, 135-147.

Palmer, A., Zimmer, M., Erdmann, K.S., Eulenburg, V., Porthin, A., Heumann, R., Deutsch, U., and Klein, R. (2002). EphrinB phosphorylation and reverse signaling: regulation by Src kinases and PTP-BL phosphatase. Mol Cell *9*, 725-737.

Park, K.W., Crouse, D., Lee, M., Karnik, S.K., Sorensen, L.K., Murphy, K.J., Kuo, C.J., and Li, D.Y. (2004). The axonal attractant Netrin-1 is an angiogenic factor. Proc Natl Acad Sci U S A *101*, 16210-16215.

Pasquale, E.B. Eph receptors and ephrins in cancer: bidirectional signalling and beyond. Nat Rev Cancer *10*, 165-180.

Pasquale, E.B. (2004). Eph-ephrin promiscuity is now crystal clear. Nat Neurosci *7*, 417-418.

Pasquale, E.B. (2005). Eph receptor signalling casts a wide net on cell behaviour. Nat Rev Mol Cell Biol *6*, 462-475.

Pasquale, E.B. (2008). Eph-ephrin bidirectional signaling in physiology and disease. Cell *133*, 38-52.

Patan, S. (2000). Vasculogenesis and angiogenesis as mechanisms of vascular network formation, growth and remodeling. J Neurooncol *50*, 1-15.

Patel, N.S., Li, J.L., Generali, D., Poulsom, R., Cranston, D.W., and Harris, A.L. (2005). Up-regulation of delta-like 4 ligand in human tumor vasculature and the role of basal expression in endothelial cell function. Cancer Res *65*, 8690-8697.

Pawson, T., and Scott, J.D. (1997). Signaling through scaffold, anchoring, and adaptor proteins. Science *278*, 2075-2080.

Pellinen, T., and Ivaska, J. (2006). Integrin traffic. J Cell Sci *119*, 3723-3731.

Pereira, F.A., Qiu, Y., Zhou, G., Tsai, M.J., and Tsai, S.Y. (1999). The orphan nuclear receptor COUP-TFII is required for angiogenesis and heart development. Genes Dev *13*, 1037-1049.

Perrin, R.M., Konopatskaya, O., Qiu, Y., Harper, S., Bates, D.O., and Churchill, A.J. (2005). Diabetic retinopathy is associated with a switch in splicing from anti- to pro-angiogenic isoforms of vascular endothelial growth factor. Diabetologia *48*, 2422-2427.

Peter, B.J., Kent, H.M., Mills, I.G., Vallis, Y., Butler, P.J., Evans, P.R., and McMahon, H.T. (2004). BAR domains as sensors of membrane curvature: the amphiphysin BAR structure. Science *303*, 495-499.

Phng, L.K., and Gerhardt, H. (2009). Angiogenesis: a team effort coordinated by notch. Dev Cell *16*, 196-208.

Poliakov, A., Cotrina, M., and Wilkinson, D.G. (2004). Diverse roles of eph receptors and ephrins in the regulation of cell migration and tissue assembly. Dev Cell *7*, 465-480.

Pugh, C.W., and Ratcliffe, P.J. (2003). Regulation of angiogenesis by hypoxia: role of the HIF system. Nat Med *9*, 677-684.

Rafii, S., Lyden, D., Benezra, R., Hattori, K., and Heissig, B. (2002). Vascular and haematopoietic stem cells: novel targets for anti-angiogenesis therapy? Nat Rev Cancer *2*, 826-835.

Rastinejad, F., Polverini, P.J., and Bouck, N.P. (1989). Regulation of the activity of a new inhibitor of angiogenesis by a cancer suppressor gene. Cell *56*, 345-355.

Risau, W., and Flamme, I. (1995). Vasculogenesis. Annu Rev Cell Dev Biol *11*, 73-91.

Robinson, C.J., and Stringer, S.E. (2001). The splice variants of vascular endothelial growth factor (VEGF) and their receptors. J Cell Sci *114*, 853-865.

Roca, C., and Adams, R.H. (2007). Regulation of vascular morphogenesis by Notch signaling. Genes Dev *21*, 2511-2524.

Rocca, D.L., Martin, S., Jenkins, E.L., and Hanley, J.G. (2008). Inhibition of Arp2/3-mediated actin polymerization by PICK1 regulates neuronal morphology and AMPA receptor endocytosis. Nat Cell Biol *10*, 259-271.

Rossman, K.L., Der, C.J., and Sondek, J. (2005). GEF means go: turning on RHO GTPases with guanine nucleotide-exchange factors. Nat Rev Mol Cell Biol *6*, 167-180.

Rothberg, K.G., Heuser, J.E., Donzell, W.C., Ying, Y.S., Glenney, J.R., and Anderson, R.G. (1992). Caveolin, a protein component of caveolae membrane coats. Cell *68*, 673-682.

Rubenstein, J.L., Kim, J., Ozawa, T., Zhang, M., Westphal, M., Deen, D.F., and Shuman, M.A. (2000). Anti-VEGF antibody treatment of glioblastoma prolongs survival but results in increased vascular cooption. Neoplasia *2*, 306-314.

Sabatier, C., Plump, A.S., Le, M., Brose, K., Tamada, A., Murakami, F., Lee, E.Y., and Tessier-Lavigne, M. (2004). The divergent Robo family protein rig-1/Robo3 is a negative regulator of slit responsiveness required for midline crossing by commissural axons. Cell *117*, 157-169.

Sadowski, L., Pilecka, I., and Miaczynska, M. (2009). Signaling from endosomes: location makes a difference. Exp Cell Res *315*, 1601-1609.

Sahin, M., Greer, P.L., Lin, M.Z., Poucher, H., Eberhart, J., Schmidt, S., Wright, T.M., Shamah, S.M., O'Connell, S., Cowan, C.W.*, et al.* (2005). Eph-dependent tyrosine phosphorylation of ephexin1 modulates growth cone collapse. Neuron *46*, 191-204.

Sakurai, Y., Ohgimoto, K., Kataoka, Y., Yoshida, N., and Shibuya, M. (2005). Essential role of Flk-1 (VEGF receptor 2) tyrosine residue 1173 in vasculogenesis in mice. Proc Natl Acad Sci U S A *102*, 1076-1081.

Sanchez-Soriano, N., Tear, G., Whitington, P., and Prokop, A. (2007). Drosophila as a genetic and cellular model for studies on axonal growth. Neural Dev *2*, 9.

Santiago, A., and Erickson, C.A. (2002). Ephrin-B ligands play a dual role in the control of neural crest cell migration. Development *129*, 3621-3632.

Schwarz-Romond, T., Fiedler, M., Shibata, N., Butler, P.J., Kikuchi, A., Higuchi, Y., and Bienz, M. (2007). The DIX domain of Dishevelled confers Wnt signaling by dynamic polymerization. Nat Struct Mol Biol *14*, 484-492.

Segura, I., Essmann, C.L., Weinges, S., and Acker-Palmer, A. (2007). Grb4 and GIT1 transduce ephrinB reverse signals modulating spine morphogenesis and synapse formation. Nat Neurosci *10*, 301-310.

Senger, D.R., Galli, S.J., Dvorak, A.M., Perruzzi, C.A., Harvey, V.S., and Dvorak, H.F. (1983). Tumor cells secrete a vascular permeability factor that promotes accumulation of ascites fluid. Science *219*, 983-985.

Seo, S., and Kume, T. (2006). Forkhead transcription factors, Foxc1 and Foxc2, are required for the morphogenesis of the cardiac outflow tract. Dev Biol *296*, 421-436.

Serini, G., Valdembri, D., Zanivan, S., Morterra, G., Burkhardt, C., Caccavari, F., Zammataro, L., Primo, L., Tamagnone, L., Logan, M.*, et al.* (2003). Class 3 semaphorins control vascular morphogenesis by inhibiting integrin function. Nature *424*, 391-397.

Shalaby, F., Rossant, J., Yamaguchi, T.P., Gertsenstein, M., Wu, X.F., Breitman, M.L., and Schuh, A.C. (1995). Failure of blood-island formation and vasculogenesis in Flk-1-deficient mice. Nature *376*, 62-66.

Shawber, C.J., Das, I., Francisco, E., and Kitajewski, J. (2003). Notch signaling in primary endothelial cells. Ann N Y Acad Sci *995*, 162-170.

Sheldon, H., Andre, M., Legg, J.A., Heal, P., Herbert, J.M., Sainson, R., Sharma, A.S., Kitajewski, J.K., Heath, V.L., and Bicknell, R. (2009). Active involvement of Robo1 and Robo4 in filopodia formation and endothelial cell motility mediated via WASP and other actin nucleation-promoting factors. FASEB J *23*, 513-522.

Shen, T.L., Park, A.Y., Alcaraz, A., Peng, X., Jang, I., Koni, P., Flavell, R.A., Gu, H., and Guan, J.L. (2005). Conditional knockout of focal adhesion kinase in endothelial cells reveals its role in angiogenesis and vascular development in late embryogenesis. J Cell Biol *169*, 941-952.

Shi, L., Fu, W.Y., Hung, K.W., Porchetta, C., Hall, C., Fu, A.K., and Ip, N.Y. (2007). Alpha2-chimaerin interacts with EphA4 and regulates EphA4-dependent growth cone collapse. Proc Natl Acad Sci U S A *104*, 16347-16352.

Shin, D., Garcia-Cardena, G., Hayashi, S., Gerety, S., Asahara, T., Stavrakis, G., Isner, J., Folkman, J., Gimbrone, M.A., Jr., and Anderson, D.J. (2001). Expression of ephrinB2 identifies a stable genetic difference between arterial and venous vascular smooth muscle as well as

endothelial cells, and marks subsets of microvessels at sites of adult neovascularization. Dev Biol *230*, 139-150.

Siekmann, A.F., and Lawson, N.D. (2007). Notch signalling limits angiogenic cell behaviour in developing zebrafish arteries. Nature *445*, 781-784.

Sigismund, S., Argenzio, E., Tosoni, D., Cavallaro, E., Polo, S., and Di Fiore, P.P. (2008). Clathrin-mediated internalization is essential for sustained EGFR signaling but dispensable for degradation. Dev Cell *15*, 209-219.

Simons, M., Gault, W.J., Gotthardt, D., Rohatgi, R., Klein, T.J., Shao, Y., Lee, H.J., Wu, A.L., Fang, Y., Satlin, L.M.*, et al.* (2009). Electrochemical cues regulate assembly of the Frizzled/Dishevelled complex at the plasma membrane during planar epithelial polarization. Nat Cell Biol *11*, 286-294.

Somanath, P.R., Malinin, N.L., and Byzova, T.V. (2009). Cooperation between integrin alphavbeta3 and VEGFR2 in angiogenesis. Angiogenesis *12*, 177-185.

Sorkin, A., and von Zastrow, M. (2009). Endocytosis and signalling: intertwining molecular networks. Nat Rev Mol Cell Biol *10*, 609-622.

Spudich, G., Chibalina, M.V., Au, J.S., Arden, S.D., Buss, F., and Kendrick-Jones, J. (2007). Myosin VI targeting to clathrin-coated structures and dimerization is mediated by binding to Disabled-2 and PtdIns(4,5)P2. Nat Cell Biol *9*, 176-183.

Stalmans, I., Ng, Y.S., Rohan, R., Fruttiger, M., Bouche, A., Yuce, A., Fujisawa, H., Hermans, B., Shani, M., Jansen, S.*, et al.* (2002). Arteriolar and venular patterning in retinas of mice selectively expressing VEGF isoforms. J Clin Invest *109*, 327-336.

Stein, E., Lane, A.A., Cerretti, D.P., Schoecklmann, H.O., Schroff, A.D., Van Etten, R.L., and Daniel, T.O. (1998). Eph receptors discriminate specific ligand oligomers to determine alternative signaling complexes, attachment, and assembly responses. Genes Dev *12*, 667-678.

Steketee, M.B., and Tosney, K.W. (2002). Three functionally distinct adhesions in filopodia: shaft adhesions control lamellar extension. J Neurosci *22*, 8071-8083.

Stone, J., Itin, A., Alon, T., Pe'er, J., Gnessin, H., Chan-Ling, T., and Keshet, E. (1995). Development of retinal vasculature is mediated by hypoxia-induced vascular endothelial growth factor (VEGF) expression by neuroglia. J Neurosci *15*, 4738-4747.

Suchting, S., Freitas, C., le Noble, F., Benedito, R., Breant, C., Duarte, A., and Eichmann, A. (2007). The Notch ligand Delta-like 4 negatively regulates endothelial tip cell formation and vessel branching. Proc Natl Acad Sci U S A *104*, 3225-3230.

Swart-Mataraza, J.M., Li, Z., and Sacks, D.B. (2002). IQGAP1 is a component of Cdc42 signaling to the cytoskeleton. J Biol Chem *277*, 24753-24763.

Takahashi, T., Takahashi, K., St John, P.L., Fleming, P.A., Tomemori, T., Watanabe, T., Abrahamson, D.R., Drake, C.J., Shirasawa, T., and Daniel, T.O. (2003). A mutant receptor tyrosine phosphatase, CD148, causes defects in vascular development. Mol Cell Biol *23*, 1817-1831.

Takahashi, T., Yamaguchi, S., Chida, K., and Shibuya, M. (2001). A single autophosphorylation site on KDR/Flk-1 is essential for VEGF-A-dependent activation of PLC-gamma and DNA synthesis in vascular endothelial cells. EMBO J *20*, 2768-2778.

Tammela, T., Zarkada, G., Wallgard, E., Murtomaki, A., Suchting, S., Wirzenius, M., Waltari, M., Hellstrom, M., Schomber, T., Peltonen, R.*, et al.* (2008). Blocking VEGFR-3 suppresses angiogenic sprouting and vascular network formation. Nature *454*, 656-660.

Tanaka, M., Sasaki, K., Kamata, R., and Sakai, R. (2007). The C-terminus of ephrin-B1 regulates metalloproteinase secretion and invasion of cancer cells. J Cell Sci *120*, 2179-2189.

Torres-Vazquez, J., Gitler, A.D., Fraser, S.D., Berk, J.D., Van, N.P., Fishman, M.C., Childs, S., Epstein, J.A., and Weinstein, B.M. (2004). Semaphorin-plexin signaling guides patterning of the developing vasculature. Dev Cell *7*, 117-123.

Torres, R., Firestein, B.L., Dong, H., Staudinger, J., Olson, E.N., Huganir, R.L., Bredt, D.S., Gale, N.W., and Yancopoulos, G.D. (1998). PDZ proteins bind, cluster, and synaptically colocalize with Eph receptors and their ephrin ligands. Neuron *21*, 1453-1463.

Tozer, G.M., Kanthou, C., and Baguley, B.C. (2005). Disrupting tumour blood vessels. Nat Rev Cancer *5*, 423-435.

Traub, L.M., and Lukacs, G.L. (2007). Decoding ubiquitin sorting signals for clathrin-dependent endocytosis by CLASPs. J Cell Sci *120*, 543-553.

Vasioukhin, V., Bauer, C., Yin, M., and Fuchs, E. (2000). Directed actin polymerization is the driving force for epithelial cell-cell adhesion. Cell *100*, 209-219.

Vieira, A.V., Lamaze, C., and Schmid, S.L. (1996). Control of EGF receptor signaling by clathrin-mediated endocytosis. Science *274*, 2086-2089.

Wang, B., Xiao, Y., Ding, B.B., Zhang, N., Yuan, X., Gui, L., Qian, K.X., Duan, S., Chen, Z., Rao, Y.*, et al.* (2003). Induction of tumor angiogenesis by Slit-Robo signaling and inhibition of cancer growth by blocking Robo activity. Cancer Cell *4*, 19-29.

Wang, H.U., Chen, Z.F., and Anderson, D.J. (1998). Molecular distinction and angiogenic interaction between embryonic arteries and veins revealed by ephrin-B2 and its receptor Eph-B4. Cell *93*, 741-753.

Wang, Y., Chang, J., Chen, K.D., Li, S., Li, J.Y., Wu, C., and Chien, S. (2007). Selective adapter recruitment and differential signaling networks by VEGF vs. shear stress. Proc Natl Acad Sci U S A *104*, 8875-8879.

Wang, Y., Nakayama, M., Pitulescu, M.E., Schmidt, T.S., Bochenek, M.L., Sakakibara, A., Adams, S., Davy, A., Deutsch, U., Luthi, U.*, et al.* Ephrin-B2 controls VEGF-induced angiogenesis and lymphangiogenesis. Nature *465*, 483-486.

Wang, Y., Ying, G.X., Liu, X., Wang, W.Y., Dong, J.H., Ni, Z.M., and Zhou, C.F. (2005). Induction of ephrin-B1 and EphB receptors during denervation-induced plasticity in the adult mouse hippocampus. Eur J Neurosci *21*, 2336-2346.

Warner, A.J., Lopez-Dee, J., Knight, E.L., Feramisco, J.R., and Prigent, S.A. (2000). The Shc-related adaptor protein, Sck, forms a complex with the vascular-endothelial-growth-factor receptor KDR in transfected cells. Biochem J *347*, 501-509.

Watson, F.L., Heerssen, H.M., Bhattacharyya, A., Klesse, L., Lin, M.Z., and Segal, R.A. (2001). Neurotrophins use the Erk5 pathway to mediate a retrograde survival response. Nat Neurosci *4*, 981-988.

Wegmeyer, H., Egea, J., Rabe, N., Gezelius, H., Filosa, A., Enjin, A., Varoqueaux, F., Deininger, K., Schnutgen, F., Brose, N.*, et al.* (2007). EphA4-dependent axon guidance is mediated by the RacGAP alpha2-chimaerin. Neuron *55*, 756-767.

Weis, S., Shintani, S., Weber, A., Kirchmair, R., Wood, M., Cravens, A., McSharry, H., Iwakura, A., Yoon, Y.S., Himes, N.*, et al.* (2004). Src blockade stabilizes a Flk/cadherin complex, reducing edema and tissue injury following myocardial infarction. J Clin Invest *113*, 885-894.

Wharton, K.A., Jr. (2003). Runnin' with the Dvl: proteins that associate with Dsh/Dvl and their significance to Wnt signal transduction. Dev Biol *253*, 1-17.

Whitehead, K.J., Chan, A.C., Navankasattusas, S., Koh, W., London, N.R., Ling, J., Mayo, A.H., Drakos, S.G., Jones, C.A., Zhu, W.*, et al.* (2009). The cerebral cavernous malformation signaling pathway promotes vascular integrity via Rho GTPases. Nat Med *15*, 177-184.

Wijelath, E.S., Rahman, S., Namekata, M., Murray, J., Nishimura, T., Mostafavi-Pour, Z., Patel, Y., Suda, Y., Humphries, M.J., and Sobel, M. (2006). Heparin-II domain of fibronectin is a vascular endothelial growth factor-binding domain: enhancement of VEGF biological activity by a singular growth factor/matrix protein synergism. Circ Res *99*, 853-860.

Williams, C.K., Li, J.L., Murga, M., Harris, A.L., and Tosato, G. (2006). Up-regulation of the Notch ligand Delta-like 4 inhibits VEGF-induced endothelial cell function. Blood *107*, 931-939.

Wilson, B.D., Ii, M., Park, K.W., Suli, A., Sorensen, L.K., Larrieu-Lahargue, F., Urness, L.D., Suh, W., Asai, J., Kock, G.A.*, et al.* (2006). Netrins promote developmental and therapeutic angiogenesis. Science *313*, 640-644.

Witze, E.S., Litman, E.S., Argast, G.M., Moon, R.T., and Ahn, N.G. (2008). Wnt5a control of cell polarity and directional movement by polarized redistribution of adhesion receptors. Science *320*, 365-369.

Wu, C., Ramirez, A., Cui, B., Ding, J., Delcroix, J.D., Valletta, J.S., Liu, J.J., Yang, Y., Chu, S., and Mobley, W.C. (2007). A functional dynein-microtubule network is required for NGF signaling through the Rap1/MAPK pathway. Traffic *8*, 1503-1520.

Wybenga-Groot, L.E., Baskin, B., Ong, S.H., Tong, J., Pawson, T., and Sicheri, F. (2001). Structural basis for autoinhibition of the Ephb2 receptor tyrosine kinase by the unphosphorylated juxtamembrane region. Cell *106*, 745-757.

Xia, J., Zhang, X., Staudinger, J., and Huganir, R.L. (1999). Clustering of AMPA receptors by the synaptic PDZ domain-containing protein PICK1. Neuron *22*, 179-187.

Xu, N.J., and Henkemeyer, M. (2009). Ephrin-B3 reverse signaling through Grb4 and cytoskeletal regulators mediates axon pruning. Nat Neurosci *12*, 268-276.

Yamanaka, T., Horikoshi, Y., Suzuki, A., Sugiyama, Y., Kitamura, K., Maniwa, R., Nagai, Y., Yamashita, A., Hirose, T., Ishikawa, H.*, et al.* (2001). PAR-6 regulates aPKC activity in a novel way and mediates cell-cell contact-induced formation of the epithelial junctional complex. Genes Cells *6*, 721-731.

Yamaoka-Tojo, M., Ushio-Fukai, M., Hilenski, L., Dikalov, S.I., Chen, Y.E., Tojo, T., Fukai, T., Fujimoto, M., Patrushev, N.A., Wang, N.*, et al.* (2004). IQGAP1, a novel vascular endothelial growth factor receptor binding protein, is involved in reactive oxygen species--dependent endothelial migration and proliferation. Circ Res *95*, 276-283.

Yang, L.T., Nichols, J.T., Yao, C., Manilay, J.O., Robey, E.A., and Weinmaster, G. (2005). Fringe glycosyltransferases differentially modulate Notch1 proteolysis induced by Delta1 and Jagged1. Mol Biol Cell *16*, 927-942.

You-Ten, K.E., Muise, E.S., Itie, A., Michaliszyn, E., Wagner, J., Jothy, S., Lapp, W.S., and Tremblay, M.L. (1997). Impaired bone marrow microenvironment and immune function in T cell protein tyrosine phosphatase-deficient mice. J Exp Med *186*, 683-693.

You, L.R., Lin, F.J., Lee, C.T., DeMayo, F.J., Tsai, M.J., and Tsai, S.Y. (2005). Suppression of Notch signalling by the COUP-TFII transcription factor regulates vein identity. Nature *435*, 98-104.

Yu, A., Rual, J.F., Tamai, K., Harada, Y., Vidal, M., He, X., and Kirchhausen, T. (2007). Association of Dishevelled with the clathrin AP-2 adaptor is required for Frizzled endocytosis and planar cell polarity signaling. Dev Cell *12*, 129-141.

Yu, J.L., Rak, J.W., Coomber, B.L., Hicklin, D.J., and Kerbel, R.S. (2002). Effect of p53 status on tumor response to antiangiogenic therapy. Science *295*, 1526-1528.

Zhang, H., Berg, J.S., Li, Z., Wang, Y., Lang, P., Sousa, A.D., Bhaskar, A., Cheney, R.E., and Stromblad, S. (2004). Myosin-X provides a motor-based link between integrins and the cytoskeleton. Nat Cell Biol *6*, 523-531.

Zhang, H., Webb, D.J., Asmussen, H., Niu, S., and Horwitz, A.F. (2005). A GIT1/PIX/Rac/PAK signaling module regulates spine morphogenesis and synapse formation through MLC. J Neurosci *25*, 3379-3388.

Zhang, Y., Singh, M.K., Degenhardt, K.R., Lu, M.M., Bennett, J., Yoshida, Y., and Epstein, J.A. (2009). Tie2Cre-mediated inactivation of plexinD1 results in congenital heart, vascular and skeletal defects. Dev Biol *325*, 82-93.

Zhong, T.P., Childs, S., Leu, J.P., and Fishman, M.C. (2001). Gridlock signalling pathway fashions the first embryonic artery. Nature *414*, 216-220.

Zimmer, M., Palmer, A., Kohler, J., and Klein, R. (2003). EphB-ephrinB bi-directional endocytosis terminates adhesion allowing contact mediated repulsion. Nat Cell Biol *5*, 869-878.

Zisch, A.H., Pazzagli, C., Freeman, A.L., Schneller, M., Hadman, M., Smith, J.W., Ruoslahti, E., and Pasquale, E.B. (2000). Replacing two conserved tyrosines of the EphB2 receptor with glutamic acid prevents binding of SH2 domains without abrogating kinase activity and biological responses. Oncogene *19*, 177-187.

10. *Curriculum Vitae*

PERSONAL INFORMATION AND CONTACT DETAILS

Name	Suphansa Sawamiphak
Nationality	Thai
Date of birth	May 31, 1980
Place of birth	Nakhonpathom, Thailand

EDUCATION

Oct 2008 – Present PhD student position at the Institute of Cell Biology and Neuroscience, Goethe University, Frankfurt, Germany

Oct 2005 – Sep 2008 PhD student position at the Max Planck Institute of Neurobiology, Martinsried, Germany.

Jun 2002 – Mar 2004 Master student at Mahidol University, Bangkok, Thailand
Master Degree of Science (Major: Molecular Biotechnology), International program, GPA 3.66 (out of 4.00)

Jun 1998 – Mar 2002 Bachelor student at Kasetsart University, Bangkok, Thailand
Bachelor Degree of Science (Major: Genetics), GPA 3.23 (out of 4.00)

RESEARCH EXPERIENCE

Oct 2005 – Present Max Planck Insitute of Neurobiology, Martinsried, Germany and continued reserch work at Insttitue of Cell Biology and Neuroscience, Goethe University, Frankfurt, Germany
Project: EphrinB2 regulates VEGFR2 function in developmental and tumor angiogenesis
Position: PhD student
PI: Prof. Dr. Amparo Acker-Palmer

Nov 2004 – Mar 2005 Kyorin University, Tokyo, Japan

Project: Basolateral transporsomes and renal function
Position: Guest scientist
PI: Prof. Dr. Yoshikatsu Kanai

Jun 2002 – Mar 2004 Mahidol University, Bangkok, Thailand
Project: Expression and functional characterization of the rat organic anion transpoter 1 (rOAT1) in yeast *Saccharomyces cerevisiae*
Position: Master student
PI: Dr. Chuenchit Boonchird

Jun 1998 – Mar 2002 Kasetsart University, Bangkok, Thailand
Project: Examination of DNA fingerprint of radioactive-induced *Canna Generalis* phenotypic mutant using RAPD marker
Position: Bachelor student
PI: Dr. Surin Piyashokanakul

Jun 1996 – Jun 1998 Sriboonyanon school, Nonthaburi, Thailand
Project: Three practical projects (duration 2-3 months) in different fields of biology and chemistry
Position: High school student

Oct 1996 – Nov 1996 Ministry of Public Health, Nonthaburi, Thailand
Project: Plant tissue culture and drug toxicological test in murine model
Position: Trainee

TEACHING EXPERIENCE

Jan 2009 – Present Supervisor of a PhD student of the Graduate Program for the Cluster of Excellent Frankfurt, Goethe University, Frankfurt

Jan 2010 Supervisor of undergraduate students presentation in a cell biology journal club

Jul 2008 – Sep 2008 Supervisor of an undergraduate student from Dartmouth University, Hanover, USA, for practical work

PUBLICATIONS

Sawamiphak S., Seidel S. Essmann C. L., Wilkinson G. A., Pitulescu M., Acker T., Acker-Palmer A. (2010) EphrinB2 regulates VEGFR2 function in developmental and tumour angiogenesis. Nature 2010 May; 465(7297): 487/91.

Sawamiphak S., Sophasan S., Endou H., Boonchird C. (2005) Functional expression of the rat organic anion transporter 1 (rOAT1) in *Saccharomyces cerevisiae*. Biochim. Biophys. Acta. 1720(1-2), 44-51.

FELLOWSHIP AND AWARDS

Jun 1996-Mar 2004 Fellowship from the Development and Promotion of Science and Technology Talents Project of Thailand, a prestigious fellowship from Thai government given to less than 40 students from all over the country each year.

Feb 2006 Best master thesis award from the Faculty of Science, Mahidol University, Bangkok, Thailand.